AD 265 514

ARF

ARMOUR RESEARCH FOUNDATION OF ILLINOIS INSTITUTE OF TECHNOLOGY

TECHNOLOGY CENTER

ARF Project No. 8130

LONG RANGE STUDY PROGRAM
LIGHTWEIGHT ARTILLERY WEAPON

Final Report

R.M. Brach

Completed in April, 1961

for

Commanding Officer
Rock Island Arsenal
Rock Island, Illinois

25 years of research

ARMOUR RESEARCH FOUNDATION
of
ILLINOIS INSTITUTE OF TECHNOLOGY
Technology Center
Chicago 16, Illinois

Final Report

LONG-RANGE STUDY PROGRAM
LIGHTWEIGHT ARTILLERY WEAPON

Completed in April, 1961

for

Commanding Officer
Rock Island Arsenal
Rock Island, Illinois

under

Contract No. DA-11-022-ORD-2543
Ordnance Project TW-201
D/A Project No. 5U17-07-021
ILS No. 1-4-1-11
ARF Project No. 8130

FOREWORD

In June 1957, Armour Research Foundation completed a feasibility study of a lightweight field artillery weapon intended for use by the Marine Corps. The study specifically explored the possibility of development of a helicopter-transportable field weapon with a high-rate-of-fire burst capability. The results of this study indicated that a lightweight field artillery weapon could be developed to use boosted rocket ammunition, be capable of helicopter transport, and fire six rounds in approximately two seconds. A project was then initiated at ARF to design and develop such a launcher.

The first phase of the program consisted of the design and fabrication of the XM70 Launcher, Prototype No. 1. This prototype displayed an exceptionally optimistic performance such that a second phase of the program was initiated. The second phase consisted of the incorporation design improvements and construction of two more prototypes, XM70E1, Prototypes 2 and 3. Subsequently, Prototypes 4 and 5, XM70E2, were designed and built.

Although the early performance of the XM70 Launcher was satisfactory, it was realized that improvements in performance were possible and necessary. In order to determine the best methods of improving performance, specifically the launcher dynamic response and its effect upon accuracy, a long-range study program was initiated. This program consisted of a concentrated effort of both experimental and analytical investigations of the launcher dynamics.

This long-range study program was begun in October of 1959 and concluded in March, 1961. Progress reports concerning this program were included in the bi-monthly reports of the design and development project. The following staff members contributed significantly to the results of this program: P. Eakins, R. A. Eubanks, L. Gardiner, C. Murray, K. Norikane, N. Pearson, R. Pratt, J. Ross, R. H. Van Beek, and C. Youngdahl.

Respectfully submitted,

ARMOUR RESEARCH FOUNDATION
of Illinois Institute of Technology

R. M. Brach

R. M. Brach
Associate Research Engineer

APPROVED:

W. D. Bobco

W. D. Bobco
Assistant Director
Mechanics Research

LONG RANGE STUDY PROGRAM
LIGHTWEIGHT ARTILLERY WEAPON

ABSTRACT

Prototype No. 3 Launcher, XM70E1, 115 mm was instrumented with strain, pressure and displacement gages; these furnished the actual loading and motion of the launcher structure. In addition to certain simple dynamic analyses, a 3-degree-of-freedom, nonlinear mathematical model of the launcher dynamics was derived and programmed for solution on Armour Research Foundation's Univac 1105. The output of the computer program was correlated with experiment and used to study the effect of physical parameter variations.

Regions of instability of the launcher motions were shown to exist for burst firings; relationships between component stiffness and damping were found which optimized the launcher response to firing loads, based upon a simple accuracy criterion. Certain design suggestions were evaluated and shown to benefit the accuracy of the launcher.

TABLE OF CONTENTS

TABLE OF CONTENTS (Continued)

LIST OF ILLUSTRATIONS

LIST OF ILLUSTRATIONS (Continued)

LIST OF ILLUSTRATIONS (Continued)

LIST OF ILLUSTRATION (Continued)

LIST OF ILLUSTRATIONS (Continued)

LIST OF TABLES

DISTRIBUTION LIST

Copies of this report are being distributed as follows

Copy No.	Recipient	Copy No.	Recipient
[illegible]	[illegible]	[illegible]	[illegible]

[illegible]

LONG-RANGE STUDY PROGRAM
LIGHTWEIGHT ARTILLERY WEAPON

I. INTRODUCTION

A unique automatic rocket launcher in the field artillery weapon class has been designed and developed by Armour Research Foundation under the technical supervision of Rock Island Arsenal. This weapon is a 115mm launcher capable of firing single shots or bursts of up to six rounds. Boost charge variations combined with rocket thrust increments and variable elevation provide an exceptionally wide range capability. The launcher can be traversed $\pm 20^{\circ}$ without disturbing its original emplacement. Based upon early feasibility studies and also upon the performance of the first prototype, this lightweight, automatic launcher concept showed itself to be unusually capable as an effective weapon. It was realized, however, that production schedule requirements for succeeding prototypes might hinder the development of the concept, because of the tendency to freeze important design features. As a result, this long-range study program was initiated to investigate the dynamic behavior of the launcher during burst firing, relate this behavior to accuracy, and determine the important physical parameter values which will insure good accuracy.

The program was comprised of theoretical and experimental studies of the dynamics of the launcher. These consisted of finding the effects of certain parameter variations upon the launcher motion; accuracy was related to the motion by simple criteria. Some of the important launcher parameters which were considered are: structural rigidity, damping, recoil system characteristics, launcher geometry, and ground restraints.

The majority of the work accomplished, both theoretical and experimental, is presented in the appendices. A description of the work and results as well as the important conclusions are presented in the following sections. Section II is an introductory portion of the report containing a description of the launcher structure and its relationship to its dynamic response. Some of the operational characteristics of the launcher system, as they affect the response, are also discussed.

Section III presents the results of the experimental work, and is broken into three parts. These respectively describe stiffness measurements of the structural components and two separate firing programs. Stiffness measurements were made, both statically, of all the major structural components, and dynamically of the entire supporting structure assembly (carriages and trails). The second experimental effort was a firing program wherein approximately 75 proof slugs were fired. During these firings the launcher was instrumented with pressure gages, displacement transducers, and strain gages to provide information on the force input, the response of the launcher, and accuracy in the vertical plane. Finally, horizontal dispersion was significantly reduced, as shown by targets, with the use of two fixtures -- one restraining the trails from horizontal motion while the second stiffened the recoiling assembly framework.

In Section IV, the theoretical analyses are described; they consist of the following mathematical models:

1. A planar, nonlinear 3-degree-of-freedom model (called Mathematical Model V in progress reports),
2. A third-order, linear model,
3. A linear, 2-degree-of-freedom model,
4. A three-dimensional, nonlinear, n-degree-of-freedom system,
5. A second-order, linear system.

The first of these was implemented with a computer program and was widely applied to study launcher motion. It contained representations of the hydropneumatic recoil system, the indexing cams, and flexibilities and damping of both the supporting structure and elevating system. Information about the response of linear, third-order systems led to a structural optimization of the elevating system. The 2-degree-of-freedom system was an approximation of the launcher used to determine the best location for auxiliary dampers. The fourth model is a relatively complex representation of the launcher; its significant contribution was the inclusion of structural flexibilities of both the recoiling assembly framework and firing tube and also consideration of motion out of the vertical plane. Unfortunately, this model could only be developed to the point where it was programmed for the Univac but not run. The final system was a single-degree-of-freedom system used

to investigate the important parameter values which can cause the response to decay by a desired amount between rounds of a burst.

The 3-degree-of-freedom model was used to correlate theoretical response curves with the experimental response obtained with various structural changes. The correlation was very good for certain parameter combinations, but the theoretical response curves lacked certain characteristics as some parameters were varied. The reason for this is postulated; allowing conclusions to be drawn which indicate the desirability of certain combinations of structural parameters which correspond to improved accuracy.

A theoretical investigation was made of a specific design recommendation -- delayed recoil rods. Because the 3-degree-of-freedom model had an explicit representation of the recoil system, the behavior resulting from increasing the orifice area during the time the rocket is in the launcher could be studied. This cutback on the recoil rods resulted in near free recoil for a short time.

The final item studied was done as a matter of interest; the terms representing the Coriolis acceleration of the recoiling assembly were neglected during one computer run. Comparison was then made with a normal response to determine the effect.

Although the launcher has a $\pm 20^{\circ}$ traverse capability, all of the studies considered only zero traverse accuracy because of its order of importance. Ground restraints and soil considerations were included in the n-degree-of-freedom model and could not be studied because of the status of the model. One method of auxiliary ground restraint, horizontal trail ties, was tried and is discussed with horizontal dispersion reduction.

II. DESCRIPTION OF THE LAUNCHER STRUCTURE

The complete launcher is shown in two firing positions, in Fig. 1 and 2. It consists of two main assemblies: the tipping assembly and the supporting structure. The total weight of the launcher, 3150 lb, is almost equally divided between these two assemblies. The tipping assembly rotates relative to the supporting structure at the trunnion; the elevating system separates them at any fixed position from -6° to 65°.

A. Tipping Assembly

The tipping assembly is composed of a cradle and recoiling assembly; the former is simply the containment for the latter. The firing tube is fixed to the front of the structural framework of the recoiling assembly (see Fig. 3); it also supports two, contrarotating breech clusters of three rounds each and holds the recuperator and recoil system. The framework consists essentially of the front plate, rear plate, two side tie bars, the recuperator cylinder and a lower tie bar; the recoil cylinders are not load bearing members of this framework. Two indexing cams extend into the hubs of the breech clusters and cause them to alternately rotate into firing position during counterrecoil. These cams are fixed to the front of the cradle.

B. Supporting Structure

The supporting structure is the name given to the portion of the launcher below the trunnions; this structure is made up of what are commonly called the upper carriage, lower carriage and trails. An exploded view of the supporting structure in Fig. 4 shows its essential components. This entire structure is composed of hollow, sheet steel construction with various necessary non-structural components accounting for 20% of its total weight. These components are the traverse and elevating mechanisms, wheels, firing base, lunnette and a jack for raising and lowering the firing base. In firing position, the trails are separated by an included angle of 40° which permits $\pm 20^{\circ}$ traverse firing; the upper box, trunnion sides and tipping assembly rotate relative to the remaining structure to attain the desired traverse positions.

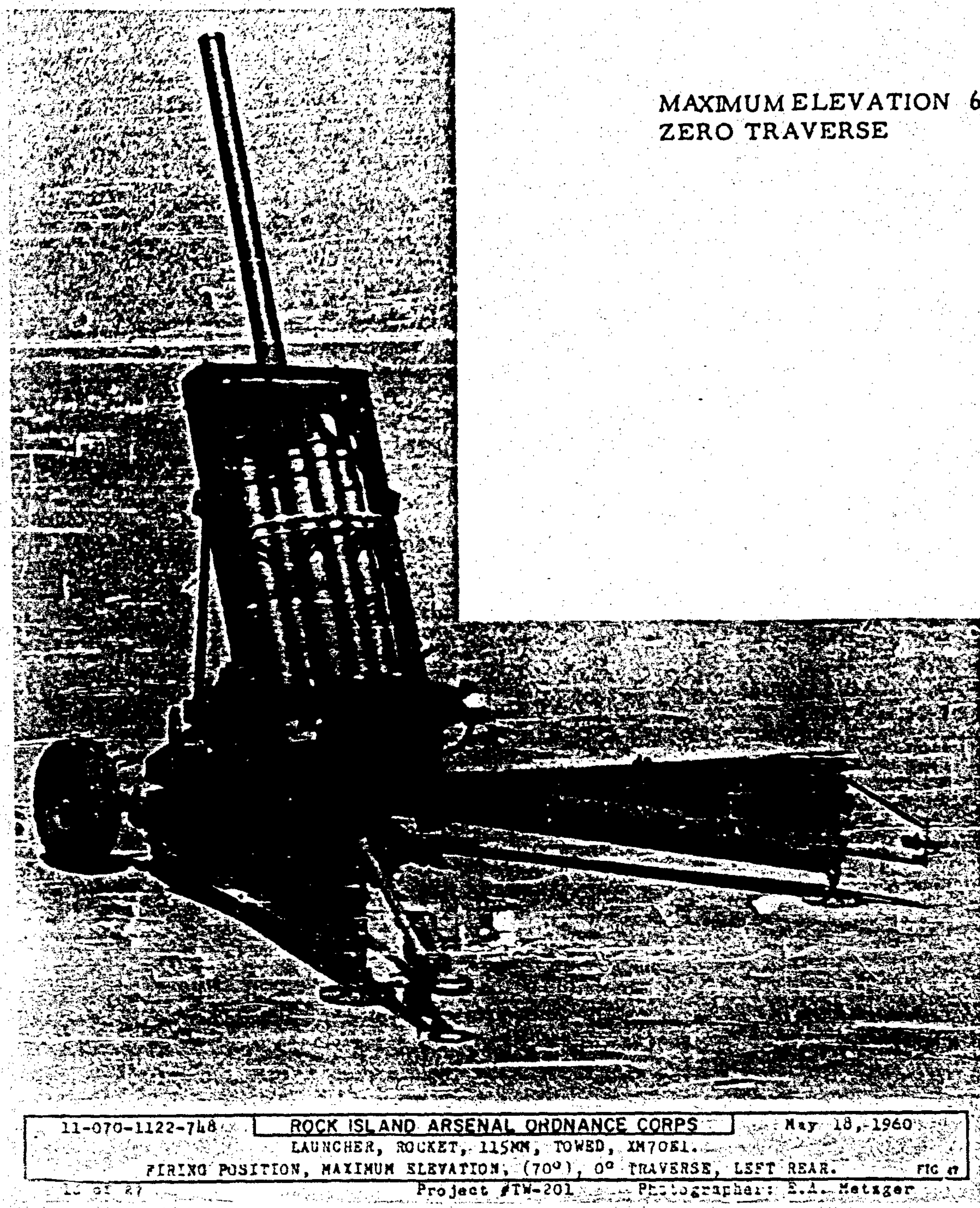

MAXIMUM ELEVATION 65°
ZERO TRAVERSE

Fig. 1 PHOTOGRAPH OF LAUNCHER

MINIMUM ELEVATION, -6°
ZERO TRAVERSE

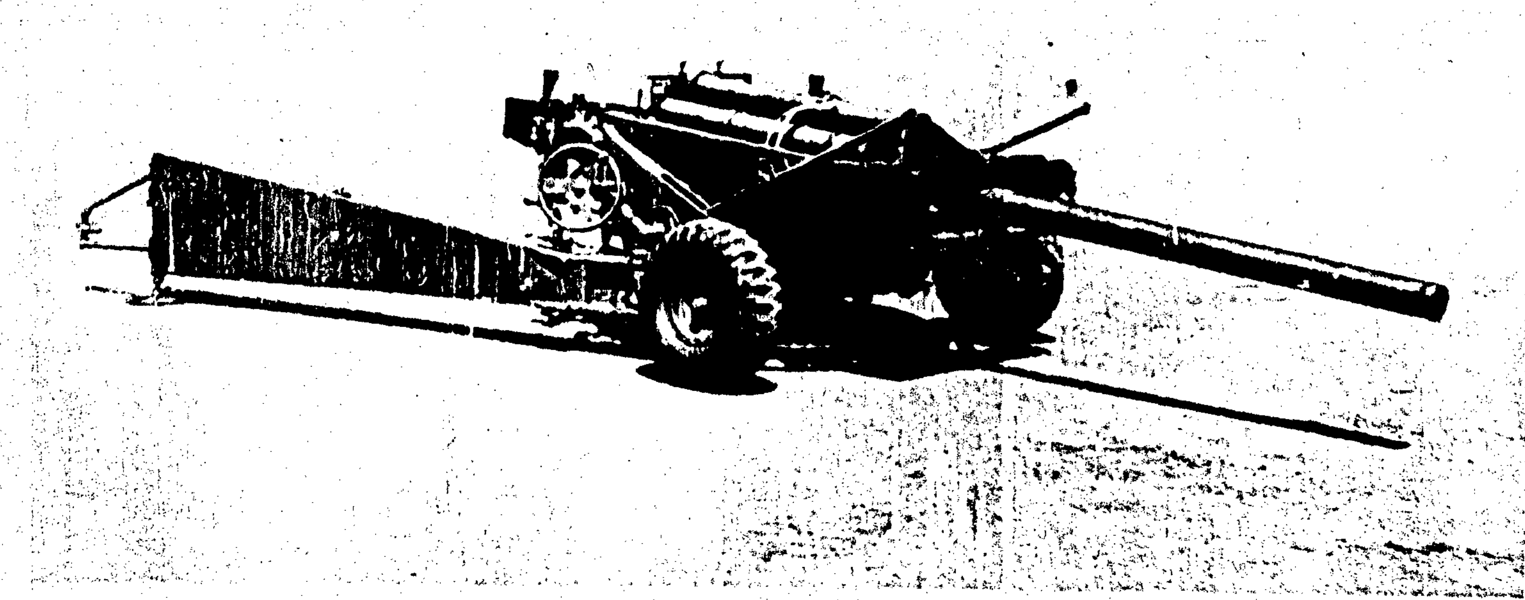

11-070-1122-746 ROCK ISLAND ARSENAL ORDNANCE CORPS May 18, 1960
LAUNCHER, ROCKET, 115MM, TOWED, XM70E1.
FIRING POSITION, MINIMUM ELEVATION, (-6°), 0° TRAVERSE, RIGHT FRONT. FIG 48
16 of 27 Project #TW-201 Photographer: E.A. Metzger

Fig. 2 PHOTOGRAPH OF LAUNCHER

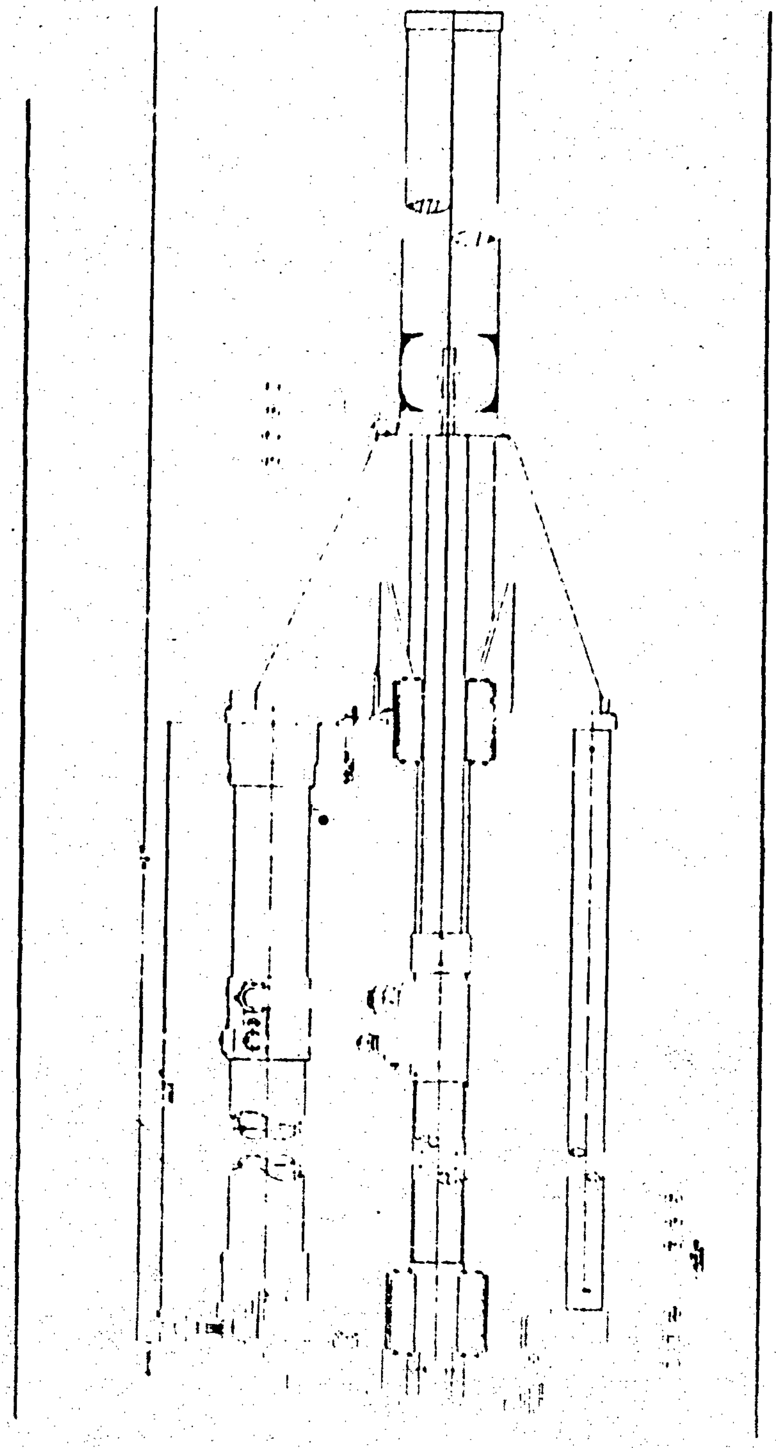

Fig. 3 SKETCH OF RECOILING ASSEMBLY

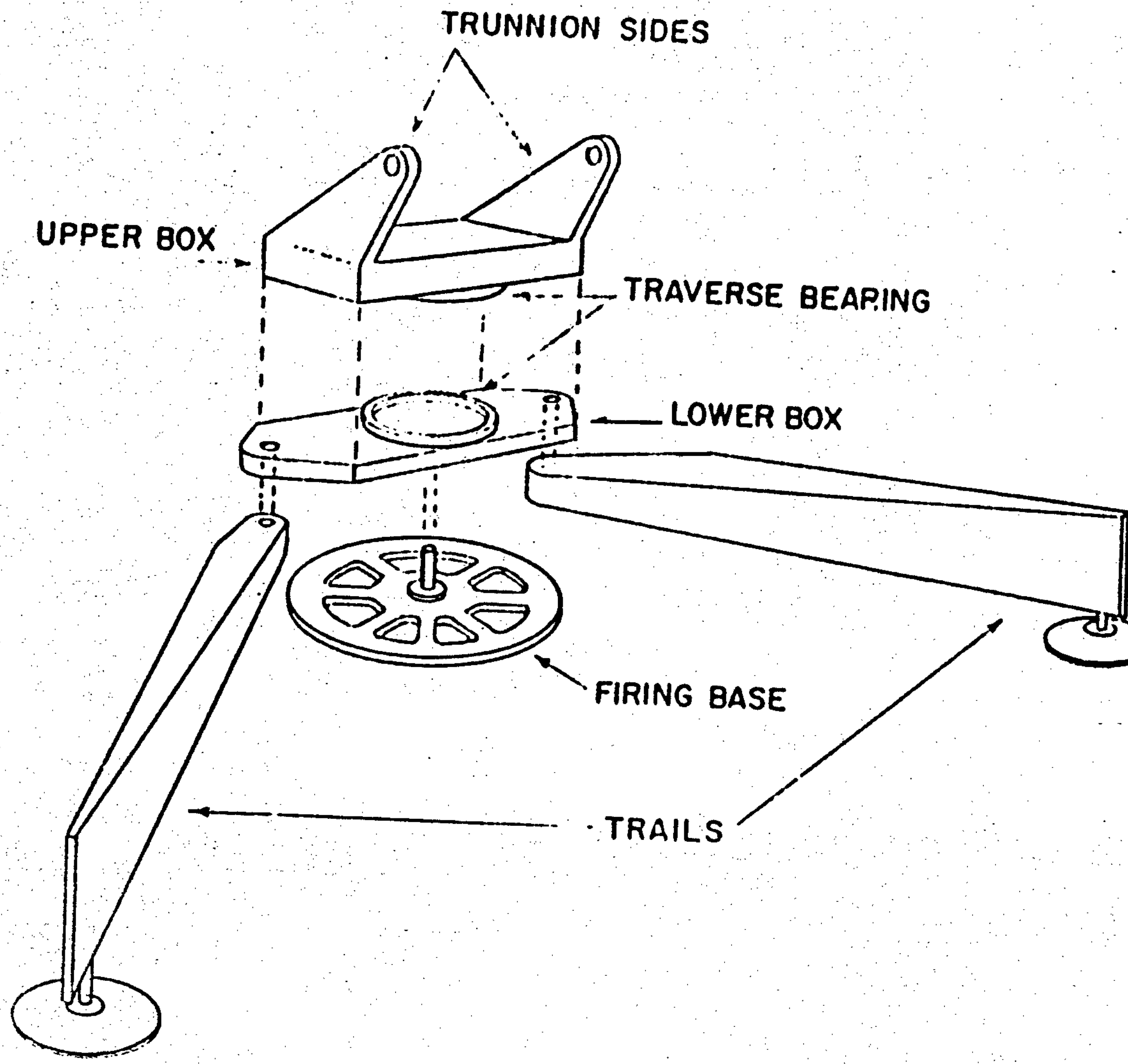

Fig. 4 EXPLODED VIEW OF THE SUPPORTING STRUCTURE

C. Elevating System

The elevating system plays an important role in the dynamic response of the launcher and deserves some discussion. This system is composed of hollow threaded rods passing through ball bearing nut assemblies held in brackets on each side of the cradle. The lower ends of these rods are inserted into the trunnion sides where they are supported by a thrust bearing in a gear box. The rods themselves are relatively stiff in tension and compression; certain other components of this system, however, comprise a significant flexibility. The brackets at the cradle are cantilevered and are inherently flexible; torsion of the cradle sides also contributes to effective relative motion of the tipping assembly and supporting structure. The ball bearings in the screw-nut mechanism, due to unavoidable clearances also add to the system flexibility in the form of nonlinearities. Likewise, the lower connections, through local deflections of the sheet metal box and trunnion sides, are relatively flexible. Thus, significant rotation of the tipping assembly mass center can occur about the trunnions (in the vertical plane) during firing,due to the flexibility of the elevating system.

D. Damping

As designed, damping of the launcher motions can occur from four sources:

1. Structural material damping,
2. Interaction with the soil,
3. The hydraulic recoil system,
4. The support buffers.

The first damping source is negligible in the presence of the others. The second source varies with the type of soil and can be either negligible or significant. The third source of damping is important because relative motion between the cradle and recoiling assembly can cause relatively large amounts of energy to be damped out by forcing oil through the orifice in each recoil cylinder. The support buffers consist of two cylinder and piston assemblies attached to the front of the lower carriage; the cylinders are fixed to the carriage and the piston rods rest against the firing base. When the supporting structure rotates forward, about the ball joint connection to the base, the

pistons force oil through orifices and damp out this forward motion. Small springs in parallel with the pistons restore the position of the supporting structure. These buffers are mainly to prevent the launcher from tipping over following the final shot of a burst when the recoiling assembly returns to battery. These buffers operate during bursts, however, when any forward rotation of the supporting structure occurs.

E. Deflection

Before discussing the dynamic response of the launcher structure to firing loads, it is necessary to first examine the supporting structure to see how it deflects to a load at the trunnions. We will consider zero traverse, a completely symmetric structure and loads in the vertical plane only. Let us assume that the tipping assembly and elevating system are removed; a force at the trunnions (for example, at 45° with respect to the ground) causes the trunnion sides to deflect relative to the upper box. Since these members are essentially short, stubby beams, both bending and shear are of equal significance. We now have a shear force and moment at the sides of the upper box; this causes bending and shear of both sides of this member relative to the bearing. However, this loading also causes torsion of the upper box section, and is the most significant deflection of this member compared to shear and bending deflections. The shear load is further transferred through the bearing down to the ground at the firing base. The moment reaction, however, is transferred through the bearing and causes torsion of the lower box, which eventually places a bending moment on the front of each trail. With respect to trunnion deflection in the vertical plane we then see that the following values of stiffness of the structure components are important:

1. Bending and shear of the trunnion sides,
2. Torsion of the upper and lower box,
3. Separation of the traverse bearing,
4. Bending of the trails.

Significant deflections occur both from the supporting structure and from the elevating system and cause a nonlinear relationship between the various deflections, due to the geometry.

F. Experimental Structure Modifications

During the experimental firings conducted on this program, various modifications to the structure were made. These took essentially two forms, changes in stiffness and changes in damping. Modifications of the structure which essentially affect only the response in the vertical plane are discussed first. The stiffening fixtures are:

1. Variable stiffness elevating rods,
2. Upper and lower box end-clamps,
3. Trunnion-to-trail struts.

The utility of the first fixture is self explanatory. The second and third sets of fixtures were designed to permit a temporary increase in the stiffness of the supporting structure by decreasing the torsion of the upper and lower boxes. The clamps were 1/2 in. thick steel brackets which joined each of the four corners of the boxes and transferred the moment reaction from the base of the trunnion sides directly to the trails. The trunnion-to-trail struts caused most of the trunnion reaction to be directly transferred to the trails. For these struts, the trails had to be rotated inward until they were set directly beneath the trunnions. Having the trails straight back caused an additional stiffness increase in this configuration.

Damping was added to the elevating system in either of two ways. Auxiliary, hydraulic dampers were placed between the cradle front and trunnion sides in parallel to the elevating screws. Figure 5 shows these dampers on the launcher. Provisions were made to change the damping source by the use of frictional ring springs in the variable flexibility elevating rods. A more complete description of these fixtures is presented in Appendix G.

The above fixtures were intended to cause a direct change of the launcher response in the vertical plane (neglecting coupling of vertical and horizontal motions). Another temporary change to the launcher structure was made, this time for the purpose of affecting the horizontal motion of the launcher. This change was the addition of a thin, sheet metal shell which surrounded the recoiling assembly and was attached to the side tie bars. This shell stiffened the framework in a manner such that the front plate and rear plate would be more securely restrained from rotating with respect to

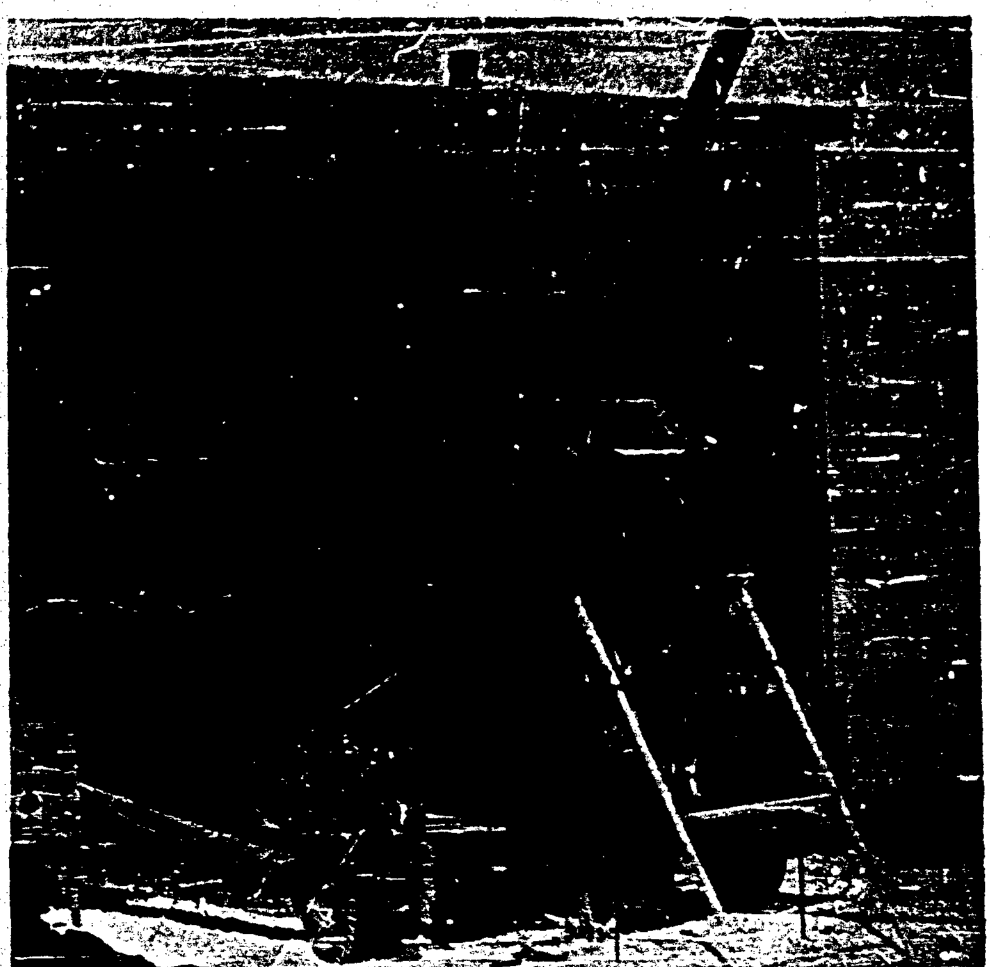

Fig. 5 EXPERIMENTAL LAUNCHER EMPLACEMENT

each other about a vertical axis. This type of rotation was experienced in the launcher and caused a significant horizontal dispersion. For the same purpose, reduction of horizontal dispersion, the trail ends were fastened by cables to small stakes at the side of each trail. This prevented the trails from rotating (in the plane of the ground) and caused a decrease in horizontal dispersion.

III. EXPERIMENTAL WORK

The experimental effort was composed of three separate ventures:

1. The determination of the structural component flexibilities,
2. Determination of the dynamic response of the launcher in the vertical plane,
3. Testing of fixtures which were to decrease horizontal dispersion.

The values of stiffness of the structural components were needed for two reasons: first, as input to the theoretical studies and second, to determine if the particular structural designs yielded the desired stiffness, as required by earlier analyses. The stiffness was found experimentally because of the complexity of the structure; it was more efficient than corresponding calculations. In cases where calculations were made, the measurements afforded a method of checking.

The dynamic response in the vertical plane was determined for correlation with theory and thereby used to validate the corresponding mathematical model, and/or point out its deficiencies.

A. Physical Parameter Measurements

Static stiffness measurements of the following components or assemblies were made:

1. The entire supporting structure,
2. The entire supporting structure with the upper and lower boxes clamped,
3. The entire supporting structure with the box clamps and with the trunnion-to-trail struts.
4. The entire supporting structure in traverse position,
   a. 20° right
   b. 20° left
5. The lower elevating screw support,
6. Trails,
7. Elevating screw - upper bracket combination.

Since rotational motion is the sole significant contributor to dispersion, the moment of the recoil force per unit rotation of a line through the ball joint and the trunnions (in the vertical plane), is used as an indication of supporting structure stiffness. The static stiffness of the

supporting structure is therefore given in units of in. -lb/radian. For the entire supporting structure at zero traverse, this was measured to be 32×10^6 in. -lb/radian. When the box clamps were added, this stiffness became 38.5×10^6, approximately 20% greater. A much larger increase occurred when the trunnion-to-trail struts were added; the stiffness rose to 55.5×10^6, a 73% increase. This was due not only to the direct load transfer from the trunnion to the trails but is also because the trails were straight back; in this position they contributed more rigidity to moments in the vertical plane. During traverse (20° left or right) the stiffness of the supporting structure dropped to 25×10^6 in. -lb/radian for the "as-designed" structure. This decrease is expected since the stiffness of one trail is almost completely lost in this configuration.

The trail stiffness (total, for both trails straight back) for a bending moment applied at the forward end resulted in 145×10^6 in. -lb/radian. In this case, the stiffness was lower than predicted by calculation, and is believed due to local deflections in the area of the trail hinge pins.

Measurement of the stiffness of the lower elevating screw supports illustrated an unanticipated result. The left support was nonlinear up to a load of 800 lb; at this load it assumed a relatively linear, load-deflection curve shape, with a slope of 3.5×10^5 lb/in. The right support had a linear stiffness of 3.5×10^5 lb/in. from zero load. This would indicate that unsymmetrical elevating system deflections would occur. This actually happened and can be seen in the experimental records in Appendix J.

The elevating rods with their upper brackets attached exhibited nonlinear load-deflection curves as assemblies. In this situation, the nonlinearities are due to either or both of the following reasons:

1. Clearances between the ball-nut and the ball bearings.
2. Nonlinear local deflections of the balls and ball-nut.

The clearances can cause nonlinearities because as more balls come into contact at higher loads, the stiffness increases until all the balls are in contact. The resulting stiffness curves are shown in Fig. H-12.

In addition to the static stiffness measurements, dynamic measurements were made of the supporting structure. As opposed to the

static measurements where the deflection is measured under a very slowly varying load, the dynamic stiffness is a measurement of the rms value of a sinusoidally varying force and the rms value of the displacement. (Maximum values also could have been used.) This, of course, varies with frequency.

A standard 600 lb electrodynamic vibration shaker was used to excite the launcher structure for the dynamic stiffness measurements. Figure H-2c shows the physical arrangement. The tipping assembly and elevating rods were removed and a relatively stiff bar was placed across the trunnions. The shaker was coupled to the bar with a dynamic force transducer which yielded the input force. Accelerometers were placed on the trunnions to yield the motion output; the dymamic stiffness, k_D, is simply,

$$k_D = \frac{F\omega^2}{a}$$

where

F = Measured, input force, rms (or peak),

ω = Input force frequency,

a = Measured, linear trunnion acceleration, rms (or peak).

Although the repeatability of the magnitude of the measurements was not good, the shape of the stiffness-frequency curve was the same for each of the two runs. The relative minimum values of this curve (Fig. H-11) correspond to resonance frequencies of the structure. The first mode frequency (the frequency at the first resonant point) of the entire supporting structure is near 70 cps. Since the firing frequency of a burst is slightly less than 3 rounds per second, we can be confident that an undesirable structural resonance will not occur. The recoil force itself could possibly contain variations at a frequency near 70 cps, however, previous experimental and calculated curves show that the magnitude of the recoil force does not have these high frequency variations. The result is that for this launcher, calculation of the first mode response should be sufficient to predict the response accurately.

A rough check of the magnitude of this frequency can be made, combining the measured, static stiffness with the result of a calculation of an equivalent structure inertia. The equivalent structure inertia was found by assuming that the structure and its equivalent both respond harmonically

in the static deflection shape of the actual structure. Imposing the conditions that the maximum deflection and kinetic energy of both systems are identical yields an equivalent inertia; for this structure it is 115 in.-lb-sec^2. The first mode frequency is found by treating the equivalent system as a 1-degree-of-freedom system. This frequency is:

$$f = \frac{1}{2\pi} \cdot \sqrt{\frac{k_s}{I_e}} = \frac{1}{2\pi} \cdot \sqrt{\frac{32 \times 10^6}{115}}$$

$$f = 84$$

where

k_s = measured static stiffness,

I_e = calculated equivalent inertia about the ball joint.

These two frequencies correspond sufficiently close when experimental errors and simplified calculations are considered. (The methods of determination of the values of stiffness of the launcher structural components are described more fully in Appendix H.)

B. Launcher Response Determination

The dynamic response (both displacement and velocity) of the launcher in the vertical plane to firing loads was obtained directly by instrumenting the launcher during a controlled firing program. The general procedure was to fire a two or three round burst for each structural condition, followed by two single shots. The reason six-round bursts were not necessary for each condition is that the response to rounds 3, 4, 5, and 6 do not differ appreciably from the second. The short test bursts, therefore, illustrated full burst conditions and the single shots provided a reasonable check on repeatability of the type of response. The firing program with the instrumentation and structural configurations listed for each test is shown in Table I-1. A list of the type and use of recorded data is as follows:

1. Strain adjacent to the firing pin (on the rear plate of the recoiling assembly), for a firing signal proportional to the boost charge,
2. Strain of the upper trail flanges near the forward pin connections to indicate the supporting structure rotation.

3. Cradle displacement, in the vertical plane, at the tip of the cradle. (Combined with similar trunnion motion, this furnishes cradle rotation).
4. Elevating rod strain to furnish the force in the rods,
5. Displacement of the trunnion, parallel and perpendicular to the cradle (some firings only),
6. Damper-support strain to furnish the damper force,
7. Recoil system pressure to indicate the recoil force.

The rotational response of the cradle and the trail strain (structure rotation) comprised the response data of primary significance. The cradle rotation was used as the primary indication of the effectiveness of a particular structural change in reducing dispersion. The trail strain formed an important quantity in correlating theory and experiment. The forcing functions in the form of rear plate strain and recoil system pressure were also necessary quantitites. (It should be mentioned that the trail strain measured is linearly proportional to the trail rotation only during positive rotation, the initial direction of deflection. This is because during negative rotation, the supporting structure rotates forward, the trail ends leave the ground and the strain is then a measurement of the trail inertial loads.)

Table 1 summarizes the launcher conditions during the various bursts which are discussed here. Except for the modifications listed, the launcher was as designed.

Table 1

Burst No.	Modifications to Launcher
B-2	None
B-5	Elevating system -- coil springs (total rate of 14,000 lb/in.) and little damping.
B-6	Elevating system -- coil springs and much damping.
B-7	Elevating system -- same as B-6, stiffened supporting structure.
B-8	Elevating system -- stiff rods and much damping, stiffened supporting structure.
B-9	Elevating system -- ring springs (self damping).
B-10	Elevating system -- coil spring (low boost charge, 720 fps muzzle velocity).

All the burst response curves are shown in Appendix J for each of the significant structural configurations. These response curves indicate that the structure, although theoretically symmetric about the vertical plane, has an unsymmetric response. The difference in stiffness between right and left elevating systems (as determined by measurements) is probably the major cause of this unsymmetrical response. Unsymmetrical supporting structure deflections were noted during the measurements also, but these were much smaller. These differences in response from one side of the launcher to the other increases the difficulty in analyzing these curves especially when comparing them to theoretical, planar response curves. Although these unsymmetrical deflections can increase dispersion, we will discuss the response curves as though they were identical.

In order to judge relative accuracy of these experimental response curves let us use a simple criterion. Since the recoiling assembly is relatively rigid in the plane of motion we are considering, its motion relative to the cradle due to its own flexibilities will be at a higher frequency and should damp out more quickly than the launcher response. Therefore, prior to each subsequent shot of a burst the only residual motion of significant magnitude is the gross launcher motion. The amount of residual gross launcher motion should then indicate the amount of dispersion, since if each round fires with identical initial conditions, the response of the launcher should be the same, neglecting recoil force variations due to weight changes.

Fig. J-5 shows the cradle rotation for burst B-5, fired with a softened and lightly damped elevating system. This burst had the greatest nonsymmetrical response in comparison to all the other firings. This could be due to additional nonsymmetry from the dampers. In discussing the general response, we will still neglect the difference in the curves. The cradle oscillation for this burst is a well damped response; the maximum slope of the response prior to the second shot is near 0.2 radians/sec. The time of shot ejection was not recorded; however, for maximum boost rounds (muzzle velocity of 1000 fps), this time is about 20 msec following ignition. The ignition time is marked, and we see that the slope or velocity is near zero. The trail strain, or supporting structure response in Fig. J-6 indicates some trail hop by the relatively high frequency oscillations about zero, immediately

following the large initial response. This response is also well damped. Fig. J-7 shows the cradle rotation for burst B-6 which had approximately 15 times more damping in the elevating system. As expected, the cradle response decays more rapidly, but not as much as was expected. The trail strain, Fig. J-8, still shows evidence of rebound of the structure. The maximum cradle velocity of the last oscillation prior to the second shot was reduced to 0.08 radians/sec. At the estimated time of shot ejection the cradle response is very unsymmetrical where one side has a positive velocity near 0.5 radians/sec and the other has a negative velocity near 0.08 radians/sec. Theoretically, the actual rotational velocity in the vertical plane is the average, however, since motion existed out of the plane, this number may be meaningless. The important fact is that the overall response damped out more quickly.

When the supporting structure was stiffened with the box clamps and trunnion to trail struts, burst B-7, the launcher response changed significantly. Fig. J-9 shows the cradle response and Fig. J-10 the corresponding trail strain. The cradle rotation essentially remained positive at all times as did the trail strain. In addition, the magnitude of the cradle rotation was significantly lower; the peak trail strain was slightly lower. The most important change, however, is the shape of the cradle response just prior to the second shot; the slope remains close to zero with only small variations. This indicates small cradle velocity and improved accuracy.

Another modification was made to the launcher by replacing the soft coil springs in the elevating rods by relatively rigid members in burst B-8. The dampers and supporting structure stiffeners were retained. The response of this system (Fig. J-11) was very similar to that of the previous one with possibly a small increase in the residual cradle oscillations. This would seem to indicate that elevating rod flexibility is not a significant parameter. Another possibility exists, however, and is more likely the situation. As indicated in the section describing the launcher, significant elevating system flexibilities occur from sources other than the rods themselves. For this reason, when the rods were stiffened, the system flexibility was not significantly changed. This is due to the fact that for a series system of flexibilities, the overall flexibility is always less than the smallest of the

component flexibilities. An interesting cradle response occurred during this burst (three rounds). The cradle rotation had a larger mean residual value between each of the succeeding rounds; in other words, the response had a tendency to climb. Although the cradle velocity was insignificant prior to each shot, the displacement was increasing. This leads to an undesirable effect upon accuracy.

Burst B-9, Fig. J-13 and J-14, shows the result of using ring springs in the elevating system; ring springs have inherent damping since their deflection is accompanied by sliding upon each other. These were designed to furnish near the maximum possible damping for the stiffness equivalent to the coil springs. Apparently, this amount is insufficient to furnish a good response.

The final firing of a modified launcher, burst B-10, consisted of a two-round burst with a zone 7 boost charge (muzzle velocity of 720 fps). The only change in the launcher structure was the addition of coil springs into the elevating system; a lower zone of boost ammunition was necessary to prevent bottoming of the springs. The cradle response (Fig. J-15) is very similar in shape to the response of burst B-5. The newer response has a generally lower magnitude because of the lower projectile boost. It is very interesting to note that the response is still very well damped even though no damping was added. This is pointed out again and discussed when the response of the unmodified launcher is discussed.

A very important characteristic of this launcher is illustrated in burst B-10, i.e., the variation in rate independent of the response. The second round fired at approximately 0.7 seconds after the first, compared to less than 0.6 seconds in the other bursts. Although the variation in this burst was later discovered to be caused by mechanical interference in the indexing cams, other changes can produce the same effect. For example, changing the bypass valve in the counterrecoil flow can vary the duration of counterrecoil and therefore the firing rate. Also, variations in recuperator preload (which is sensitive to ambient temperature) can also cause rate changes. The point is that a negative cradle velocity prior to ignition of the rounds such as in burst B-5, cannot be depended upon to decrease the value of the initial positive response following ignition. This is because firing time, relative to the cradle

oscillation, would be very difficult to control. The proposed alternative, sought here, is to reduce the cradle oscillations to a minimum and rely on consistency. This was implicit in the simple criterion previously stated.

One last point to be mentioned about the response of burst B-10 is the very slow initial rise time of the cradle on both shots. This is in comparison to all the other bursts. It is due mainly to the slower rise time of the recoil force for the smaller boost. The type of recoil system used has this characteristic feature.

We will now discuss how these response curves differ from those of the launcher in its as-designed condition. Fig. J-1 shows the cradle response during a 6-round burst, B-2. In comparison to the launcher with a more flexible elevating system, the response is similar in that the negative cradle rotation has appreciable magnitude; the residual oscillation, however, has a very small magnitude as well as negligible variation. (Because of the perfectly flat, residual response, the consideration of instrument error must be made. However, two other 6-round bursts yielded the same result.) It appears that the as-designed structural configuration, by the simple criterion set up, should produce the best burst accuracy. To a limited extent this is true, but there are two important considerations which must be mentioned. The first consideration is the reason why the as-designed structure responded the way it did. If we look at the corresponding trail strain curves (Fig. J-2 and J-3) we can see that because of the high frequency oscillation about zero, the rear of the trails must have lifted from the ground. This is due simply to the elastic rebound, or overshoot, of the structure caused by the recoil force characteristics. This means that the supporting structure rotated forward about the ball joint and compressed the two support buffers between the lower box and the firing base. The amount of trail hop is dependent upon the following quantities:

1. Shape and magnitude of the recoil force,
2. Drop off time of the recoil force relative to the natural period of the system.

Variations in the structural stiffness or the inertia of the launcher can alter the occurrence of hop. This was shown when the supporting structure was stiffened -- the hop was absent.

The second consideration is that while the supporting structure is tipped forward, the launcher can turn about a vertical axis through the ball joint. This allows the launcher to lose its aimed orientation and cause horizontal dispersion. Since a method exists to eliminate this rotation during hop (discussed in the next section), choice can be made to either eliminate the hop, by a stiffer carriage for example, or eliminate the rotation during hop. Either is an acceptable method to insure good horizontal dispersion. Other considerations may enter into a choice of whether or not trail hop should be eliminated, such as the safety of the crew.

C. Horizontal Dispersion

Early tests of the XM70E1 tipping parts indicated that horizontal dispersion was larger than vertical and followed a left-right-left sequence of impact points in burst firings. No analytical attack was made on the dispersion problem when it was first recognized because at that time no logical theory of the behavior could be constructed. In particular, the powder couple did not offer a logical explanation because it does not change direction after each shot.

A test program was planned to investigate the sequential horizontal dispersion. The weapon was prepared and the tests were conducted with the extensive cooperation of the Rock Island Arsenal. It was possible to conduct the tests on the force mount at Rock Island Arsenal because the dispersion evidenced itself with a high degree of repeatability during the proof tests of both Prototype No. 2 and Prototype No. 3.

The first group of tests showed that any round fired from a breech tube in the left cluster would fall 5 in. or more to the left of the vertical boresight line and that any round fired from the right would fall 5 in. or more to the right, at an 85-yd range, for all conditions tried. The boresight spot on the target coincided before and after each firing.

Instrumentation changes were made, and the weapon was prepared for a second series of tests. The tests showed no substantial improvement with slugs more accurately centered in the breech tubes or with disconnected igniter tubes, but some improvement was obtained with the clusters shimmed tight between the front and back plates. The instrumentation indicated that

the hub of the cluster being fired was not being properly loaded with the inertia force of the cluster.

Instrumentation changes were made, and the weapon was prepared for a third series of tests. These tests showed that a round could be fired accurately from either cluster if that cluster were drawn back tight against the back plate when the round was in the firing position. This was accomplished by preloading the cluster thrust bearing located in the back plate of the recoiling assembly framework. Indexing during firing was then impossible and was prevented by removing the indexing cam followers.

At this time, it was realized that the breech tube being fired was being driven back against the back plate and was carrying the connected cluster rearward with it. This resulted in the application of a large moment to the rear plate since the inertia force of the non-firing cluster was being applied at its thrust bearing.

A final series of tests was conducted with the breech tubes permitted a few thousandths of an inch axial movement in the retaining spiders. This allowed the tube being fired to move rearward without carrying its cluster with it. The horizontal dispersion was very substantially reduced. Several 6-rd bursts at zone 10 (1000 fps muzzle velocity) were fired through targets at 85-yd range. The target pattern was nearly rectangular with overall dimensions of approximately 5 in. vertical by 10 in. horizontal.

The remaining horizontal dispersion is still sequential. Calculations show that because the breech tube being fired is driven rearward primarily by the powder-gas pressure acting on a belled portion at the front of the tube, its mass is lost from the cluster assembly and the loss of that mass then produces the sequential horizontal dispersion. Figure 6 and 7 show schematically how the cluster inertia forces are distributed throughout the recoiling framework.

A series of firing tests[1/] was conducted with Prototype No. 3 during September and October, 1960 at Redstone Arsenal to determine the effect of increased rigidity between the front and rear plates (i.e. rigidity

---

1/ Armour Research Foundation Report 8130-20, P. II-4.

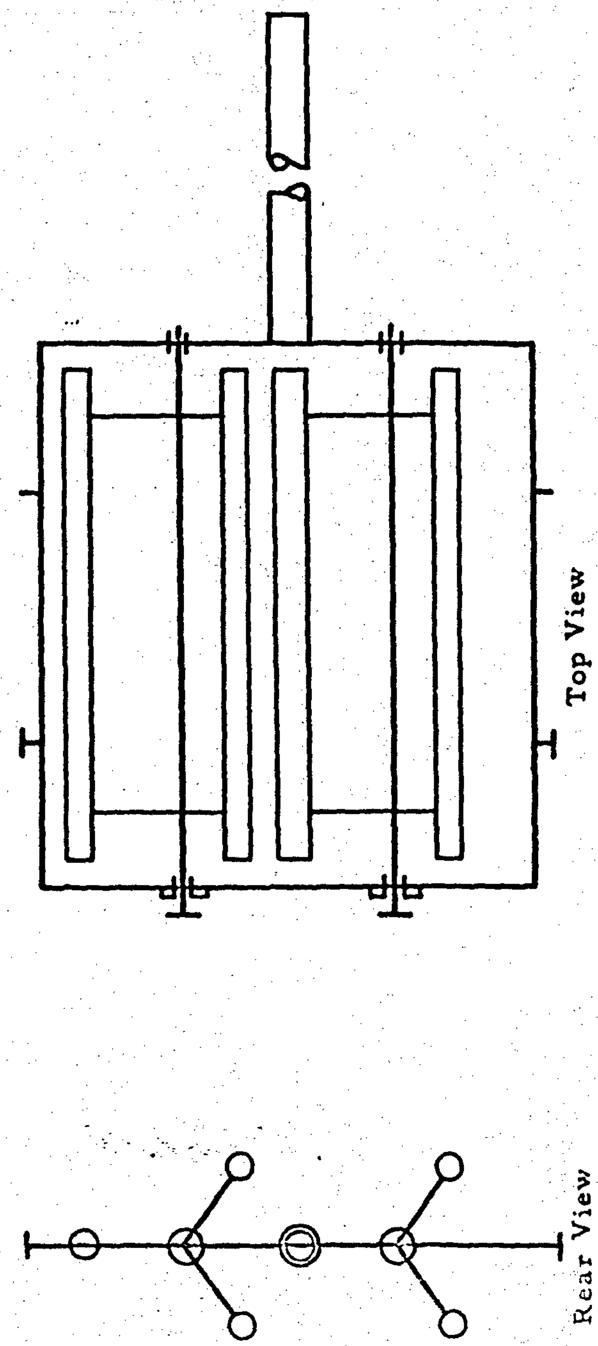

Fig. 5 SCHEMATIC OF RECOILING ASSEMBLY

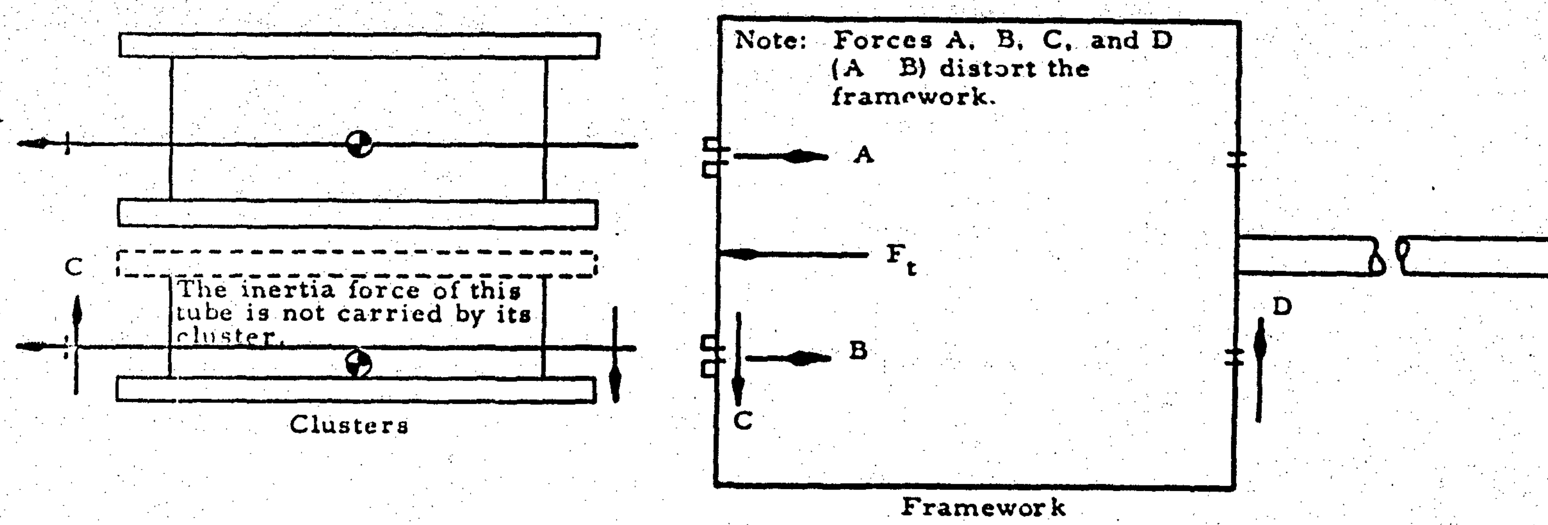

Fig. 7 REACTIONS BETWEEN CLUSTERS AND FRAMEWORK

of the recoiling assembly framework) on the sequential horizontal dispersion.

A calculation showed that sequential horizontal dispersion would be very small if the recoiling assembly framework was very rigid. The problem then was to find a lightweight structure that would greatly increase the stiffness of the framework. It was decided that the most efficient structure would be a thin metal skin or shell enclosing the entire framework.

The firing program was set up to fire 6-round bursts with and without the shell. To measure shell effectiveness, two quantities were recorded: (1) the bending strain of the firing tube near its base in the horizontal plane, and (2) the target patterns. Six bursts were fired, three with and three without the shell. (The launcher also contained additional stiffening fixtures used in the previous Fort Sheridan firings, consisting of carriage clamps at the front and rear corners of the box sections, trunnion-to-trail struts.)

The records of bending strain in the firing tube without the shell exhibited the alternating direction of initial bending moment. With the shell, the initial direction of the bending moment was consistently in one direction, which can be logically explained by the rifling torque; see Fig. 8. The target patterns, however, did not show any reduction in horizontal dispersion. It was decided that the rigid body rotation of the launcher, due to the trail pads shifting along the ground, was hindering the effectiveness of the shell.

A portion of the test was thus repeated in an attempt to obtain less horizontal dispersion. This time the trails were restrained from rotating about the ball joint in the plane of the ground by placing a pinned connection between a stake and a trail on each side of the launcher. This permitted small rearward and upward trail motions. In this condition, four 6-round bursts were fired, two with and two without the shell. The resulting target patterns are shown in Fig. 9. The two bursts with the shell are rounds No. 93 - 98 and 99 - 104; the two bursts without the shell are No. 106 - 111 and 112 - 117. The firings with the shell had a total horizontal dispersion of approximately 1.5 and 1.9 mils, while the two without the shell had a total horizontal dispersion of 3.7 and 2.9 mils. Because of the single-hole targets, it is impossible to calculate the standard deviation, but it can be inferred

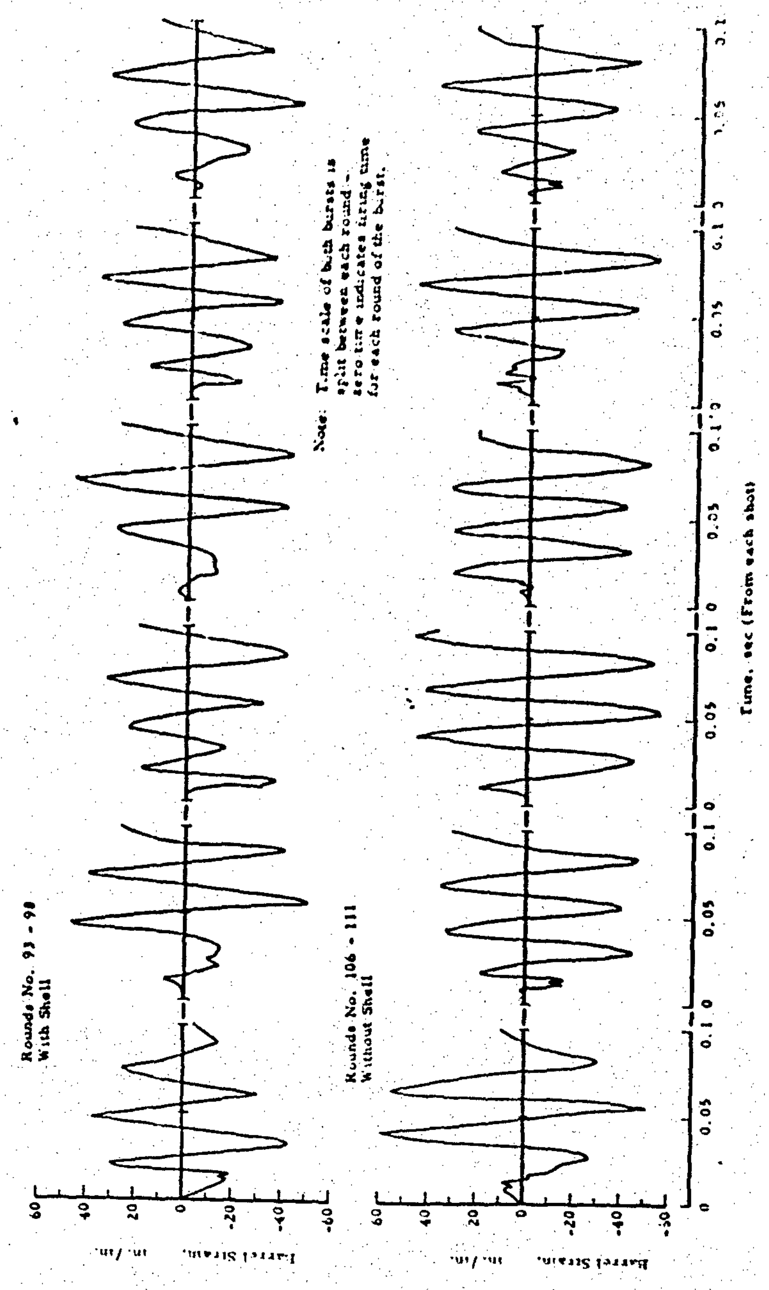

Fig. 8 BARREL STRAIN

Fig. 9 TARGET PATTERNS

that, for the two bursts with the shell, the standard deviation is less than 1 mil.

The results of these tests indicate that the shell offers a reduction of horizontal dispersion of nearly 100%. (The trial ties showed a reduction of 200 to 300%.) The reliability or consistency is fairly satisfactory since these targets represent four consecutive bursts fired from Prototype No. 3 under identical conditions. But in order to obtain these results, it must be emphasized that the trails were restrained from rotating about a vertical axis through the ball joint.

IV. THEORETICAL ANALYSES

The theoretical analyses of the launcher dynamics consist of two specific mathematical models to determine launcher motion, and three supplemental studies which used very simple dynamic models in order to directly study the effects of certain parameter variations. The two models which were developed to calculate the launcher motion are:

1. A planar, nonlinear, 3-degree-of-freedom system,
2. A three-dimensional, nonlinear, n-degree-of-freedom system.

The three supplemental studies include:

1. A linear, 2-degree-of-freedom analysis to study the effectiveness of various locations for auxiliary damper locations,
2. A third-order, linear single-degree-of-freedom model to determine optimum elevating system structural parameters.
3. A linear, second-order system to determine the parameters which bring about an optimum response decay.

The derivation, assumptions, and some results of these models and studies are presented in the appendices; a discussion of their development, applications and results are presented in this section.

The derivation and discussion of a mathematical accuracy criterion is also included in this section. This criterion is based upon the sensitivity of the rocket to the different launcher motions studied in the mathematical models.

A. Planar, Nonlinear, 3-Degree-of-Freedom Model

Prior to the initiation of this Long-Range Study Program, some dynamic studies were conducted which aided the formulation of this model. One study, in particular, was a similar, planar, 3-degree-of-freedom model with the following degrees of freedom:

1. Rigid body rotation of the launcher about the trail ends; base hop,
2. Recoil motion,
3. Elastically restrained rotation about the ball joint.

The last type of motion was assumed to the first mode response of the relatively flexible supporting structure, with a rigid tipping mass and rigid elevating system.

Subsequent experience, both from the use of the above model and from actual launcher firings, provided valuable information for making assumptions for the new model. For example, instrumented firings and the output of the above model both showed that rotation about the trail ends was very small. It was therefore neglected in the new model. Recoil motion calculated in the above model agreed fairly well with experiment except during counterrecoil. The difference was traced to seal friction and indexing forces. The former results in longer counterrecoil durations, while the latter brings about two changes. Indexing forces cause small changes in the recoil motion but more important, they significantly affect the cradle response. Consequently, they were both included in the new model. Inability to obtain a good correlation of the experimental response with the output of the prior model led to the conclusion that the elevating system was flexible. Again, this flexibility was therefore included. The assumption of the first mode response of the supporting structure was supported by previous experimental firings, and was reconfirmed with the dynamic analysis described earlier; this assumption was retained. The three degrees of freedom of the model developed on this program correspond to:

1. Elastically restrained rotation of the supporting structure about the ball joint, φ_1.
2. Recoil motion relative to the cradle, u,
3. Rotation of the tipping parts about the trunnion relative to the supporting structure, φ_2.

The last motion is a consequence of the flexible elevating system. Although no auxiliary damping in the elevating system was included in the as-designed launcher, linear damping terms were placed in the equations for dampers in parallel with the elevating rods and also a damper between the lower box and the ground.

The frictional forces were added in the form of a constant frictional force due to the preload plus a term proportional to the recoil pressure. This corresponds to the type of seals employed. The equation of motion of the recoiling mass in the u direction also includes terms representing the constant-force, constant-stopping distance recoil system used in the launcher.

The final equations of motion consisted of three, second-order, nonlinear differential equations. In order to solve these without making any restrictive, simplifying assumptions, they were programmed for ARF's Univac 1105 in the Univac Scientific Exchange (USE) language. This program is described in Appendix D. Solution of the three, second-order differential equations was effected by using the Runge-Kutta numerical integration technique. Launcher parameters such as damping, stiffness, recoil rod shape, initial boost charge force, etc. were all included as input data; a sample output sheet is shown in Fig. D-2.

The purpose of the computer solutions of launcher motion can be grouped into three divisions by considering their purpose. The first group of solutions was aimed at matching the experimental launcher response. The second was to verify the existence of an optimum response and determine the optimum parameters. (This is described later when the optimum system is discussed.) The final group of computer runs was to show the results of various changes, e.g., low zone response, efforts of elevation changes, and delayed recoil.

1. Correlation of Theory with Experiment

The success of correlation between computed and experimental response curves varied and depended upon launcher parameters; in general the agreement was better when less negative carriage rotation occurred. The difficulty was due to the fact that the original model did not represent the nonlinear stiffness and damping displayed by the launcher supporting structure. This was subsequently corrected and closer correlation obtained, though not entirely satisfactory.

Figures 10 through 21 show typical information obtained from the computer program. Figure 18 shows a full burst response. The numerical input corresponded to either measured or calculated values of physical parameters of Prototype No. 3 Launcher. Certain parameters were varied, however, to obtain the correlation. All of the parameters not designated on the curves are listed on the computer program in Appendix D.

The two curves shown superimposed in Fig. 23 are the cradle response from Fig. 15 and the experimental cradle response from firing

R-38, listed in Table I-1. This experimental response was from a single shot with identical launcher conditions to burst B-8, Fig. J-11. The supporting structure stiffness measured for this condition was 5.5×10^7 in.-lb/radian. The numerical value of carriage stiffness used in the computer program was 4.5×10^7 in.-lb/radian and is significantly lower. The fact that this lower value was necessary to match the experimental response is probably due to the flexibility added to the system by the soil in the actual firing. (The structural stiffness measurements were made on concrete.) The measured elevating system stiffness for shot R-38 was approximately 4.5×10^5 compared to 1.4×10^4 used in the computer. The difference, though very large, is probably due to the unmeasured elevating system flexibilities discussed earlier. (Burst B-7 had an elevating system stiffness of 1.4×10^4 lb/in. but had a very similar response to burst B-8, even though the latter supposedly had a much stiffer elevating system. This further supports the conclusion that the high, measured stiffness value is not correct.)

A further comparison can be made between the computed carriage rotation (Fig. 13) and the trail strain from burst B-8, Fig. J-11. These curves agree in less detail, but their main characteristics are the same. The computed curve is generally smoother since it does not contain any higher mode response characteristics.

Figures 26 and 27 show experimentally obtained strain from the elevating screw and damper supports. These curves are tensile and compressive strain in circular, pinned rods and are directly proportional to the forces. They compare reasonably well with the spring force and damper force shown in Fig. 18 and 19 respectively.

Because of the similarity of the response of burst B-7 and B-8, we see that the computed response also agrees reasonably well with B-7. In this case the actual launcher had an elevating stiffness of 1.4×10^4. Burst B-6, Fig. J-7, reveals a large negative dip after the initial positive displacement, which did not occur in burst B-7 or B-8. The only difference is that B-6 did not have a stiffened supporting structure. Reduction of only the supporting structure stiffness in the computer model produced the response in Fig. 24. The expected correspondence does not occur; the cradle response remains essentially positive. The negative supporting structure response, however, doubled compared to the previous theoretical response which indi-

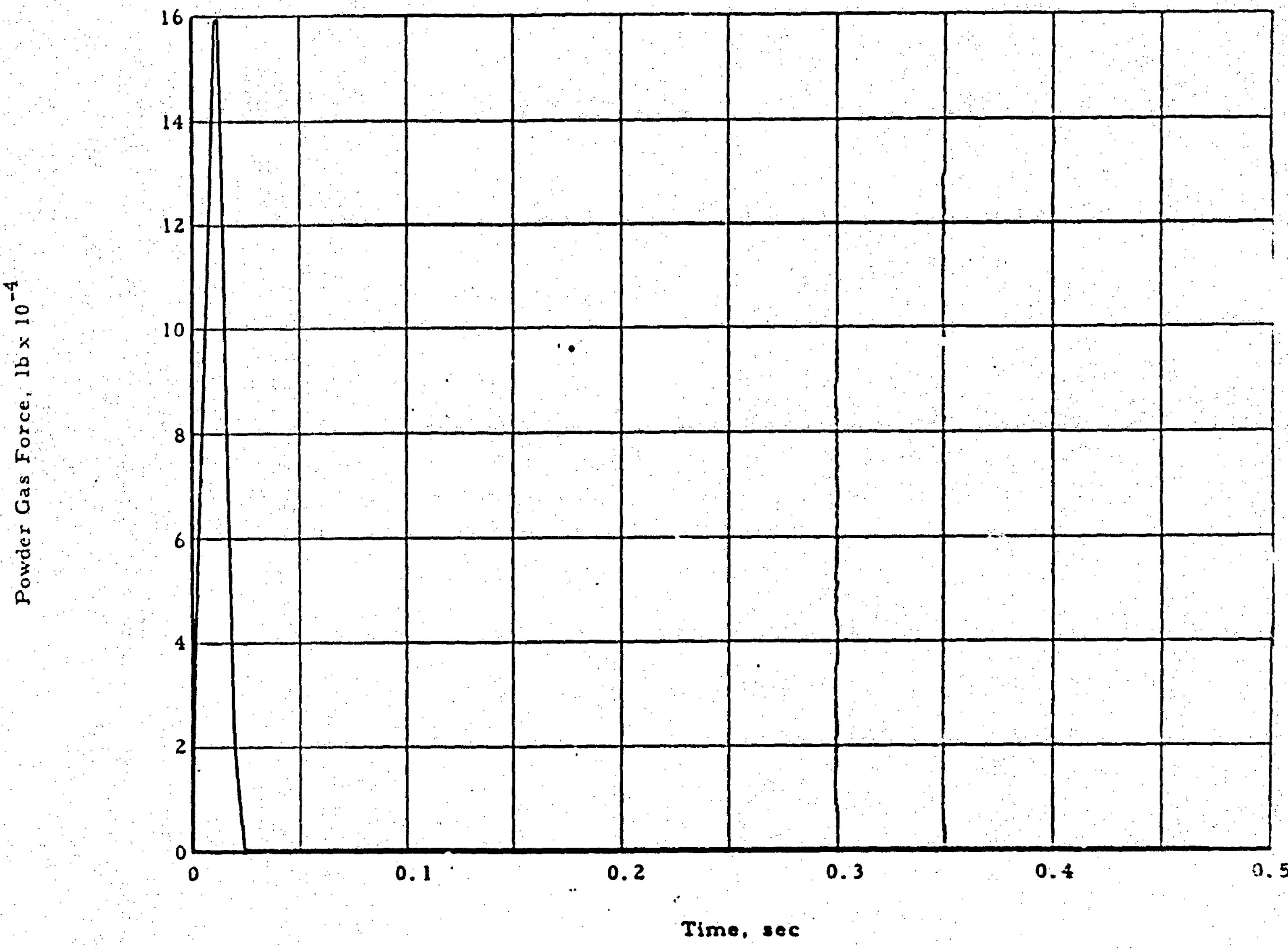

Fig. 10 TYPICAL COMPUTER SOLUTION -- POWDER GAS FORCE

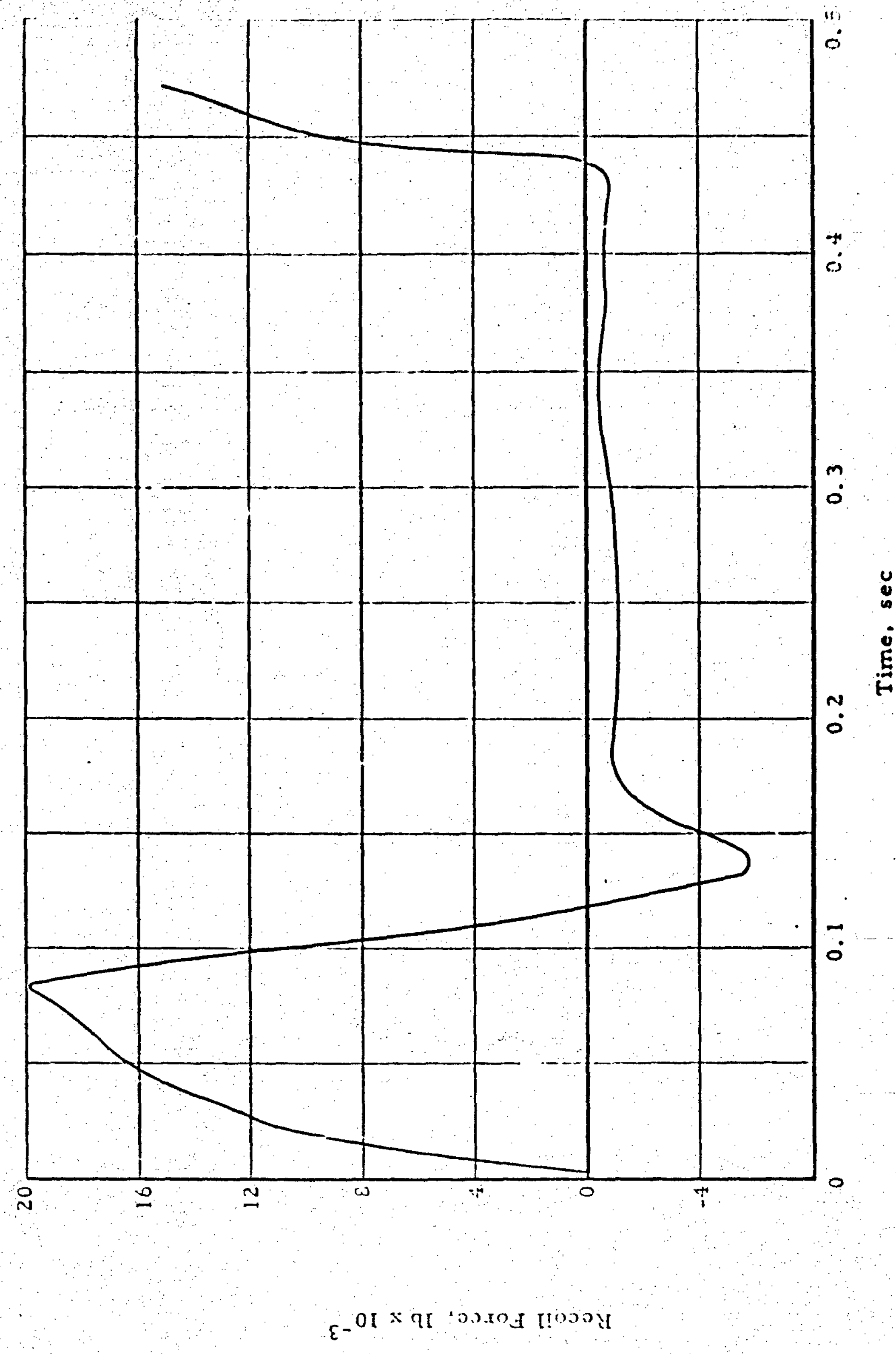

Fig. 11 TYPICAL COMPUTER SOLUTION -- RECOIL FORCE

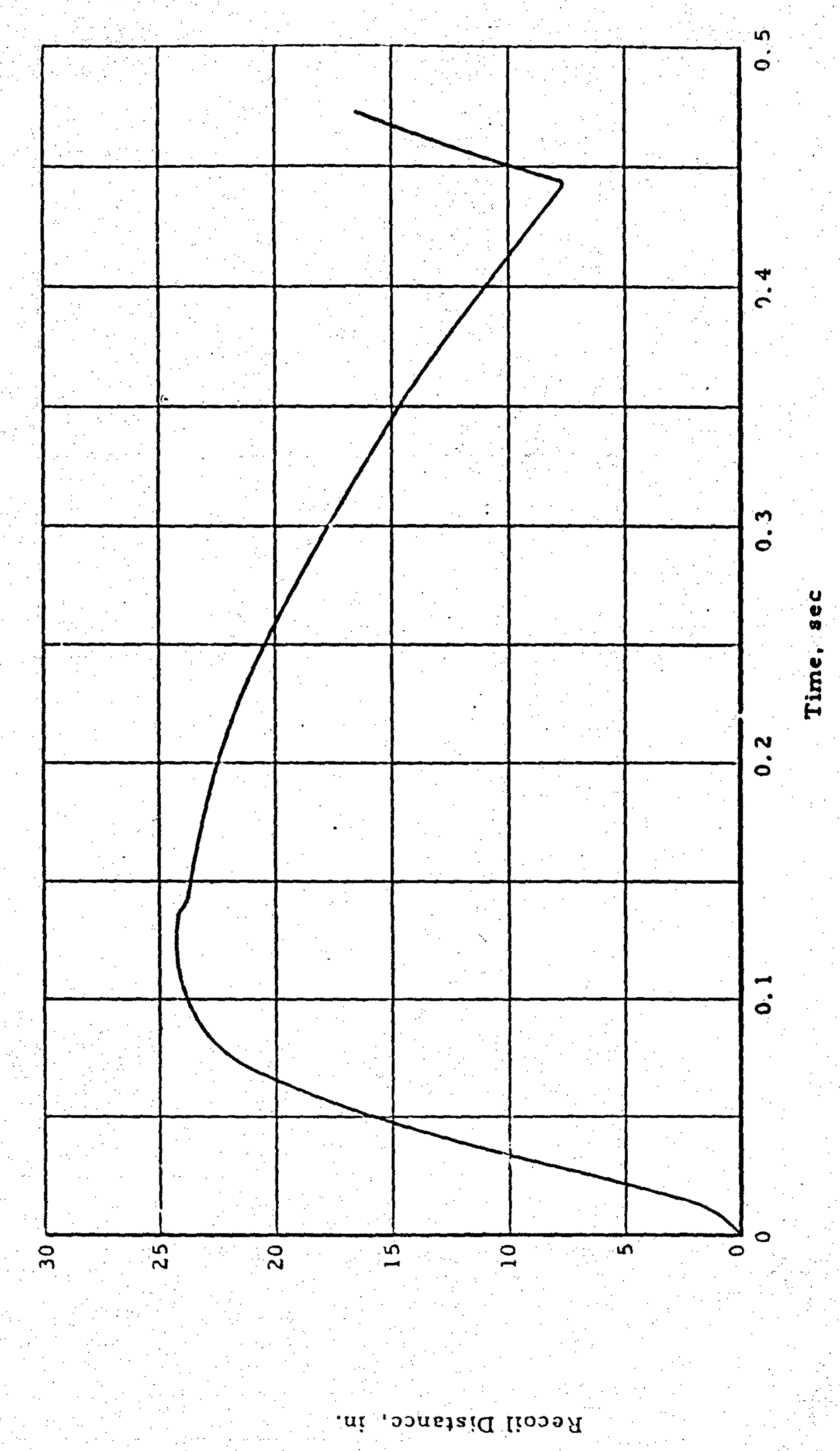

Fig. 12 TYPICAL COMPUTER SOLUTION -- RECOIL DISPLACEMENT

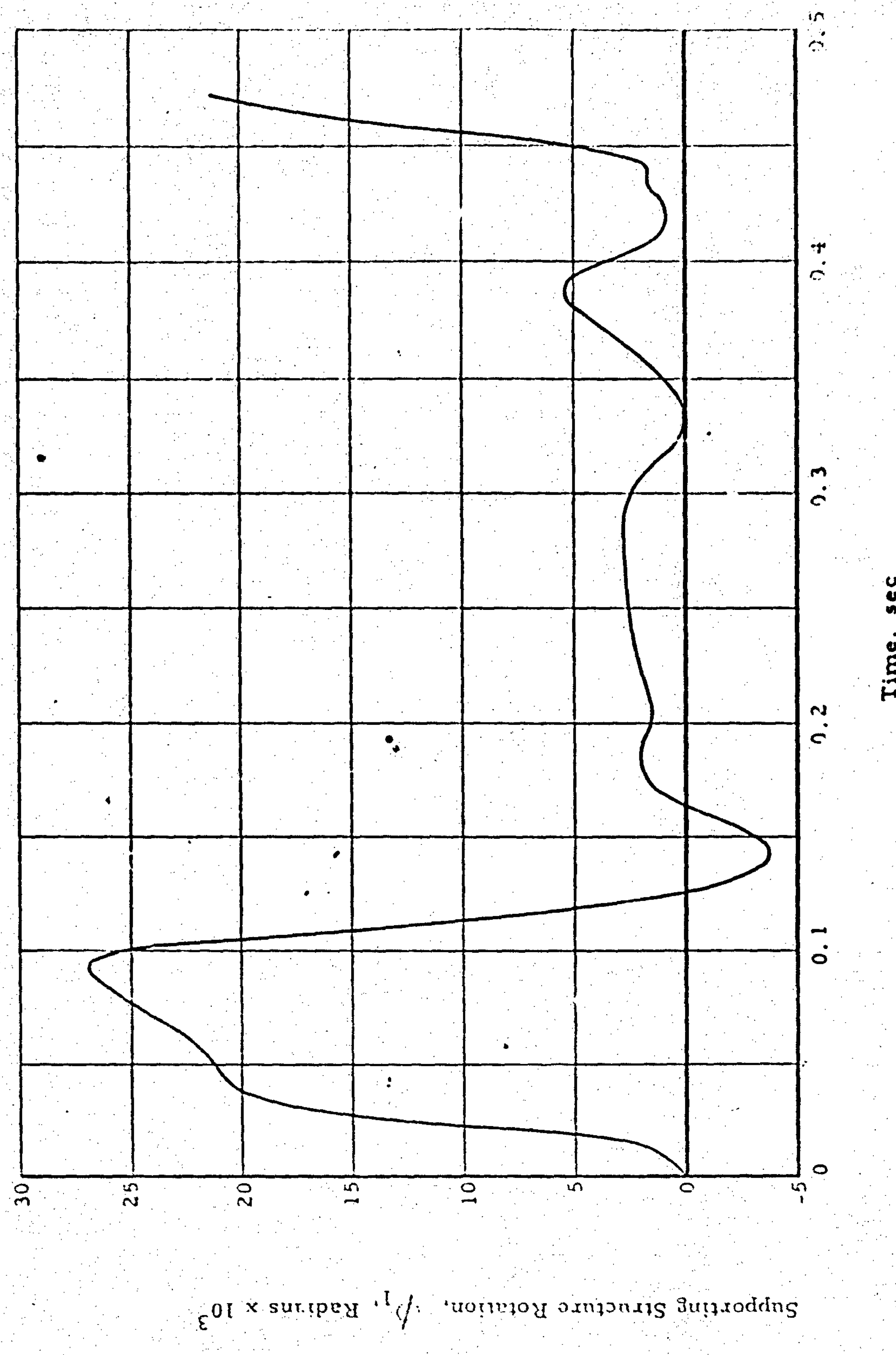

Fig. 13 TYPICAL COMPUTER SOLUTION -- CARRIAGE ROTATION

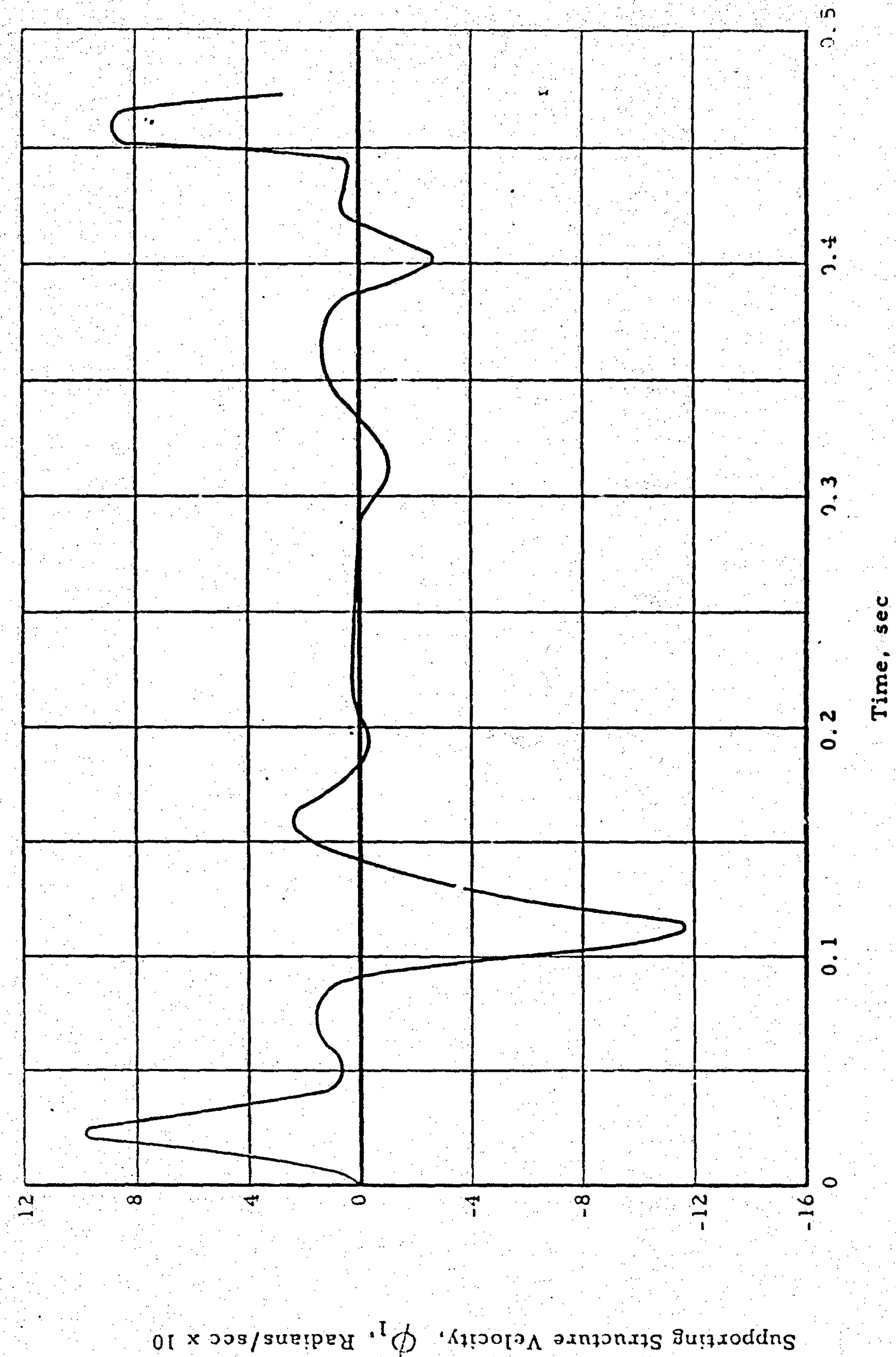

Fig. 14 TYPICAL COMPUTER SOLUTION -- CARRIAGE ROTATIONAL VELOCITY

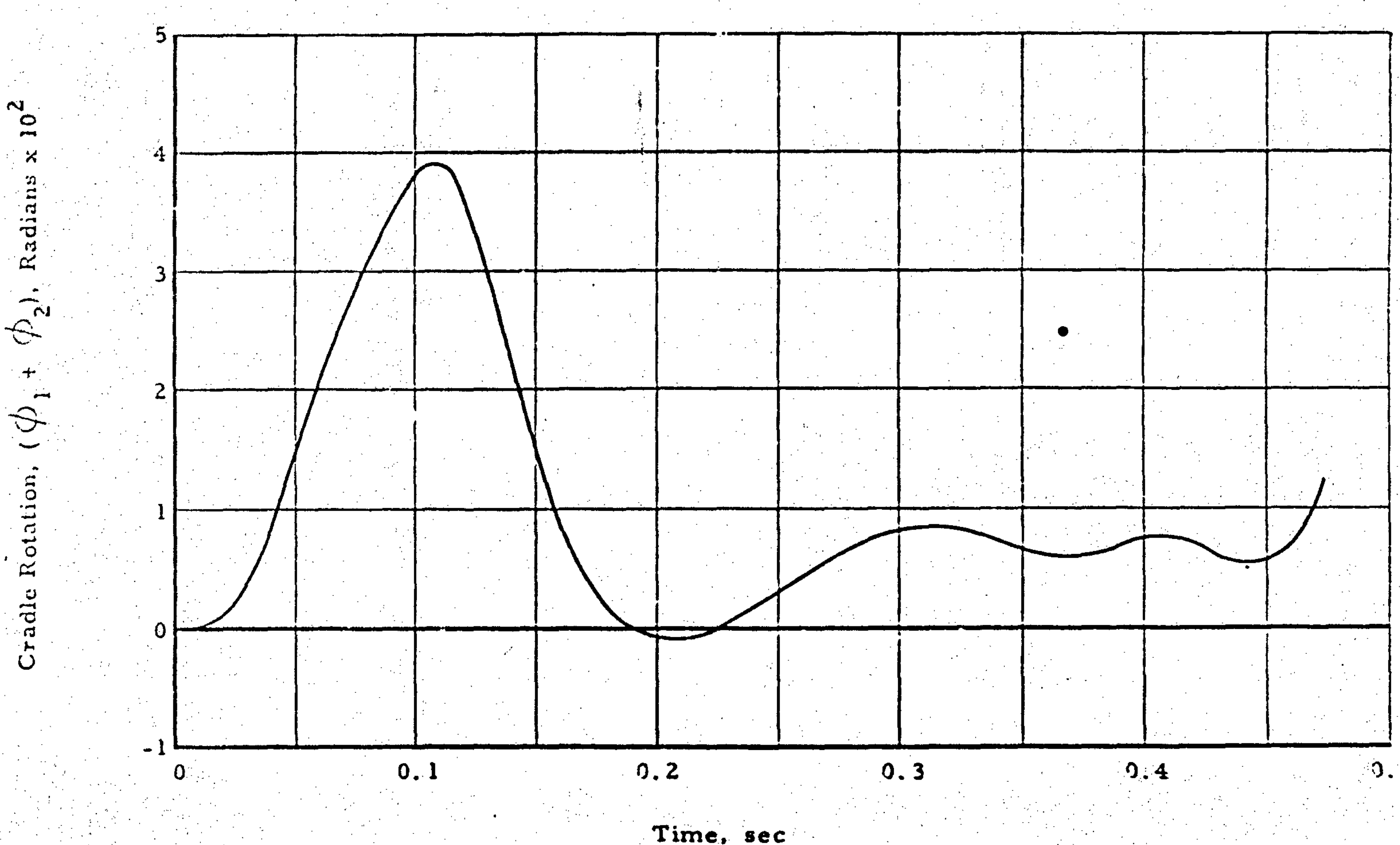

Fig. 15 TYPICAL COMPUTER SOLUTION -- CRADLE ROTATION

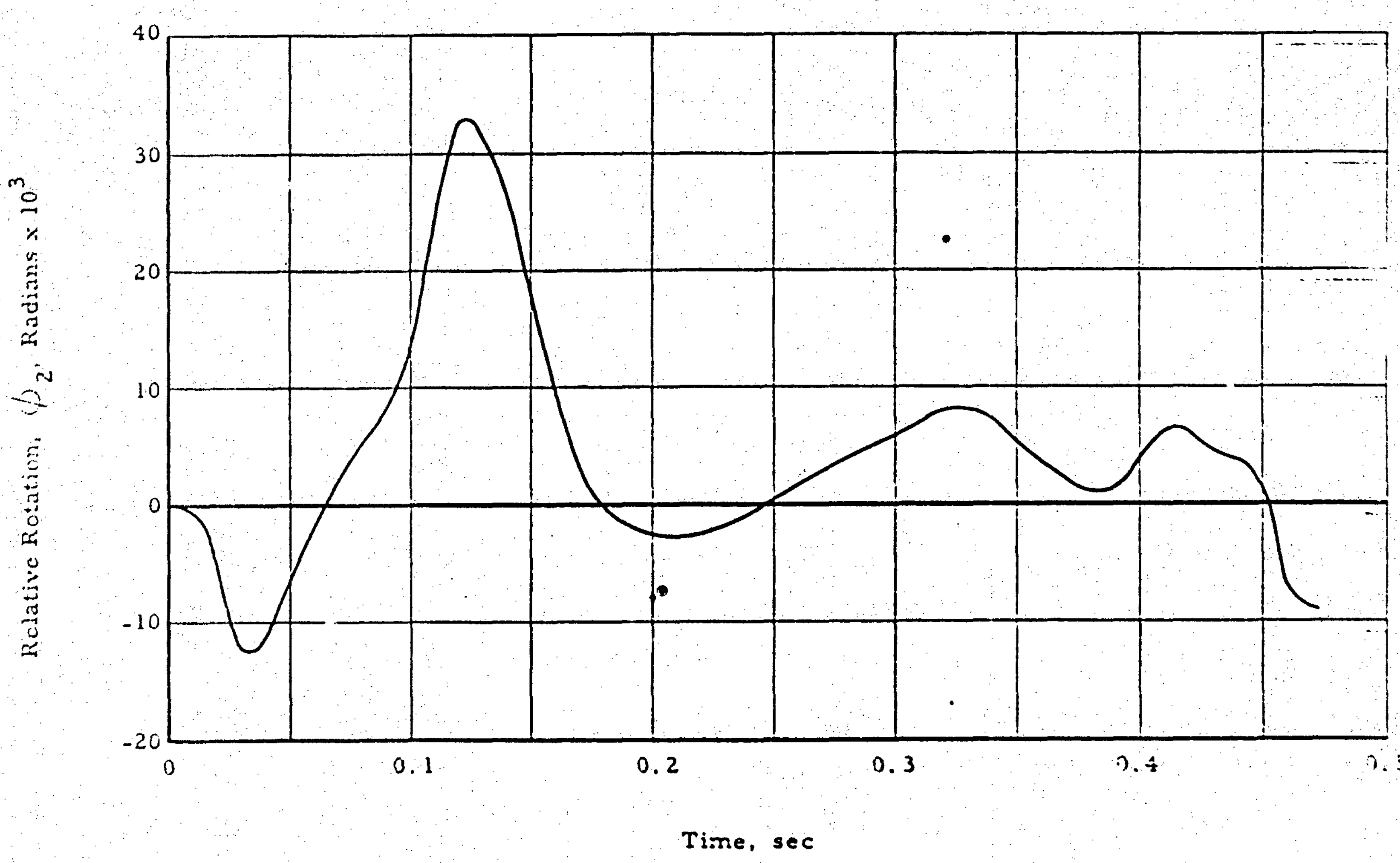

Fig. 16 TYPICAL COMPUTER SOLUTION -- CRADLE-CARRIAGE RELATIVE ROTATION

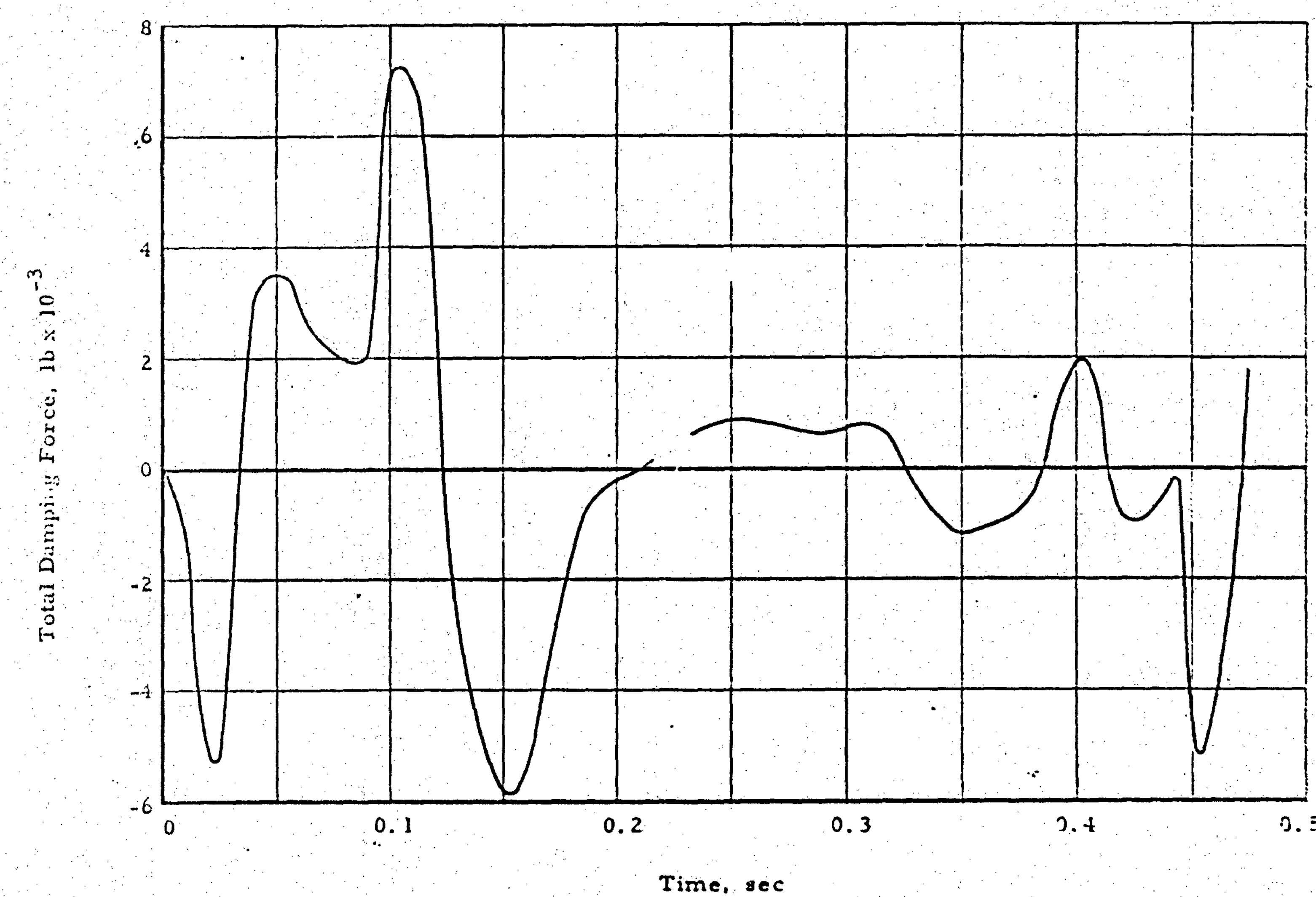

Fig. 17 TYPICAL COMPUTER SOLUTION -- CRADLE-CARRIAGE RELATIVE ROTATIONAL VELOCITY

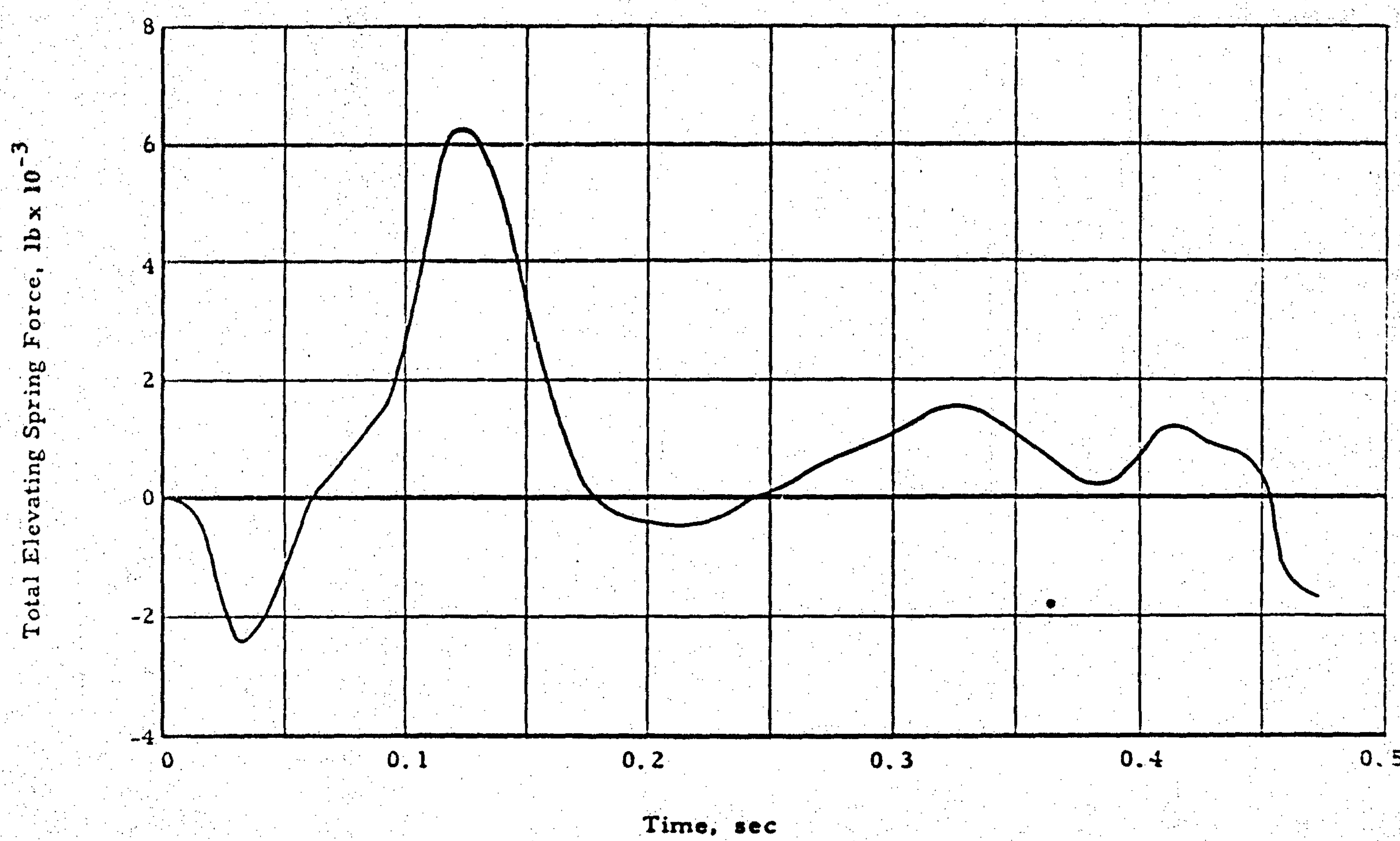

Fig. 18 TYPICAL COMPUTER SOLUTION -- ELEVATING SYSTEM SPRING FORCE

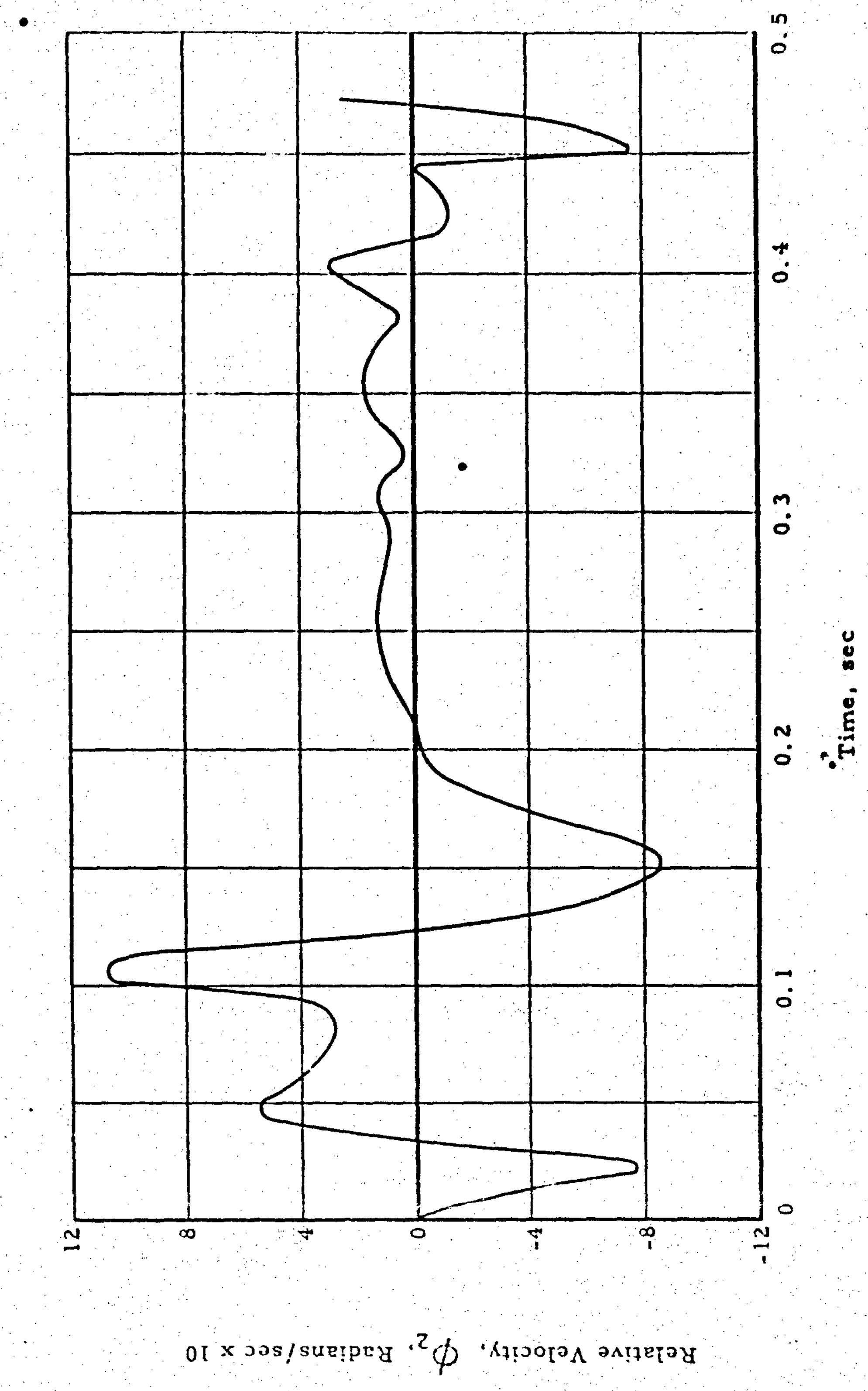

Fig. 19 TYPICAL COMPUTER SOLUTION -- ELEVATING SYSTEM DAMPER FORCE

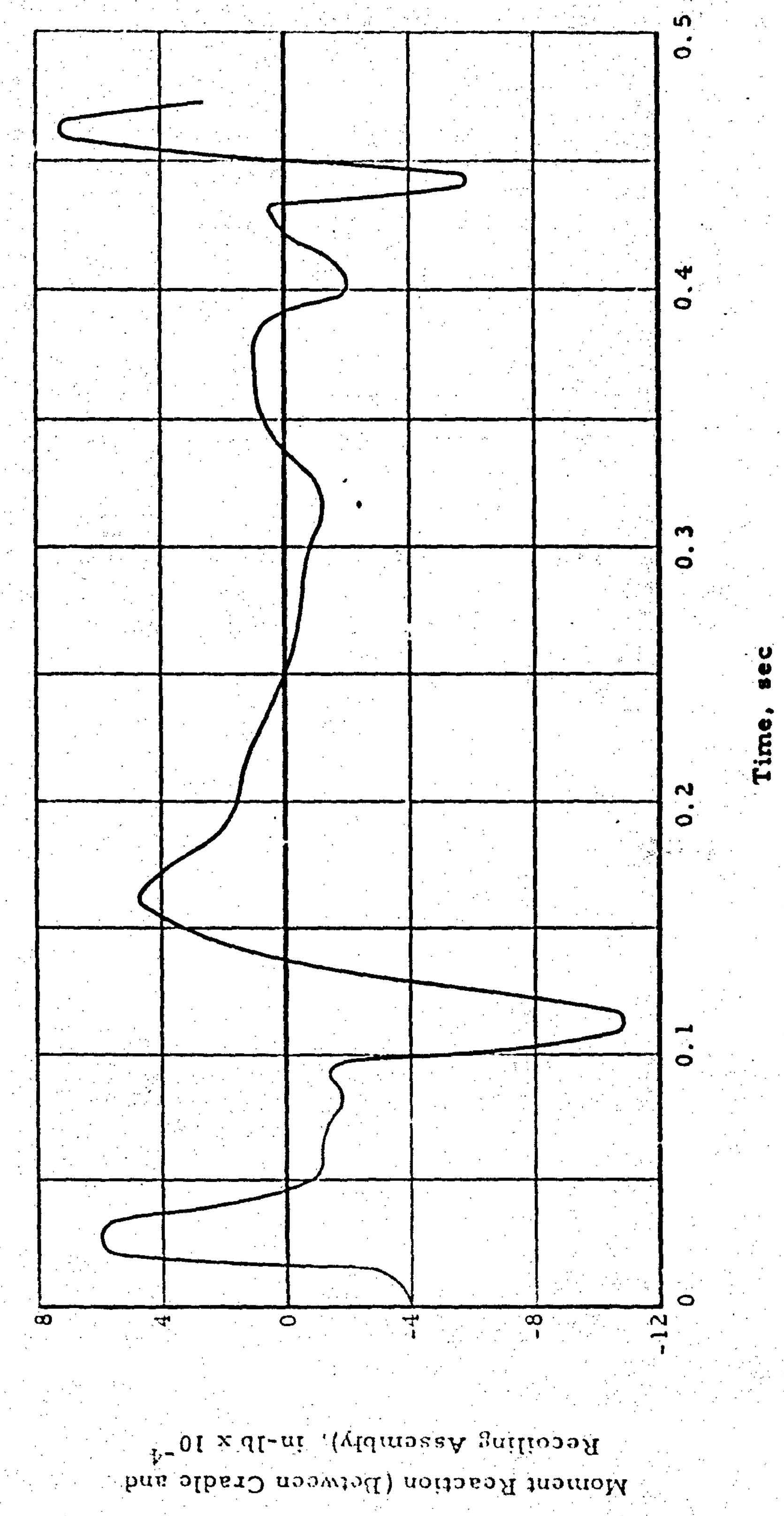

Fig. 20 TYPICAL COMPUTER SOLUTION -- RECOILING ASSEMBLY - CRADLE MOMENT REACTION

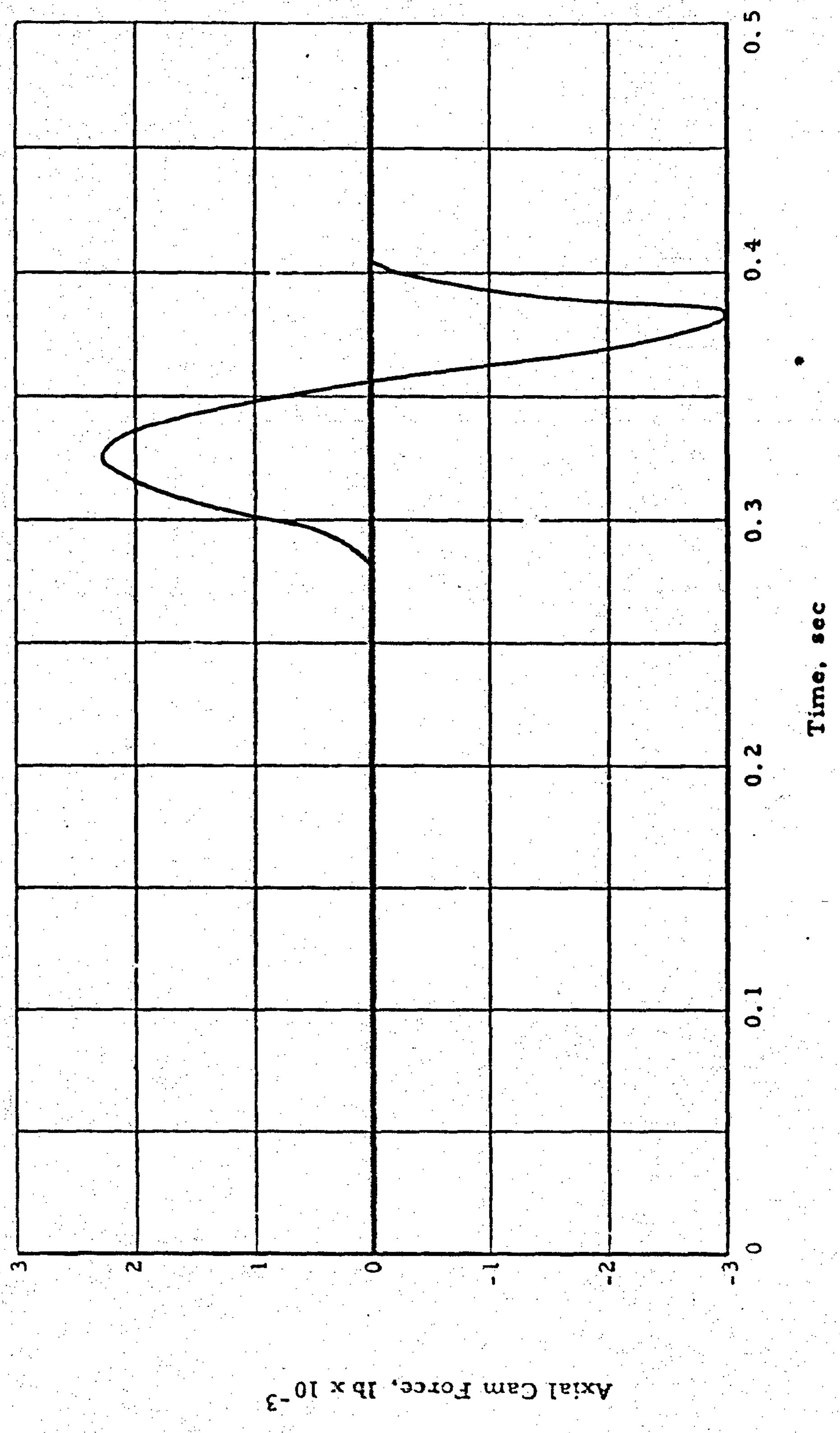

Fig. 21 TYPICAL COMPUTER SOLUTION -- AXIAL CAM FORCE

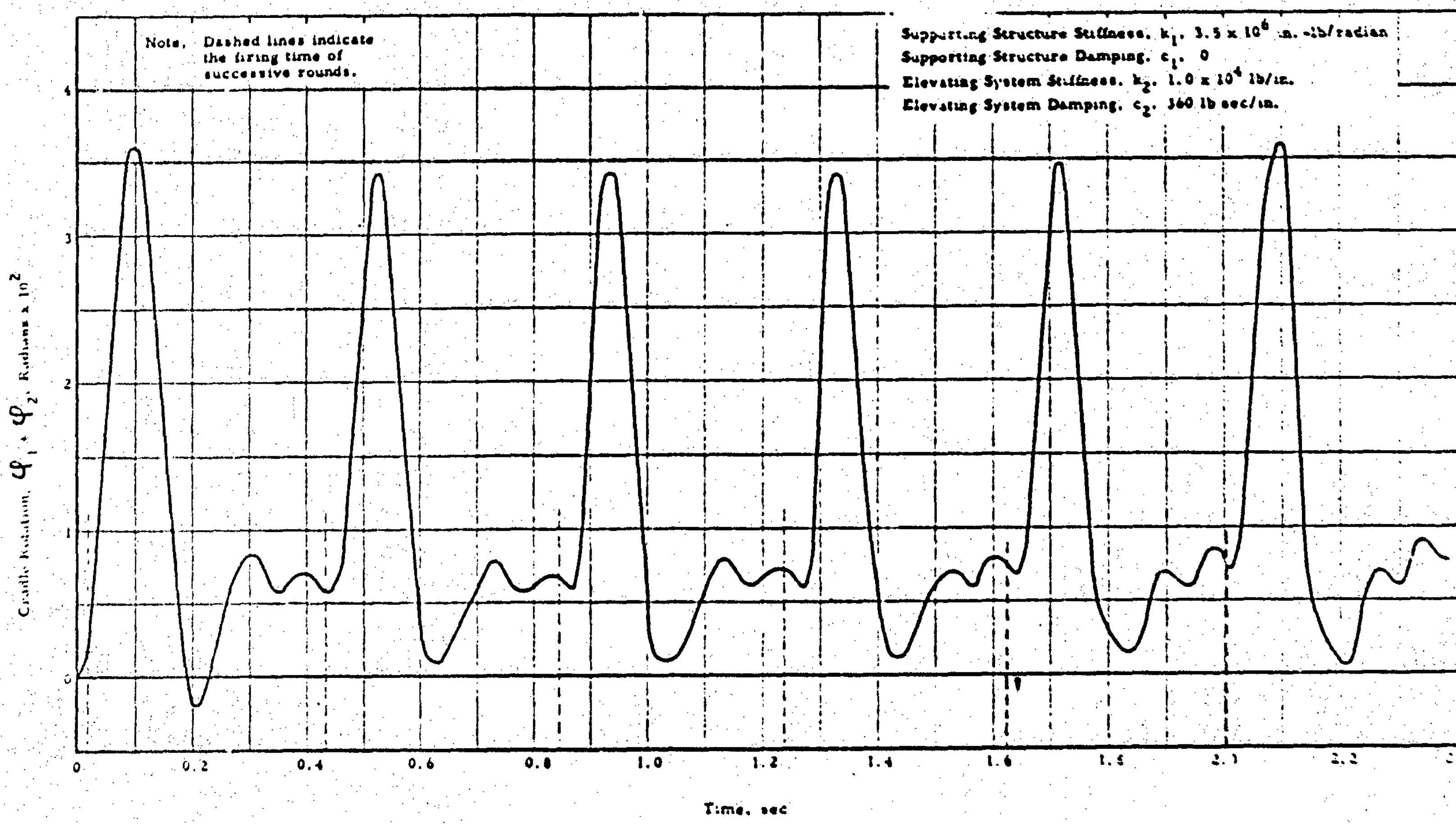

Fig. 22 TYPICAL COMPUTER SOLUTION -- CRADLE ROTATION, 6-RD BURST

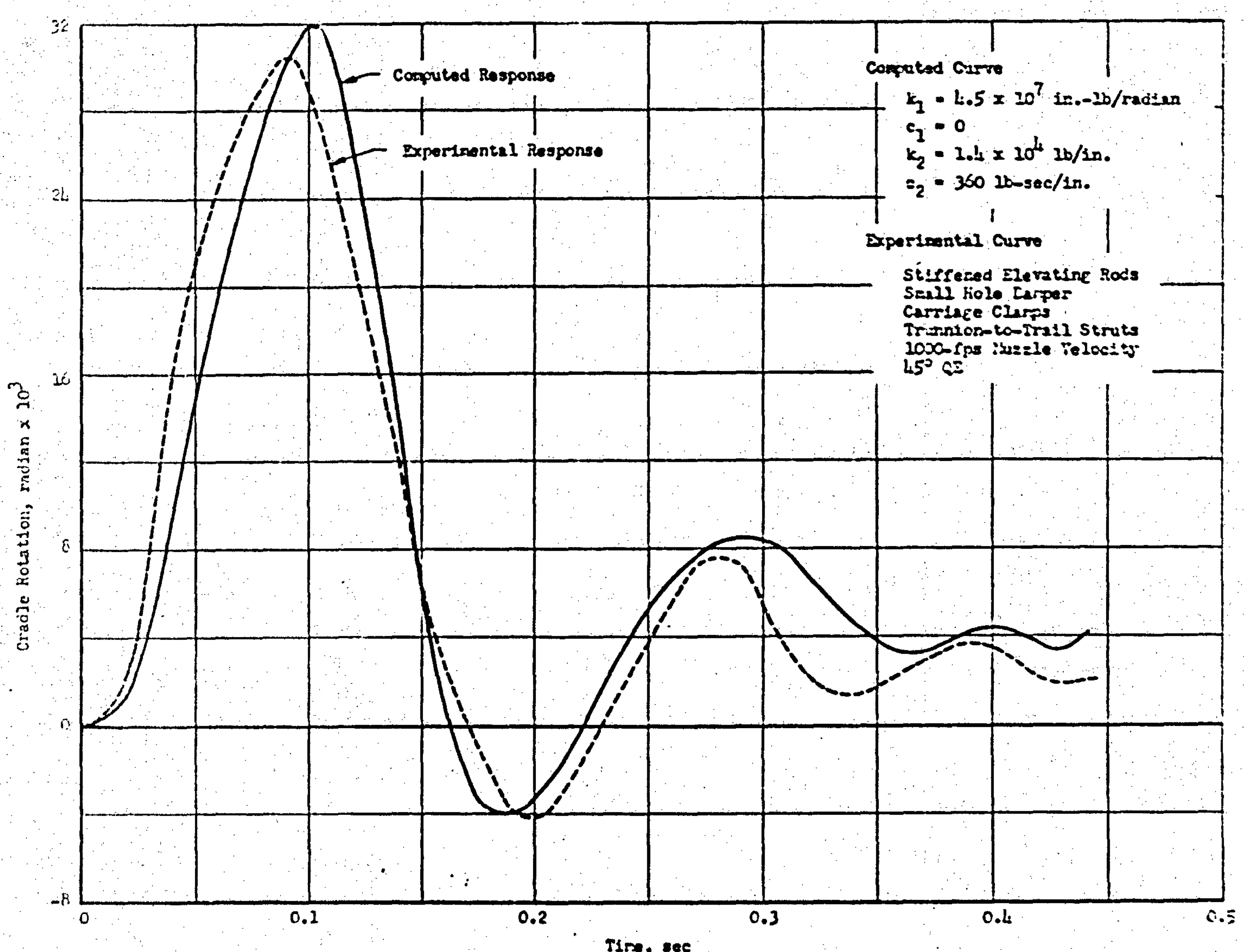

Fig. 23 COMPARISON OF COMPUTED AND EXPERIMENTAL RESPONSE CURVES

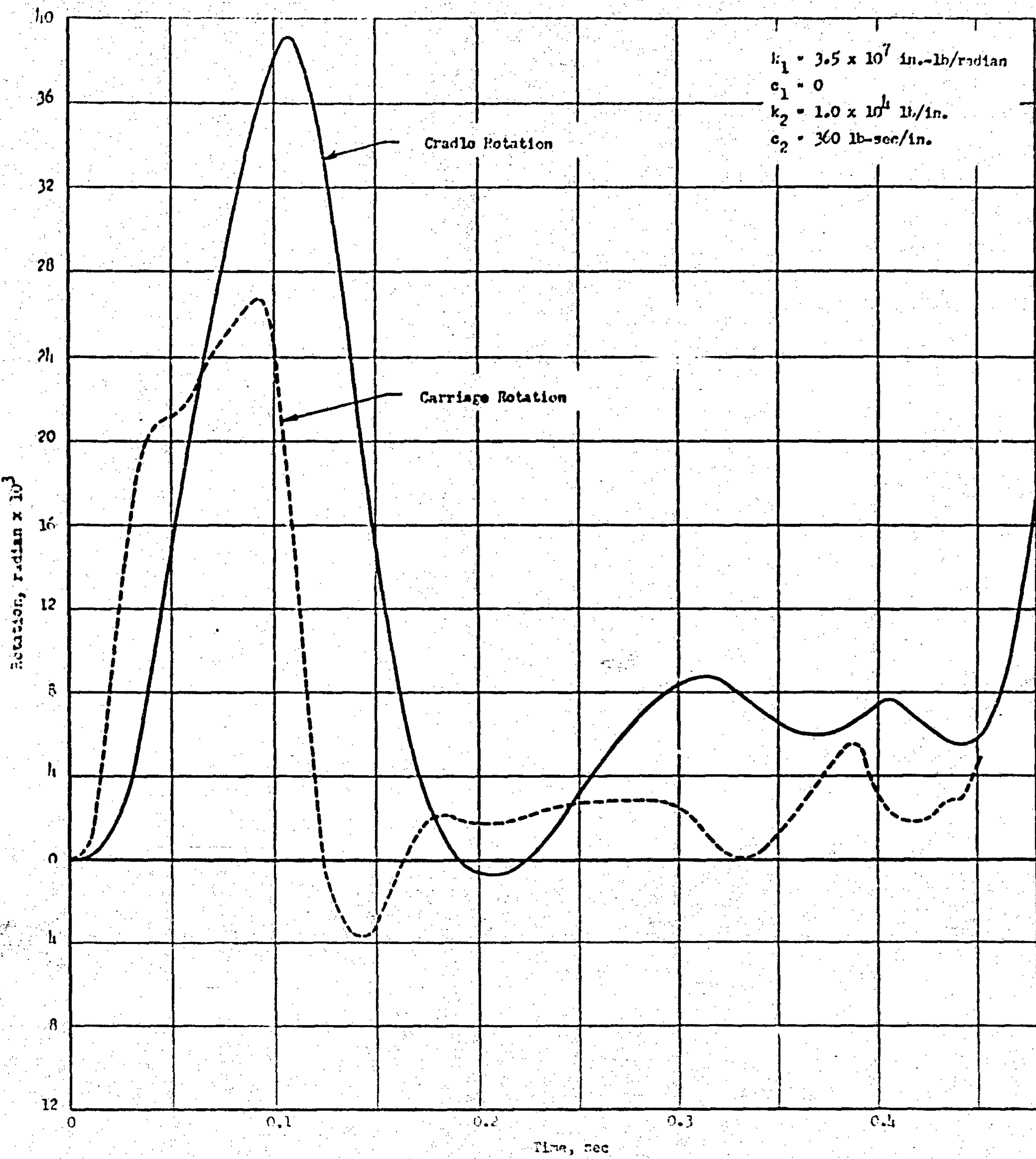

Fig. 24 THEORETICAL RESPONSE WITH REDUCED STRUCTURAL STIFFNESS

cates that the nonlinear negative supporting structure characteristics are very significant here. To investigate the effects of a bilinear stiffness the computer program was modified. Figure 25 shows the cradle response using a bilinear supporting structure stiffness. Although the agreement is much better, it could probably be improved with slightly different values of stiffness and also the additional simulation of a bilinear damping coefficient. The effect of these nonlinearities has been demonstrated, however, even though perfect correlation was not obtained.

2. Effects of Elevation Changes

It was important to investigate the effects of elevation changes upon the response of the launcher. This was done easily, because the elevation was an input to the computer program. Figures 28 and 29 show the cradle response of the launcher with structural parameters identical to those in the previously computed curves. These responses are at 20° and 60° elevation, respectively. (The previous ones were at (45°). There are some definite changes in the details of the response, especially at the time immediately following the ignition of the rounds. At 20° elevation, the initial rise time (velocity at shot ejection) is significantly higher than at 45°, and at 45° the initial response is higher than that corresponding to 60°. There is a very simple reason for this. The geometry change brings about a change in the inertial moment of the tipping assembly. To demonstrate this, Fig. 30 illustrates that as the supporting structure deflects due to the application of the recoil force, the trunnion moves in a direction perpendicular to a line through the trunnion and ball joint. At 20° elevation, this motion causes the tipping assembly to react with an initial counterclockwise rotation which adds to the normal response. At 60°, however, the initial tendency of the tipping assembly is to rotate clockwise which opposes the normal counterclockwise rotation. The result here is a delay in the cradle response, which occurs at every round of the burst. The response at 45° elevation is similar to 60°, but the delay is smaller in magnitude. We now have a situation where increases in elevation bring about greater accuracy -- an inherent characteristic of this launcher. This characteristic has less importance when delayed recoil is used and is apparent when delayed recoil is discussed in Section IV-E.

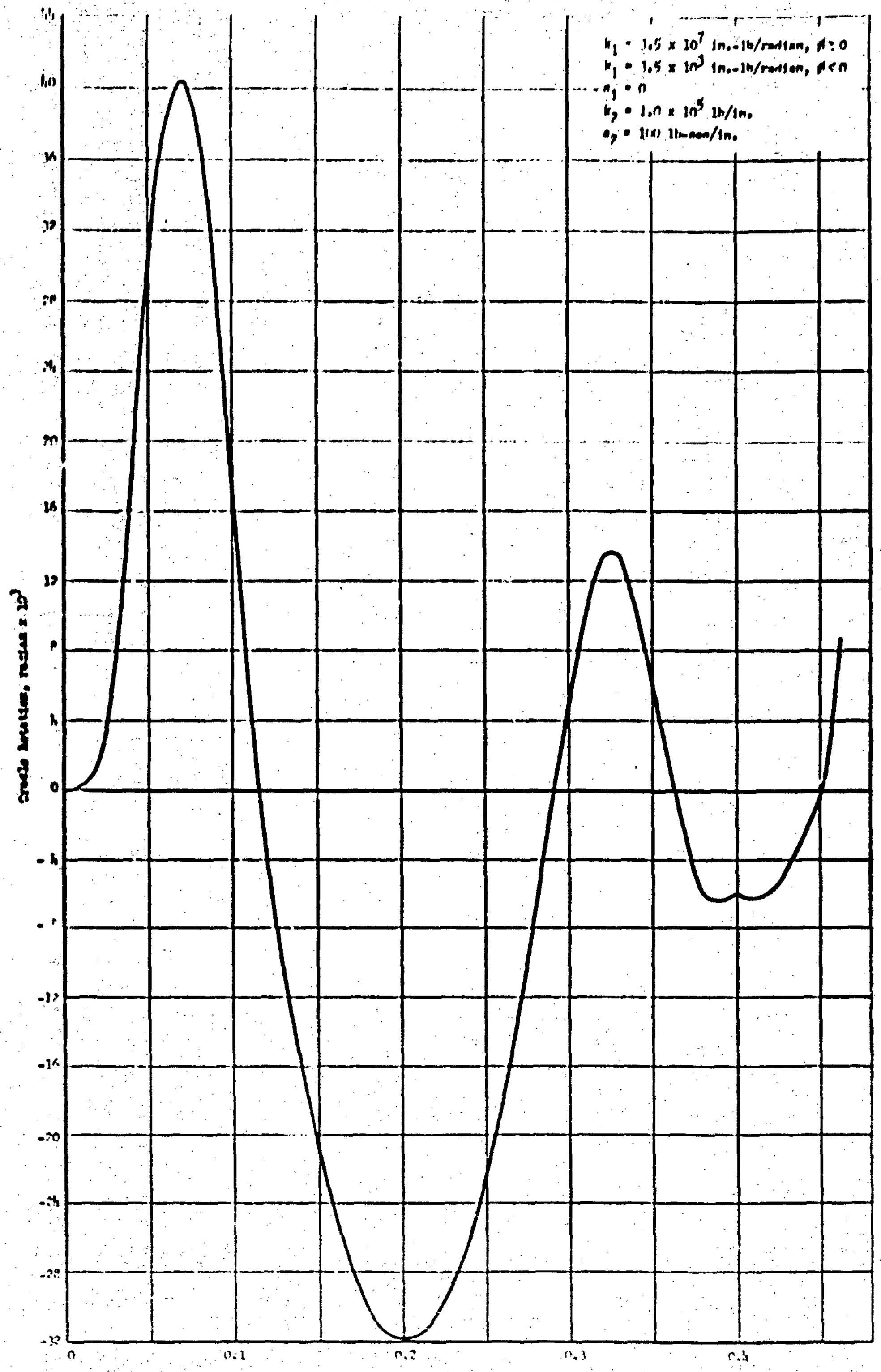

Fig. 25 THEORETICAL RESPONSE WITH A BILINEAR STIFFNESS

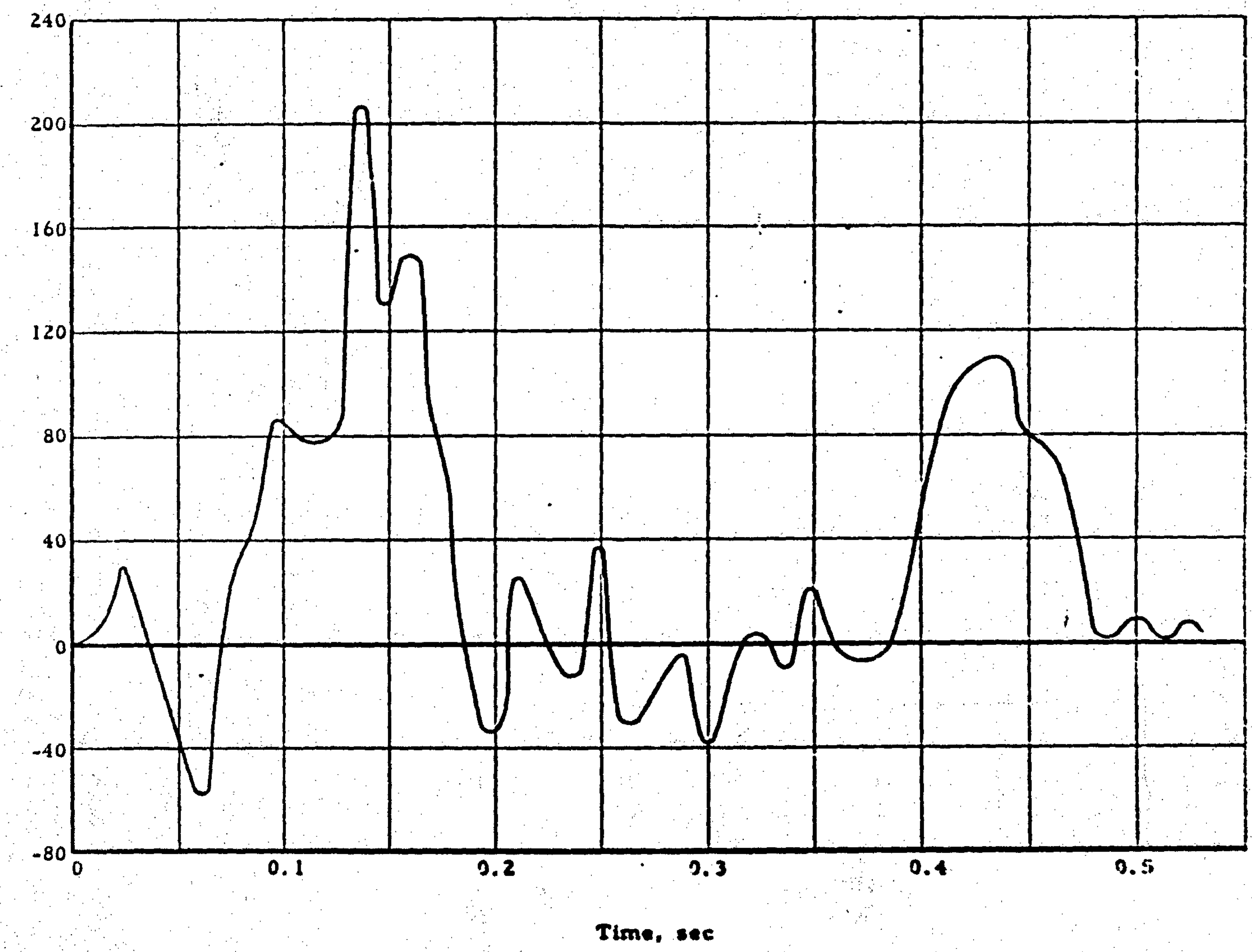

Fig. 26 EXPERIMENTAL ELEVATING ROD STRAIN

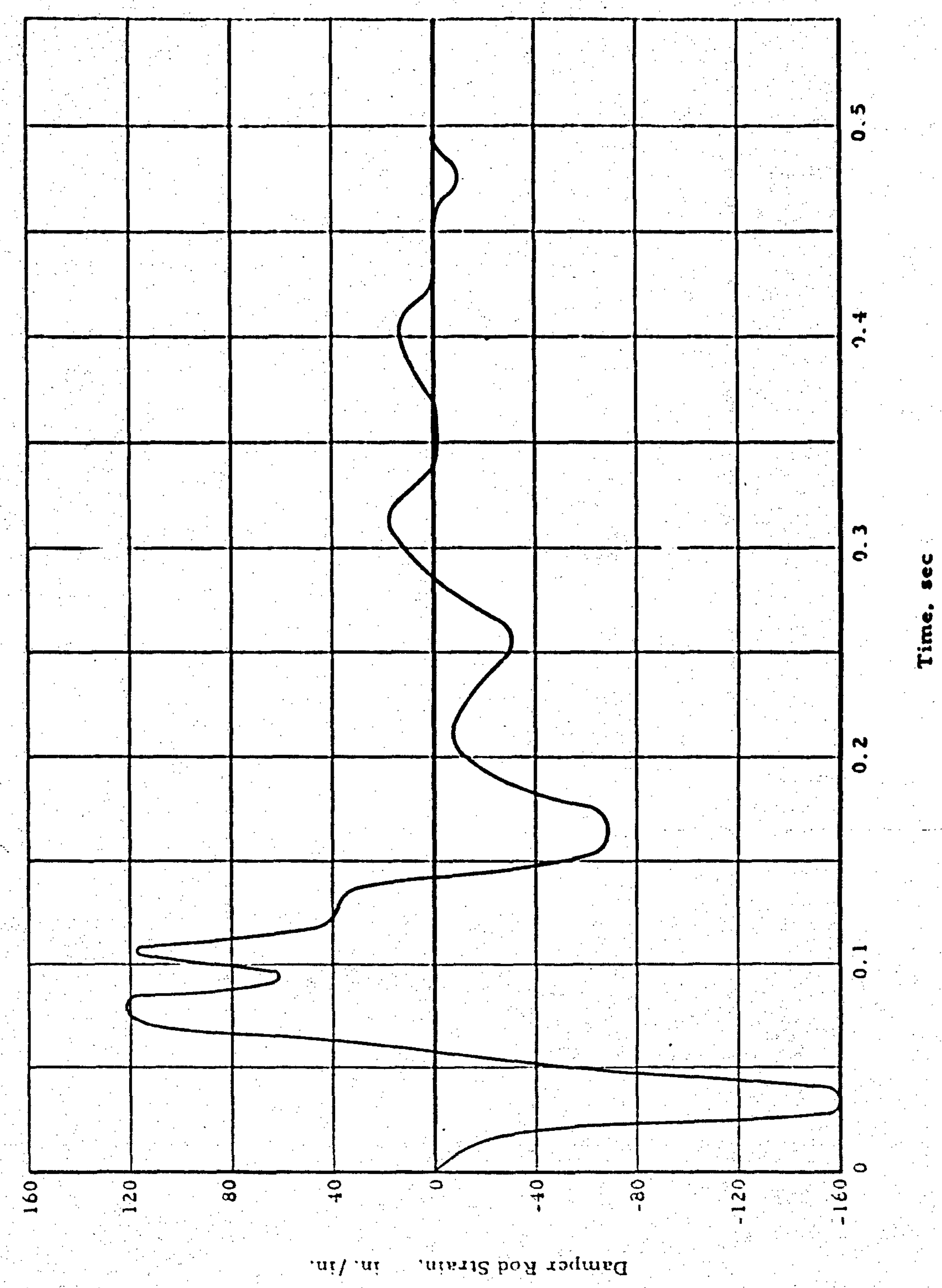

Fig. 27 EXPERIMENTAL ELEVATING SYSTEM DAMPER SUPPORT STRAIN

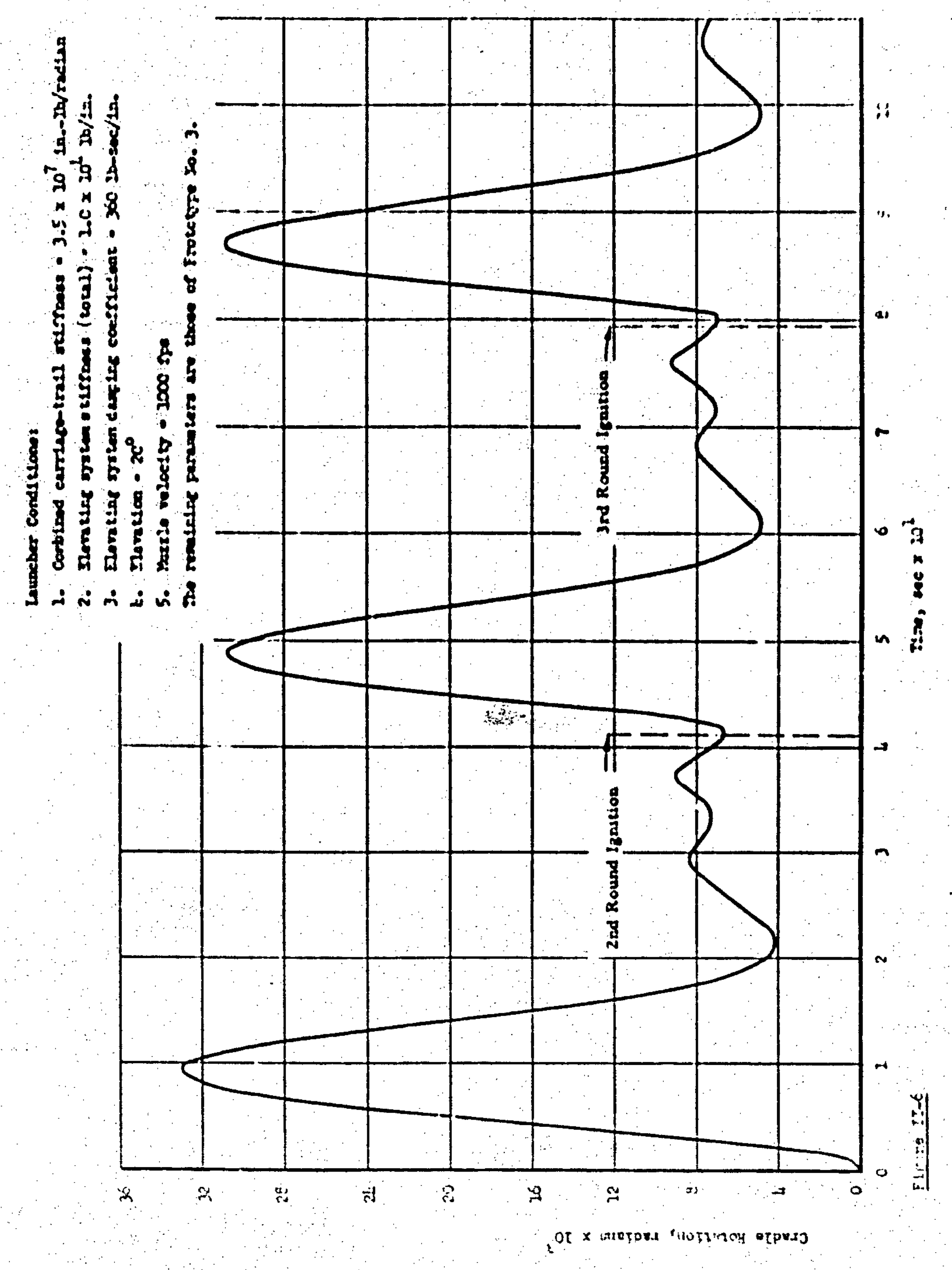

Fig. 28 CRADLE RESPONSE AT 20° ELEVATION

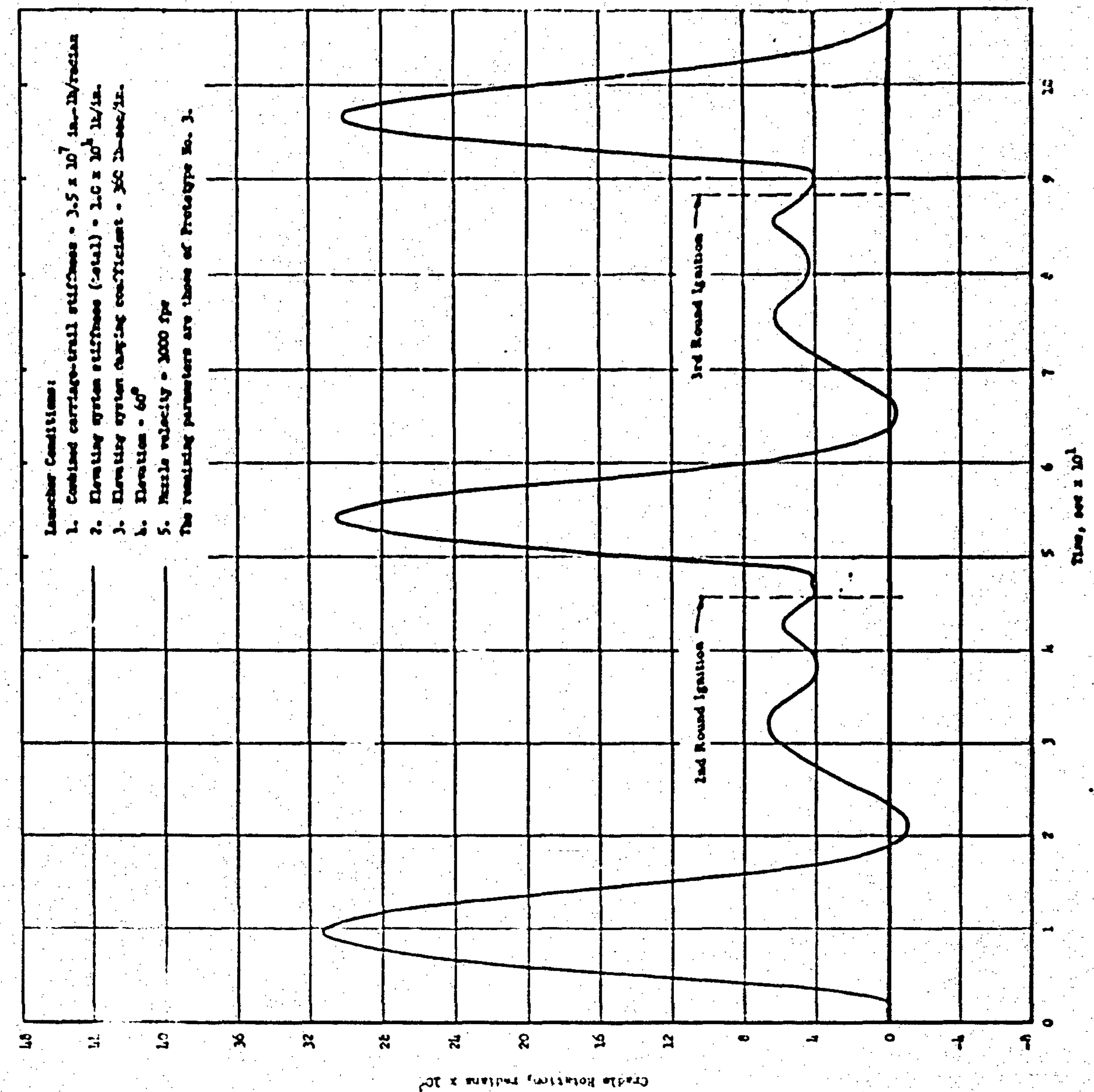

Fig. 29 CRADLE RESPONSE AT 60° ELEVATION

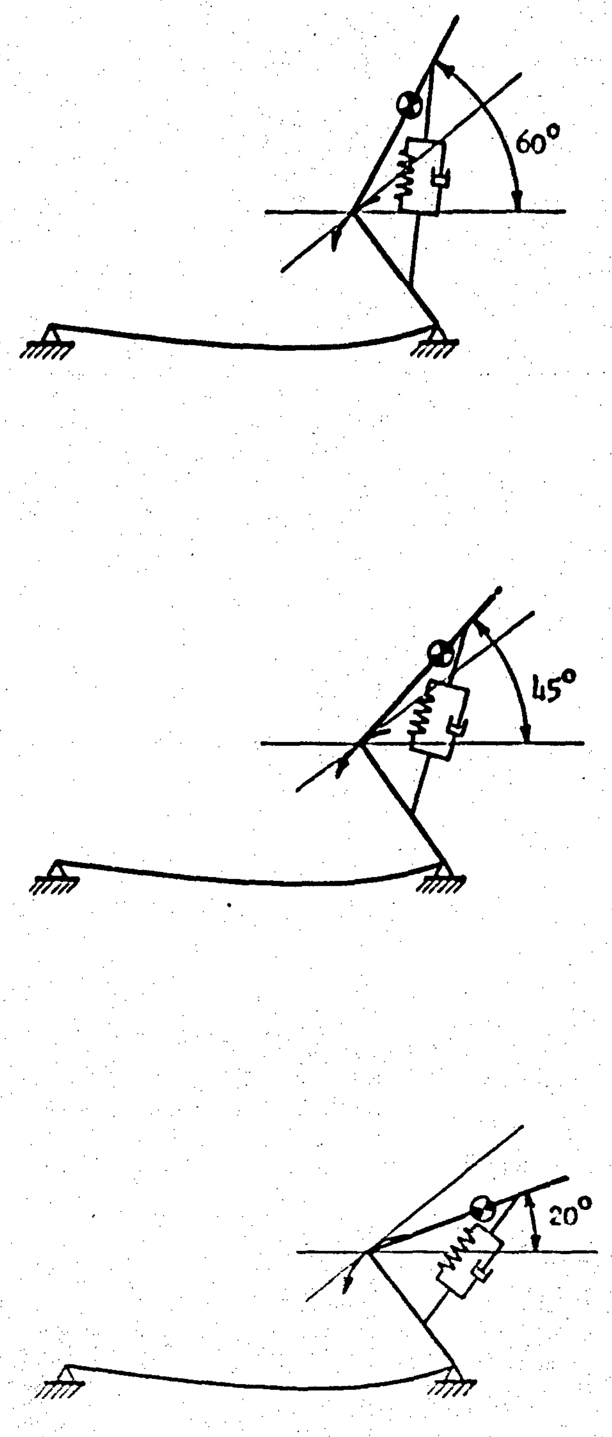

Fig. 30 GEOMETRY OF ELEVATION CHANGES

3. Low Boost Firings

This launcher has the capability of firing rockets with various muzzle velocities (zones of ammunition) simply by varying the amount of gunpowder. The powder-gas force curve corresponding to a muzzle velocity of 380 fps was used in the computer program. Figure 31 shows the cradle response for 60° elevation at this low boost. (The high value of elevation was necessary to insure a large enough recoil distance to cause automatic indexing.) As would be expected, the rise time of the initial cradle response is much smaller than for the high boost rounds and was due to the slower rise time in the recoil force. The amplitude of the residual motion prior to successive shots is also less, but it is still significant. The variation in the residual motion, however, is very similar to the high zone bursts since the counterrecoil forces developed are a function of the recuperator force and the indexing forces. These are both relatively independent of the boost, because of the constant stopping distance recoil system. The maximum recoil distance for this burst was near 20 inches compared to 24 at higher zones. As a result of the slower rise times of the recoil force, we see that it is much more possible to have a negative cradle velocity at shot ejection. In addition, delayed recoil will have less of an effect in changing the response.

4. Importance of Coriolis Acceleration

Because of the high recoil velocity (400 in./sec) combined with the rotational velocity of the tipping assembly, a question arose concerning the importance of the Coriolis acceleration. This acceleration is proportional to the product of these two velocities. For this mathematical model, because of computer solution, there was no particular reason to neglect this term; in other situations, this might lead to a convenient simplification in the equations of motion. For this reason, Coriolis' effect upon the cradle response was investigated. Because the term is proportional to the product of the velocities $\dot{u}$ and $(\dot{\varphi}_1 + \dot{\varphi}_2)$, a set of parameters was selected where these velocities were high. The recoil velocity $\dot{u}$ is almost independent of the structural parameters, so the selection was reduced to finding parameters which increased $(\dot{\varphi}_1 + \dot{\varphi}_2)$. This is done by increasing the stiffness of the elevating system. Figures 32 and 33 show the cradle response with and without the Coriolis terms. The overall response shape has not changed

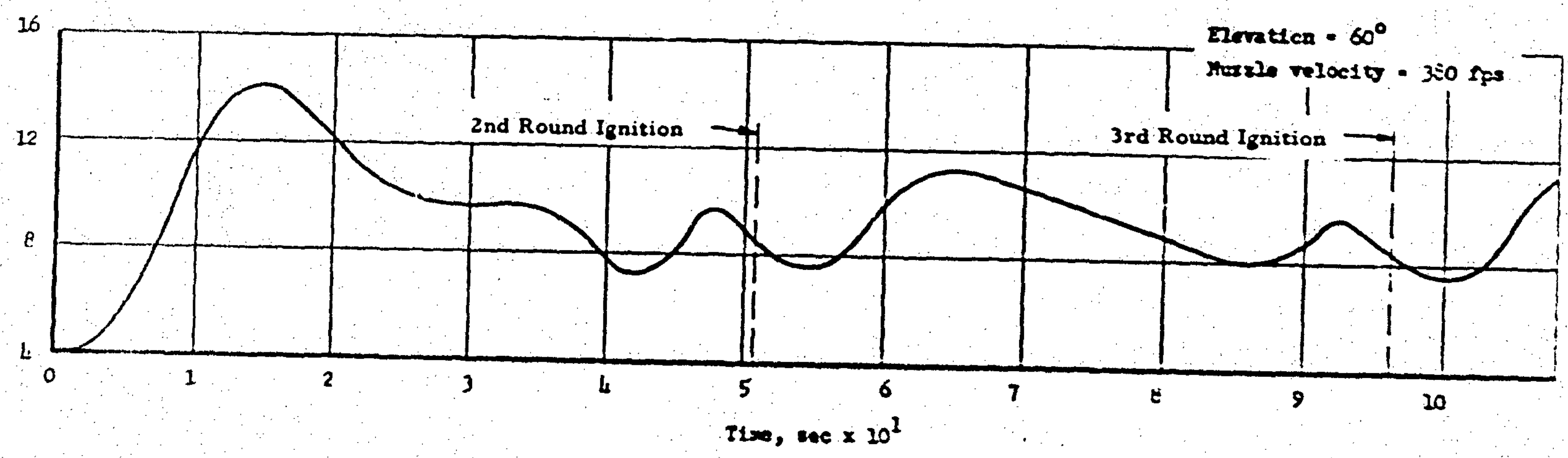

Fig. 31 CRADLE RESPONSE, LOW ZONE BOOST

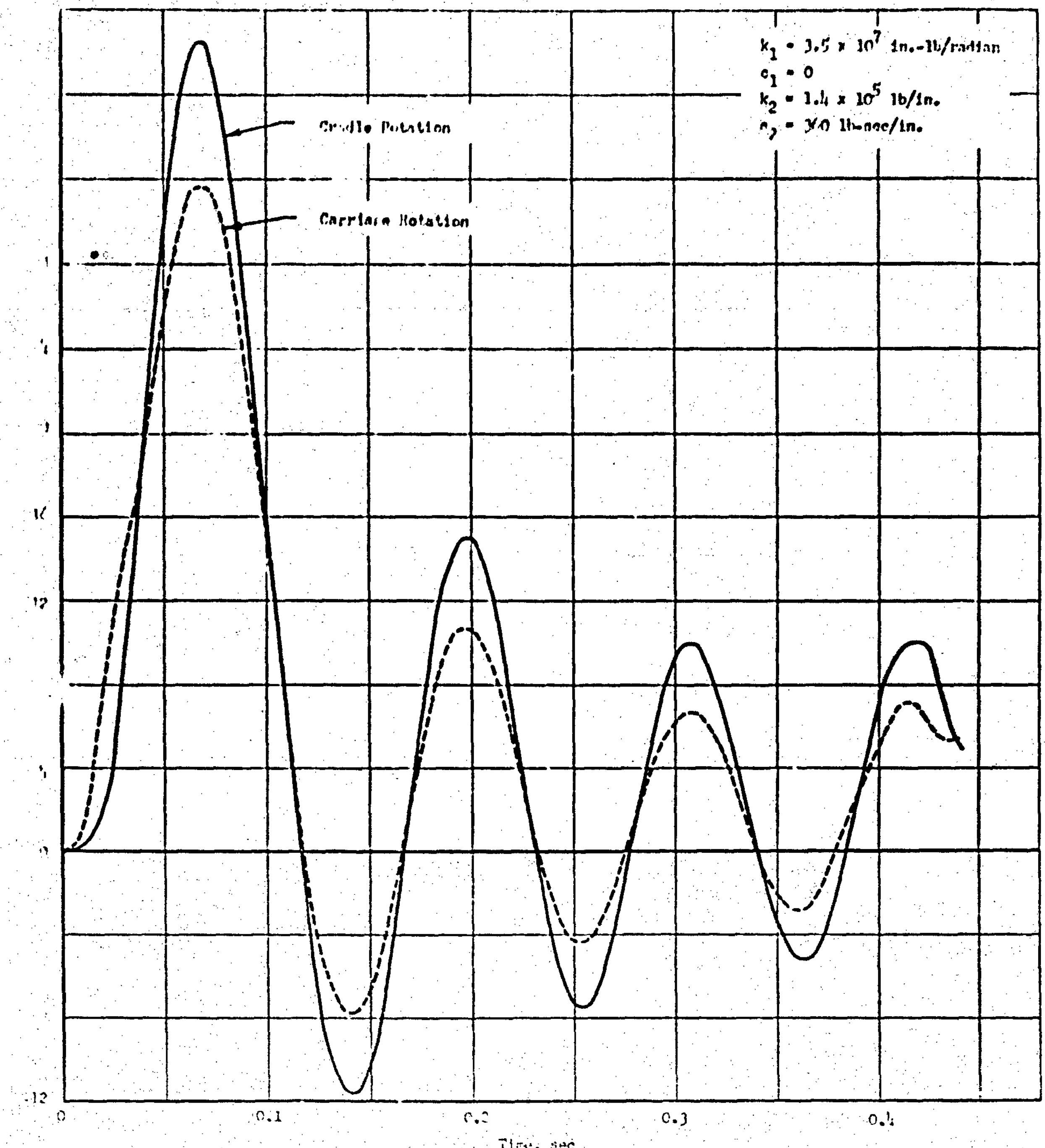

Fig. 32 CRADLE RESPONSE WITH A VERY STIFF ELEVATING SYSTEM

ARMOUR RESEARCH FOUNDATION OF ILLINOIS INSTITUTE OF TECHNOLOGY

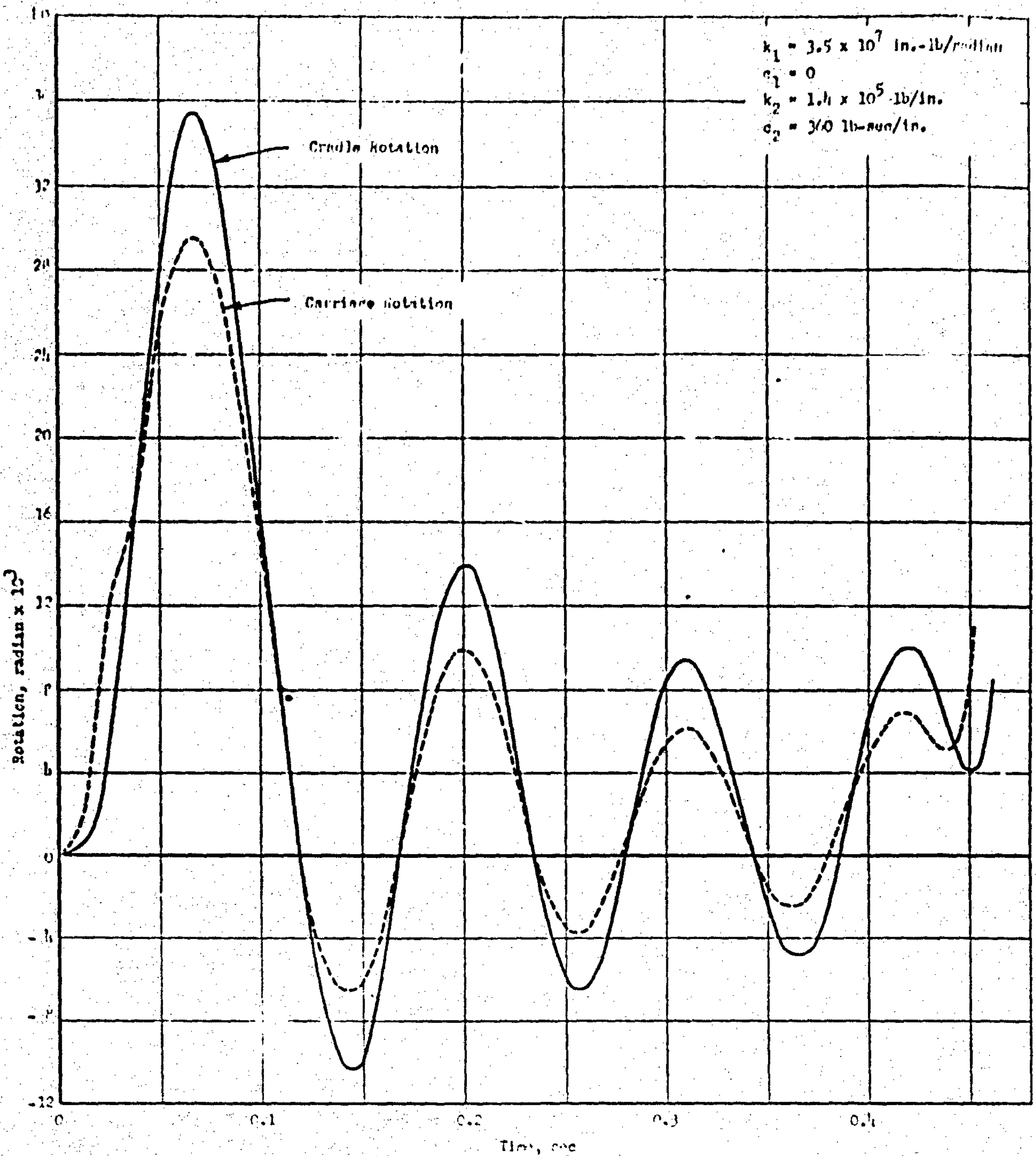

Fig. 33 CRADLE RESPONSE WITH A VERY STIFF ELEVATING SYSTEM NEGLECTING THE CORIOLIS ACCELERATION

ARMOUR RESEARCH FOUNDATION OF ILLINOIS INSTITUTE OF TECHNOLOGY

while the peak response has a difference of 7%. This indicates that the Coriolis acceleration is of second order importance with respect to the shape of the cradle response, though the change in magnitude may be significant. This serves to indicate that some of the simplified models used in the supplementary analyses may be a reasonable representation of the launcher for predicting large scale changes in the response.

5. Delayed Recoil

The recoil system on the XM70 Launcher makes use of a variable area orifice which was designed to stop the recoiling assembly in a constant distance with a constant force. The orifice area varies as a function of the recoil distance; this was effected by pulling variable diameter rods through a fixed area orifice plate. A design suggestion was made to modify the recoil system in such a way that the recoil force is zero (or of negligible magnitude) until the rocket has left the firing tube. In this way the carriage deflections will be zero (for the first shot of a burst), the velocity will be small, and the launcher accuracy will be near perfect. Certain problems arise with delayed recoil; the magnitude of the recoil force increases due to the shorter distance over which the recoil force acts, because of the constant stopping distance system. A question also arose about the effect of the delay on shots following the first.

The 3-degree-of-freedom mathematical model was used to study the effect of delayed recoil since the recoil rod shape is entered into the model as a tabular function of the recoil displacement. Inserting a rod shape into this mathematical model corresponds identically to inserting new recoil rods into an actual launcher.

The first rod shape tried was a standard rod with a decreased diameter (increase in orifice area) for the first 11-1/2 in. of recoil motion. The first rocket leaves the launcher at about 3 to 4 in. of recoil; subsequent shots are fired by an adjustable cam, 9 in. out of battery. Because of the residual counterrecoil velocity during all shot ignitions except the first, these rockets leave the launcher at a recoil distance near 11-1/2 in. Figure 34 shows the cradle rotation and the recoil force much larger than obtained for the standard rod. Figure 5 shows a peak force near 20,000 lb compared with the new force

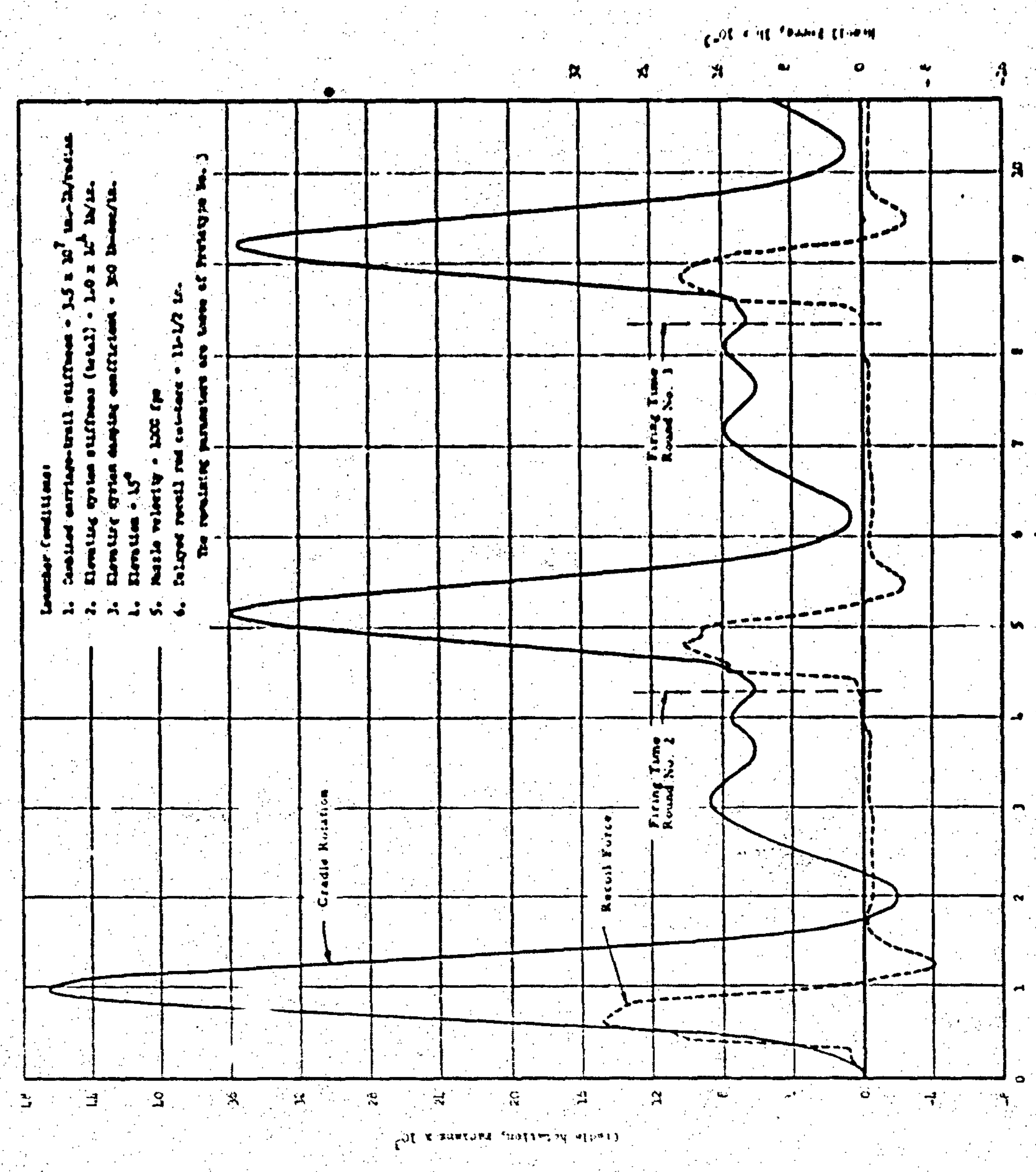

Fig. 34 CRADLE RESPONSE FOR DELAYED RECOIL ROD CUTBACK 11-1/2 IN.

near 30,000 lb. The later shots, however, are near the 20,000 lb peak reflecting the fact that of the 11-1/2 in. cutback, only about 2-1/2 in. of it affect the later shots, compared to the entire 11-1/2 for the first shot. Comparison of the response to that shown in Fig. 20 (optimum elevating system parameters) shows that delayed recoil cut the cradle rotation by about 50% at shot ejection (approximately 20 msec after t = 0) and lowered the velocity by approximately 30%. The displacement effect for later shots is almost negligible because it is fairly large to begin with. Close inspection of the curves shows that the velocity reduction is significant for the second shot. The third rocket, however, left the launcher when the cradle had a negative velocity (for the regular control rod). The use of the cutback rods changed the burst characteristics such that the third shot fired prior to a region of positive cradle velocity. We then realize the situation that delayed recoil does not aid the accuracy if the cradle would normally have a negative velocity at the time a round is ignited. The normal launcher response tends to lessen this negative velocity with a desirable result. This leads us to the conclusion that in order to gain the benefits of delayed recoil, the residual cradle motion should be as small as possible. In this situation, delayed recoil is definitely useful.

In order to decrease the high, first-round recoil force a rod was tried with two diameter cutbacks, the first from 0 to 3 in. and the second from 8 to 11-1/2 in. It was expected that the extra raised portion between 3 and 8 in. would help decrease the first force level. Figure 35 shows the result; the peak force is reduced from 30,000 to 26,000 lb. The peak cradle rotation was also reduced. The later rounds were unaffected because the section of the rod over which they operate was unchanged.

We saw earlier that firings at 60° elevation have less initial cradle rotation due to the geometry of the elevating system and tipping assembly mass center. A computed response for a 60° firing using a cutback recoil rods is shown in Fig. 36. In this situation, the cradle velocity is nowhere near that of the cradle for the ordinary launcher. In the same respect, the response for 20° elevation (with a cutback rod) is probably near the ordinary response.

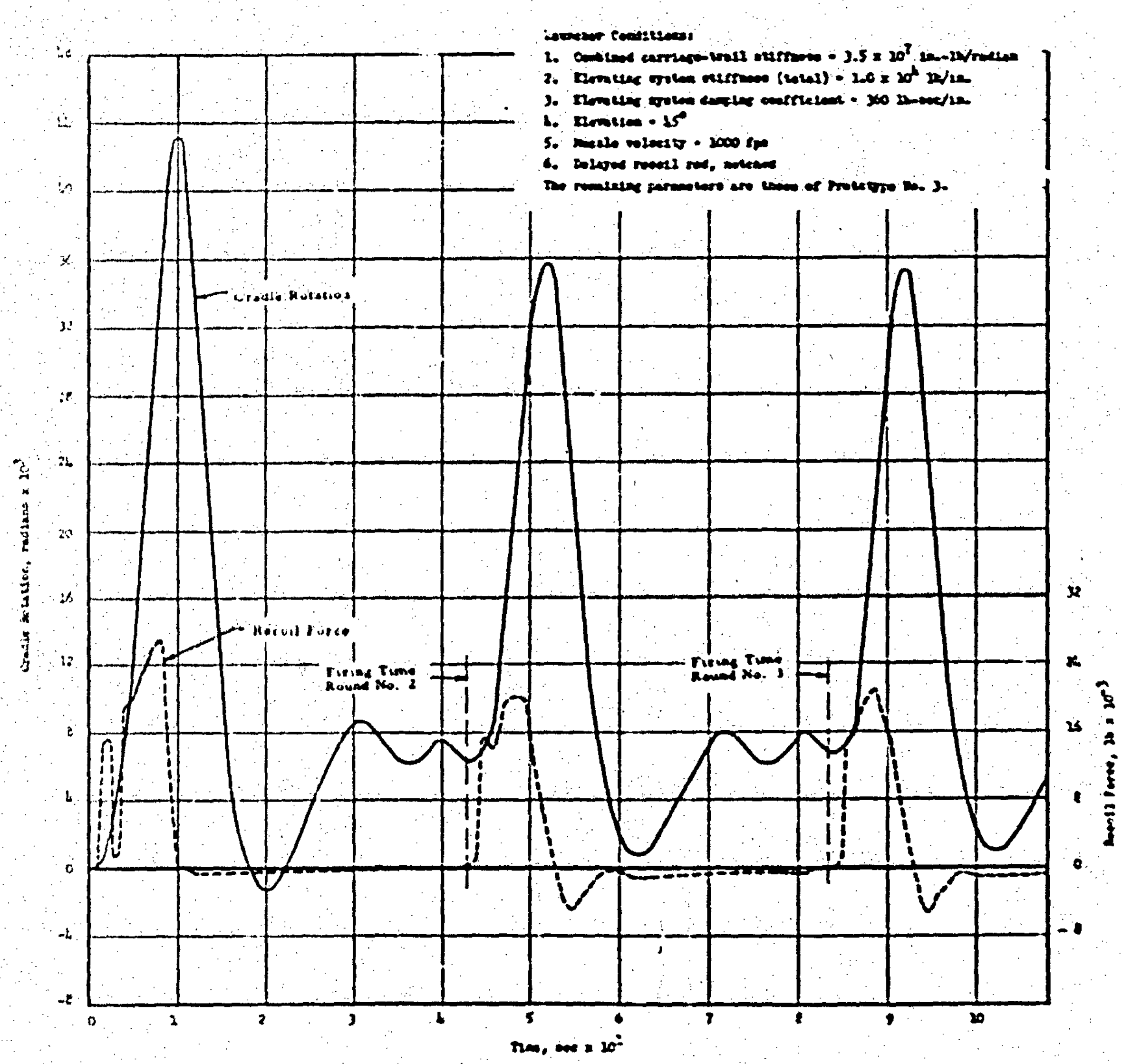

Fig. 35 CRADLE RESPONSE FOR DELAYED RECOIL, NOTCHED ROD

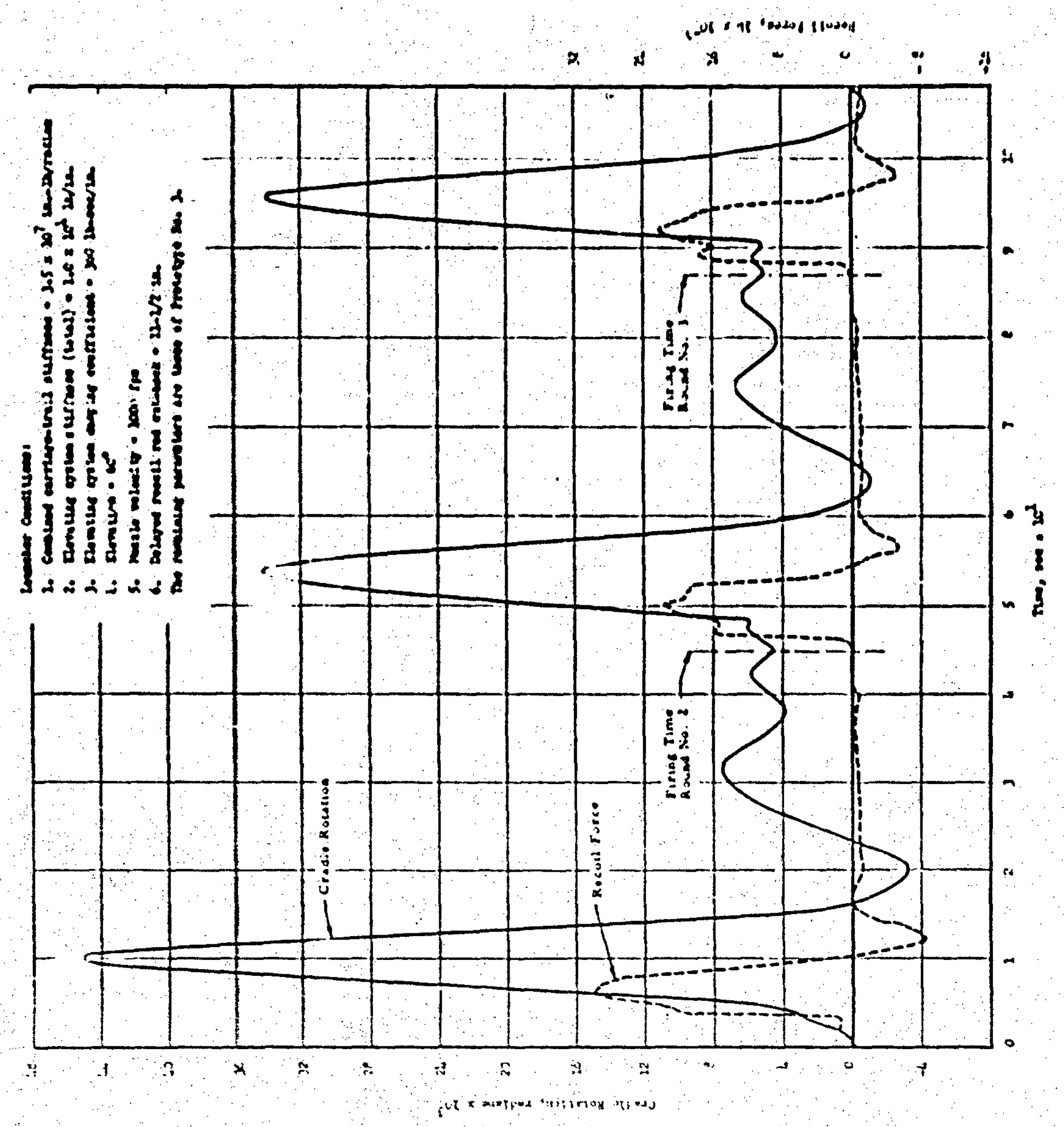

Fig. 36 CRADLE RESPONSE FOR DELAYED RECOIL ROD CUTBACK 11-1/2 IN.

B. Supplementary Analyses

1. Third-Order System

A third-order linear system was developed as a mathematical model and used to find the stiffness and damping which should be incorporated into the elevating system of the launcher. This model was obtained by simplification of the launcher representation shown in Fig. C-1. The simplifications were:

1. The inertia of the carriage and trails, I_o, was assumed negligible compared to the moment of inertia of the tipping assembly -- a ratio of approximately 115:8000.
2. Nonlinear coupling terms between the motion of tipping assembly and supporting structure were neglected.
3. The recoiling motion was neglected.
4. The recoil force was treated as the primary disturbance and was approximated by an impulse.

These assumptions are considered valid because the resulting solution is not intended to represent the actual launcher motion, but rather to indicate the variation of the response behavior for a wide range of parameter variations. The linear analog of the resulting model is shown in Fig. E-1.

The responses of this third-order system were determined by using the response plots contained in "Dynamic Response Plots and Design Charts for Third-Order Linear Systems" 1/. This report contains the solution of such systems in the form of dimensionless response plots for forty-eight different combinations of parameters. These plots were obtained from evaluation of Equation E-5, as a function of time, on a digital computer.

The design charts in the report 1/ show areas of three types of responses.

1. Parameter combinations which produce a normal damped response.
2. Parameter combinations which produce an unstable response.
3. Parameters which result in three real roots to Eq. E-3.

In order to establish the undesirability of the third type of response, a set of

1/ Meyfarth, P., Dynamic Response Plots and Design Charts for Third-Order Linear Systems, Research Memo No. R. M. 7401-3, Massachusetts Institute of Technology, 1958.

parameters which produce this was used in the computer solution for the 3-degree-of-freedom system. The resulting cradle response was continuously increasing (non-oscillating), as shown in Fig. E-3, for 150 lb-sec/in. damping and 100 lb/in. stiffness.

Despite the various assumptions, the response curves obtained were a fair representation of the actual launcher motion for a single shot. (Compare Figures E-2 and E-4.) The optimum response for this system was defined as one with both a low first peak displcaement and a low ratio of second peak to first peak displacement. Three response plots which satisfy this definition are shown in Figure E-2. The corresponding optimum elevating system parameters are a stiffness of 1.0×10^4 to 1.4×10^4 lb/in. and damping of 360 to 540 lb-sec/in.

2. An Approximate Dynamic Analysis of the Minimum Weapon Weight Required for a Specified Accuracy

A relatively simple mathematical model of the XM70 and a simple dynamic performance requirement for accuracy was formulated in order to evaluate several basic design parameters including the minimum total weight of the weapon. Mathematically, the procedure was one of finding a second order system which had a specified response decay. The details of the analysis are contained in Appendix B of this report.

For the purposes of this analysis, the complete weapon was represented by a linear, forced, damped, single-degree-of-freedom oscillator. The displacement of the oscillator represented angular rotation of the firing tube in a vertical plane. This representation was shown to be useful[1] when the stiffness is taken to be the total stiffness of the weapon structure and the mass is a computed dynamic equivalent. Values of the damping coefficient were chosen to be consistent with experimental data of the weapon's response to firing loads. The force applied to the oscillator to simulate firing was a rectangular pulse whose amplitude and duration were chosen to represent the recoil force of the actual weapon.

As a criterion for adequate dynamic performance, it was assumed

[1] See ARF Project K130, Bimonthly Report No. 11, Appendix A.

that the amplitude of firing tube oscillations (in a vertical plane) must be less than some small value, which is considered to produce negligible error at the target, prior to firing of each round of a burst.

Under the assumptions of the analysis, a closed form solution can be obtained to the equation of motion of the weapon. The solutions consists of the displacement of the firing tube as a function of time and the stiffness, damping and mass of the weapon but what is ultimately desired from the analysis is the time required for adquate damping of the response as a function of the weapon weight.

The weight of the weapon was explicity introduced into the solution by writing expressions for the stiffness, damping coefficient, and equivalent mass of the weapon as functions of the weight of the major subassemblies of the XM70. These expressions were obtained by assuming linear relationships and using the XM70 Prototype Model No. 1 weights for reference. Using the solution containing these expressions, it was possible to obtain a time-displacement curve, and hence the time required for adequate damping, for a particular total weapon weight. Several solutions must be obtained in order to obtain a plot of required damping time versus total weight from which the minimum weight can be obtained. The analysis procedure is facilitated by using the envelope of the response curves rather than the curves themselves.

This analysis formed the basis for the computation of the optimum recoiling assembly weight for the XM70 which is reported upon in ARF Project K130 Bimonthly Report No. 8 Appendix B. In addition, this analysis was used to estimate the minimum weight of a weapon having a small recoiling assembly weight (500 lb) and a delayed recoil force. The minimum weight of such a weapon was found to be only 1340 lb., but the resulting ground reaction was too large and the calculated carriage weight was inadequate from a strength standpoint. These calculations led to the development of an auxiliary strength criterion for the carriage and hence to the procedure referred to above for calculating optimum recoiling assembly weight.

3. Linear, 2-Degree-of-Freedom Model

A classical, 2-degree-of-freedom system was another system studied

to obtain information about the best location for auxiliary damping of the cradle motion. Because only qualitative information was desired, the lack of representation of system nonlinearities is not considered important. Fig. A-1 shows the system which was studied where m_2 represented the tipping assembly, and m_1, the supporting structure. The three damper locations which were considered correspond to the following:

1. c_1; damping between the supporting structure and the ground (the ground was assumed to be capable of furnishing a tensile load).
2. c_2; damping between the supporting structure and tipping assembly.
3. c_3; damping between the tipping assembly and the ground.

The equations of motion were solved by digital computation where the input disturbance, F_1, was a tabular representation of an actual recoil force. All three damper locations are physically attainable, though the second is certainly the most convenient location. Equivalent damping between the three locations was determined by estimating the amount of forcible damping for the same weight contribution to the launcher from the respective dampers.

As expected, damping directly between the cradle and ground was most effective, of the three locations. However, damping between the tipping assembly and supporting structure was relatively effective, especially compared to damping between the supporting structure and ground. Combinations of the latter two, c_1 and c_2, was better, but on the estimated weight basis, the improvement was not significant. Since c_3-damping is the most difficult to attain, the most promising damper location was concluded to be relative to the supporting structure and tipping assembly.

C. Three-Dimensional, n-Degree-of-Freedom Model

This mathematical model (called Mathematical Model VI in progress reports) was developed with a view toward the incorporation of several of the modes of motion which were not included in earlier models. It contains all of the freedom of the previous models and, in addition, permits the investigation of the following types of behavior.

1. Ground Flexibility

Results of some of the experiments showed that an elastic and plastic deformation of the earth underneath the ball joint and the trail paths can

sizably affect the burst accuracy of the weapon. The new model, consequently, will allow the introduction of an arbitrary force-displacement relationship at the support points.

2. Sidewise Rotation at the Ball Joint

Incorporation of this freedom necessitated that a full three-dimensional representation be utilized. This representation should permit simulation of a portion of the lateral dispersive action associated with the weapon.

3. Left-Right Sequencing

This is also a three-dimensional effect; it arises because the inertial unbalance in the recoiling assembly cannot be eliminated. Left-right sequencing is discussed in detail in another portion of this report. Its incorporation into this model was somewhat simplified through the interpretation of the recoiling assembly framework flexibility in the form of a single torsional spring.

4. Flexible Barrel

The barrel flexibility was considered to be very important to the overall burst dispersion of this weapon. In particular, it would appear that phasing between the barrel vibration and the time of firing of the various rounds is quite significant. This barrel vibration is even more important because it is evidently coupled with the rotation of the weapon about the ball joint to Coriolis force terms and gyroscopic moments which arise due to the moving projectile.

5. Moving Projectile

The flexible barrel is excited by the traveling load induced through a projectile as well as through the gross forces which arise through firing. This operation motivated the inclusion in the model of a representation for the coupled motion of a traveling mass and the barrel proper. This representation is so organized that an experimentally determined time-displacement relationship can be introduced to describe the axial projectile behavior. It is thus possible to determine the instantaneous muzzle position orientation and velocity at the time of projectile exit. It is felt that this

information should be of aid in the development of more complete accuracy criteria for rocket launchers of this type.

This 3-dimensional mathematical model was not completed until near the close of the present project. The equations were programmed for the UNIVAC 1105 digital computer at Armour Research Foundation, but the program was not run on the machine because it was felt that the time and efforts which remained on the project could be more efficiently applied to other facets of launcher behavior. The equations for this model are presented in Appendix F of the present report. These equations are quite complex; their full solution should prove to be time consuming. Conversely, specific items of interest to future rocket launcher programs can certainly be obtained through specilization of these very general equations.

D. Accuracy Criterion

The main direction of effort on this program has been to study the response of the XM70 Launcher structure in the vertical plane due to burst firing loads. The intention was to find that combination of launcher parameters, e.g., weight, stiffness, moment of inertia, mass distribution, recoil force, etc., which would optimize or at least improve the response. In order to evaluate the effects of parameter changes, a simple accuracy criterion was used. This criterion was: the most accurate burst has the smallest residual angular cradle displacement and velocity prior to each succeeding round. This was not expressed mathematically, but was applied simply by examining graphs of both computer and experimental responses. A mathematical accuracy criterion is presented here that permits a more accurate basis for judgment. This criterion is a relationship between the launcher response and the points of projectile impact. General application of this criterion is limited only by the fact that it employs the motion characteristics of a short-burning-time, ballistic rocket. Because the development of this criterion came late in this program, its application was not completed. It is presented here, however, because of its generality.

The significant sources of rocket dispersion (of a rocket with a relatively short burning time) are:

1. Initial cross spin, i.e., angular yaw (pitch) velocity when the rocket leaves the launcher,

2. Launch mal-point, i.e., initial yaw (pitch) when the rocket leaves the launcher,
3. Dynamic unbalance of rocket,
4. Cross winds during burning,
5. Total rocket impulse variations,
6. Rocket spin at burnout,
7. Thrust malalignment.

Only the first three of these are influenced by the launcher. The particular launcher motion that can contribute significantly to dispersion by influencing these three quantities is the cradle motion in combination with the firing tube motion relative to the cradle. The cradle angular displacement and angular velocity in the vertical plane are considered here. At present, we are limited to consider only these because all completed mathematical models assume a rigid firing tube and plane motion only. Because of these two limitations, dynamic unbalance must also be neglected. In addition, during the transition period when the rocket is partially out of the firing tube, the rocket is assumed to have the orientation of the tip of the tube.

The purpose of this criterion is to permit a comparison of launcher responses to burst firings (or a group of single shot firings with the same launcher) and a subsequent selection of the best response; with this in mind, the following characteristics can be imposed upon the criterion:

1. Only relative changes in dispersion or accuracy between burst responses need be indicated by the criterion.
2. In the case of computed responses, an indication of accuracy improvement by the mathematical output of the criterion must correspond to an actual accuracy improvement. (This can be checked experimentally or with a complete, bailistics mathematical model). This correspondence will not be required to be linear, however.
3. The criterion will yield a numerical answer for each burst and will be zero for a perfect burst. (A perfect burst is attained when all rounds impact at the same point.)
4. The criterion must allow for the different contributions to dispersion from unit deviations in initial yaw and initial cross spin.
5. Each round of a burst is to be considered separately, and its sequential position will be neglected.

These are the criterion characteristics that are inferred prior to the development of the criterion simply by considering its purpose and application. The implications of each of these are: Item 1 states that the criterion output for a single burst will not indicate anything about the accuracy of that burst, when compared to the criterion output of another burst; however, it will indicate which of the two is better, i.e., more accurate. Item 2 states that the indication of which of two bursts was more accurate must correspond to the indication of relative accuracy of an actual launcher firing of two bursts under the same conditions: the criterion must agree with reality. In order that the criterion contain the characteristics implied by Item 3, the deviations of both displacement and velocity of the cradle will be measured with respect to their mean. Item 4 states that the criterion must account for the fact that a unit deviation in angular cradle displacement does not necessarily produce the same dispersion as a unit deviation in angular cradle velocity; this is accomplished by using what are known as "unit effects", coefficients determined by the magnitude of dispersion due to a unit deviation in each quantity. The last item, No. 5 merely states that no priority is given to any of the six rounds of a burst.

The combination of the above characteristics narrows the choice of mathematical expressions describing this accuracy criterion to a point where an expression can be deduced:

$$L = U_y \sum_{k=1}^{6} \left|\Delta_y\right|_k + U_s \sum_{k=1}^{6} \left|\Delta_s\right|_k ,$$

where

L	=	the numerical output from the above expression indicating relative burst accuracy,
U_y	=	unit effect for mal-point or initial yaw,
U_s	=	unit effect for initial cross spin,
Δ_y	=	deviation from the mean in initial yaw,
Δ_s	=	deviation from the mean in initial cross spin,
k	=	index.

The two deviations are written as:

$$\left|\Delta_y\right|_k = \left|\phi_k - \phi_m\right| \qquad \left|\Delta_s\right|_k = \dot{\phi}_k - \dot{\phi}_m ,$$

where ϕ_k and ϕ_m are the initial yaw and cross spin, respectively. In this criterion, the smaller the value of L, the better the burst. Other criteria may be deduced that conform to the given conditions, but for small deviations they will reduce to the above expression.

This criterion was to be incorporated directly into the computer program of the 3-degree-of-freedom mathematical model. A 6-rd burst computation would then automatically give the quantity, L. The unit effects are obtained from solutions of the equations of motion of the rocket; the unit effects for the XM54 rocket were tabulated in previous progress reports of this project. [1]

---

[1] For more information of the unit effects of rocket dispersion, see: Bi-Monthly Report No. 18, ARF Project D124, January 22, 1960.

V. CONCLUSIONS

All the results derived from this study are based upon considerations of cradle motion near the time of shot ejection of each round of a burst. There was no intention of neglecting the effects of firing tube flexibilities, but this effort represents a first step to increase the weapon accuracy. There was no reason to suspect that flexible firing tube motions may be simply additive to cradle motion because of the coupling which exists. However, the correlation obtained between theory and experiment, despite neglecting this coupling theoretically, indicates that the effects upon gross cradle rotation are small. This points to the conclusion that the accuracy criterion based upon cradle motion was valid, i.e., a reduction in the residual cradle motion prior to the successive rounds of a burst will improve accuracy.

The residual cradle oscillations of the as-designed launcher (Prototype No. 3) were seen experimentally to be small. The only disturbing factor was that the as designed structure was subjected to elastic rebond, or trail hop; this permitted serious, gross horizontal dispersion to occur. This horizontal dispersion was eliminated by simple ties restraining the trails from moving in a horizontal plane. An alternative was shown to exist where trail hop was eliminated -- this was shown to be accomplished by stiffening the supporting structure. With this stiffened structure, the ties at the trails are unnecessary.

When trail hop does not occur, an optimum combination of elevating system structural parameters was found. This was based upon a study which showed that the best location (based upon effectiveness per weight) at which auxiliary damping should be added to the launcher is between the tipping assembly and the supporting structure. The optimum elevating system had the following structural parameters:

k_2 (total stiffness) = 1.4×10^4 lb/in.

c_2 (Damping coefficient) = 400 lb-sec/in.

This combination caused a minimum of residual cradle oscillation between shots of a burst, and is independent of the stiffness of the supporting

structure. The possibility of an unstable response during a burst was demonstrated for very low elevating system stiffness. It should be mentioned that due to the damping of the hydraulic recoil system and possibly soil interaction, the launcher, as designed, displayed much inherent damping.

Elevation changes were shown theoretically to influence the accuracy because of the corresponding geometry changes. The overall effect was to increase accuracy with elevation. Changes in accuracy were also observed due to difference in ammunition boost charge. The difference, however, was much less than might be expected because of the large reduction in the recoil force at the lower zones. This was because the forces developed during counterrecoil, from the recuperator and indexing system, are of the same order of magnitude as during the high boost bursts.

Delayed recoil is effective in reducing the velocity and displacement of the cradle response for single shots. For bursts, the effectiveness is questionable since it will improve accuracy when the ignition of the round occurs simultaneously with positive cradle velocity, but it does not help when ignition occurs during a duration of a negative cradle velocity. Rods cut back to delay the recoil force for the first shot only will probably yield the best overall accuracy improvement. This improves single shot accuracy while it eliminates the possibility of detracting during later shots.

When considering horizontal dispersion, the shell which stiffens the recoiling assembly framework reduces the dispersion by more than 100%. In addition, when trail hop is present, horizontal ties between the trails and the ground are necessary to achieve good accuracy. They may also improve dispersion in the absence of hop if a tendency exists for the trail pads to slide.

Finally, inclusion of Coriolis acceleration was shown to be significant in the calculation of peak response magnitude, but neglecting it did not alter the overall response shape.

In order to completely investigate launcher contributions to dispersion, two additional efforts are recommended. These are a completion of the development of the three-dimensional mathematical model begun in this

project, and a comprehensive experimental program utilizing the stiffening fixtures developed. This experimental program should include firing tube motion instrumentation as well as rocket instrumentation. It is felt that this combined effort can produce a weapon whose accuracy in burst fire exceeds that of present single shot artillery.

APPENDIX A

A STUDY OF THE RELATIVE EFFECTIVENESS OF VARIOUS DAMPER LOCATIONS

N. P. Pearson, R. M. Brach, and R. H. Van Beek

I. INTRODUCTION

This appendix concerns the theoretical possibility of damping the motions of the supporting structure and tipping parts of an XM70-type launcher between consecutive shots of a burst. Ideal viscous dampers are considered to be located between the ground and supporting structure, and/or between the supporting structure and the tipping parts, and/or between the ground and the tipping parts.

II. THE MATHEMATICAL MODEL

Figure A-1 is a schematic drawing of an XM70-type launcher simplified and idealized to the point where it has only two degrees-of freedom. The general procedure for forming such a discrete system from an elastic system consists of lumping equivalent masses at points where the stiffness is known and/or loads are applied and determining the values of the equivalent masses in such a way that the actual and reduced systems have the same kinetic and potential energy during their first-mode oscillation.[1] The accuracy of the technique depends upon the nature of the forcing function and upon the location where the motion is desired. Deflection magnitudes at any given instant are not expected to be accurate because important features, such as the indexing forces, are not considered. However, the relative effectiveness of the three damper locations is expected to be correctly represented. Clearly, in this particular case, if the calculations showed the motions to be thoroughly damped after some relatively long time, say t_o, and if the actual weapon were equipped with analogous dampers, the motion of the actual carriage or cradle would be thoroughly damped after t_o also.

---

1. Jacobsen, L. S., Ayre, R. S., Engineering Vibrations, McGraw Hill Book Co., Inc., New York, 1958.

The equations of motion of the system shown in Fig. A-1 are;

$$I_2 \ddot{\phi}_2 = -k_2 (\phi_2 - \phi_1) - c_2 (\dot{\phi}_2 - \dot{\phi}_1) - c_3 \dot{\phi}_2 \qquad \text{A-1}$$

and

$$(I_e + m_r \ell^2) \ddot{\phi}_1 = k_2 (\phi_2 - \phi_1) + \ell F(t) - k_1 \phi_1 - c_1 \dot{\phi}_1 + c_2 (\dot{\phi}_2 - \dot{\phi}_1) \qquad \text{A-2}$$

or, letting

$$I_e + m_r \ell^2 = I_1$$

and

$$\ell F(t) = M(t)$$

then

$$I_1 \ddot{\phi}_1 - k_2 (\phi_2 - \phi_1) + k_1 \phi_1 + c_1 \dot{\phi}_1 + c_2 (\dot{\phi}_2 - \dot{\phi}_1) = M(t) \qquad \text{A-3}$$

$$I_2 \ddot{\phi}_2 + k_2 (\phi_2 - \phi_1) + c_2 (\dot{\phi}_2 - \dot{\phi}_1) + 3 \dot{\phi}_2 \qquad \text{A-4}$$

Equations A-3 and A-4 have been solved with a forcing function, M (t), derived from an experimental record of recoil pressure. Figure A-2 shows the forcing function used for all the solutions given in this appendix. The value of the function is just the recoil pressure multiplied by the appropriate area and moment arm. Figures A-3 through A-8 show the calculated response for various choices of the parameters. The stiffness values, k_1 and k_2, represent the values either measured or calculated for the existing weapons. In addition to the values of damping and stiffness, each of the graphs is labeled with the maximum value of the quantity $c_2 (\dot{\phi}_1 - \dot{\phi}_2)$ which is the maximum force developed in the damper between the supporting structure and the tipping parts.

III. DISCUSSION AND CONCLUSIONS

Figure A-3 describes the undamped response of the system, which is not representative of the actual weapon response, primarily because the actual weapon contains inherent damping. The figure does show, however, that significantly larger amplitudes may be obtained on shots after the first. This phenomenon was observed experimentally for Prototype No. 1. It is worthwhile noting that, in all of these response plots, the negative values of ϕ_1 may be taken as a rough indication of the system's tendency to produce trail hop.

The parameters used in the calculation represented by Fig. A-4, A-5, and A-6 are identical except for the values of damping, with c_1, c_2, and c_3 alternately taking on the value 1.25×10^5 lb-sec^2/in., the other two being zero in each case. Note from Fig. A-6 that damping between the ground and the tipping parts, c_3-damping, gives the best results. The relative effectiveness of c_2-damping, as shown by Fig. A-5, and the relative ineffectiveness of c_1-damping, as shown by Fig. A-4, constitute the most important result of this study.

Damping between the tipping parts and the ground, c_3-damping, is the most difficult type to obtain practically. Figure A-7 shows an attempt to obtain the effectiveness of c_3-damping using only c_1- and c_2-damping. The results are seen to be not as good as c_3-damping alone. This is particularly discouraging when the weight added by the two dampers is considered. Figure A-8 shows the results of attempts to compensate for the weight of the two dampers by reducing the supporting structure stiffness and, hence, its weight. This performance is seen to be slightly less satisfactory, but further conclusions are unwarranted because of the simplicity of the model which does not include indexing forces and elevating system geometry. Because these factors affect the optimum stiffness-damping relationship, this relationship will be studied by means of a more elaborate mathematical model.

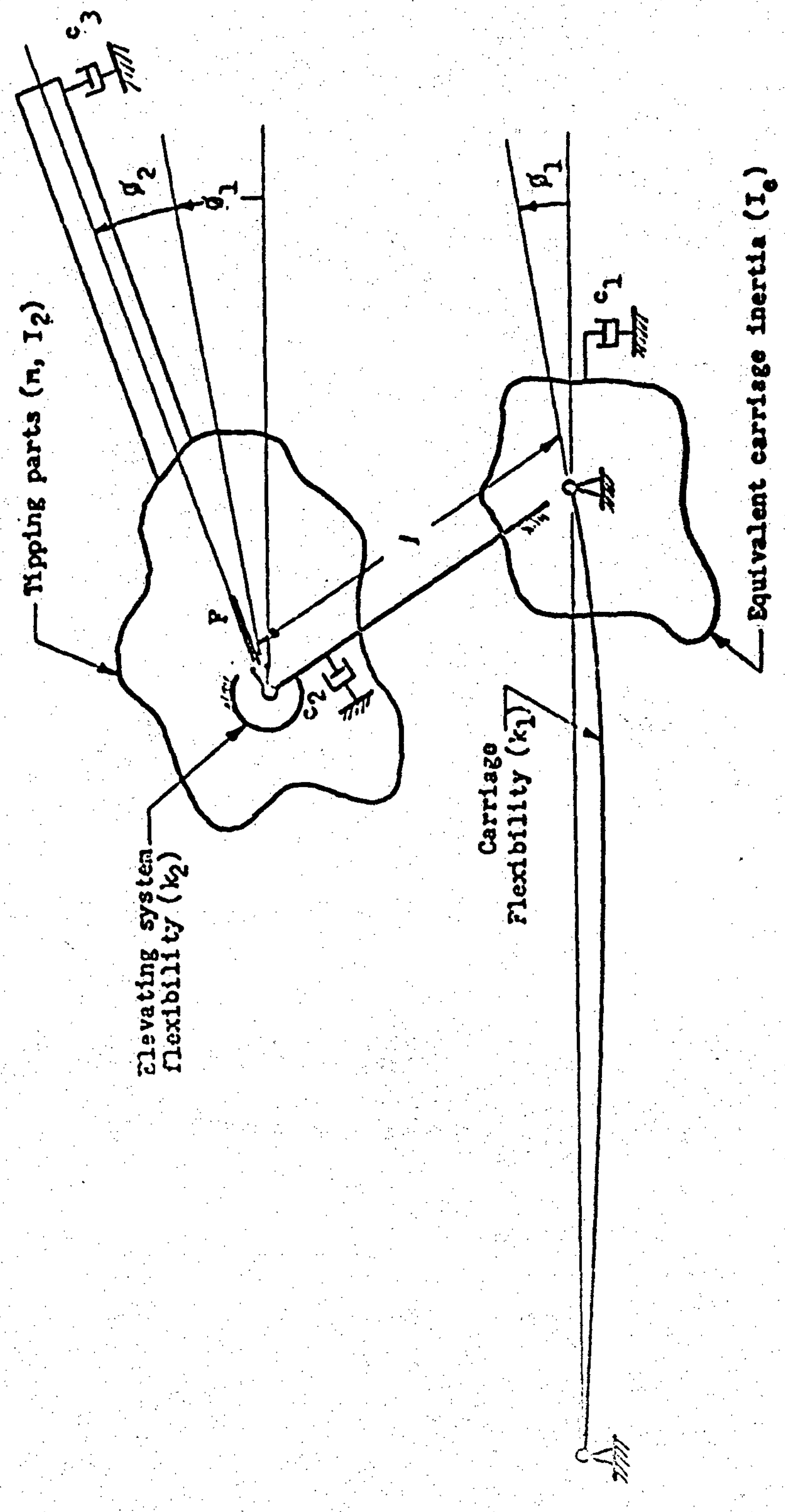

Fig. A-1 **TWO-DEGREE-OF-FREEDOM REPRESENTATION OF A XM70 LAUNCHER**

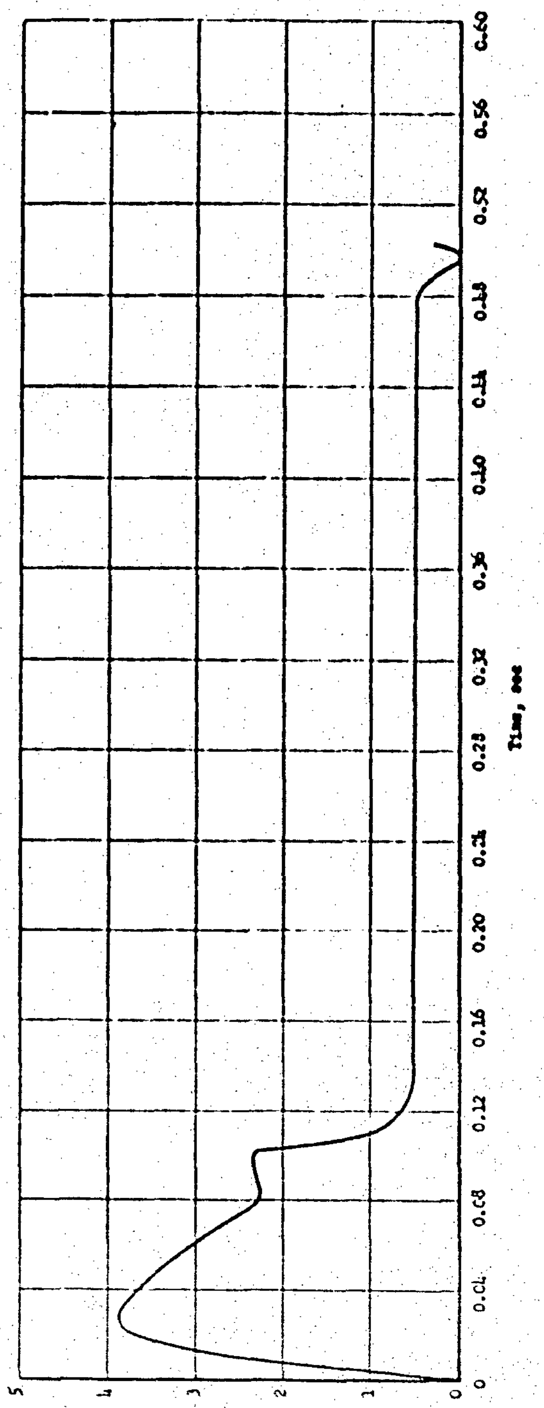

Fig. A-2 MOMENT PRODUCED BY THE RECOIL FORCE

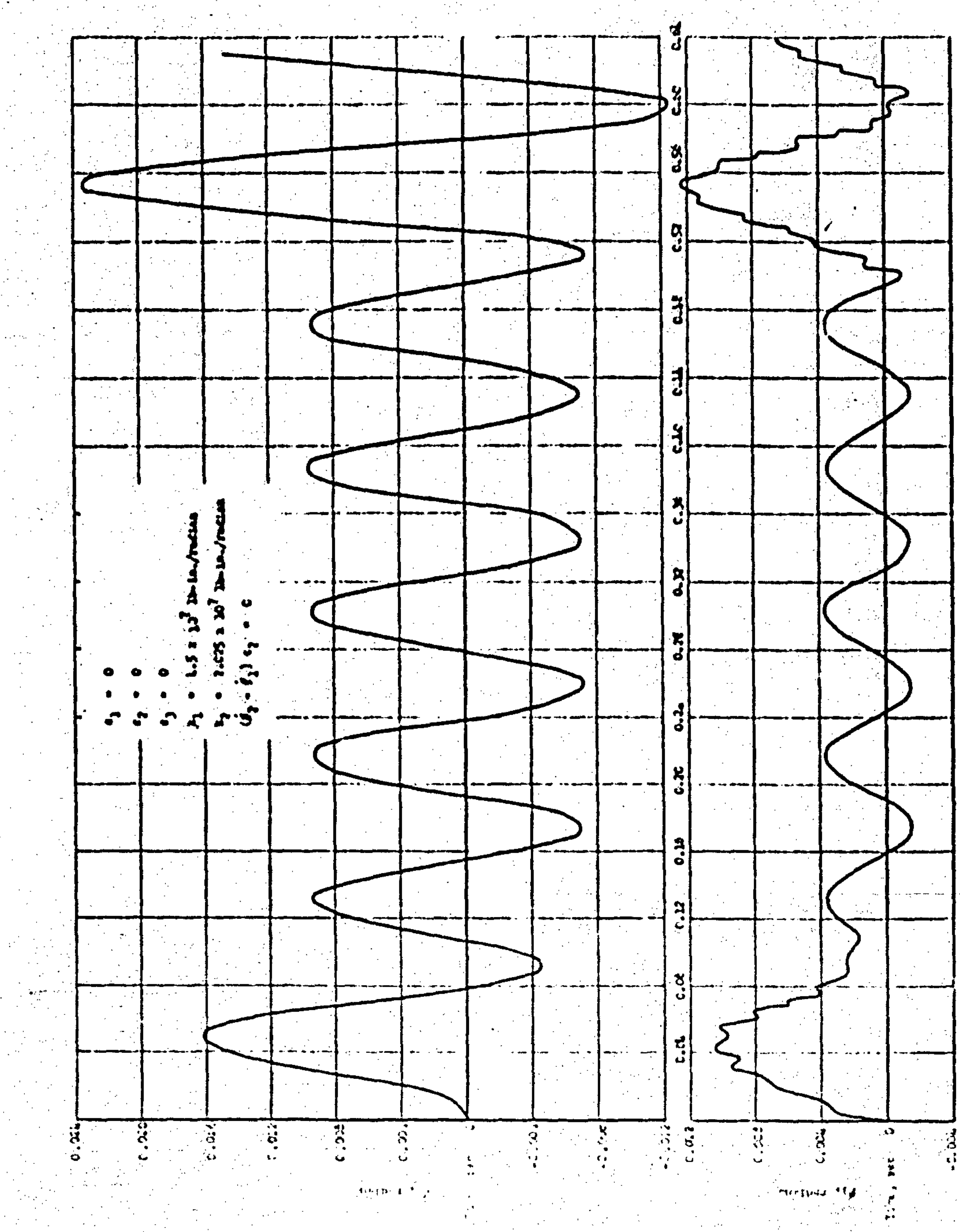

Fig. A-3 CALCULATED UNDAMPED RESPONSE OF AN XM70-TYPE LAUNCHER

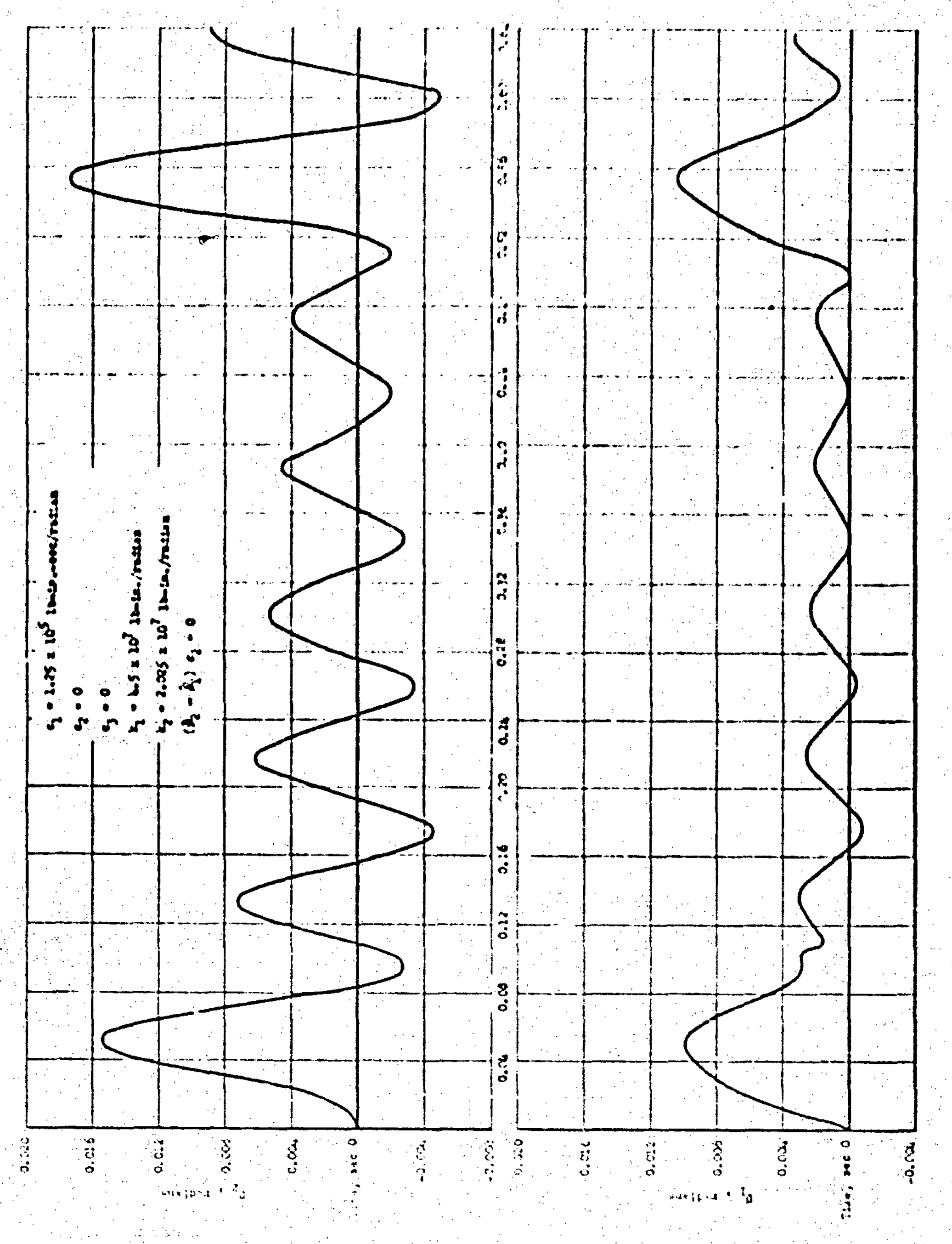

Fig. A-4 CALCULATED RESPONSE OF AN XM70-TYPE LAUNCHER WITH c_1-DAMPING ONLY

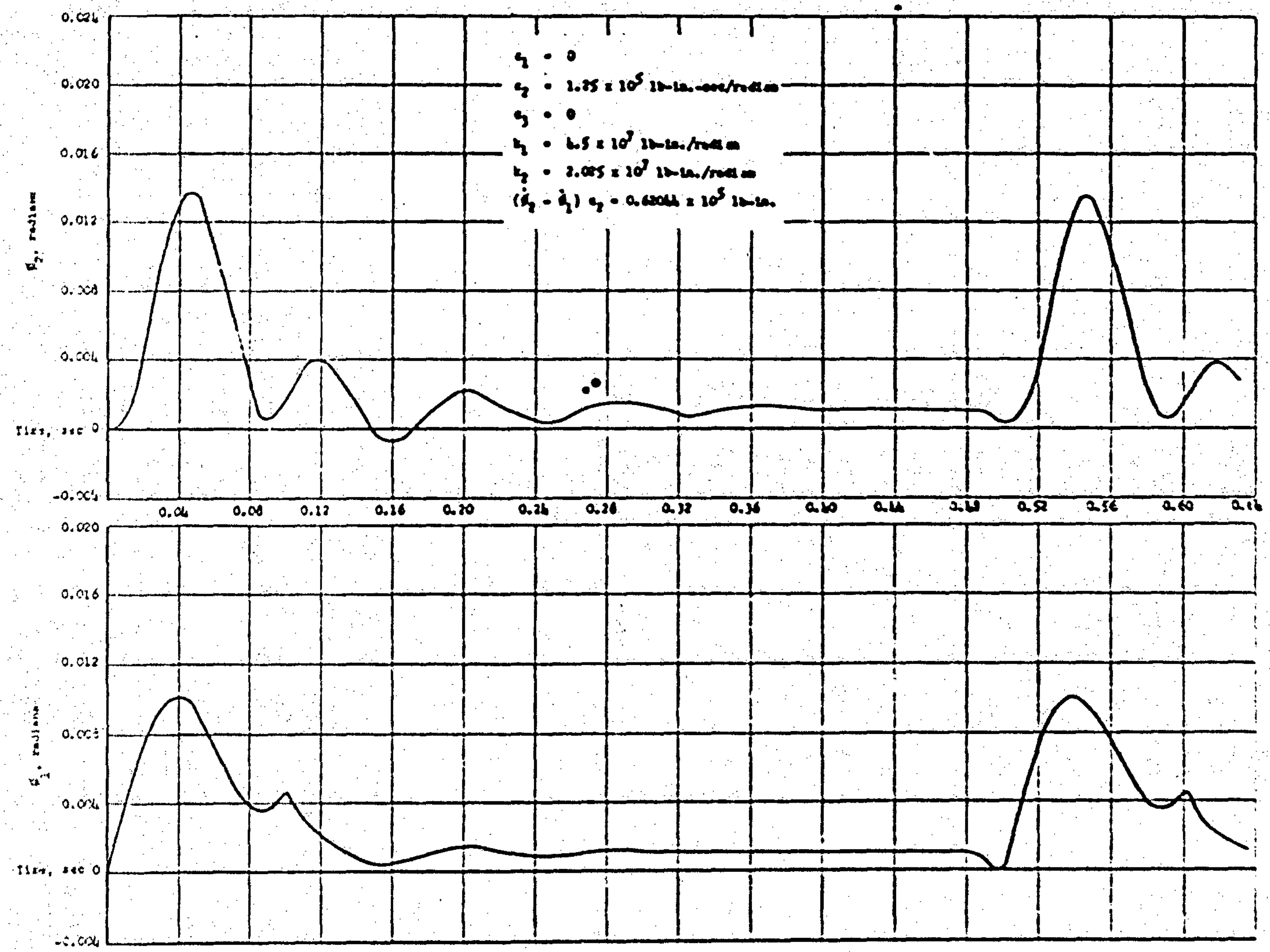

Fig. A-5 CALCULATED RESPONSE OF AN XM70-TYPE LAUNCHER WITH c_2-DAMPING ONLY

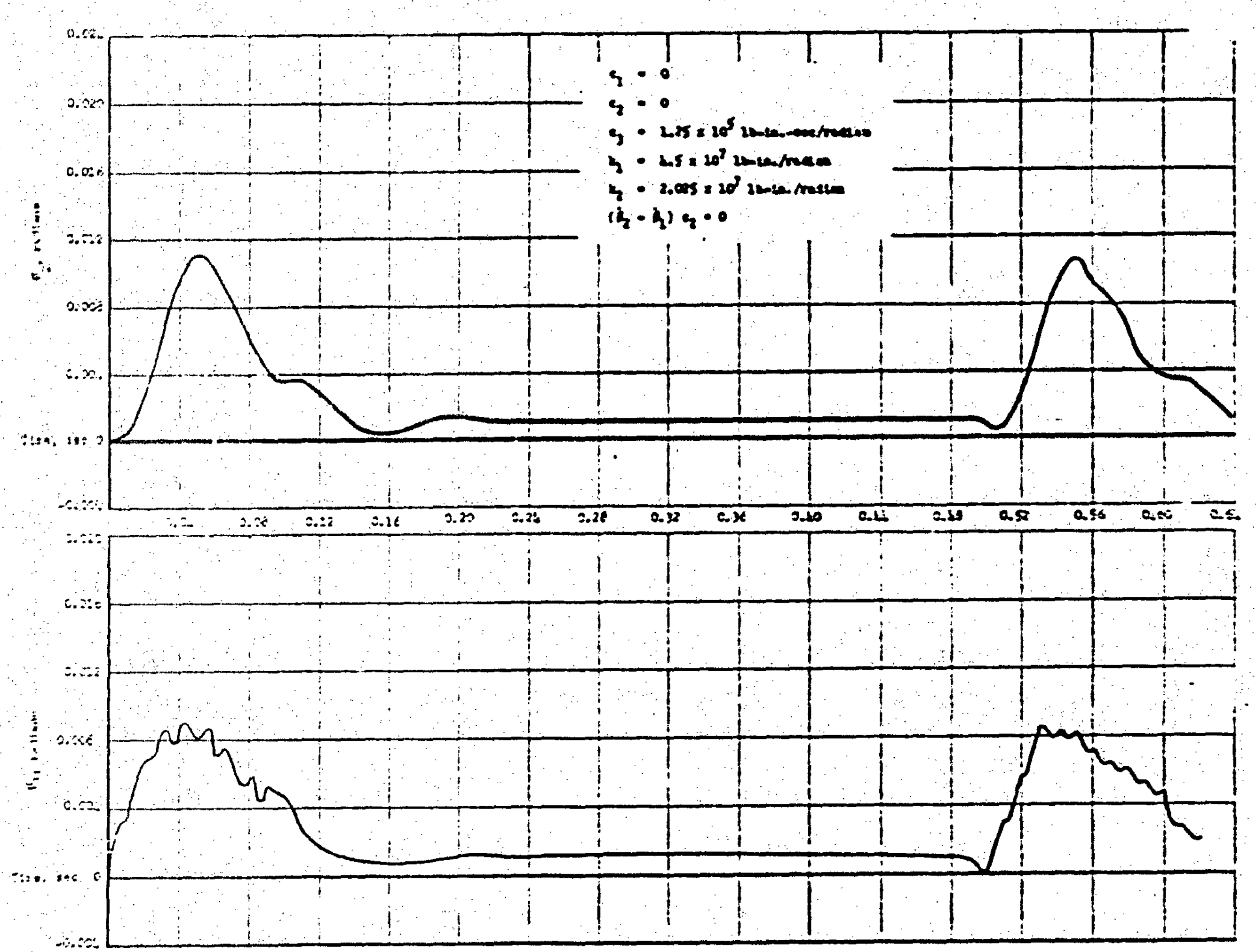

Fig. A-6 CALCULATED RESPONSE OF AN XM70-TYPE LAUNCHER WITH c_3 - DAMPING ONLY

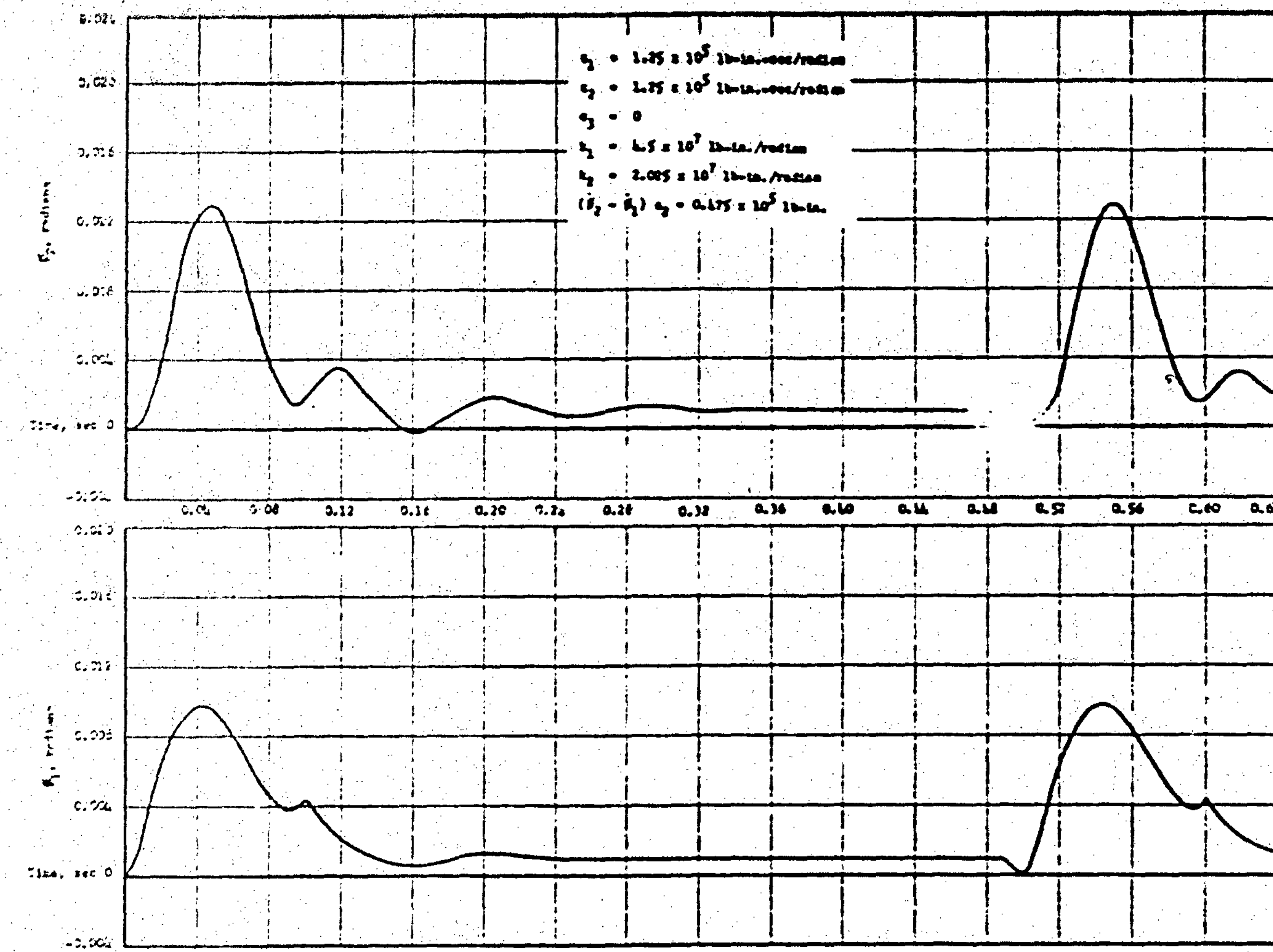

Fig. A-7 CALCULATED RESPONSE OF AN XM70-TYPE LAUNCHER WITH c_1- AND c_2 - DAMPING COMBINED

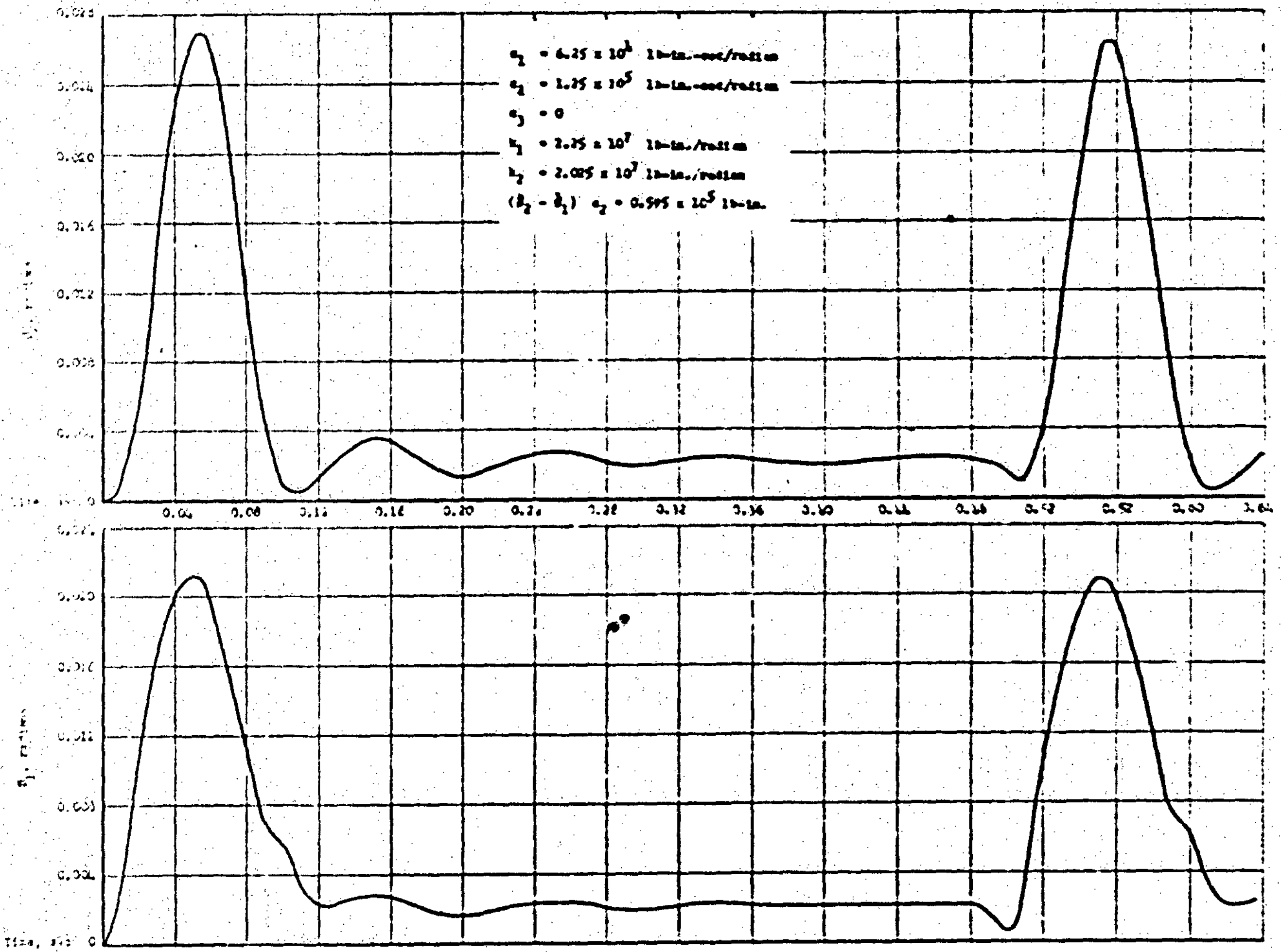

Fig. A-8 CALCULATED RESPONSE OF AN XM70-TYPE LAUNCHER WITH c_1- AND c_2-DAMPING COMBINED AND WITH REDUCED CARRIAGE STIFFNESS

APPENDIX B

A DYNAMIC ANALYSIS OF SOME BASIC DESIGN PARAMETERS

By R. H. Van Beek

I. INTRODUCTION

This appendix contains a dynamic analysis which was intended to aid in determinimg some of the basic design parameters, such as weight and stiffnesses, of weapons of the XM70 type. This analysis uses a relatively simple mathematical model of a weapon together with semiempirical data from the XM70 Prototype Model No. 1. A nomenclature list is at the end of this Appendix.

II. ANALYSIS

It has been shown that the weapon can be represented by a single-degree-of-freedom dynamic model with the recoil force (rod pull) as a forcing function. The assumed model and forcing function are shown in figures B-1 and B-2.

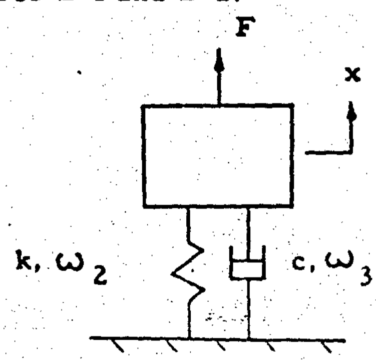

Fig. B-1 MATHEMATICAL MODEL

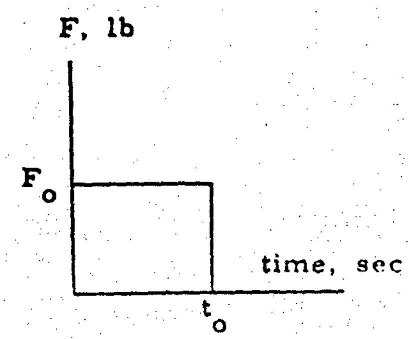

Fig. B-2 FORCING FUNCTION

The differential equation for the system of figure B-1 is

$$M = \ddot{x} + c\dot{x} + kx = F \qquad \text{Eq. (B-1)}$$

$$\text{Let } \eta \equiv \sqrt{\frac{K}{M}}\, t_o\,, \quad \mu \equiv \frac{c}{2\sqrt{KM}}\,, \quad \tau \equiv \frac{t}{t_o}\,, \quad \mathcal{X} \equiv \frac{XM}{F_o t_o^2} \qquad \text{Eq. (B-2)}$$

The solution to differential equation (B-1) in terms of these quantities is

$$x(\tau) = \frac{1}{\eta^2}\left[1 - e^{-\eta\mu\tau}\left(\frac{\mu}{\sqrt{1-\mu^2}}\sin\eta\sqrt{1-\mu^2}\,\tau + \cos\eta\sqrt{1-\mu^2}\,\tau\right)\right] \quad \text{for } 0 \leq \tau \leq 1 \qquad \text{Eq. (B-3)}$$

$$x(\tau) = e^{-\eta\mu\tau}\left[L_1 \sin\eta\sqrt{1-\mu^2}\,\tau + L_2 \cos\eta\sqrt{1-\mu^2}\,\tau\right]$$

$$\text{for } \tau \geq 1 \qquad \text{Eq. (B-4)}$$

$$\text{where } L_1 = \frac{1}{\eta^2}\left[\frac{-\mu}{\sqrt{1-\mu^2}} + e^{\mu\eta}\left(\frac{\mu}{\sqrt{1-\mu^2}}\cos\eta\sqrt{1-\mu^2} + \sin\eta\sqrt{1-\mu^2}\right)\right] \qquad \text{Eq. (B-5)}$$

$$\text{and } L_2 = -\frac{1}{\eta^2}\left[1 + e^{\mu\eta}\left(\frac{\mu}{\sqrt{1-\mu^2}}\sin\eta\sqrt{1-\mu^2} - \cos\eta\sqrt{1-\mu^2}\right)\right] \qquad \text{Eq. (B-6)}$$

For a single degree-of-freedom torsional system, the same solution holds with the dimensionless variables given by

$$x = \frac{\theta I}{T_o t_o^2}, \quad \eta = \sqrt{\frac{k}{I}}\, t_o, \quad \mu = \frac{c}{2\sqrt{kI}}, \quad \tau = \frac{t}{t_o} \qquad \text{Eq. (B-7)}$$

A typical displacement time plot is shown in figure B-3.

Adequate dynamic performance, i.e. acceptable accuracy, results when t_c is less than the time to a subsequent firing and θ_c is a displacement which produces negligible error at the target. Several primary design parameters can be logically determined by finding the minimum weight weapon which will give the required performance.

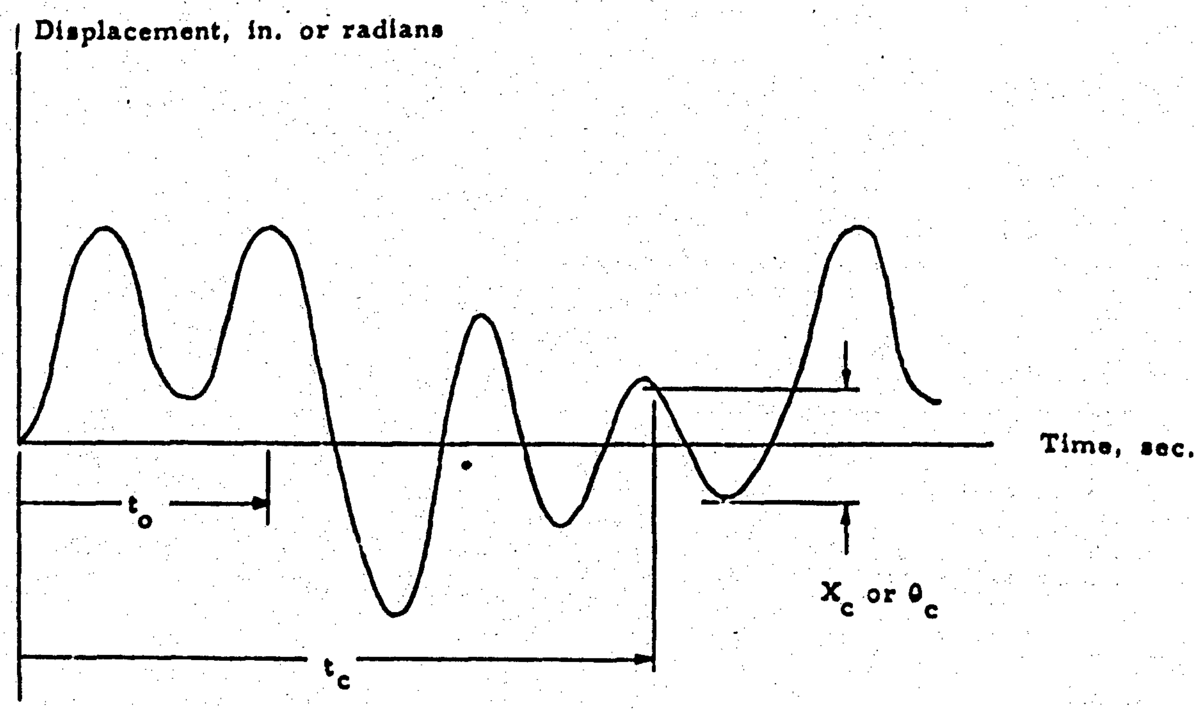

FIG. B-3 TYPICAL TIME DISPLACEMENT CURVE OF THE XM70 LAUNCHER

For given μ and η the graph of x versus τ can be drawn. The last intersection of the curve with $\theta = \pm \theta_c$ determines τ_c. Repeating this procedure for a number of combinations of μ and η gives data for a plot of τ_c versus η for various values of μ. For a given τ_c, a plot of η versus μ can then be drawn. All points on this curve are such that the corresponding η and μ produce a displacement of θ_c at $\tau = \tau_c$ and $\theta < \theta_c$ for $\tau > \tau_c$. All points give values of μ and η for which τ_c is less than the value of τ for which the curve is drawn. Figure B-4 shows a typical graph of τ versus η.

As an approximation, the envelope of equation (B-4) can be used. It is given by

$$\theta_e = L_1^2 + L_2^2 \quad e^{-\eta\mu\tau} \qquad \text{Eq. (B-8)}$$

$$L_1^2 + L_2^2 = \frac{\sqrt{1 - 2e^{\mu\eta} \cos\eta \sqrt{1-\mu^2} + e^{2\mu\eta}}}{\eta^2\sqrt{1-\mu^2}} \qquad \text{Eq. (B-9)}$$

Then

$$(\theta_e)_c = L_1^2 + L_2^2 \quad e^{-\eta\mu\tau_c} \qquad \text{Eq. (B-10)}$$

This eliminates the necessity of drawing the first two of the above mentioned graphs, since, given τ_c and θ_c, for each μ the corresponding η can be found numerically by trial and error. In all cases where the graphs of μ versus η were found by both methods the difference between the graphs was negligible.

Let the total weight of the weapon be given by

$$W_t = W_1 + W_2 + W_3 + W_{NS} \qquad \text{Eq. (B-11)}$$

Assume that the weight of the carriage is related to its rotational stiffness by the linear relation

$$W = \alpha k \qquad \text{Eq. (B-12)}$$

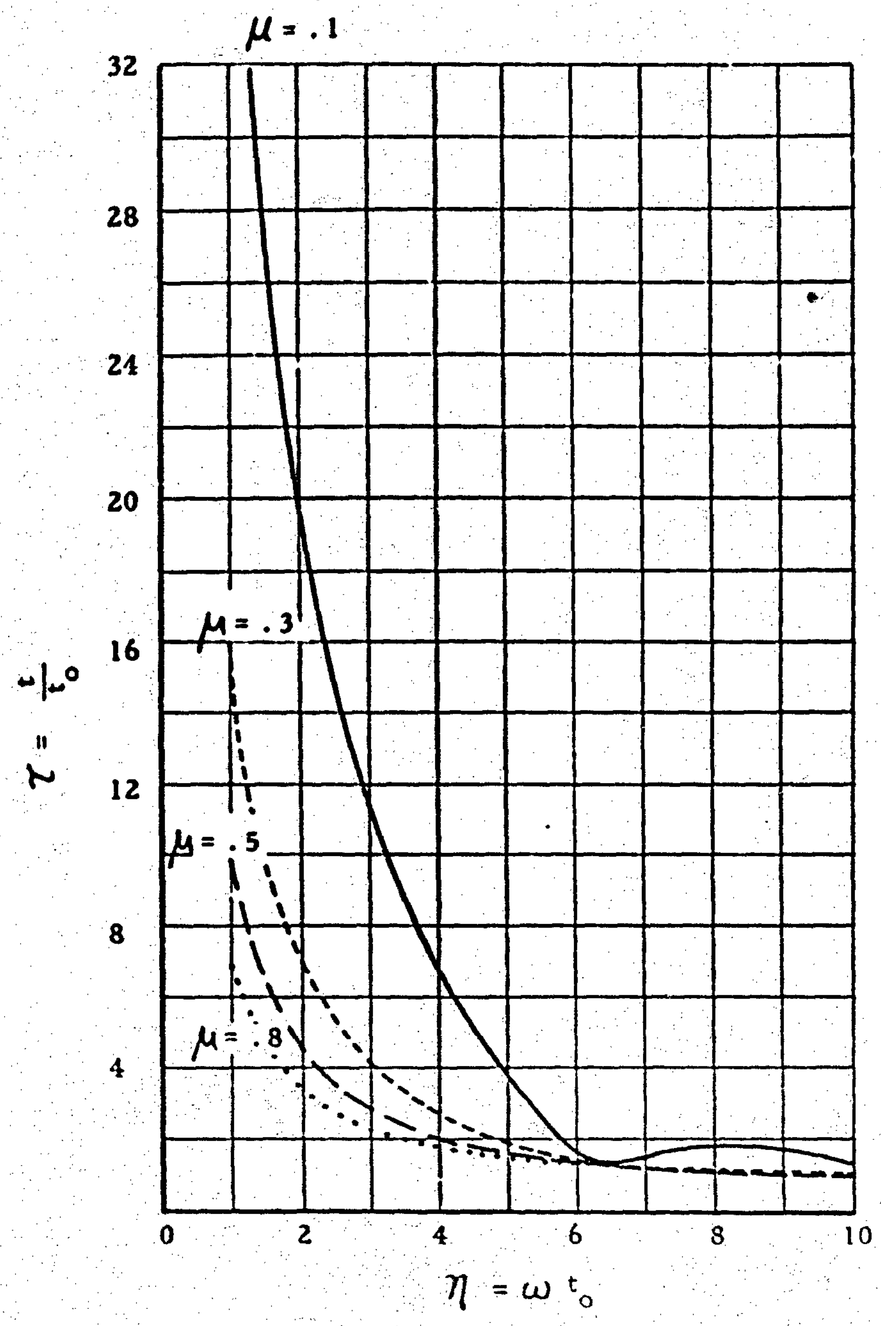

FIG. B-4 TYPICAL GRAPH OF DIMENSIONLESS TIME VERSUS FREQUENCY FOR VARIOUS DAMPING RATIOS

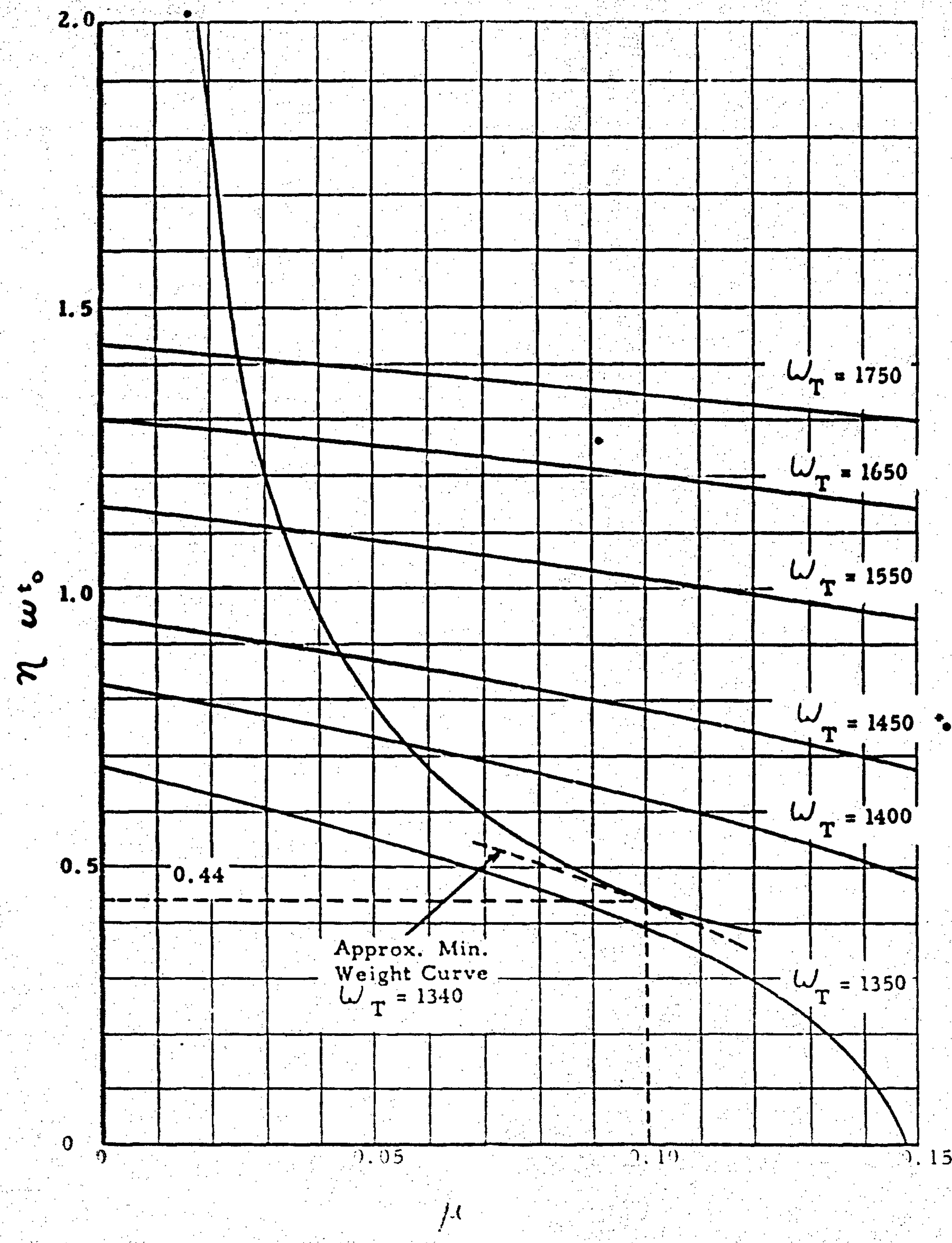

FIG. B-5 MINIMUM WEIGHT REQUIRED TO SATISFY ACCURACY CRITERION

In addition, assume that the weight of the damper is related to the damping ratio by the linear relation

$$W_3 = \beta\mu \qquad \text{Eq. (B-13)}$$

By (B-1), (B-2), and (B-3)

$$W_T - W_H - W_1 = \alpha k + \beta\mu \qquad \text{Eq. (B-14)}$$

By definition

$$\eta = \omega t_o = \frac{k}{I} t_o \qquad \text{Eq. (B-15)}$$

Assuming that one-third of the moment of inertia of the carriage should be added to the moment of inertia of the recording assembly given

$$I = I_1 + 1/3\, I_2$$

$$I = \frac{W_1}{g} r_1^2 + \frac{W_2}{3g} r_2^2$$

$$I = \frac{W_1}{g} r_1^2 + \frac{2k}{3g} r_2^2 \qquad \text{Eq. (B-16)}$$

By eliminating k and I between Eq. (B-4), (B-5), and (B-6), the relation between η and μ for constant W_T is obtained, assuming W_1 and W_H are constants.

$$\eta^2 = \frac{3gt_o^2}{2r_2^2} \left[\frac{\gamma}{3\frac{r_1^2}{r_2^2} + \gamma} \right] \qquad \text{Eq. (B-17)}$$

where $$\gamma \equiv \frac{W_T - W_H - W_1 - \beta\mu}{W_1} \qquad \text{Eq. (B-18)}$$

III. RESULTS

From this relationship, curves of η versus μ for various values of W_T can be plotted. If a curve of η versus μ for the desired value of τ is plotted on the same graph, the lowest possible weight giving acceptable accuracy can be determined. The situation is illustrated in Fig. 5. The constant γ curve can be thought of as representing acceptable performance and the other curves are the constant weight curves. Then the lowest weight curve which just intersects the performance curve gives the minimum total weight and the point of intersection determines the desired damping ratio and η. Then by the use of equations (B-11), (B-12), and (B-13), the carriage stiffness and weight and the damper weight can be calculated. Fig. 5 also shows the results of applying this analysis with the following input data:

Projectile weight*	50 lb.
Muzzle velocity*	1000 ft/sec.
Firing rate	20 rnds/min.
Maximum Amplitude of Vibration at triggering (θ_c)	0.0005 rad.
Maximum Recoil Displacement (Free Recoil until shot ejection is assumed and requires 12 in. of recoil)	24 in.
Recoiling Assembly Weight	500 lb.

The inertia-weight relationships and the carriage stiffness- weight relationship, (α), of the XM 70 were assumed. It will be noted that the hypothetical weapon has a very low firing rate and small recoiling assembly weight and hence has a small mimimum weight. From the graph, the minimum total weight which gives the desired accuracy is 1340 lb. Included in this is a total accessory or non-structural weight which is assumed to be 750 lb. This is the same as the XM70 and includes everything except the recoiling assembly and the carriage structure. Using the values of μ and η from the graph, the damper weight is found to be 67.5 lb. and the carriage weight

* these quantities determine the forcing function

22.5 lb. The carriage stiffness required is 1.12×10^6 lb. in./rad.

This example design, although it theoretically satisfies the accuracy criterion, is impossible because a carriage weighing 22.5 lb. could not carry the rod pull. This result led to the development of strenghth criterion and a method of optimizing recoiling assembly weight. This latter method was used for the XM70 Prototype Model No. 2 and is presented in ARF Project K130 Bi-monthly Report No. 8, Appendix B.

IV. NOMENCLATURE

W_T	total weight of gun
W_{NS}	weight of gun hardware
W_1	weight of recoiling assembly
W_2	weight of carriage
W_3	weight of damper
k	torsional stiffness of carriage
K	spring stiffness for linear vibration system
c	damping stiffness for linear vibration system
M	mass stiffness for linear vibration system

$b = \frac{c}{2M}$

$\omega = \sqrt{\frac{K}{M}} = \sqrt{\frac{k}{I}}$, natural frequency of undamped system

I	effective moment of inertia of torsional vibration system
μ	ratio of damping to critical damping

$\eta = \omega t_o$, non-dimensional frequency

x	displacement for linear vibration system
θ	displacement for torsional vibration system
t	time

$\chi = \frac{Mx}{F_o t_o^2} = \frac{I_\theta}{T_o t_o^2}$ non-dimensional displacement

t_o length of pulse

F_o amplitude of pulse-linear vibration system

T_o amplitude of pulse-torsional vibration system

$\tau = t/t_o$ non-dimensional time

I_1 moment of inertia of recoiling assembly about the base

I_2 moment of inertia of carriage about the base

APPENDIX C

EQUATIONS OF MOTION OF THE LAUNCHER WITH THREE DEGREES OF FREEDOM

R. M. Brach

I. INTRODUCTION

The following equations apply to launchers with a structural geometry corresponding to that of the XM70 automatic rocket launcher. It is a three-degree-of-freedom analysis of gross launcher motion in the vertical plane. These equations are to be used to investigate the stability of the system and the influence on stability of changes in: (1) elevating system stiffness and damping, (2) carriage and trail stiffness, (3) mass distribution, (4) recoil force, and (5) indexing cam length. They can also furnish an indication of the effects due to variations in the muzzle momentum of the projectile. However, because the analysis considers a rigid firing tube, it cannot predict the precise projectile motion at the time of muzzle ejection.

The three degrees of freedom (see Fig. C-1) are the following: (1) the linear displacement of the recoiling mass relative to the cradle, u, (2) the angular motion of the tipping parts relative to the carriage, ϕ_2, and (3) the absolute angular motion of the supporting structure, ϕ_1. The supporting structure in this analysis is taken to be the entire structure that supports the tipping parts; i.e., the supporting structure includes a rigid, massless, trunnion side, an inertia, and a massless, flexible trail. The inertia is an equivalent inertia found by letting the above support contain kinetic and potential energy equal to that of the actual launcher vibrating in its static deflection shape. The supporting structure is assumed to rotate about the ball joint, point 0 in Fig. C-1; a provision for damping the rotation is included. The elevating system is assumed to be a massless spring and damper. The cradle and recoiling mass are both assumed to be rigid bodies.

The equations of motion of the recoiling mass include those describing the constant-force, constant-stopping-distance recoil system,

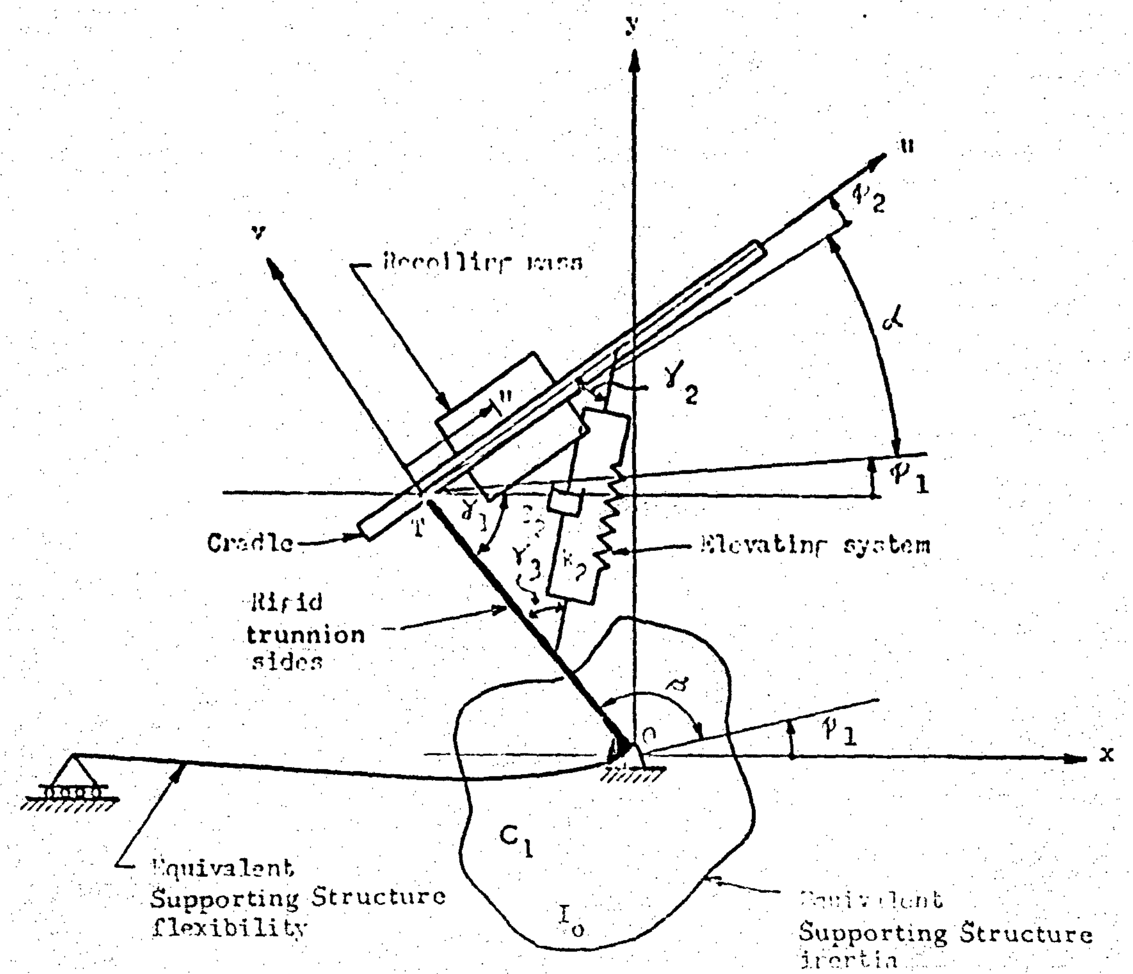

Fig. C-1 SCHEMATIC REPRESENTATION OF THE LAUNCHER

used in the XM70, and also the axial reactions of the indexing cam since these have been found to be significant from past experience.

II. ANALYSIS

A. Kinematics

If the motion of the recoiling mass is described by x_r and y_r with respect to the ground and by u with respect to the cradle, we see from Fig. C-2 that

$$x_r = \ell \cos(\beta + \phi_1) + u \cos(\alpha + \phi_1 + \phi_2)$$

and C-1

$$y_r = \ell \sin(\beta + \phi_1) + u \sin(\alpha + \phi_1 + \phi_2)$$

In these equations, ℓ is the distance from the point 0 to the trunnion, point T , β is the fixed obtuse angle made with ground and the trunnion sides, α is the angle of elevation, ϕ_1 is the angular motion of the supporting structure and ϕ_2 is the angular motion of the tipping parts with respect to the supporting structure. The velocities, $\dot{x}_r$ and $\dot{y}_r$, and the accelerations, $\ddot{x}_r$ and $\ddot{y}_r$, are found by differentiation to be

$$\dot{x}_r = -\ell\dot{\phi}_1 \sin(\beta + \phi_1) + \dot{u} \cos(\alpha + \phi_1 + \phi_2)$$
$$- u(\dot{\phi}_1 + \dot{\phi}_2) \sin(\alpha + \phi_1 + \phi_2)$$

$$\dot{y}_r = \ell\dot{\phi}_1 \cos(\beta + \phi_1) + \dot{u} \sin(\alpha + \phi_1 + \phi_2)$$
$$+ u(\dot{\phi}_1 + \dot{\phi}_2) \cos(\alpha + \phi_1 + \phi_2) \qquad \text{C-2}$$

and

$$\ddot{x}_r = -\ell\ddot{\phi}_1 \sin(\beta + \phi_1) - \ell\dot{\phi}_1^2 \cos(\beta + \phi_1)$$
$$+ \ddot{u} \cos(\alpha + \phi_1 + \phi_2) - \dot{u}(\dot{\phi}_1 + \dot{\phi}_2) \sin(\alpha + \phi_1 + \phi_2)$$
$$- u(\ddot{\phi}_1 + \ddot{\phi}_2) \sin(\alpha + \phi_1 + \phi_2) - \dot{u}(\dot{\phi}_1 + \dot{\phi}_2) \sin$$
$$(\alpha + \phi_1 + \phi_2) - u(\dot{\phi}_1 + \dot{\phi}_2)^2 \cos(\alpha + \phi_1 + \phi_2) \qquad \text{C-3}$$

$$\ddot{y}_r = \ell \ddot{\phi}_1 \cos(\beta + \phi_1) - \ell \dot{\phi}_1^2 \sin(\beta + \phi_1) + \ddot{u} \sin(\alpha + \phi_1 + \phi_2) + \dot{u}(\dot{\phi}_1 + \dot{\phi}_2) \cos(\alpha + \phi_1 + \phi_2) + u(\ddot{\phi}_1 + \ddot{\phi}_2) \cos(\alpha + \phi_1 + \phi_2) + \dot{u}(\dot{\phi}_1 + \dot{\phi}_2) \cos(\alpha + \phi_1 + \phi_2) - u(\dot{\phi}_1 + \dot{\phi}_2)^2 \sin(\alpha + \phi_1 + \phi_2) \qquad \text{C-4}$$

The vector sum of the component $\ddot{x}_r$ and $\ddot{y}_r$ may be resolved into components in the u- and v- directions. These components are denoted as η and ξ, respectively. From Fig. C-3, these are:

$$\ddot{\eta} = \ddot{x}_r \cos \omega_1 + \ddot{y}_r \sin \omega_1 \qquad \text{C-5}$$

$$\ddot{\xi} = \ddot{y}_r \cos \omega_1 - \ddot{x}_r \sin \omega_1 \, , \qquad \text{C-6}$$

where

$$\omega_1 = \alpha + \phi_1 + \phi_2 \, . \qquad \text{C-7}$$

Substituting Eq. C-3 and 4 into Eq. C-5 and 6 gives the following expression,

$$\ddot{\eta} = -\ell \ddot{\phi}_1 \sin \omega_2 - \ell \dot{\phi}_1^2 \cos \omega_2 + \ddot{u} - u(\dot{\phi}_1 + \dot{\phi}_2)^2 \qquad \text{C-8}$$

$$\ddot{\xi} = \ell \ddot{\phi}_1 \cos \omega_2 - \ell \dot{\phi}_1^2 \sin \omega_2 + 2\dot{u}(\dot{\phi}_1 + \dot{\phi}_2) + u(\ddot{\phi}_1 + \ddot{\phi}_2) \, . \qquad \text{C-9}$$

where

$$\omega_2 = \beta - \alpha - \phi_2 \, . \qquad \text{C-10}$$

B. Equations of Motion

Equations C-8 and C-9 are the components of the absolute acceleration of the recoiling mass. The free body diagram of the recoiling mass is shown in Fig. C-4. Summing forces acting through the mass center, we obtain

$$m_r \ddot{\eta} = -F(t) + \Phi(t) + e\mu |N| - m_r g \sin \omega_1 \, . \qquad \text{C-11}$$

$$m_r \ddot{\xi} = N - m_r g \cos \omega_1 \, . \qquad \text{C-12}$$

In these equations the following nomenclature is used:

F (t) applied force

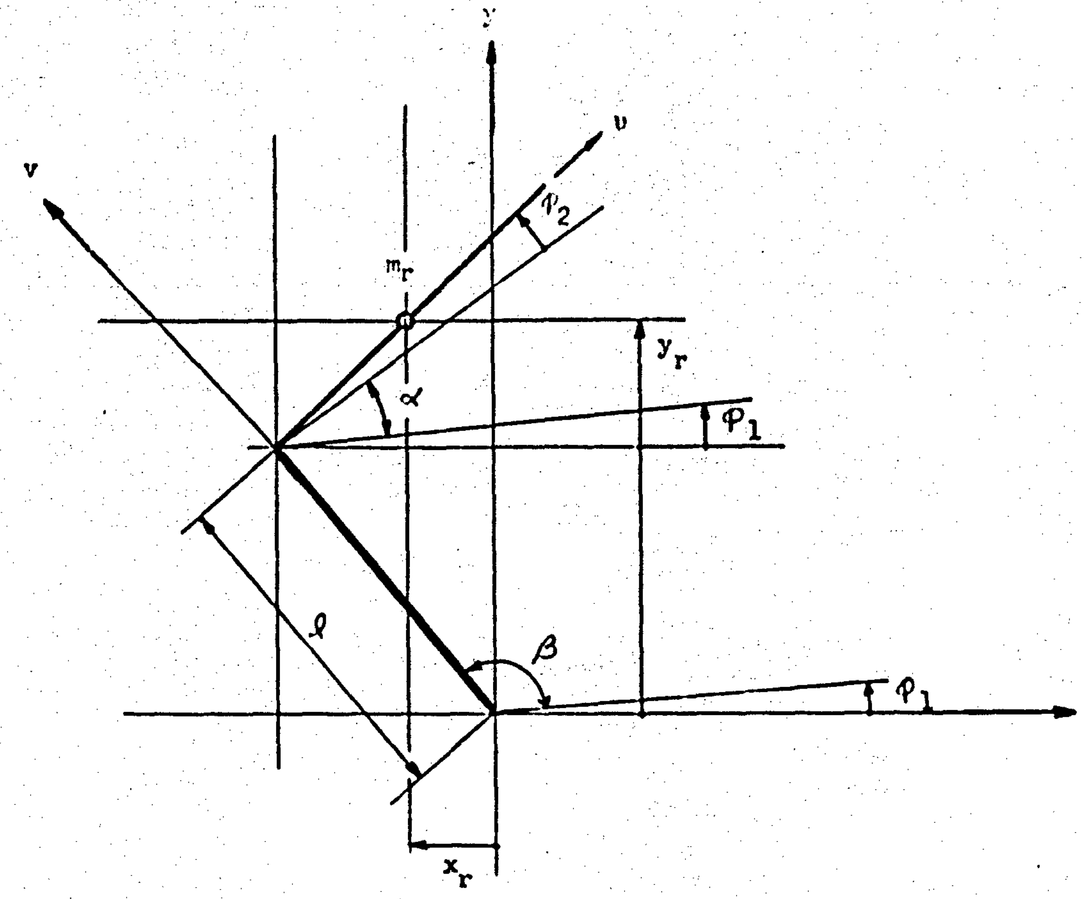

Fig. C-2 GEOMETRIC REPRESENTATION OF AN XM70-TYPE LAUNCHER

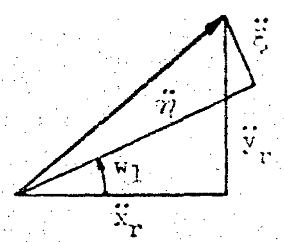

Fig. C-3 VECTOR COMPONENT TRANSFORMATION

$T'(t)$	applied moment (powder couple equal to $\epsilon F(t)$ where ϵ is the moment arm from the bore center to the recoiling mass cg.
$\Phi(t)$	reactions of the recoil system and cam
N	normal reaction force between the cradle and recoiling mass
T	moment reaction between the cradle and recoiling mass
μ	coefficient of Coulomb friction between the cradle and recoiling mass
e	$e = 1,\ \dot{u}<0;\ e = -1,\ \dot{u}>0;\ e = 0,\ \dot{u} = 0$

The XM70 launchers have very low friction ball bearings between the cradle and recoiling parts; the force $\mu|N|$ is therefore negligible compared to the seal friction. Because the absolute value sign, the term becomes unwieldy in later expressions and is neglected at this point.

If I_r is the moment of inertia of the recoiling mass about an axis through the mass center, we may write

$$I_r(\ddot{\phi}_1 + \ddot{\phi}_2) = T + T' \qquad \text{C-13}$$

In order to evaluate the retarding force, $\Phi(t)$, we must know what type of resistance is furnished by the recoil system. The system used in the XM70 launchers contains a preloaded recuperator or air spring to hold the mass in battery position at angles of elevation. Sufficient accuracy will be obtained if a linear spring rate is used to represent the recuperator. The recoil force is furnished by forcing oil through a variable-area orifice. The total retarding force is then made up of the following terms:*

$$K,\ k(u_o - u),\ R(\dot{u}^2, u),\ H_1,\ H_3(\dot{u}^2, u) \quad . \qquad \text{C-14}$$

The nomenclature used is

K	recuperator preload
k	recuperator spring rate
R	hydraulic resistance
H_1	constant friction force
H_3	hydraulic system seal frictional force
u_o	in-battery position of the recoiling mass

* For a more complete description of the recoil system, see Bimonthly Report No. 7 of this Project (8130)

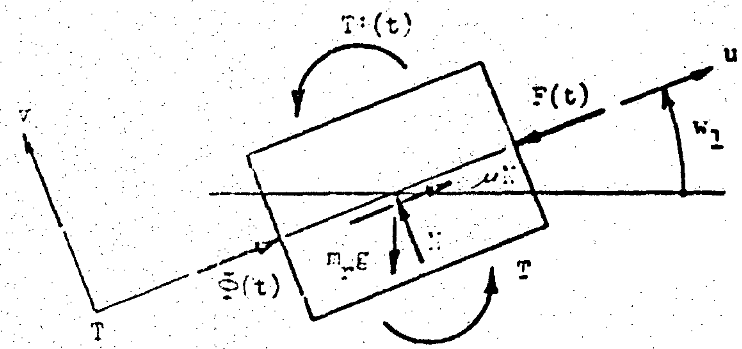

Fig. C-4 FREE BODY DIAGRAM OF THE RECOILING MASS

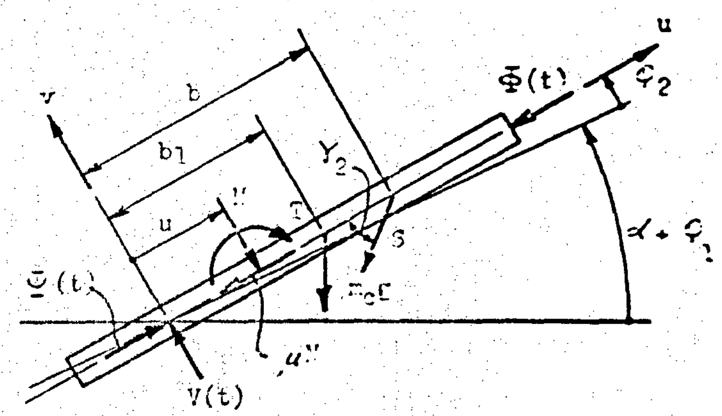

Fig. C-5 FREE BODY DIAGRAM OF THE CRADLE

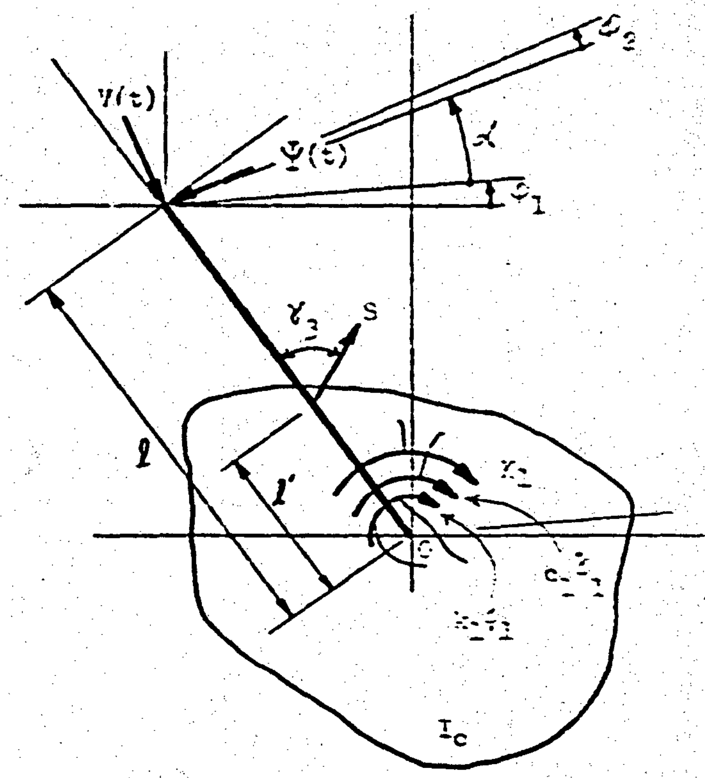

Fig. C-6 FREE BODY DIAGRAM OF THE EQUIVALENT FIRING SUPPORT

The cam reaction force in the direction of recoil may be represented by $C(\ddot{u}, \dot{u}, u)$; the actual functions will be introduced later, in order to keep the lengths of the expressions to a minimum. The total retarding force is, then,

$$\Phi(t) = K + k(u_o - u) + eR(\dot{u}^2, u) + eH_1 + eH_3(\dot{u}^2, u) + efC(\ddot{u}, \dot{u}, u). \qquad \text{C-15}$$

In this expression, $f = 0$, except when $u_1 < u < u_2$ and $u < 0$, that is when the recoiling mass is counterrecoiling through the cam, beginning at u_1 and ending at u_2, otherwise $f = +1$.

We will now consider a rigid cradle with a free body diagram as shown in Fig. C-5. It is assumed that there is no relative angular motion between the cradle and recoiling mass; because of this, the coordinates of the mass center of the cradle may be immediately written from Eq. C-1. This is done by substituting the constant length b_1 for u. These equations are

$$x_c = \ell\cos(\beta + \phi_1) + b_1\cos\omega_1$$

and $\qquad$ C-16

$$y_c = \ell\sin(\beta + \phi_1) + b_1\sin\omega_1$$

The length b_1 is the distance along the u-axis from the trunnion to the cradle mass center, and x_c and y_c are the absolute coordinates of the mass center of the cradle. The corresponding velocity and acceleration components may be found by differentiation of Eq. C-16 or by similar substitution of b_1 for u in Eq. C-2, 3, and 4. The components of acceleration of the cradle mass center are:

$$\ddot{x}_c = -\ell\ddot{\phi}_1\sin(\beta + \phi_1) - \ell\dot{\phi}_1^2\cos(\beta + \phi_1) - b_1(\ddot{\phi}_1 + \ddot{\phi}_2)\sin\omega_1 - b_1(\dot{\phi}_1 + \dot{\phi}_2)^2\cos\omega_1 \qquad \text{C-17}$$

$$\ddot{y}_c = \ell\ddot{\phi}_1\cos(\beta + \phi_1) - \ell\dot{\phi}_1^2\sin(\beta + \phi_1) + b_1(\ddot{\phi}_1 + \ddot{\phi}_2)\cos\omega_1 - b_1(\dot{\phi}_1 + \dot{\phi}_2)^2\sin\omega_1 \qquad \text{C-18}$$

If we let the vector sum of the components of x_c and y_c be resolved into components ζ and λ, respectively, in the u-, v-coordinate system using Fig. C-3, we have

$$\ddot{\zeta} = -\ell\ddot{\phi}_1\sin\omega_2 - \ell\dot{\phi}_1^2\cos\omega_2 - b_1(\dot{\phi}_1 + \dot{\phi}_2) \qquad \text{C-19}$$

and

$$\ddot{\lambda} = \ell \ddot{\phi}_1 \cos \omega_2 - \ell \dot{\phi}_1^2 \sin \omega_2 - b_1 (\ddot{\phi}_1 + \ddot{\phi}_2) \qquad \text{C-20}$$

The equations of motion of the cradle mass center may now be found by summing forces in the u- and v-directions. These are:

$$m_c \ddot{\zeta} = \Psi(t) - \Phi(t) - S \cos \gamma_2 - m_c g \sin \omega_1 \qquad \text{C-21}$$

$$m_c \ddot{\lambda} = V(t) - N - m_c g \cos \omega_1 - S \sin \gamma_2 \ , \qquad \text{C-22}$$

where the following nomenclature is used:

Ψ (t)	trunnion reaction in the u-direction
V (t)	trunnion reaction in the v-direction
S	force in the elevating system.

The displacement of one end of the elevating system relative to the other is given by $b\phi_2 \sin \gamma_2$. The force developed, assuming a linear spring and damping proportional to the first derivative of the displacement, is

$$S = K_2 + k_2 b(\sin \gamma_2)\phi_2 + c_2 b(\sin \gamma_2)\dot{\phi}_2 \qquad \text{C-23}$$

The preload is given by K_2, the rate by k, and the damping coefficient by c_2. In this expression, the angle γ_2 is assumed constant. The angular equation of motion of the cradle is found by summing moments about the mass center. From this we get

$$I_c (\ddot{\phi}_1 + \ddot{\phi}_2) = - b_1 V(t) - T + N(b_1 - u) - S(b - b_1) \sin \gamma_2 \qquad \text{C-24}$$

In Eq. C-24, I_c is the moment of inertia of the cradle about the mass center. The preload K_2 is the preload necessary to balance the component of force due to the weight of the recoiling mass and the cradle itself.

The final equation of motion may now be found by summing moments on the firing support about the fixed point 0 (see Fig. C-6):

$$I_o \ddot{\phi}_1 = \Psi(t) \ell \sin \omega_2 - V(t) \ell \cos \omega_2 - S \ell' \sin \gamma_3$$
$$- K_1 - k_1 \phi_1 - c_1 \dot{\phi}_1 \qquad \text{C-25}$$

For any angle of elevation, it will be assumed that γ_3 is a constant; also the following relationship will be used:

$$\gamma_3 \approx \gamma_3\Big|_{\alpha=0} - \alpha \equiv \gamma_o - \alpha \qquad \text{C-26}$$

We must now express the recoil and cam forces in terms of the variables of this analysis. The recoil force is given as

$$eR(\dot{u}^2, u) = \frac{e\,\gamma A_p^{\,3}}{2\,g\,C_o^{\,2}\alpha_o^{\,2}}\quad \dot{u}^2 \ , \qquad \text{C-27}$$

where the following nomenclature is used:

γ	density of the oil
A_p	piston area
C_o	orifice coefficient
α_o	orifice area (function of u)

For this analysis, it is assumed that the seal friction is directly proportional to the recoil pressure (or force) and may be expressed as

$$H_3 = \delta R \ , \qquad \text{C-28}$$

where δ is a constant.

A cycloidal indexing cam shape is used in this analysis (as on the XM70 launcher). The axial component of force is

$$C = \frac{I_B}{R_1^2}\left[\frac{h^2}{(u_2 - u_1)^2}\right]\left[\frac{2\pi}{u_2 - u_1}\ \sin\ 2\pi\frac{u - u_1}{u_2 - u_1}\right.$$

$$\left.\left(1 - \cos 2\pi\frac{u - u_1}{u_2 - u_1}\right)\dot{u}^2 + \left(1 - \cos 2\pi\frac{u - u_1}{u_2 - u_1}\right)^2 \ddot{u}\right] \qquad \text{C-29}$$

The launcher has two breech clusters containing three rounds each. For this analysis, it is assumed that only one cluster exists containing six rounds; however, the proper moment of inertia, I_B, corresponding to the combined, double cluster will be used. In Eq. C-29, h is the height of the cam path development and R_1 is the pitch radius.

Substituting the last three relationships into Eq. C-11, 12, 13, 21, 22, 24, and 25, and eliminating the four unknown reactions, T, V, N, and Ψ, leaves three equations. These three equations are second order, non-linear, differential equations, with the variables ϕ_1, ϕ_2, and u.

They are:

$$m_r\,(\ell\sin\omega_2+u)\,\ddot{\phi}_1+\left[ef\,\frac{I_B}{R_1{}^2}\,\frac{h^2}{(u_2-u_1)^2}\,\left(1-\cos 2\pi\frac{u-u_1}{u_2-u_1}\right)^2-m_r\right]\ddot{u}$$

$$=-m_r u\,(\dot{\phi}_1+\dot{\phi}_2)^2+F(t)-K-k\,(u_o-u)+m_r\ell\cos\omega_2\,\dot{\phi}_1{}^2$$

$$-e\left[(1+\delta)\left(\frac{\gamma A_p{}^3}{2g\,C_o{}^2\alpha_o{}^2}\right)+f\,\frac{I_B}{R_1{}^2}\,\left(\frac{2\pi h^2}{(u_2-u_1)^3}\,\sin 2\pi\frac{u-u_1}{u_2-u_1}\right)\cdot\right.$$

$$\left.\cdot\left(1-\cos 2\pi\,\frac{u-u_1}{u_2-u_1}\right)\right]\,\dot{u}^2\qquad -cH_1+m_r g\sin\omega_1 \qquad \text{C-30}$$

and

$$\ddot{\phi}_1\left[\dot{I}_o+m_c\ell^2+(\ell\cos\omega_2+u)\,m_r\ell\cos\omega_2+m_c\,b_1\ell\cos\omega_2\right]+$$

$$+\ddot{\phi}_2\left[m_r\,u\ell\cos\omega_2+m_c\,b_1\ell\cos\omega_2\right]+\ddot{u}\left[-ef\ell\sin\omega_2\cdot\right.$$

$$\left.\cdot\frac{I_B\,h^2}{R_1{}^2\,(u_2-u_1)^2}\,\left(1-\cos 2\pi\,\frac{u-u_1}{u_2-u_1}\right)^2\right]=\ell\sin\omega_2\left[-\,b_1\,m_c\cdot\right.$$

$$\left.\cdot(\dot{\phi}_1+\dot{\phi}_2)^2+m_r\ell\cos\omega_2+K+k\,(u_o-u)+m_c g\sin\omega_1\right]+$$

$$\ell\cos\omega_2\left[-2\,m_r\dot{u}\,(\dot{\phi}_1+\dot{\phi}_2)-g\cos\omega_1\,(m_r+m_c)\right]+$$

$$+\;e\,\ell\sin\omega_2\left[(1+\delta)\,\frac{\gamma A_p{}^2}{2g\,C_o{}^2\alpha_o{}^2}\quad\dot{u}^2+H_1+f\,\frac{I_B\,2\pi\,h^2}{R_1{}^2\,(u_2-u_1)^3}\right.$$

$$\left.\sin 2\pi\,\frac{u-u_1}{u_2-u_1}\,\left(1-\cos 2\pi\frac{u-u_1}{u_2-u_1}\right)\,\dot{u}^2\right]\qquad -C_1\,\dot{\phi}_1+$$

$$-k_1\,\phi_1-K_1+\left[K_2+k_2 b(\sin\gamma_2)\phi_2+C_2\,b(\sin\gamma_2)\dot{\phi}_2\right]\cdot$$

$$\cdot\left[\ell\sin(\omega_2-\gamma_2)-\ell'\sin(\gamma_o-\alpha)\right]\qquad \text{C-31}$$

and

$$\ddot{\phi}_1\left[I_c+I_r+m_r\,u\,(\ell\cos\omega_2+u)+b_1\,m_c\,(\ell\cos\omega_2+b_1)\right]$$

$$+\ddot{\phi}_2\left[I_c+I_r+m_r\,u^2+m_c\,b_1{}^2\right]=\dot{\phi}_1{}^2\,\ell\sin\omega_2\,(m_r\,u+m_c\,b_1)+$$

$$- 2 m_r u \dot{u} (\dot{\phi}_1 + \dot{\phi}_2) - g \cos \omega_1 (m_r u + m_c b_1) + \epsilon F(t)$$

$$- b \sin \gamma_2 \left[K_2 + b \sin \gamma_2 (k_2 \phi_2 + c_2 \dot{\phi}_2) \right] . \qquad \text{C-32}$$

III. DISCUSSION

Based upon the assumption made, the solution to the three differential equations of motion just derived will furnish the first mode response of the launcher in the vertical plane. The reaction forces and moments may also be found when the equations of motion are solved. Because of the complexity of these expressions, their solution is obtained on the Technology Center Univac 1105 digital computer. The programming of these equations and the results obtained is presented in other appendices.

APPENDIX D

DIGITAL COMPUTER PROGRAM, THREE-DEGREE-OF-FREEDOM MATHEMATICAL MODEL

R. M. Brach

I. INTRODUCTION

The equations of motion of a three-degree-of-freedom system representing an XM70-type launcher are presented in Appendix C. Because of the complexity of these equations, they are being solved numerically on Armour Research Foundation's Univac 1105 digital computer. In this appendix, the computer program is described and some results are compared with previous work.

II. COMPUTER PROGRAM

Basically, the computer program constitutes the numerical solution of a set of three, second-order, non-linear differential equations. The solution was programmed in a non-algebraic, symbolic language called USE (Univac Scientific Exchange). A side-by-side listing of the program, as written, and its octal representation are shown in Fig. D-3. Program output format is illustrated in Fig. D-4, which is the first page of output of a typical run.

A subroutine was written for general use by Robert Floyd of Armour Research Foundation based on the numerical technique of Runge and Kutta for the solution of up to 50, first-order, simultaneous differential equations. It is applied here to solve the three, second-order equations after a reduction of their order by three trivial substitutions, such as $\dot{u} = s$. The subroutine is shown listed after the main program with the call address, RWF999. One other special subroutine was written, RWF998, to allow the use of two tabular functions: in this case, an experimental powder-gas forcing function and a table of recoil-system orifice areas. This subroutine employs linear interpolation between points. It is also listed after the main program. All other subroutines used are from the standard ARF library.

Fig. D-1 shows a general program flow diagram. A detailed flow diagram showing how the time of application of the powder gas force is derived from the position and velocity of the recoiling parts is shown in Fig. D-2.

III. RESULTS

Two comparisons of the output of this program will be made in this appendix: (1) a comparison with a previous computer program of the parent project and (2) a comparison with experimental curves obtained from firings of the Prototype No. 1 launcher.

The physical launcher parameters used for the first comparison are taken from Prototype No. 1. The response curve from an early computer program is shown in Fig. D-5; the corresponding response curve from the present computer program is shown in Fig. D-6. Table D-1 points out the significant similarities of and differences between the two sets of equations of motion and launcher parameters.

The two curves are seen to differ slightly in amplitude and frequency. The amplitude differences may be accounted for by the difference in recoil forces between the two: the recoil force in the current program peaks significantly near the end of recoil as does the recoil force of the actual launcher, whereas in the early program, the recoil force remains nearly constant. The frequency differences probably are due to the inclusion of the elevating system flexibility in the current program, even though that system is very stiff.

The second comparison utilizes the experimental record of the first shot of Burst No. L68-L73, which was fired at Redstone Arsenal on February 22, 1959 (presented in Appendix II-A of Report No. 11 of the parent project). Figure D-7 shows the trail strain, cradle motion, and recoil force measured during that burst. The response as given by the current computer program is shown in Fig. D-8. The input data to the computer program to be compared are shown in Table D-2. The chosen elevating system stiffness value is seen to be relatively low; it may be recalled that the elevating screw brackets on the Prototype No. 1 were found to be relatively flexible.

Table D-1

COMPARISON OF MODELS AND LAUNCHER PARAMETERS

Item	Old Program	New Program
Degrees of freedom	Recoil motion, carraige rotation, hop of firing base	Recoil motion, carraige rotation, cradle rotation relative to the carriage
Launcher Geometry	Pilot No. 1 at 15° elevation	Pilot No. 1 at 15° elevation
Values of Mass	Pilot No. 1	Pilot No. 1
Elevating System Stiffness	Rigid	1×10^6 lb/in.
Equivalent Carriage Stiffness	100×10^6 in. -lb/radian	100×10^6 in. -lb/radian
Recoil System	Computed from equations of a theoretical recoil system	Computed from equations of a theoretical recoil system using actual orifice areas from Pilot No. 3 rods.
Auxiliary damping	None	None

Table D-2

INPUT DATA TO COMPUTER PROGRAM

Item	Value in Program
Launcher Geometry	Pilot No. 3 at 45° elevation
Values of Mass	Pilot No. 3 (See parameter list in Program, Fig. D-3)
Elevating System Stiffness	1.405×10^4 lb/in.
Elevating System Damping Coefficient	90 lb-sec/in.
Equivalent Carriage Stiffness	45×10^6 in. -lb/radian

The similarity between the experimental and computed curves is striking, even down to details such as the influence of indexing forces between times 0.26 and 0.4. Especially important is the reproduction of the computed curve of cradle motion in the experimental curve just prior to the time of firing of the second round. This cradle motion, the most undesirable part of the gross response of the Prototype No. 1 launcher, was subsequently reduced by designing a stiffer elevating system. By means of an accurate computer program, however, the optimum combination of parameters can easily be found for a desired response.

IV. CONCLUSIONS

The examples presented in this appendix indicate: (1) that the current computer program corresponds closely to previous theoretical work, which means that errors do not exist either in the equations that were programmed or in the program itself; and (2) that the data derived from the current computer program represent gross experimental launcher response very accurately, which means that the program may be used to improve that response.

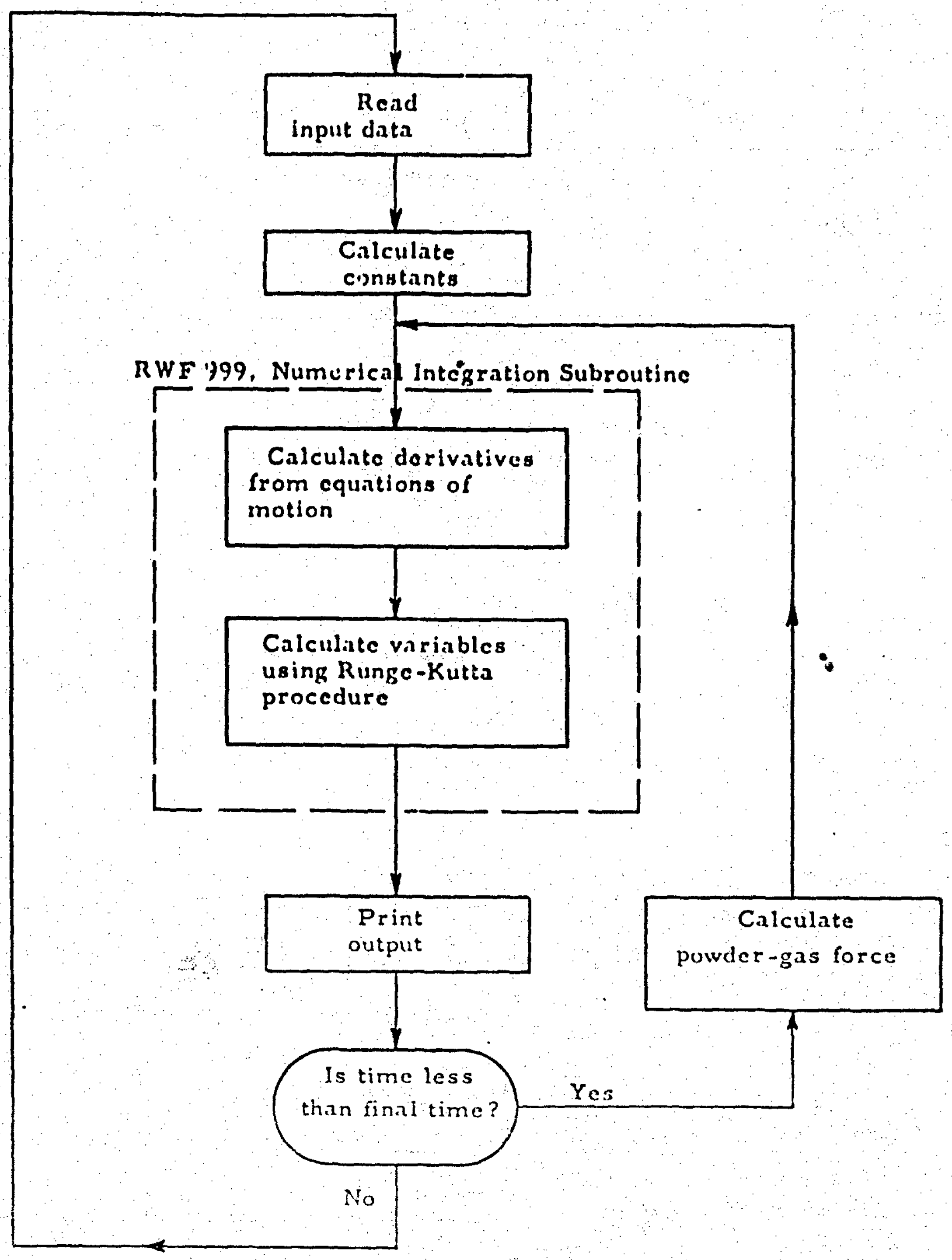

Fig. D-1 COMPUTER PROGRAM FLOW CHART

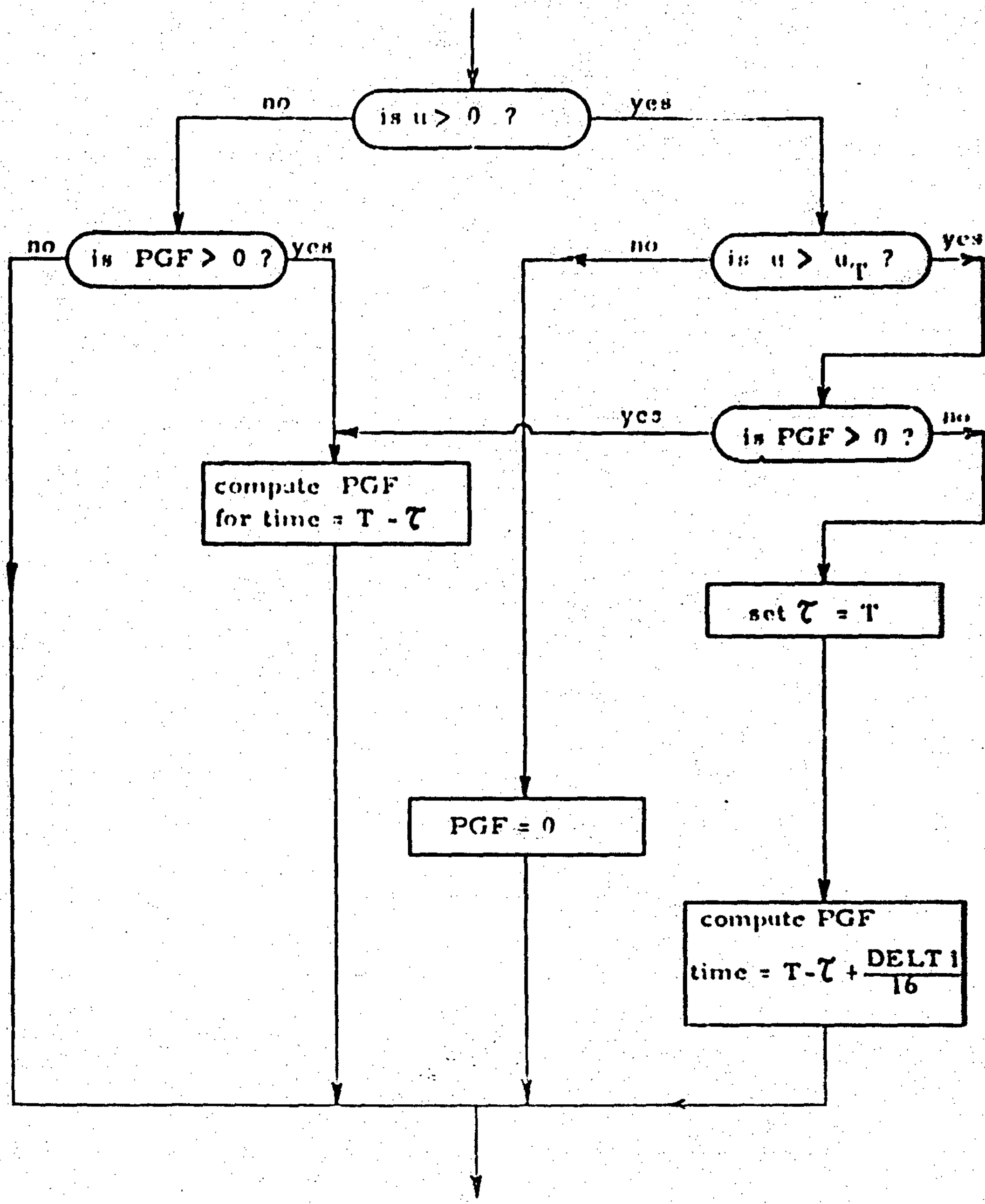

PGF . . . . . . Powder-gas force

T . . . . Time

UT . . . . Trigger Position

τ . . . . Time between shots of a burst

DELT 1 . . . . . Increment of tabular powder-gas force function

Fig. D-2 POWDER-GAS FORCE SELECTION FLOW DIAGRAM

```
                                  110.  . DELT   . EQUALS .309     .309   .TABULAR TIME INTERVAL LOCATIONS$
                                  111.  . A      . EQUALS .4       .4     .$
                                  112.  . M      . EQUALS .5       .5     .$
                                  113.  . I      . EQUALS .6       .6     .$
                                  114.  . INTA1  . EQUALS .9       .9     .$

                                  115.  . INTA2  . EQUALS .10      .10    .$
                                  116.  . B      . EQUALS .11      .11    .$
                                  117.  . AM11   . EQUALS .12      .12    .$
                                  118.  . AM12   . EQUALS .13      .13    .$
                                  119.  . W      . EQUALS .14      .14    .$
                                  120.  . JINTA1 . EQUALS .59      .59    .$
                                  121.  . JINTA2 . EQUALS .60      .60    .$
                                  122.  . JB     . EQUALS .61      .61    .$
                                  123.  . JAM11  . EQUALS .62      .62    .$
                                  124.  . JAM12  . EQUALS .63      .63    .$
                                  125.  . JW     . EQUALS .64      .64    .$
                                  126.  .        . SETLOC .310     .310   .*

00465  00466  00 00000 00000      127.  . TML1   . F      .0       .      .TABLE OF FORCE,PGES
                                  128.  .        . SETLOC .310     .310   .$
00632  00632  00 00000 00000      129.  . TML2   . F      .0       .      .TABLE OF 1 REC.CYL. ORFICE AREAS
                                  130.  .        . SETLOC .510     .510   .$
                                  131.  . RES1   . RESERV .2       .2     .$
                                  132.  . RES2   . RESERV .2       .2     .$
                                  133.  . LAT    . RESERV .2       .2     .$
01004  01004  20 15435 37310      134.  . MC     . F      .1.3894  .      .MASS,CRADLES
01005  01005  20 24131 37461      135.  . MR     . F      .3.2749  .      .MASS,RECOILING ASSEMBLYS
01006  01006  20 54441 30132      136.  . IM     . F      .51.429  .      .MOM.OF INER.,BREECH CLUSTERS$
01007  01007  21 34355 14472      137.  . IC     . F      .1174.4  .      .MOM.OF INER.,CRADLES
01010  01010  21 44770 00000      138.  . IR     . F      .2852.0  .      .MOM.OF INER.,REC.ASSEMBLYS
```

FIG. D-3 COMPUTER PROGRAM

```
01011  01011  21 35274 00000   139.  • AS     • F   •1975.0      •   •PRELOAD•RECUPERATORS
01012  01012  20 75540 00000   140.  • A      • F   •91.0        •   •RATE•RECUPERATORS
01013  01013  00 00000 00000   141.  • KK1    • F   •0           •   •PRELOAD•CARRIAGE FLEXIBILITYS
01014  01014  00 00000 00000   142.  • KK2    • F   •0           •   •PRELOAD•ELEVATING SYSTEMS
01015  01015  20 44400 00000   143.  • L      • F   •38.         •   •LENGTH•TRUNNION TO ELEVATING SYS.S
01016  01016  20 56514 63146   144.  • L1     • F   •24.6        •   •LENGTH• TRUNNION TO CRADLE C. OEM.S
01017  01017  20 44400 00000   146.  • LT     • F   •34.         •   •LENGTH•BALL JOINT TO TRUNNIONS
01020  01020  20 17000 00000   147.  • R1     • F   •1.75        •   •CAMPAIN PITCH RADIUSS
01021  01021  20 17347 73717   148.  • H      • F   •1.932       •   •HEIGHT OF CYCLOIDAL CAM DEVEL.S
01022  01022  21 16027 00000   149.  • G      • F   •386.        •   •ACCELERATION OF GRAVITYS
01023  01023  17 44035 41755   150.  • GAMA   • F   •0.0313      •   •OIL DENSITYS
01024  01024  20 24554 57211   151.  • AP     • F   •2.35619     •   •AREA OF 1 REC.SYS.PISTONS

01025  01025  20 75144 34451   152.  • CD     • F   •0.65        •   •ORIFICE COEFFICIENTS
01026  01026  20 77530 00000   153.  • BETA   • F   •173.5       •   •ANGLE OF TRUNNION SIDE PAT GROOVES.S
01027  01027  17 75075 34122   154.  • DELTA  • F   •0.01        •   •COEFFICIENT OF SEAL FRICTIONS
01030  01030  17 45075 34122   155.  • MU     • F   •0.04        •   •COEFFICIENT OF CRADLE BRG.FRICTIONS
01031  01031  20 75047 61115   156.  • LMS    • F   •0.633       •   •BRAKE CONTROL MOMENT ARMS
01032  01032  20 75237 14001   157.  •        • F   •0.654       •   •SAMES
01033  01033  17 77427 40421   158.  •        • F   •0.497       •   •SAMES
01034  01034  17 74441 62410   159.  •        • F   •0.321       •   •SAMES
01035  01035  17 75724 30641   160.  •        • F   •0.315       •   •SAMES
01036  01036  20 04151 30152   161.  •        • F   •0.557       •   •SAMES
01037  01037  15 76111 50457   162.  • DELT1  • F   •0.0015      •   •INTERVAL OF TPL1S
01040  01040  17 74000 00000   163.  • DELT2  • F   •0.25        •   •INTERVAL OF TPL2S

01041  01041  20 04000 00000   164.  • SING2  • F   •0.5         •   •SIN(GAMMA2)•ELEVATING SYS:S
01042  01042  20 06731 17204   165.  • COSG2  • F   •0.866025    •   •COS(GAMMA2)•ELEVATING SYS:S
01043  01043  20 07151 60020   166.  • SINGA  • F   •0.964049    •   •SIN(GAMMA)AT ALPHA EQUAL ZEROS
01044  01044  20 34530 41217   167.  • LTP    • F   •9.42        •   •LENGTH•BALL JOINT TO ELEVATING BRACKETS
01045  01045  00 00000 00000   168.  • I      • X   •0           •   •PRINTOUT CONSTANTSS
01046  01046  00 00000 00004   169.  • II     • X   •4           •   •NO. OF TIME INTERVALS BETW. PRINTOUTSS
01047  01047  20 36220 77325   170.  • PI     • F   •3.14159265• •   •S
01050  01050  00 00000 00000   171.  • ZERO   • F   •0           •   •S
01051  01051  20 14000 00000   172.  • ONE    • F   •1           •   •S
01052  01052  37 63777 77777   173.  • MONE   • F   •-1.0        •   •S
01053  01053  20 24000 00000   174.  • TWO    • F   •2.          •   •S
01054  01054  20 15735 17307   175.  • SQ3    • F   •1.732051    •   •S

01055  01055  20 14715 60213   176.  • IR     • F   •1.226       •   •MOM. OF INER.•PROJECTILE IN ROLLS
01056  01056  17 54157 31156   177.  • MP     • F   •.13180      •   •MASS•PROJECTILES
01057  01057  20 35400 00000   178.  • RP     • F   •5.5         •   •CLUSTER RADIUSS
01060  01060  20 37420 30447   179.  • IPP    • F   •7.532       •   •MOM.OF INER.•PROJECTILE IN PITCHS
01061  01061  00 00000 00000   180.  • TAU    • F   •0           •   •FIRING INTERVAL(COMPUTED IN PROG.)S
01062  01062  00 00000 00005   181.  • NO     • I   •5           •   •NUMBER OF EQUATIONSS
01063  01063  16 74051 11555   182.  • DELTAT • F   •1.00-3      •   •TIME INTERVAL(INTEGRATION)•
01064  01064  00 00000 00000   183.  •        • F   •0           •   •ALWAYS ZEROS
01065  01065  00 00000 00000   184.  •        • F   •0           •   •ALWAYS ZEROS
01066  01066  00 00000 00000   185.  • TO     • F   •0           •   •INITIAL TIMESS
01067  01067  00 00000 00000   186.  • TETA10 • F   •0           •   •INITIAL CONDITIONS
01070  01070  00 00000 00000   187.  • TETA20 • F   •0           •   •SAMES
```

FIG. D-3 COMPUTER PROGRAM (Continued)

```
01071  01071  00 00000 00000   188.  * S0      * F      *0         *          *SAMES
01072  01072  00 00000 00000   189.  * PHI10   * F      *0         *          *SAMES
01073  01073  00 00000 00000   190.  * PHI20   * F      *0         *          *SAMES
01074  01074  20 57153 14632   191.  * U0      * F      *29.9      *          *INITIAL POSITIONS
01075  01075  00 00001 00000   192.  * IA      * 300    *00001     *00000     *NCTAL CONSTANTS
01076  01076  20 14000 00000   193.  * IP      * F      *1.0       *          *NO. OF ROUNDS FIRED
01077  01077  20 77110 00000   194.  * IO      * F      *115.      *          *NOM.OF INERTIA.CARRIAGE EQUIVALENTS
01100  01100  00 00000 00000   195.  * K2      * F      *0         *          *RATE.ELEVATING SYS.S
01101  01101  00 00000 00000   196.  * C2      * F      *0         *          *DAMPING COEFF..ELEVATING SYS.S
01102  01102  00 00000 00000   197.  * K1      * F      *0         *          *RATE.CARRIAGE FLEXIBILITY
01103  01103  00 00000 00000   198.  * C1      * F      *0         *          *DAMPING COEFF..CARRIAGES
01104  01104  20 54753 14632   199.  * U2      * F      *19.9      *          *END OF CAMPATMS

01105  01105  20 14736 31443   200.  * W1      * F      *9.9       *          *BEGINNING OF CAMPATMS
01106  01106  20 76200 00000   201.  * H1      * F      *100.      *          *CONSTANT RECOIL FRICTION FORCESS
01107  01107  20 55500 00000   202.  * ALPHA   * F      *45.       *          *ANGLE OF ELEVATION.DEGREES
01110  01110  20 55353 14632   203.  * UT      * F      *21.9      *          *TRIGGER POSITIONS
01111  01111  17 76314 03146   204.  * TS      * F      *0.4       *          *PROGRAM STOP AT THIS TIMES
01112  01112  11 01114 17770   205.  * START   * TP     *PAR       *1770013   *S
01113  01113  17 17759 17753   206.  *         * RJ     *1775519   *1775319   *S
01114  01114  45 00000 01114   207.  *         * TJ     *          *L+2       *S
01115  01115  00 31000 00012   208.  * PAR     * 00     *0         *10        *S
01116  01116  11 01124 16000   209.  *         * ARF031 *21        *          *S
01117  01117  17 15777 13775
01120  01120  45 00000 01155   210.  *         * TJ     *          *NEXT1     *S

01121  01121  75 30002 01123   211.  *         * ARF035 *          *AL        *S
01122  01122  11 00000 16516
01123  01123  17 16515 16515
01124  01124  00 01751 01125   212.  * 21      * 00     *1001      *L+1       *S
01125  01125  00 01131 27540   213.  *         * 00     *NI        *17000     *S
01126  01126  00 00000 16513   214.  *         * 00     *          *AL        *S
01127  01127  00 00000 00000   215.  *         * 00     *          *          *S
01130  01130  00 00000 00000   216.  *         * 00     *          *          *S
01131  01131  54 30250 33445   217.  * *1      * XS3-5  *RECOIL-MASS----CARRIAGE-INERTS
01132  01132  01 47215 56531
01133  01133  01 02010 24674
01134  01134  54 54342 43230

01135  01135  01 34533 03446
01136  01136  34 24210 13424   218.  *         * XS3-5  *IABC-RATE-C-DAMPING-COEFF........
01137  01137  46 30210 12754
01140  01140  47 52315 03251
01141  01141  26 03333 13122
01142  01142  01 01010 10131
01143  01143  02 01023 04630   219.  *         * XS3-5  *---ELEVATING-SYSTEM-RELUAC-RS
01144  01144  70 24553 43032
01145  01145  01 55734 56530
01146  01146  47 01525 43045
01147  01147  03 24272 10154
01150  01150  24 46302 10127   220.  *         * XS3-5  *ATERC-DAMPING-CO.EFF.............S
```

FIG. D-3 COMPUTER PROGRAM (Continued)

```
01151  01151  34 37523 45032
01152  01152  31 26333 03131
01153  01153  33 01010 10101
01154  01154  31 01010 10101
01155  01155  11 01150 10000      221.  * EXT1 * ARF031 *27                 *          *$
01156  01156  17 15777 15775
01157  01157  15 00000 01211      222.  *              * NJ     *          *NEXT2     *$
01160  01160  00 01751 01151      223.  * 27           * 00     *1031      *L+1       *$
01161  01161  00 01150 27350      224.  *              * 00     *N2        *12000     *$
01162  01162  00 00000 10513      225.  *              * 00     *          *8L        *$
01163  01163  00 00000 00000      226.  *              * 00     *          *          *$
01164  01164  00 00000 00000      227.  *              * 00     *          *          *$

01165  01165  35 24172 12530      228.  * 12           * XS3-3  *CAM=CHEGINNING+M=.CAM=C+END---COS*$
01166  01166  32 14535 03453
01167  01167  32 01312 62427
01170  01170  21 01335 02732
01171  01171  31 02350 33045
01172  01172  56 72015 43035      229.  *              * XS3-3  *T+WHEEL_FRICT+ION--ELEVATIONS
01173  01173  33 34150 13154
01174  01174  34 26535 40357
01175  01175  32 01325 04553
01176  01176  30 24553 40353
01177  01177  32 01325 53024      230.  *              * XS3-3  *---SEAL_FRICT----+-HG.FRICT.=C*$
01200  01200  45 01314 43455

01201  01201  56 72020 10225
01202  01202  54 52220 13154
01203  01203  34 26552 20135
01204  01204  53 30515 14232      231.  *              * XS3-3  *OFFF.---SEC.MR.ELOAD---T=IG.ER.*$
01205  01205  51 02515 02652
01206  01206  31 52515 04553
01207  01207  34 27020 10265
01210  01210  54 34325 23054
01211  01211  11 01217 10090      232.  * EXT2 * ARF031 *25                 *          *$
01212  01212  17 15777 15775
01213  01213  15 00000 01240      233.  *              * NJ     *          *NEXT3     *$
01214  01214  75 30002 01215      234.  *              * ARF030 *          *FL        *$

01215  01215  11 00000 10550
01216  01216  17 16515 10515
01217  01217  00 01751 01200      235.  * 25           * 00     *1001      *L+1       *$
01220  01220  00 01105 02425      236.  *              * 00     *M0        *1302      *$
01221  01221  00 00000 10543      237.  *              * 00     *          *FL        *$
01222  01222  00 01077 02425      238.  *              * 00     *IO        *1302      *$
01223  01223  00 00000 10543      239.  *              * 00     *          *FL        *$
01224  01224  00 01102 02426      240.  *              * 00     *K1        *1302      *$
01225  01225  00 00000 10543      241.  *              * 00     *          *FL        *$
01226  01226  00 01103 02425      242.  *              * 00     *C1        *1302      *$
01227  01227  00 00000 10513      243.  *              * 00     *          *FL        *$
01230  01230  00 01314 02425      244.  *              * 00     *KF2       *1302      *$
```

FIG. D-3 COMPUTER PROGRAM (Continued)

```
01231  01231  00 00000 10513    245.  .        . 00       .          .FL      .$
01232  01232  00 01130 02425    246.  .        . 00       .K2        .1302    .$
01233  01233  00 00000 10513    247.  .        . 00       .          .FL      .$
01234  01234  00 01131 02425    248.  .        . 00       .C2        .1302    .$
01235  01235  00 00000 10513    249.  .        . 00       .          .FL      .$
01236  01236  00 00000 00000    250.  .        . 00       .          .        .$
01237  01237  00 00000 00000    251.  .        . 00       .          .        .$
01240  01240  11 01243 16000    252.  . NEXT3  . 1PF0D1   .Z8        .        .$
01241  01241  37 15777 15775
01242  01242  15 00000 01246    253.  .        . 1J       .          .NEXT4   .$
01243  01243  00 01751 01244    254.  . Z4     . 00       .1001      .L+1     .$
01244  01244  00 01130 02425    255.  .        . 00       .U1        .1302    .$

01245  01245  00 00000 10513    256.  .        . 00       .          .FL      .$
01246  01246  00 01134 02426    257.  .        . 00       .U2        .1302    .$
01247  01247  00 00000 10513    258.  .        . 00       .          .FL      .$
01250  01250  00 01130 02425    259.  .        . 00       .M1        .1302    .$
01251  01251  00 00000 10513    260.  .        . 00       .          .FL      .$
01252  01252  00 01137 02426    261.  .        . 00       .ALPHA     .1302    .$
01253  01253  00 00000 10513    262.  .        . 00       .          .FL      .$
01254  01254  00 01127 02425    263.  .        . 00       .DELTA     .1302    .$
01255  01255  00 00000 10513    264.  .        . 00       .          .FL      .$
01256  01256  00 01130 02426    265.  .        . 00       .W1        .1302    .$
01257  01257  00 00000 10513    266.  .        . 00       .          .FL      .$
01260  01260  00 01311 02425    267.  .        . 00       .KK        .1302    .$

01261  01261  00 00000 10513    268.  .        . 00       .          .FL      .$
01262  01262  00 01110 02425    269.  .        . 00       .UT        .1302    .$
01263  01263  00 00000 10513    270.  .        . 00       .          .FL      .$
01264  01264  00 00000 00000    271.  .        . 00       .          .        .$
01265  01265  01 00000 00000    272.  .        . 01       .          .        .$
01266  01266  11 01271 15000    273.  . NEXT4  . 1PF0D1   .Z4        .        .$
01267  01267  37 15777 15775
01270  01270  15 00000 01327    274.  .        . 1J       .          .NEXT5   .$
01271  01271  00 01751 01272    275.  . Z5     . 00       .1001      .L+1     .$
01272  01272  00 01314 01141    276.  .        . 00       .N9        .599     .$
01273  01273  00 00000 10513    277.  .        . 00       .          .AL      .$
01274  01274  00 01315 01141    278.  .        . 00       .N8        .699     .$

01275  01275  00 00000 10513    279.  .        . 00       .          .AL      .$
01276  01276  00 01314 01141    280.  .        . 00       .N5        .499     .$
01277  01277  00 00000 10513    281.  .        . 00       .          .AL      .$
01300  01300  00 01317 01141    282.  .        . 00       .N6        .699     .$
01301  01301  00 00000 10513    283.  .        . 00       .          .AL      .$
01302  01302  00 01320 02263    284.  .        . 00       .N7        .1203    .$
01303  01303  00 00000 10513    285.  .        . 00       .          .AL      .$
01304  01304  00 01322 02263    286.  .        . 00       .N8        .1203    .$
01305  01305  00 00000 10513    287.  .        . 00       .          .AL      .$
01306  01306  00 01324 01141    288.  .        . 00       .N9        .699     .$
01307  01307  00 00000 10513    289.  .        . 00       .          .AL      .$
01310  01310  00 01326 02263    290.  .        . 00       .N10       .1203    .$
```

FIG. D-3 COMPUTER PROGRAM (Continued)

```
01311  01711  00 00000 10513     291*   *       * 00      *                *AL      *$
01312  01712  00 00000 00000     292*   *       * 00      *                *        *$
01313  01713  00 00000 00000     293*   *       * 00      *                *        *$
01314  01714  55 34473 00151     294*   * *3    * X53     *TIME**          *        *$
01315  01715  32 33140 20491     295*   * *4    * X53     *PHI-1*          *        *$
01316  01716  32 33140 20591     296*   * *5    * X53     *PHI-2*          *        *$
01317  01717  57 01010 10191     297*   * *6    * X53     *U*****          *        *$
01320  01720  32 33140 20492     298*   * *7    * X53-2   *PHI-1-DOT****            *$
01321  01721  57 03450 10191
01322  01722  52 33140 20592     299*   * *8    * X53-2   *PHI-2-DOT****            *$
01323  01723  57 03450 10191
01324  01724  57 02270 30551     300*   * *9    * X53     *U-DOT*          *$

01325  01725  54 30250 33415     301*   * *10   * X53-4   *RECOIL*FORCE*            *$
01326  01726  01 31035 42510
01327  01727  11 01332 10010     302*   * *EXTD * ARFNS1  *ZA              *        *$
01330  01730  57 15777 10775
01331  01731  45 00000 01375     303*   *       * 00      *                *NEXT0   *$
01332  01732  00 01731 01333     304*   * *69   * 00      *1031            *L*1     *$
01333  01733  00 01354 02253     305*   *       * 00      *N11             *1203    *$
01334  01734  00 00000 10513     306*   *       * 00      *                *AL      *$
01335  01735  00 01357 02253     307*   *       * 00      *N12             *1203    *$
01336  01736  00 00000 10513     308*   *       * 00      *                *AL      *$
01337  01737  00 01351 02253     309*   *       * 00      *N13             *1203    *$
01340  01740  00 00000 10513     310*   *       * 00      *                *AL      *$

01341  01741  00 01353 02253     311*   *       * 00      *N14             *1203    *$
01342  01742  00 00000 10513     312*   *       * 00      *                *AL      *$
01343  01743  00 01355 02253     313*   *       * 00      *N15             *1203    *$
01344  01744  00 00000 10513     314*   *       * 00      *                *AL      *$
01345  01745  00 01357 02253     315*   *       * 00      *N16             *1203    *$
01346  01746  00 00000 10513     316*   *       * 00      *                *AL      *$
01347  01747  00 01371 02253     317*   *       * 00      *N17             *1203    *$
01350  01750  00 00000 10513     318*   *       * 00      *                *AL      *$
01351  01751  00 01373 02253     319*   *       * 00      *N18             *1203    *$
01352  01752  00 00000 10513     320*   *       * 00      *                *AL      *$
01353  01753  00 00000 00000     321*   *       * 00      *                *        *$
01354  01754  00 00000 00000     322*   *       * 00      *                *        *$

01355  01755  27 30165 62491     323*   * *11   * X53-2   *DELTA*T******            *$
01356  01756  45 01010 10191
01357  01757  24 72417 44091     324*   * *12   * X53-2   *AXIAL*CA4****            *$
01360  01760  26 24470 10191
01361  01761  45 24535 23033     325*   * *13   * X53-2   *TANGENT**CAN*            *$
01362  01762  46 22717 62417
01363  01763  17 03173 03056     326*   * *14   * X53-2   *MOME..T*REACT*           *$
01364  01764  01 54432 42555
01365  01765  50 03514 72416     327*   * *15   * X53-2   *NORMAL*REACT*            *$
01366  01766  01 54432 42055
01367  01767  55 52515 45032     328*   * *15   * X53-2   *SPRI.G*FORCE*            *$
01370  01770  01 31035 42513
```

FIG. D-3 COMPUTER PROGRAM (Continued)

```
01371  01371  27 24375 44291      324.   .  .17    . XS3-2  .DAMW.MFORCE..           .S
01372  01372  41 03562 65031
01373  01373  32 03712 73051      330.   .  .19    . XS3-2  .PROOFMUFORCE.           ..
01374  01374  71 41035 42010
01375  01375  11 01430 10030      331.   .  VEXTB  . ANFO31 .Z2         .            .S
01376  01376  37 15777 15775
01377  01377  15 00000 01432      332.   .         . W      .           .VEXTB       .S
01400  01400  30 01731 02431      333.   .  Z4     . DS     .1031       .L+1         .S
01401  01401  30 01417 02111      334.   .         . DS     .U17        .S0S         .S
01402  01402  30 00000 10513      335.   .         . DS     .           .AL          .S
01403  01403  30 01120 02253      336.   .         . DS     .U20        .1703        .S
01404  01404  30 00000 10513      337.   .         . DS     .           .AL          .S

01405  01405  30 01127 02253      338.   .         . DS     .U21        .1703        .S
01406  01406  30 00000 10513      339.   .         . DS     .           .AL          .S
01407  01407  30 01124 02253      340.   .         . DS     .U22        .1703        .S
01410  01410  30 00000 10513      341.   .         . DS     .           .AL          .S
01411  01411  30 01126 02253      342.   .         . DS     .U23        .1703        .S
01412  01412  30 00000 10513      343.   .         . DS     .           .AL          .S
01413  01413  30 01130 02253      344.   .         . DS     .U24        .1703        .S
01414  01414  30 00000 10513      345.   .         . DS     .           .AL          .S
01415  01415  30 00000 00000      346.   .         . DS     .           .            .S
01416  01416  31 00000 00000      347.   .         . DI     .           .            .S
01417  01417  31 01217 10131      348.   .  .13    . XS3    .000000     .            .S
01420  01420  44 03675 02791      349.   .  .29    . XS3-2  .ROUP NUMBER.            .S

01421  01421  30 47472 53054
01422  01422  34 30750 33445      350.   .  .21    . XS3-2  .MFCOIL.DIST..           .S
01423  01423  31 27346 50022
01424  01424  36 54202 74630      351.   .  .22    . XS3-2  .CRADLE.RJT...           .S
01425  01425  31 41036 62491
01426  01426  54 30750 33415      352.   .  .23    . XS3-2  .MFCOIL.FRICT.           .S
01427  01427  31 41565 46456
01430  01430  32 71275 40125      353.   .  .24    . XS3-2  .PROJ.CAL.ARM.           .S
01431  01431  32 46712 40417
01432  01432  75 40413 01434      354.   .  VEXTB  . APS    .11         .L+2         .S
01433  01433  11 01352 00034      355.   .         . TP     .U          .M           .S
01434  01434  47 01347 10755      356.   .         . FD     .PI         .L(F190.)    .S

01435  01435  11 41700 10540      357.   .         . TP     .3          .CONV        .S
01436  01436  65 01137 10540      358.   .         . FM     .ALPHA      .CONV        .S
01437  01437  11 41700 01137      359.   .         . TP     .3          .ALPHA       .S
01440  01440  55 01024 10540      360.   .         . FM     .BETA       .CONV        .S
01441  01441  11 41700 01035      361.   .         . TP     .3          .BETA        .S
01442  01442  11 01137 00775      362.   .         . TP     .ALPHA      .MEG1        .S
01443  01443  11 01131 00777      363.   .         . TP     .ONE        .MEG1+1      .S
01444  01444  75 40002 01446      364.   .         . ARFOTN .MEG1       .LOC1        .S
01445  01445  11 00774 17057
01446  01446  37 17756 17053
01447  01447  11 17734 10541      365.   .         . TP     .LOC1+3     .COSALF      .COSALPS
01450  01450  46 01474 01035      366.   .         . FM     .UA         .MM          .S
```

FIG. D-3 COMPUTER PROGRAM (Continued)

```
01451  01451  32 01014 00034      367.    .         . FI     .31      .MC       .$
01452  01452  57 31030 00015      368.    .         . FO     .3       .9        .$
01453  01453  56 31030 15561      369.    .         . FM     .3       .COSALF   .$
01454  01454  56 31030 00032      370.    .         . FM     .3       .S        .$
01455  01455  56 31030 00053      371.    .         . FM     .3       .TMG      .$
01456  01456  13 31030 00014      372.    .         . TN     .3       .KK2      .KK2$
01457  01457  55 01326 00157      373.    .         . FS     .BETA    .ALPHA    .$
01460  01460  11 31030 15653      374.    .         . TP     .3       .GMA      .$
01461  01461  11 15553 00775      375.    .         . TP     .GMA     .NEG1     .$
01462  01462  11 01137 00033      376.    .         . TP     .ALPHA   .NEG2     .$
01463  01463  11 01030 00777      377.    .         . TP     .ZERO    .NEG1+1   .$
01464  01464  11 01030 01031      378.    .         . TP     .ZERO    .NEG2+1   .$

01465  01465  75 30032 01447      379.    .         . ARFO78 .NEG1    .LOC1     .$
01466  01466  11 00776 17057
01467  01467  37 17035 17053
01470  01470  11 17736 15543      380.    .         . TP     .LOC1+3  .SINMMA   .SINMMA$
01471  01471  75 30032 01473      381.    .         . ARFO78 .NEG2    .LOC1     .$
01472  01472  11 01030 17057
01473  01473  37 17035 17053
01474  01474  11 17736 15554      382.    .         . TP     .LOC1+3  .SINALF   .SINALF$
01475  01475  11 15553 00775      383.    .         . TP     .GMA     .NEG1     .$
01476  01476  11 01031 00777      384.    .         . TP     .ONE     .NEG1+1   .$
01477  01477  75 30032 01001      385.    .         . ARFO78 .NEG1    .LOC1     .$
01500  01500  11 00776 17057

01501  01501  37 17035 17053
01502  01502  11 17735 15545      386.    .         . TP     .LOC1+3  .COSMMA   .COSMMA$
01503  01503  46 01322 15554      387.    .         . FM     .3       .SINALF   .$
01504  01504  46 31030 01034      388.    .         . FM     .3       .MC       .$
01505  01505  32 01014 01042      389.    .         . FI     .KK2     .COSQ2    .$
01506  01506  46 31030 15543      390.    .         . FM     .3       .SINMMA   .$
01507  01507  46 31030 01017      391.    .         . FM     .3       .LT       .$
01510  01510  11 31030 15555      392.    .         . TP     .3       .S1       .S1$
01511  01511  44 01034 00035      393.    .         . FA     .MC      .MP       .$
01512  01512  46 31030 15551      394.    .         . FM     .3       .COSALF   .$
01513  01513  46 31030 00032      395.    .         . FM     .3       .S        .$
01514  01514  32 01014 00011      396.    .         . FI     .KK2     .SINQ2    .$

01515  01515  56 31030 15555      397.    .         . FM     .3       .COSMMA   .$
01516  01516  46 31030 00017      398.    .         . FM     .3       .LT       .$
01517  01517  13 31030 15557      399.    .         . TN     .3       .S2       .S2$
01520  01520  55 01014 00015      400.    .         . FM     .KK2     .SINMA    .$
01521  01521  56 31030 00014      401.    .         . FM     .3       .LTP      .$
01522  01522  13 31030 31030      402.    .         . TN     .3       .3        .$
01523  01523  54 31030 15557      403.    .         . FA     .3       .S2       .$
01524  01524  54 31030 15555      404.    .         . FA     .3       .S1       .$
01525  01525  11 31030 01013      405.    .         . TP     .3       .KK1      .KK1$
01526  01526  11 01011 15570      406.    .         . TP     .KK      .MSFS
01527  01527  11 01532 00035      407.    .         . TP     .ALG     .A        .$
01530  01530  37 17171 17171      408.    . SUB     . ARFO99 .        .         .$
```

FIG. D-3   COMPUTER PROGRAM (Continued)

```
01531  01531  45 00000 01721   407*   .       . SJ     .         .FORCE    .$
01532  01532  45 00000 01533   410*   . ALS   . SJ     .         .L+1      .$
01533  01533  11 00010 15671   411*   .       . TP     .T        .TT       .$
01534  01534  54 01137 00014   412*   .       . FA     .ALPHA    .MN11     .$
01535  01535  54 01000 00015   413*   .       . FA     .0        .MN12     .$
01536  01536  11 01000 00776   414*   .       . TP     .0        .NEG1     .$
01537  01537  45 01124 01137   415*   .       . FS     .DELTA    .ALPHA    .$
01540  01540  55 01000 00015   416*   .       . FS     .0        .MN12     .$
01541  01541  11 01000 01000   417*   .       . TP     .0        .NEG2     .$
01542  01542  11 15774 00777   418*   .       . TP     .LIF01    .NEG1+1   .$
01543  01543  75 10002 01515   419*   .       . ARFO7R .MF31     .LOC1     .$
01544  01544  11 00776 17057

01545  01545  37 17054 17053
01546  01546  11 17054 15672   420*   .       . TP     .LOC1+3   .SIN1     .$
01547  01547  11 15774 01001   421*   .       . TP     .LIF01    .NEG2+1   .$
01550  01550  75 10002 01552   422*   .       . ARFO7R .MF32     .LOC1     .$
01551  01551  11 01000 17057
01552  01552  37 17054 17053
01553  01553  11 17054 15673   423*   .       . TP     .LOC1+3   .SIN2     .$
01554  01554  11 15757 00777   424*   .       . TP     .LIF1.1   .NEG1+1   .$
01555  01555  11 15757 01001   425*   .       . TP     .LIF1.1   .NEG2+1   .$
01556  01556  75 10002 01557   426*   .       . ARFO7R .MF31     .LOC1     .$
01557  01557  11 00776 17057
01560  01560  37 17054 17053

01561  01561  11 17054 15674   427*   .       . TP     .LOC1+3   .COS1     .$
01562  01562  75 10002 01564   428*   .       . ARFO7R .MF32     .LOC1     .$
01563  01563  11 01000 17057
01564  01564  37 17054 17053
01565  01565  11 17054 15675   429*   .       . TP     .LOC1+3   .COS2     .$
01566  01566  56 01017 15672   430*   .       . FM     .LT       .SIN1     .$
01567  01567  11 01000 15675   431*   .       . TP     .0        .LSIM1    .$
01570  01570  55 01017 15674   432*   .       . FM     .LT       .COS1     .$
01571  01571  11 01000 15677   433*   .       . TP     .0        .LCOS1    .$
01572  01572  56 01017 15673   434*   .       . FM     .LT       .SIN2     .$
01573  01573  11 01000 15700   435*   .       . TP     .0        .LSIM2    .$
01574  01574  56 01017 15675   436*   .       . FM     .LT       .COS2     .$

01575  01575  11 01000 15701   437*   .       . TP     .0        .LCOS2    .$
01576  01576  11 00015 32000   438*   .       . TP     .5        .4        .SET E AND F$
01577  01577  17 01604 01533   439*   .       . ZJ     .L+4      .L+1      .$
01600  01600  11 01057 15752   440*   .       . TP     .ZERO     .E        .$
01601  01601  11 01057 15753   441*   .       . TP     .ZERO     .F        .$
01602  01602  45 00000 01616   442*   .       . SJ     .         .JUMPX    .$
01603  01603  46 01604 00557   443*   .       . SJ     .L+1      .L+4      .$
01604  01604  11 01051 15752   444*   .       . TP     .ONE      .E        .$
01605  01605  11 01057 15753   445*   .       . TP     .ZERO     .F        .$
01606  01606  45 00000 01615   446*   .       . SJ     .         .JUMPX    .$
01607  01607  11 01052 15752   447*   .       . TP     .MOVE     .E        .$
01610  01610  11 00014 32000   448*   .       . TP     .U        .4        .$
```

FIG. D-3 COMPUTER PROGRAM (Continued)

```
01611  01411  12 01134 01613     449*     *          * TJ     *U1      *L+2      *$
01612  01412  42 01134 01615     450*     *          * TJ     *U2      *L+3      *$
01613  01413  11 01037 15703     451*     *          * TP     *ZERO    *F        *$
01614  01414  45 00000 01615     452*     *          * TJ     *        *L+2      *$
01615  01415  11 01031 15703     453*     *          * TP     *ONE     *F        *$
01616  01416  55 15734 01037     454*     * JUMPX    * FM     *E       *M)       *$
01617  01417  11 31037 15704     455*     *          * TP     *3       *EMU      *$
01620  01420  55 15734 15701     456*     *          * FM     *EMU     *LCOS2    *$
01621  01421  12 15704 00015     457*     *          * FI     *EMU     *T        *$
01622  01422  55 31037 01035     458*     *          * FM     *3       *MR       *$
01623  01423  32 01035 15703     459*     *          * FI     *SM      *LSIN2    *$
01624  01424  11 31037 15705     460*     *          * TP     *4       *A11      *A11$

01625  01425  55 15734 01035     461*     *          * FM     *EMU     *MR       *$
01626  01426  56 31037 01015     462*     *          * FM     *4       *T        *$
01627  01427  11 31037 15705     463*     *          * TM     *3       *A12      *A12$
01630  01430  11 15703 32037     464*     *          * TM     *F       *1        *$
01631  01431  17 01534 01432     465*     *          * ZJ     *L+3     *L+1      *$
01632  01432  11 01137 15707     466*     *          * TN     *MR      *A13      *$
01633  01433  45 00000 01675     467*     *          * TJ     *        *MASS1    *$
01634  01434  55 01037 01033     468*     *          * FM     *A1      *R1       *$
01635  01435  57 01135 31037     469*     *          * FD     *IM      *3        *$
01636  01436  11 31037 15713     470*     *          * TM     *3       *T1       *T1 IS IS (FI...
01637  01437  56 01321 01021     471*     *          * FM     *M       *4        *$
01640  01440  11 31037 15711     472*     *          * TM     *4       *M5       *$

01641  01441  55 01134 01135     473*     *          * FS     *U2      *U1       *$
01642  01442  11 31037 15712     474*     *          * TP     *3       *U2-U1    *$
01643  01443  55 31037 15712     475*     *          * FM     *4       *U2-U1    *$
01644  01444  57 15711 31037     476*     *          * FD     *M52     *M        *$
01645  01445  11 31037 15713     477*     *          * TP     *3       *T2       *T2 IS (MINUS...
01646  01446  55 00015 01135     478*     *          * FS     *U       *U1       *$
01647  01447  57 31037 15712     479*     *          * FD     *3       *U2-U1    *$
01650  01450  56 31037 01053     480*     *          * FM     *3       *TRU      *$
01651  01451  55 31037 01017     481*     *          * FM     *3       *PI       *$
01652  01452  11 31037 01032     482*     *          * TP     *3       *PAR      *$
01653  01453  11 01037 01033     483*     *          * TP     *ZERO    *TEMP1    *$
01654  01454  75 30037 01655     484*     *          * ARFD/A *CAR     *LOCI     *$

01655  01455  11 01037 17057
01656  01456  17 17035 17053
01657  01457  11 17035 15714     485*     *          * TP     *LOCI+3  *SINCAM   *$
01660  01460  11 01031 01033     486*     *          * TP     *ONE     *TEMP1    *$
01661  01461  75 30037 01653     487*     *          * ARFD/A *CAR     *LOCI     *$
01662  01462  11 01037 17057
01663  01463  37 17035 17053
01664  01464  11 17035 15715     488*     *          * TP     *LOCI+3  *COSCAM   *$
01665  01465  55 01031 15715     489*     *          * FS     *ONE     *COSCAM   *$
01666  01466  11 31037 15715     490*     *          * TP     *3       *A93      *A93=(1-COS...
01667  01467  56 31037 15715     491*     *          * FM     *3       *A93      *$
01670  01470  11 31037 15717     492*     *          * TP     *4       *A9       *A9=(1-COS...
```

FIG. D-3   COMPUTER PROGRAM (Continued)

```
01671  01471  56 31000 15734    493.   .         . FM    .0       .C        .$
01672  01472  55 31000 15710    494.   .         . FM    .0       .T1       .$
01673  01473  56 31000 15711    495.   .         . FM    .Q       .T2       .$
01674  01474  55 31000 01055    496.   .         . FS    .0       .MQ       .$
01675  01475  11 31000 15737    497.   .         . TP    .0       .A13      .A13. NOTOPS
01676  01476  54 70011 00012    498.   . PASS1   . FA    .TETA1   .TETA2    .$
01677  01477  11 31000 15720    499.   .         . TP    .0       .T8       .T8=THETA1+THETA2S
01700  01700  55 31000 15720    500.   .         . FM    .0       .T8       .$
01701  01701  56 31000 01055    501.   .         . FM    .0       .MQ       .$
01702  01702  55 31000 00015    502.   .         . FM    .0       .11       .$
01703  01703  13 31000 15555    503.   .         . TN    .0       .S1       .FIRST TERM OF AXIS
01704  01704  56 15720 00013    504.   .         . FM    .T8      .S        .$

01705  01705  55 31000 15734    505.   .         . FM    .0       .FMU      .$
01706  01706  56 31000 01055    506.   .         . FM    .Q       .MQ       .$
01707  01707  55 31000 01053    507.   .         . FM    .0       .TMU      .$
01710  01710  13 31000 15557    508.   .         . TN    .0       .S2       .SECOND TERM OF AXIS
01711  01711  56 15730 01055    509.   .         . FM    .EMU     .MQ       .$
01712  01712  55 31000 15573    510.   .         . FM    .0       .SIN2     .$
01713  01713  32 01000 15675    511.   .         . FI    .MM      .COS2     .$
01714  01714  56 31000 00011    512.   .         . FM    .C       .TETA1    .$
01715  01715  56 31000 00011    513.   .         . FM    .C       .TETA1    .$
01716  01716  56 31000 01017    514.   .         . FM    .0       .LT       .$
01717  01717  11 31000 15721    515.   .         . TP    .0       .S3       .3RDTERM OF AXIS
01720  01720  45 00000 01775    516.   .         . MJ    .        .SKIP     .$

01721  01721  11 01037 00455    517.   . FORCE   . TP    .DELT1   .DELT     .$
01722  01722  11 00010 15671    518.   .         . TP    .T       .TT       .$
01723  01723  11 00010 32090    519.   .         . TP    .T       .A        .$
01724  01724  17 01727 01725    520.   .         . ZJ    .L+3     .L+1      .$
01725  01725  11 01011 15670    521.   .         . TP    .KK      .PSF      .$
01726  01726  45 00000 01773    522.   .         . MJ    .        .TAG1     .$
01727  01727  11 00013 32090    523.   .         . TP    .S       .A        .$
01730  01730  46 01752 01731    524.   .         . SJ    .TAG3    .L+1      .$
01731  01731  11 01110 32090    525.   .         . TP    .UT      .A        .$
01732  01732  42 00014 01735    526.   .         . TJ    .U       .TAG4     .$
01733  01733  11 01350 15670    527.   .         . TP    .ZERO    .PSF      .$
01734  01734  45 00000 01773    528.   .         . MJ    .        .TAS1     .$

01735  01735  11 01350 32090    529.   . TAG4    . TP    .ZERO    .A        .$
01736  01736  42 15470 01755    530.   .         . TJ    .MMF     .TAG5     .$
01737  01737  11 00010 01041    531.   .         . TP    .T       .TAU      .$
01740  01740  47 01037 15770    532.   .         . FD    .DELT1   .L(F16+)  .$
01741  01741  11 31000 00010    533.   .         . TP    .0       .T        .$
01742  01742  75 30001 01744    534.   .         . RPF9VM .LIX1)   .LOC2     .$
01743  01743  11 15771 17337
01744  01744  37 17335 17335
01745  01745  11 17335 15570    535.   .         . TP    .LOC2+3  .PSF      .$
01746  01746  55 01035 01055    536.   .         . FS    .MQ      .MQ       .$
01747  01747  11 31000 01055    537.   .         . TP    .0       .MQ       .$
01750  01750  55 01034 01055    538.   .         . FS    .IM      .IP       .$
```

FIG. D-3 COMPUTER PROGRAM (Continued)

```
01751  01751  11 31000 01036    539.  .        . TP      .Q         .I9       .$
01752  01752  55 01010 01050    540.  .        . FS      .IN        .IPP      .$
01753  01753  11 31000 01010    541.  .        . TP      .Q         .IR       .$
01754  01754  11 01754 32000    542.  .        . TP      .FRI       .4        .$
01755  01755  35 01075 01755    543.  .        . ST      .IA        .FRI      .$
01756  01756  11 01031 01031    544.  . PHI    . TP      .EPS       .EPS      .$
01757  01757  54 01051 01076    545.  .        . FA      .ZONE      .I2       .$
01760  01760  11 31000 01075    546.  .        . TP      .Q         .I2       .$
01761  01761  15 00000 01773    547.  .        . UJ      .          .TAG1     .$
01762  01762  11 01000 32000    548.  . IA33   . TP      .ZERO      .4        .$
01763  01763  42 15570 01755    549.  .        . TJ      .PNF       .L+2      .$
01764  01764  15 00000 01773    550.  .        . UJ      .          .TAG1     .$

01765  01765  55 00010 01051    551.  . IA35   . FS      .T         .TAU      .$
01766  01766  11 31000 00010    552.  .        . TP      .Q         .T        .$
01767  01767  75 30001 01701    553.  .        . R*FWW*  .L(X1)     .LOC2     .$
01770  01770  11 15771 17357
01771  01771  37 17335 17333
01772  01772  11 17335 15770    554.  .        . TP      .LOC2+9    .TSF      .$
01773  01773  11 15571 00010    555.  . IA51   . TP      .TT        .T        .$
01774  01774  15 00000 02037    556.  .        . UJ      .          .LOOP     .$
01775  01775  55 01074 00016    557.  . SKIP   . FS      .UN        .II       .$
01776  01776  01 01012 01011    558.  .        . FP      .K         .KK       .$
01777  01777  55 31000 15670    559.  .        . FS      .Q         .PSF      .$
02000  02000  13 31000 15722    560.  .        . TN      .Q         .SN       .$

02001  02001  56 01024 01053    561.  . IA52   . FM      .AM        .TWO      .$
02002  02002  11 31000 02024    562.  .        . TP      .Q         .AP       .$
02003  02003  11 02004 02031    563.  .        . TP      .L+1       .TAG2     .$
02004  02004  15 00000 02035    564.  .        . UJ      .          .L+1      .$
02005  02005  56 01024 01024    565.  .        . FM      .AM        .AP       .$
02006  02006  56 31000 01024    566.  .        . FM      .Q         .AP       .$
02007  02007  56 31000 01023    567.  .        . FM      .Q         .GAMA     .$
02010  02010  57 31000 01053    568.  .        . FD      .Q         .TWO      .$
02011  02011  57 31000 01022    569.  .        . FD      .Q         .S        .$
02012  02012  57 31000 01025    570.  .        . FD      .Q         .CO       .$
02013  02013  57 31000 01025    571.  .        . FD      .Q         .CO       .$
02014  02014  11 31000 15723    572.  .        . TP      .Q         .CONST    .$

02015  02015  55 01074 00016    573.  .        . FS      .UN        .II       .$
02016  02016  11 31000 15724    574.  .        . TP      .Q         .UOMU     .$
02017  02017  11 31000 00010    575.  .        . TP      .Q         .T        .$
02020  02020  11 31000 32000    576.  .        . TP      .Q         .4        .$
02021  02021  42 15772 02023    577.  .        . TJ      .L(F2*+1)  .L+2      .$
02022  02022  11 15772 00010    578.  .        . TP      .L(F2*+1)  .T        .$
02023  02023  11 01010 00465    579.  .        . TP      .DFLT2     .DELT     .$
02024  02024  75 30001 02026    580.  .        . R*FWW*  .L(X2)     .LOC2     .$
02025  02025  11 15773 17337
02026  02026  37 17335 17333
02027  02027  56 17335 01053    581.  .        . FM      .LOC2+3    .TWO      .$
02030  02030  11 31000 15725    582.  .        . TP      .2         .ALFAO    .$
```

FIG. D-3 COMPUTER PROGRAM (Continued)

```
02031 02031 56 15724 15735   583. ,          , FM ,ALFAO  ,ALFAO  ,$
02032 02032 57 15724 31000   584. ,          , FD ,CONST  ,0      ,$
02033 02033 11 31000 15726   585. ,          , TP ,0      ,SS     ,$
02034 02034 56 00017 00017   586. ,          , FM ,S      ,S      ,$
02035 02035 11 31000 15727   587. ,          , TP ,0      ,SSG    ,$
02036 02036 56 31000 15702   588. ,          , FM ,0      ,E      ,$
02037 02037 56 31000 15726   589. ,          , FM ,0      ,SS     ,$
02040 02040 11 31000 15730   590. ,          , TM ,0      ,RF     ,RECOIL FORCES$
02041 02041 54 01031 01057   591. ,          , FA ,ONE    ,DELTA  ,$
02042 02042 56 31000 15726   592. ,          , FM ,0      ,SS     ,$
02043 02043 56 31000 15702   593. ,          , FM ,0      ,E      ,$
02044 02044 56 31000 15727   594. ,          , FM ,0      ,SSG    ,$

02045 02045 13 31000 15735   595. ,          , TN ,0      ,SS     ,5TH TERM , F.OS
02046 02046 11 15735 32000   596. ,          , TP ,F      ,A      ,$
02047 02047 17 02337 02053   597. ,          , ZJ ,L+1    ,PASS2  ,$
02050 02050 56 15717 15713   598. ,          , FM ,T1     ,T2     ,$
02051 02051 57 31000 15712   599. ,          , FD ,0      ,UPMUL  ,$
02052 02052 56 31000 01053   600. ,          , FM ,0      ,TTO    ,$
02053 02053 55 31000 01047   601. ,          , FM ,0      ,RT     ,$
02054 02054 55 31000 15714   602. ,          , FM ,0      ,SIACAM ,$
02055 02055 55 31000 15716   603. ,          , FM ,0      ,ARG    ,$
02056 02056 55 31000 15702   604. ,          , FM ,0      ,E      ,$
02057 02057 56 31000 15727   605. ,          , FM ,0      ,SSG    ,$
02060 02060 13 31000 31000   606. ,          , TN ,0      ,0      ,$

02061 02061 54 31000 15726   607. ,          , FA ,0      ,SS     ,$
02062 02062 11 31000 15735   608. ,          , TM ,0      ,SS     ,5TH TERM +(NOT)+OS
02063 02063 56 15702 01136   609. , PASS2    , FM ,E      ,R1     ,$
02064 02064 13 31000 15731   610. ,          , TN ,0      ,S5     ,6TH TERM OF AXIS
02065 02065 56 15734 15074   611. ,          , FM ,EMU    ,COSI   ,$
02066 02066 53 31000 15072   612. ,          , FS ,0      ,SINI   ,$
02067 02067 55 31000 01022   613. ,          , FM ,0      ,S      ,$
02070 02070 56 31000 01035   614. ,          , FM ,0      ,MR     ,7TH TERM OF AXIS
02071 02071 13 31000 31000   615. ,          , TN ,0      ,0      ,$
02072 02072 54 31000 15065   616. ,          , FA ,0      ,S1     ,$
02073 02073 54 31000 15067   617. ,          , FA ,0      ,S2     ,$
02074 02074 54 31000 15721   618. ,          , FA ,0      ,S3     ,$

02075 02075 54 31000 15722   619. ,          , FA ,0      ,S4     ,$
02076 02076 54 31000 15725   620. ,          , FA ,0      ,S5     ,$
02077 02077 54 31000 15731   621. ,          , FA ,0      ,S6     ,$
02100 02100 11 31000 15732   622. ,          , TP ,0      ,AA1    ,FINISH FIRST EQUATION$
02101 02101 56 01030 01017   623. ,          , FM ,MC     ,LT     ,$
02102 02102 31 01017 01077   624. ,          , FM ,LT     ,IO     ,$
02103 02103 11 31000 15065   625. ,          , TP ,0      ,S1     ,1ST 2 TERMS OF AXIS
02104 02104 56 15734 01052   626. ,          , FM ,EMU    ,MONE   ,$
02105 02105 56 31000 01035   627. ,          , FM ,0      ,MR     ,$
02106 02106 56 31000 15730   628. ,          , FM ,0      ,LSIN2  ,$
02107 02107 52 01035 15751   629. ,          , FI ,MM     ,LCOS2  ,$
02110 02110 11 31000 15057   630. ,          , TP ,0      ,S2     ,$
```

FIG. D-3 COMPUTER PROGRAM (Continued)

```
02111  02111  54 00014 15731    531.   .   . FA   .U       .LCOS2   .$
02112  02112  56 31000 15657    532.   .   . FM   .0       .S2      .$
02113  02113  11 31000 15657    533.   .   . TP   .0       .S2      .2ND TERM OF A21S
02114  02114  56 01014 15731    535.   .   . FM   .01      .LCOS2   .$
02115  02115  55 31000 01094    536.   .   . FM   .0       .MC      .$
02116  02116  54 31000 15656    537.   .   . FA   .0       .S1      .$
02117  02117  54 31000 15657    538.   .   . FA   .0       .S2      .$
02120  02120  11 31000 15733    539.   .   . TP   .0       .A21     .A21S
02121  02121  56 15734 01052    540.   .   . FM   .EMU     .MONE    .$
02122  02122  31 15730 15731    541.   .   . FP   .LSIN2   .LCOS2   .$
02123  02123  56 31000 00015    542.   .   . FM   .0       .U       .$
02124  02124  56 31000 01095    543.   .   . FM   .0       .MR      .$

02125  02125  11 31000 15656    544.   .   . TP   .0       .S1      .1ST TERM OF A22S
02126  02126  56 01000 01015    545.   .   . FM   .MC      .S1      .$
02127  02127  31 15731 15656    546.   .   . FP   .LCOS2   .S1      .$
02130  02130  11 31000 15734    547.   .   . TP   .0       .A22     .A22S
02131  02131  54 01035 15737    548.   .   . FA   .MW      .S13     .$
02132  02132  56 31000 15730    549.   .   . FM   .0       .LSIN2   .$
02133  02133  13 31000 15735    550.   .   . TN   .0       .A23     .A23S
02134  02134  56 15720 15730    551.   .   . FM   .T4      .T4      .$
02135  02135  56 31000 01015    552.   .   . FM   .0       .S1      .$
02136  02136  55 31000 01094    553.   .   . FM   .0       .MC      .$
02137  02137  13 31000 15655    554.   .   . TN   .0       .S1      .1ST TERMS
02140  02140  55 00011 00011    555.   .   . FM   .TETA1   .TETA1   .$

02141  02141  55 31000 01095    556.   .   . FM   .0       .MR      .$
02142  02142  56 31000 15731    557.   .   . FM   .0       .LCOS2   .$
02143  02143  11 31000 15657    558.   .   . TP   .0       .S2      .2ND TERMS
02144  02144  11 15722 32030    559.   .   . TP   .SA      .4       .$
02145  02145  17 02150 02146    560.   .   . ZJ   .L+3     .L+1     .$
02146  02146  11 01030 15721    561.   .   . TP   .ZERO    .S3      .K + KUS
02147  02147  15 00000 02152    562.   .   . UJ   .        .L+3     .$
02150  02150  55 15722 15670    563.   .   . FS   .SA      .MGF     .$
02151  02151  13 31000 15721    564.   .   . TN   .0       .S3      .K + KUS
02152  02152  55 01034 01032    565.   .   . FM   .MC      .S       .$
02153  02153  31 15472 15721    566.   .   . FP   .SIN1    .S3      .$
02154  02154  54 31000 15657    567.   .   . FA   .0       .S2      .$

02155  02155  54 31000 15656    568.   .   . FA   .0       .S1      .$
02156  02156  56 31000 15730    569.   .   . FM   .0       .LSIN2   .$
02157  02157  11 31000 15655    570.   .   . TP   .0       .S1      .1ST TERM OF A42S
02160  02160  56 15720 00013    571.   .   . FM   .T4      .S       .$
02161  02161  56 31000 01095    572.   .   . FM   .0       .MR      .$
02162  02162  55 31000 01053    573.   .   . FM   .0       .TRU     .$
02163  02163  13 31000 15657    674.   .   . TN   .0       .S2      .FIRST TERMS
02164  02164  54 01035 01094    575.   .   . FA   .MW      .MC      .$
02165  02165  56 31000 01032    576.   .   . FM   .0       .S       .$
02166  02166  55 31000 15674    577.   .   . FM   .0       .COS1    .$
02167  02167  13 31000 15721    578.   .   . TN   .0       .S3      .$
02170  02170  54 15457 15721    579.   .   . FA   .S2      .S3      .$
```

FIG. D-3 COMPUTER PROGRAM (Continued)

```
02171  02171  56 31000 15701   580.   *   FM   .3      .LC0S2   .1
02172  02172  11 31000 15667   581.   *   TP   .3      .S9      .2ND TERM OF A*2S
02173  02173  56 15720 00013   582.   *   FM   .TM     .S       .$
02174  02174  56 31000 01055   583.   *   FM   .3      .W9      .$
02175  02175  56 31000 01053   584.   *   FM   .3      .W11     .$
02176  02176  56 31000 01053   585.   *   FM   .3      .TPG     .$
02177  02177  11 31000 15721   586.   *   TP   .3      .S5      .1ST TERMS
02200  02200  56 00311 00011   587.   *   FM   .TOTAL  .TOTAL   .$
02201  02201  56 31000 15707   588.   *   FM   .3      .LSIN2   .$
02202  02202  56 31000 01055   589.   *   FM   .3      .W9      .$
02203  02203  56 31000 01053   590.   *   FM   .3      .W11     .$
02204  02204  13 31000 15722   591.   *   TN   .3      .S4      .2ND TERMS

02205  02205  56 01031 00027   592.   *   FA   .ONE    .DELTA   .$
02206  02206  11 31000 15725   593.   *   TP   .3      .S5      .$
02207  02207  12 15730 30000   594.   *   TM   .S6     .2       .$
02210  02210  56 31000 15725   595.   *   FM   .3      .S5      .$
02211  02211  11 31000 15725   596.   *   TP   .3      .S5      .3RD TERMS
02212  02212  11 01105 15731   597.   *   TP   .M1     .S4      .4TH TERMS
02213  02213  11 15735 30077   598.   *   TP   .A23    .8       .$
02214  02214  47 02217 00215   599.   *   TJ   .L+3    .L+1     .$
02215  02215  11 01030 15735   700.   *   TP   .ZERO   .S7      .5TH TERM ZERO
02216  02216  15 00000 00225   701.   *   TJ   .       .PASS7   .$
02217  02217  56 15717 01055   702.   *   FM   .T1     .TT3     .$
02220  02220  56 31000 15713   703.   *   FM   .3      .T3      .$

02221  02221  57 31000 15712   704.   *   FD   .3      .UDMOL   .$
02222  02222  56 31000 15714   705.   *   FM   .3      .RT.CAP  .$
02223  02223  56 31000 15715   706.   *   FM   .3      .S9.     .$
02224  02224  56 31000 15707   707.   *   FM   .3      .SS2     .$
02225  02225  11 31000 15735   708.   *   TP   .3      .S7      .5TH TERM E CONTIONS
02226  02226  56 01022 15671   709.   * PASS7 .FM   .3      .COS1    .$
02227  02227  56 31000 01055   710.   *   FM   .3      .W9      .$
02230  02230  01 01037 15735   711.   *   FD   .W11    .S7      .$
02231  02231  54 31000 15721   712.   *   FA   .3      .S3      .$
02232  02232  54 31000 15722   713.   *   FA   .3      .S4      .$
02233  02233  54 31000 15725   714.   *   FA   .3      .S5      .$
02234  02234  54 31000 15731   715.   *   FA   .3      .S6      .$

02235  02235  56 31000 15700   716.   *   FM   .3      .LSIN2   .$
02236  02236  56 31000 15702   717.   *   FM   .3      .E       .$
02237  02237  11 31000 15721   718.   *   TP   .3      .S3      .3RD TERM OF A*2S
02240  02240  56 01105 00011   719.   *   FM   .C1     .TOTAL   .$
02241  02241  02 01107 00014   720.   *   FI   .K1     .OMEI1   .$
02242  02242  54 31000 01013   721.   *   FA   .3      .KK1     .$
02243  02243  13 31000 15722   722.   *   TN   .3      .S4      .4TH TERM OF A*2S
02244  02244  56 01107 00015   723.   *   FM   .K2     .OMEI2   .$
02245  02245  02 01101 00012   724.   *   FI   .C2     .TETA2   .$
02246  02246  56 31000 01015   725.   *   FM   .3      .7       .$
02247  02247  57 31000 01053   726.   *   FD   .3      .T9J     .SIN(GAMA2).12*
02250  02250  54 31000 01014   727.   *   FA   .3      .KK2     .$
```

FIG. D-3 COMPUTER PROGRAM (Continued)

```
02251  02251  11 31000 15726    720.   .   .TP   .0      .S5      .$
02252  02252  56 01110 01013    729.   .   .FM   .LTP    .SIGMA   .$
02253  02253  13 31000 15731    730.   .   .TN   .0      .S6      .$
02254  02254  57 15731 01053    731.   .   .FD   .LCOS2  .TWO     .$
02255  02255  13 31000 15735    732.   .   .TN   .0      .S7      .$
02256  02256  56 15730 01054    733.   .   .FM   .LSIN2  .S03     .$
02257  02257  57 31000 01053    734.   .   .FD   .0      .TWO     .$
02260  02260  54 31000 15735    735.   .   .FA   .0      .S7      .$
02261  02261  54 31000 15731    736.   .   .FA   .0      .S6      .$
02262  02262  31 15734 15732    737.   .   .FM   .S5     .S4      .$5TH TERM OF A42S
02263  02263  54 31000 15655    738.   .   .FA   .0      .S1      .$
02264  02264  54 31000 15657    739.   .   .FA   .0      .S2      .$

02265  02265  54 31000 15721    740.   .   .FA   .0      .S3      .$
02266  02266  11 31000 15737    741.   .   .TP   .0      .A42     .$A42= END SECOND EQUATIONS
02267  02267  56 01035 00016    742.   .   .FM   .XM     .U       .$
02270  02270  31 00016 01037    743.   .   .FM   .U      .IC      .$
02271  02271  54 31000 01010    744.   .   .FA   .0      .I0      .$
02272  02272  11 31000 15655    745.   .   .TP   .0      .S1      .$
02273  02273  56 01015 00015    746.   .   .FM   .Q1     .Q1      .$
02274  02274  31 01031 15655    747.   .   .FM   .NF     .S1      .$
02275  02275  11 31000 15733    748.   .   .TP   .0      .A32     .A32S
02276  02276  56 01035 00015    749.   .   .FM   .XM     .U       .$
02277  02277  32 01034 01015    750.   .   .FI   .MC     .Q1      .$
02300  02300  56 31000 15731    751.   .   .FM   .0      .LCOS2   .$

02301  02301  54 31000 15740    752.   .   .FA   .0      .A32     .$
02302  02302  11 31000 15741    753.   .   .TP   .0      .A31     .A31S
02303  02303  11 01030 15742    754.   .   .TP   .ZERO   .A33     .A33S
02304  02304  55 00311 00011    755.   .   .FM   .TETA1  .TETA1   .$
02305  02305  56 31000 15733    756.   .   .FM   .0      .LSIN2   .$
02306  02306  11 31000 15655    757.   .   .TP   .0      .S1      .$
02307  02307  56 01035 00015    758.   .   .FM   .XM     .U       .$
02310  02310  32 01034 01015    759.   .   .FI   .MC     .Q1      .$
02311  02311  56 31000 15655    760.   .   .FM   .0      .S1      .$
02312  02312  11 31000 15656    761.   .   .TP   .0      .S1      .$1ST TERM OF A43S
02313  02313  56 15570 01031    762.   .   .FM   .PNF    .S05     .$
02314  02314  11 31000 15657    763.   .   .TP   .0      .S2      .$2ND TERM OF A43S

02315  02315  56 15727 00013    764.   .   .FM   .TM     .S       .$
02316  02316  56 31000 01035    765.   .   .FM   .0      .XM      .$
02317  02317  56 31000 01053    766.   .   .FM   .0      .TWO     .$
02320  02320  56 31000 00015    767.   .   .FM   .0      .U       .$
02321  02321  13 31000 15721    768.   .   .TN   .0      .S3      .$3RD TERM OF A43S
02322  02322  56 01035 00016    769.   .   .FM   .XM     .U       .$
02323  02323  32 01034 01015    770.   .   .FI   .MC     .Q1      .$
02324  02324  56 31000 01032    771.   .   .FM   .0      .S       .$
02325  02325  56 31000 15674    772.   .   .FM   .0      .COS1    .$
02326  02326  13 31000 15732    773.   .   .TN   .0      .S4      .$4TH TERM OF A43S
02327  02327  56 01107 00015    774.   .   .FM   .K2     .PHI2    .$
02330  02330  32 01131 00012    775.   .   .FI   .C2     .TETA2   .$
```

FIG. D-3 COMPUTER PROGRAM (Continued)

```
02331  02331  56 31000 01015      770.   .     . FM   .Q     .9     .S
02332  02332  57 31000 01053      771.   .     . FD   .Q     .TWO   .S
02333  02333  56 31000 01014      776.   .     . FA   .Q     .SS2   .S
02334  02334  56 31000 01015      779.   .     . FM   .Q     .9     .S
02335  02335  57 31000 01053      780.   .     . FD   .4     .TWO   .S
02336  02336  13 31000 15735      781.   .     . TN   .Q     .S5    .S
02337  02337  54 15725 15732      782.   .     . FA   .S5    .S4    .S
02340  02340  54 31000 15721      783.   .     . FA   .Q     .S3    .S
02341  02341  54 31000 15647      784.   .     . FA   .Q     .S2    .S
02342  02342  54 31000 15646      785.   .     . FA   .Q     .S1    .S
02343  02343  11 31000 15743      786.   .     . TP   .Q     .AA3   .S
02344  02344  57 15735 15735      787.   .     . FD   .A12   .A11   .S

02345  02345  11 31000 15655      788.   .     . TP   .Q     .S1    .S
02346  02346  57 15739 15733      789.   .     . FD   .A22   .A21   .S
02347  02347  55 31000 15655      790.   .     . FS   .Q     .S1    .S
02350  02350  13 31000 15734      791.   .     . TN   .Q     .911   .+11S
02351  02351  57 15737 15735      792.   .     . FD   .A13   .A11   .S
02352  02352  11 31000 15655      793.   .     . TP   .Q     .S1    .S
02353  02353  57 15737 15733      794.   .     . FD   .A23   .A21   .S
02354  02354  55 31000 15655      795.   .     . FS   .Q     .S1    .S
02355  02355  13 31000 15715      796.   .     . TN   .Q     .912   .+12S
02356  02356  57 15732 15735      797.   .     . FD   .AA1   .A11   .S
02357  02357  11 31000 15655      798.   .     . TP   .Q     .S1    .S
02360  02360  57 15737 15733      800.   .     . FD   .AA2   .A21   .S

02361  02361  55 31000 15655      801.   .     . FS   .Q     .S1    .S
02362  02362  13 31000 15715      802.   .     . TN   .Q     .991   .+01S
02363  02363  57 15735 15735      803.   .     . FD   .A12   .A11   .S
02364  02364  11 31000 15655      804.   .     . TP   .Q     .S1    .S
02365  02365  57 15710 15741      805.   .     . FD   .A32   .A31   .S
02366  02366  55 31000 15655      806.   .     . FS   .Q     .S1    .S
02367  02367  13 31000 15717      807.   .     . TN   .Q     .921   .+21S
02370  02370  57 15737 15735      808.   .     . FD   .A13   .A11   .S
02371  02371  11 31000 15655      809.   .     . TP   .Q     .S1    .S
02372  02372  57 15712 15741      810.   .     . FD   .A33   .A31   .S
02373  02373  55 31000 15655      811.   .     . FS   .Q     .S1    .S
02374  02374  13 31000 15757      812.   .     . TN   .Q     .922   .+22S

02375  02375  57 15732 15735      813.   .     . FD   .AA1   .A11   .S
02376  02376  11 31000 15655      814.   .     . TP   .Q     .S1    .S
02377  02377  57 15743 15741      815.   .     . FD   .AA3   .A31   .S
02400  02400  55 31000 15655      816.   .     . FS   .Q     .S1    .S
02401  02401  13 31000 15751      817.   .     . TN   .Q     .992   .+02S
02402  02402  46 15744 15750      818.   .     . FM   .911   .922   .S
02403  02403  11 31000 15656      819.   .     . TP   .Q     .S1    .S
02404  02404  46 15745 15717      820.   .     . FM   .912   .921   .S
02405  02405  55 31000 15656      821.   .     . FS   .Q     .S1    .S
02406  02406  13 31000 15752      822.   .     . TN   .Q     .DET   .S
02407  02407  11 31000 32000      823.   .     . TP   .Q     .A     .S
02410  02410  17 02412 02411      824.   .     . ZJ   .L+2   .L+1   .S
```

FIG. D-3 COMPUTER PROGRAM (Continued)

```
02411  02411  45 00000 30000    425.   .     . NJ    .        .FILL     .S
02412  02412  55 15730 13716    426.   .     . FM    .J72     .3R1      .S
02413  02413  11 31000 13655    427.   .     . TP    .0       .S1       .S
02414  02414  56 15745 13751    428.   .     . FM    .J12     .9R2      .S
02415  02415  55 31000 13655    429.   .     . FS    .0       .S1       .S
02416  02416  57 31000 13752    430.   .     . FD    .0       .DET      .S
02417  02417  13 31000 00074    431.   .     . TN    .0       .DTLTA2   .JTETA2S
02420  02420  56 15744 13751    432.   .     . FM    .J11     .3R2      .S
02421  02421  11 31000 13656    433.   .     . TP    .0       .S1       .S
02422  02422  55 15747 13715    434.   .     . FM    .J21     .9R1      .S
02423  02423  55 31000 13656    435.   .     . FS    .0       .S1       .S
02424  02424  57 31000 13752    436.   .     . FD    .0       .DET      .S

02425  02425  13 31000 00075    437.   .     . TN    .0       .DS       .DSS
02426  02426  56 00074 13710    438.   .     . FM    .DTETA2   .AR2      .S
02427  02427  55 31000 13743    439.   .     . FS    .0       .AA3      .S
02430  02430  57 31000 13731    440.   .     . FD    .0       .AR1      .S
02431  02431  13 31000 00073    441.   .     . TN    .0       .DTETA1   .JTETA1S
02432  02432  11 00013 00076    442.   .     . TM    .TETA1   .DPHI1    .S
02433  02433  11 00012 00077    443.   .     . TP    .TETA2   .DPHI2    .S
02434  02434  11 00015 00100    444.   .     . TM    .S       .DU       .S
02435  02435  11 15471 00013    445.   .     . TP    .TT      .T        .S
02436  02436  45 00000 00057    446.   .     . NJ    .        .7        .S
02437  02437  11 01115 02435    447.   . LOOP . TJ   .1       .PASS3    .SUC TES (PASS3) IN PROG. STOPS
02440  02440  11 01105 01035    448.   .     . TP    .11      .1        .S

02441  02441  11 15730 32000    449.   .     . TP    .F       .A        .S
02442  02442  47 02147 02413    450.   .     . ZJ    .L+5     .L+1      .S
02443  02443  11 01000 13753    451.   .     . TP    .ZERO    .AYCAM    .S
02444  02444  11 01000 13750    452.   .     . TP    .ZERO    .TANCAM   .S
02445  02445  11 01000 13735    453.   .     . TP    .ZERO    .NONCAM   .S
02446  02446  45 00000 02471    454.   .     . NJ    .        .PASS4    .S
02447  02447  55 15710 01047    455.   .     . FM    .SINCAM  .DT       .S
02450  02450  55 31000 01053    456.   .     . FM    .0       .TAU      .S
02451  02451  57 31000 13712    457.   .     . FD    .0       .U2XU1    .S
02452  02452  55 31000 13715    458.   .     . FM    .0       .AR3      .S
02453  02453  56 31000 13727    459.   .     . FM    .0       .SS2      .S
02454  02454  72 15717 00075    460.   .     . FI    .TS      .DS       .S

02455  02455  56 31000 13713    461.   .     . FM    .0       .T2       .S
02456  02456  55 31000 13710    462.   .     . FM    .0       .T1       .S
02457  02457  11 31000 13753    463.   .     . TP    .0       .AYCAM    .S
02460  02460  56 01151 01017    464.   .     . FM    .T+0     .DT       .S
02461  02461  55 31000 13714    465.   .     . FM    .0       .SINCAM   .S
02462  02462  57 31000 13712    466.   .     . FD    .0       .U2XU1    .S
02463  02463  55 31000 13727    467.   .     . FM    .0       .SS,      .S
02464  02464  72 15715 00075    468.   .     . FI    .A+3     .DS       .S
02465  02465  55 31000 01021    469.   .     . FM    .0       .4        .S
02466  02466  57 31000 13712    470.   .     . FD    .0       .U2XU1    .S
02467  02467  56 31000 13710    471.   .     . FM    .0       .T1       .S
02470  02470  11 31000 13754    472.   .     . TM    .0       .TANCAM   .S
```

FIG. D-3 COMPUTER PROGRAM (Continued)

```
02471  02471  44 00073 00074    973.   * PASS4 * FA      *DTETA1   *DTETA2   *$
02472  02472  56 31000 01010    974.   *       * FM      *Q        *TR       *$
02473  02473  11 31000 15546    975.   *       * TP      *Q        *S1       *$
02474  02474  66 15470 01031    976.   *       * FM      *PGF      *EPS      *$
02475  02475  55 31000 15545    977.   *       * FS      *Q        *S1       *$
02476  02476  13 31000 15756    978.   *       * TN      *Q        *TORQ     *TORQUES
02477  02477  55 00073 15701    979.   *       * FM      *DTETA1   *LCOS2    *$
02500  02500  11 31000 15555    980.   *       * TP      *Q        *S1       *$
02501  02501  55 00011 00011    981.   *       * FM      *TETA1    *TETA1    *$
02502  02502  55 31000 15700    982.   *       * FM      *Q        *LSIN2    *$
02503  02503  13 31000 15557    983.   *       * TN      *Q        *S2       *$
02504  02504  44 00011 00012    984.   *       * FA      *TETA1    *TETA2    *$

02505  02505  56 31000 00013    985.   *       * FM      *Q        *S        *$
02506  02506  55 31000 01053    986.   *       * FM      *Q        *TWO      *$
02507  02507  11 31000 15721    987.   *       * TP      *Q        *S3       *$
02510  02510  44 00073 00074    988.   *       * FA      *DTETA1   *DTETA2   *$
02511  02511  55 31000 00016    989.   *       * FM      *Q        *U        *$
02512  02512  11 31000 15722    990.   *       * TP      *Q        *S4       *$
02513  02513  56 01127 15674    991.   *       * FM      *4        *COS1     *$
02514  02514  54 31000 15722    992.   *       * FA      *Q        *S4       *$
02515  02515  54 31000 15721    993.   *       * FA      *4        *S3       *$
02516  02516  54 31000 15557    994.   *       * FA      *Q        *S2       *$
02517  02517  54 31000 15556    995.   *       * FA      *Q        *S1       *$
02520  02520  56 31000 01055    996.   *       * FM      *Q        *WW       *$

02521  02521  11 31000 15757    897.   *       * TP      *Q        *NORM     *NORMS
02522  02522  56 01100 01015    898.   *       * FM      *K2       *S        *$
02523  02523  55 31000 00015    899.   *       * FM      *Q        *PHI2     *$
02524  02524  57 31000 01053    900.   *       * FD      *Q        *TWO      *$
02525  02525  11 31000 15760    901.   *       * TP      *Q        *SPRING   *$
02526  02526  55 01101 01015    902.   *       * FM      *C2       *S        *$
02527  02527  56 31000 00012    903.   *       * FM      *Q        *TETA2    *$
02530  02530  57 31000 01053    904.   *       * FD      *Q        *TWO      *$
02531  02531  11 31000 15761    905.   *       * TP      *Q        *DAMP     *$
02532  02532  44 00014 00015    906.   *       * FA      *PHI1     *PHI2     *$
02533  02533  11 31000 15762    907.   *       * TP      *Q        *ROT      *$
02534  02534  56 15730 01027    908.   *       * FM      *HF       *DELTA    *$

02535  02535  72 15702 01106    909.   *       * FI      *E        *HI       *$
02536  02536  11 31000 15743    910.   *       * TP      *Q        *FRIC     *$
02537  02537  11 02542 16070    911.   *       * ARFOS1  *27       *         *$
02540  02540  37 15777 15775
02541  02541  45 00000 02555    912.   *       * SJ      *         *NEXT7    *$
02542  02542  00 01751 02533    913.   * 27    * 00      *1001     *L+1      *$
02543  02543  00 00010 02426    914.   *       * 00      *T        *1302     *$
02544  02544  00 00000 16543    915.   *       * 00      *         *FL       *$
02545  02545  00 00014 02426    916.   *       * 00      *PHI1     *1302     *$
02546  02546  00 00000 16543    917.   *       * 00      *         *FL       *$
02547  02547  00 00015 02426    918.   *       * 00      *PHI2     *1302     *$
02550  02550  00 00000 16543    919.   *       * 00      *         *FL       *$
```

FIG. D-3 COMTPUTER PROGRAM (Continued)

```
02551 02551 00 00015 02426      920.  .           . 00   .U        .1302    .$
02552 02552 00 00000 16543      921.  .           . 00   .         .FL      .$
02553 02553 00 00011 02425      922.  .           . 00   .TETA1    .1302    .$
02554 02554 00 00000 16543      923.  .           . 00   .         .FL      .$
02555 02555 00 00012 02425      924.  .           . 00   .TETA2    .1302    .$
02556 02556 00 00000 16543      925.  .           . 00   .         .FL      .$
02557 02557 00 00013 02425      926.  .           . 00   .S        .1302    .$
02560 02560 00 00000 16543      927.  .           . 00   .         .FL      .$
02561 02561 00 15730 02425      928.  .           . 00   .MB       .1302    .$
02562 02562 00 00000 16543      929.  .           . 00   .         .FL      .$
02563 02563 00 00000 00000      930.  .           . 00   .         .        .$
02564 02564 00 00000 00000      931.  .           . 00   .         .        .$

02565 02565 11 02570 16000      932.  . NEXT/ . ANFOJ1 .Z#              .        .$
02566 02566 17 15777 13775
02567 02567 15 00000 02613      933.  .           . 00   .         .NEATIO  .$
02570 02570 00 01731 02571      934.  . Z#        . 00   .1001     .L+1     .$
02571 02571 00 01735 02425      935.  .           . 00   .DELTA1   .1302    .$
02572 02572 00 00000 16543      936.  .           . 00   .         .FL      .$
02573 02573 00 15731 02425      937.  .           . 00   .AYCAN    .1302    .$
02574 02574 00 00000 16543      938.  .           . 00   .         .FL      .$
02575 02575 00 15734 02425      939.  .           . 00   .TANCAM   .1302    .$
02576 02576 00 00000 16543      940.  .           . 00   .         .FL      .$
02577 02577 00 15736 02425      941.  .           . 00   .TORQ     .1302    .$
02600 02600 00 00000 16543      942.  .           . 00   .         .FL      .$

02601 02601 00 15757 02425      943.  .           . 00   .MMM      .1302    .$
02602 02602 00 00000 16543      944.  .           . 00   .         .FL      .$
02603 02603 00 15757 02426      945.  .           . 00   .SPRING   .1302    .$
02604 02604 00 00000 16543      946.  .           . 00   .         .FL      .$
02605 02605 00 15751 02425      947.  .           . 00   .UMM      .1302    .$
02606 02606 00 00000 16543      948.  .           . 00   .         .FL      .$
02607 02607 00 15570 02425      949.  .           . 00   .PHF      .1302    .$
02610 02610 00 00000 16543      950.  .           . 00   .         .FL      .$
02611 02611 00 00000 00000      951.  .           . 00   .         .        .$
02612 02612 00 00000 00000      952.  .           . 00   .         .        .$
02613 02613 11 02415 16000      953.  . NEXTIN. ANFOJ1 .Z10             .        .$
02614 02614 17 15777 13775

02615 02615 15 00000 02635      954.  .           . 00   .         .MASS3   .$
02616 02616 00 01731 02617      955.  . Z10       . 00   .1001     .L+1     .$
02617 02617 00 01417 01111      956.  .           . 00   .M13      .409     .$
02620 02620 00 00000 16513      957.  .           . 00   .         .AL      .$
02621 02621 00 01375 02426      958.  .           . 00   .I2       .1302    .$
02622 02622 00 00000 16543      959.  .           . 00   .         .FL      .$
02623 02623 00 15724 02426      960.  .           . 00   .UPMU     .1302    .$
02624 02624 00 00000 16543      961.  .           . 00   .         .FL      .$
02625 02625 00 15762 02426      962.  .           . 00   .RMT      .1302    .$
02626 02626 00 00000 16543      963.  .           . 00   .         .FL      .$
02627 02627 00 15765 02425      964.  .           . 00   .FMIC     .1302    .$
02630 02630 00 00000 16543      965.  .           . 00   .         .FL      .$
```

FIG. D-3 COMPUTER PROGRAM (Continued)

```
02431  02431  00 01131 02426        966.   .          . JO      .ZPS      .1502     .$
02432  02432  00 00100 10543        967.   .          . JO      .         .FL       .$
02433  02433  00 00100 00000        968.   .          . JO      .         .         .$
02434  02434  01 00100 00000        969.   .          . JI      .         .         .$
02435  02435  11 00110 32000        970.   . PASS3    . TP      .T        .A        .$
02436  02436  12 01111 01000        971.   .          . TJ      .TN       .SUB      .$
02437  02437  15 00000 01112        972.   .          . UJ      .         .START    .$
02440  02440  11 02513 15000        973.   . JIMO     . INFO31  .THE      .         .$
02441  02441  17 15777 15775
02442  02442  15 00000 30000        974.   . RETURN   . UJ      .         .FILL     .$
02443  02443  00 01751 02444        975.   . THE      . JO      .1031     .L+1      .$
02444  02444  00 15750 02571        976.   .          . JO      .IPST4    .IRUI     .$

02445  02445  00 00100 17403        977.   .          . JO      .         .NC       .$
02446  02446  00 15755 02426        978.   .          . JO      .AFSQRT   .1502     .$
02447  02447  00 00100 10513        979.   .          . JO      .         .FL       .$
02450  02450  00 00100 00000        980.   .          . JO      .         .         .$
02451  02451  00 00100 00000        981.   .          . JO      .         .         .$
02452  02452  15 00102 02455        982.   .          . INFO32  .         .NC       .$
02453  02453  11 00000 17435
02454  02454  17 17405 17403
                                    983.   .          . SUB     .HOFV     .80       .ACTUALLY 119
                                    984.   .          . TERMS   .5        .0        .$
                                    985.   .          . INOUT   .1        .1        .$
                                    986.   .          . UJ      .         .FIRST    .$

                                    987.   . ERROR    . ALARM   .         .         .$
                                    988.   . EXIT     . UJ      .         .FILL     .$
                                    989.   . ANS      . JO      .FILL     .FILL     .$
                                    990.   . PU       . JO      .FILL     .FILL     .$
                                    991.   . I        . EQUALS  .8        .8        .$
                                    992.   . DELT     . EQUALS  .307      .308      .$
                                    993.   . IMC1     . EQUALS  .313      .310      .$
                                    994.   . IMC2     . EQUALS  .410      .810      .$
                                    995.   . FIRST    . TP      .FP       .A        .$
                                    996.   .          . EJ      .K1       .L+3      .K1 IS ALWAYS 15
                                    997.   .          . TU      .TMLB     .WPO      .$
                                    998.   .          . UJ      .         .L+2      .$

                                    999.   .          . TU      .TMLA     .WPO      .$
                                   1000.   .          . FO      .T        .DEL1     .$
                                   1001.   .          . TP      .Q        .J        .$
                                   1002.   .          . JE      .1000019  .         .$
                                   1003.   .          . FA      .Q        .K2       .K2 IS 0.79327
                                   1004.   .          . TV      .Q        .INTMR    .$
                                   1005.   .          . FS      .Q        .K2       .$
                                   1006.   .          . JE      .Q        .         .$
                                   1007.   .          . FS      .Q        .J        .$
                                   1008.   .          . TN      .Q        .FRACT    .$
                                   1009.   .          . LQ      .INTGR    .A+1      .$
                                   1010.   .          . AT      .L+2      .L+2      .$
```

FIG. D-3 COMPUTER PROGRAM (Continued)

```
15770  15770  30 [illegible] 00033  4   219.                                        COUNTS [illegible]
15771  15771  30 [illegible] 00031  4   220.                                        COUNTS [illegible]
15772  15772  33 [illegible] 00033  4   221.                                        COUNTS [illegible]
                                                                                    COUNTS [illegible]
                                                                                    COUNTS [illegible]

                                     4   224.   .          . SUB    [illegible]  .38     .ACTUALLY [illegible]
17171  17171  15 [illegible] 17175   4   225.   . [illegible] . TJ  .           [illegible]  . [illegible]
17172  17172  47 [illegible] 17753   4   226.   . [illegible] . [illegible]     .   [illegible]
17173  17173  15 [illegible] 20033   4   227.   . [illegible] . TJ  .           .FILL   .1
                                     4   228.   .          . TEMPS  .0           .9      .1
                                     4   229.   .          . INPUT  .0           .9      .5

                                     4   230.   .          . EQUALS .4           .       .
                                     4   231.   .          . EQUALS .5           .       .
                                     4   232.   .          . EQUALS .5           .       .
                                     4   233.   .          . EQUALS .7           .       .
                                     4   234.   . A        . EQUALS .8           .       .
                                     4   235.   .          . EQUALS .9           .       .
                                     4   236.   .          . EQUALS [illegible]  .       .
                                     4   237.   .          . EQUALS [illegible]  .       .
                                     4   238.   .          . EQUALS [illegible]  .       .
                                     4   239.   .          . EQUALS [illegible]  .       .
                                     4   240.   .          . EQUALS [illegible]  .       .
17174  17174  15 [illegible] 20031   4   241.   .          . TJ     .            .FILL   .

[illegible]  17175  11 [illegible]   4   242.   . [illegible] . TM  [illegible]  [illegible]
[illegible]  [illegible]             4   243.   .          . [illegible]
[illegible]  17177  11 [illegible]   4   244.   .          . TM     [illegible]
[illegible]                          4   245.   .          . [illegible]
[illegible]                          4   246.   .          . TV     [illegible]
[illegible]                          4   247.   .          . [illegible]
[illegible]                          4   248.   .          . TV     [illegible]
[illegible]                          4   249.   .          . [illegible]
[illegible]                          4   250.   .          . TV     [illegible]
[illegible]                          4   251.   .          . [illegible]
[illegible]                          4   252.   .          . TV     [illegible]
[illegible]  17210  11 [illegible]   4   253.   .          . [illegible]

17211  17211  [illegible] 17217      4   254.   .          . ST     [illegible]
17212  17212  55 [illegible] 00017   4   255.   .          . [illegible]
17213  17213  [illegible] 17214      4   256.   .          . ST     [illegible]
17214  17214  [illegible]            4   257.   .          . [illegible]
17215  17215  11 [illegible] 00155   4   258.   .          . TM     [illegible]
17216  17216  [illegible]            4   259.   .          . ST     [illegible]
17217  17217  47 [illegible] 00035   4   260.   .          . TJ     [illegible]
17220  17220  11 [illegible] 17215   4   261.   .          . TM     [illegible]
17221  17221  55 [illegible] 00073   4   262.   . [illegible] . [illegible]
17222  17222  11 [illegible] 00257   4   263.   .          . TM     [illegible]
17223  17223  54 [illegible] 00155   4   264.   .          . FA     [illegible]
17224  17224  11 [illegible] 00011   4   265.   .          . TM     [illegible]
```

FIG. D-3 COMPUTER PROGRAM (CONTINUED)

```
17225 17225 75 20030 17237  A  266.  .        . JMU  .4       .L.2     .1
17226 17226 71 17321 17323  A  267.  .        . XA   .LOOP1   .<5      .6
17227 17227 11 17315 17771  A  268.  .        . IJ   .1       .LOOP1   .1
17230 17230 54 00010 17320  A  269.  .        . FA   .X       .H2      .1
17231 17231 11 31000 00010  A  270.  .        . TM   .J       .X       .1
17232 17232 17 00037 00035  A  271.  .        . XJ   .UNCK    .OUT     .1
17233 17233 11 17317 17315  A  272.  .        . TM   .N1      .I       .1
17234 17234 55 17320 00073  A  273.  . LOOP2  . FM   .H2      .F1      .1
17235 17235 11 31000 00321  A  274.  .        . TP   .J       .<21     .1
17236 17236 54 31000 00155  A  275.  .        . FA   .J       .VN1     .1
17237 17237 11 31000 00011  A  276.  .        . TM   .J       .V1      .1
17240 17240 75 20030 17252  A  277.  .        . JMU  .4       .L.2     .1

17241 17241 71 17330 17323  A  278.  .        . XA   .LOOP2   .<5      .1
17242 17242 11 17315 17236  A  279.  .        . IJ   .I       .LOOP2   .1
17243 17243 17 00037 00035  A  280.  .        . XJ   .SPCK    .OUT     .1
17244 17244 11 17317 17315  A  281.  .        . TP   .N1      .I       .1
17245 17245 55 00036 00073  A  282.  . LOOP3  . FM   .H       .F1      .1
17246 17246 11 31000 00321  A  283.  .        . TM   .J       .<21     .1
17247 17247 54 31000 00155  A  284.  .        . FA   .J       .VN1     .1
17250 17250 11 31000 00011  A  285.  .        . TM   .J       .V1      .1
17251 17251 75 20030 17253  A  286.  .        . JMU  .4       .L.2     .1
17252 17252 71 17334 17323  A  287.  .        . XA   .LOOP3   .<5      .1
17253 17253 11 17316 17245  A  288.  .        . IJ   .I       .LOOP3   .1
17254 17254 54 00012 17320  A  289.  .        . FA   .X       .H2      .1

17255 17255 11 31000 00010  A  290.  .        . TM   .J       .X       .1
17256 17256 17 00037 00035  A  291.  .        . XJ   .SECK    .OUT     .1
17257 17257 11 17317 17315  A  292.  .        . TP   .N1      .I       .1
17260 17260 55 00036 17325  A  293.  .        . FM   .H       .<9      .1
17261 17261 11 31000 17331  A  294.  .        . TM   .J       .HALTM   .1
17262 17262 55 17327 00073  A  295.  . LOOP4  . FM   .HALTM   .F1      .1
17263 17263 72 17324 00473  A  296.  .        . FI   .<7      .<41     .1
17264 17264 32 17324 00297  A  297.  .        . FI   .<7      .<11     .1
17265 17265 72 17316 00321  A  298.  .        . FI   .<6      .<21     .1
17266 17266 54 31000 00155  A  299.  .        . FA   .J       .VN1     .1
17267 17267 11 31000 00011  A  300.  .        . TM   .J       .V1      .1
17270 17270 75 20030 17272  A  301.  .        . JMU  .5       .L.2     .1

17271 17271 71 17337 17393  A  302.  .        . XA   .LOOP4   .<5      .1
17272 17272 11 17315 17262  A  303.  .        . IJ   .I       .LOOP4   .1
17273 17273 15 00000 17175  A  304.  .        . UJ   .        .EXIT    .1
17274 17274 00 00000 00073  A  305.  . S1     .      .        .F1      .1
17275 17275 00 00000 00297  A  306.  .        .      .        .<11     .1
17276 17276 00 00000 00155  A  307.  .        .      .        .VN1     .1
17277 17277 00 00000 00011  A  308.  .        .      .        .V1      .1
17300 17300 00 00000 00073  A  309.  . S2     .      .        .F1      .1
17301 17301 00 00000 00321  A  310.  .        .      .        .<21     .1
17302 17302 00 00000 00155  A  311.  .        .      .        .VN1     .1
17303 17303 00 00000 00011  A  312.  .        .      .        .V1      .1
17304 17304 00 00000 00073  A  313.  . S3     .      .        .F1      .1
```

FIG. D-3 COMPUTER PROGRAM (CONTINUED)

```
17305  17705  00 00000 00455  A   314.   .        .        .        .<31     .$
17306  17706  00 00000 00155  A   315.   .        .        .        .V01     .$
17307  17707  00 00000 00011  A   316.   .        .        .        .V1      .$
17310  17710  00 00000 00075  A   317.   . SM     .        .        .F1      .$
17311  17711  00 00000 00455  A   318.   .        .        .        .<3,     .$
17312  17712  00 00000 00237  A   319.   .        .        .        .<11     .$
17313  17713  00 00000 00321  A   320.   .        .        .        .<21     .$
17314  17714  00 00000 00155  A   321.   .        .        .        .V01     .$
17315  17715  00 00000 00011  A   322.   .        .        .        .V1      .$
17316  17716  00 00000 00000  A   323.   . I      .        .        .        .$
17317  17717  00 00000 00000  A   324.   . M1     .        .        .        .$
17320  17720  00 00000 00000  A   325.   . M2     .        .        .        .$

17321  17721  00 00000 00000  A   326.   . MATH   .        .        .        .$
17322  17722  00 00000 00000  A   327.   . SM     . F      .0M      .        .$
17323  17723  00 00000 00001  A   328.   . AM     . C      .1.      .        .$
17324  17724  17 75252 52525  A   329.   . S7     . F      ..3333   .33333   .$
17325  17725  00 05252 52525  A   330.   . SM     . F      ..65555  .666E67  .$
17326  17726  17 55252 52525  A   331.   . SM     . F      ..16565  .666E67  .$
                              A   332.   .        . ENDSUM .        .        .$
                              A   333.   .        . SUB    .MMF9.M  .80      .ACTUALLY ***
                              A   334.   .        . TEMPS  .5       .0       .$
                              A   335.   .        . INOUT  .1       .1       .$
17335  17735  15 00000 17740  A   336.   .        . TJ     .        .FIRST   .$
17336  17736  17 17750 17753  A   337.   . ERROR  . SLANT  .        .        .$

17335  17735  15 00000 30000  A   338.   . EXIT   . TJ     .        .FIL..   .$
17336  17736  00 40000 30000  A   339.   . ANS    . JO     .FILL    .FIL..   .$
17337  17737  00 40000 30000  A   340.   . FO     . JO     .FILL    .FIL..   .$
                              A   341.   . I      . EQUALS .3       .0       .$
                              A   342.   . DELT   . EQUALS .300     .300     .$
                              A   343.   . MUL1   . EQUALS .313     .313     .$
                              A   344.   . MUL2   . EQUALS .413     .810     .$
17340  17740  11 17357 32000  A   345.   . FIRST  . TP     .FO      .8       .$
17341  17741  15 17357 17344  A   346.   .        . TJ     .AT      .L+3     .<I IS ALWAYS ??
17342  17742  15 17374 17351  A   347.   .        . TU     .TMU3    .MP2     .$
17343  17743  15 00000 17315  A   348.   .        . TJ     .        .L+2     .$
17344  17744  15 17372 17351  A   349.   .        . TU     .TMLA    .MP2     .$

17345  17745  47 00010 00455  A   350.   .        . FU     .T       .DEL1    .$
17346  17746  11 51000 15435  A   351.   .        . TP     .0       .J       .$
17347  17747  05 10000 00000  A   352.   .        . JF     .1000317 .        .$
17350  17750  44 51000 17370  A   353.   .        . FA     .2       .<2      .<2 IS 0.7--27*
17351  17751  15 51000 17371  A   354.   .        . TV     .0       .INTGR   .$
17352  17752  55 51000 17370  A   355.   .        . FS     .0       .<2      .$
17353  17753  05 00000 00000  A   356.   .        . JA     .0       .        .$
17354  17754  55 51000 15435  A   357.   .        . FS     .2       .J       .$
17355  17755  13 51000 15437  A   358.   .        . TN     .0       .FRACT   .$
17356  17756  35 17371 30017  A   359.   .        . LQ     .INTGR   .A+15    .$
17357  17757  35 17351 17351  A   360.   .        . AT     .L+2     .L+2     .$
17360  17760  75 50000 17362  A   361.   .        . RPB    .2       .L+2     .$
```

FIG. D-3 COMPUTER PROGRAM (CONTINUED)

```
17361  17361  11 30000 17374  X  362.  •AP3   •TP     •FILL   •FA      •$
17362  17362  36 31000 17351  X  363.  •      •ST     •0      •L-1     •$
17363  17363  55 17375 17374  X  364.  •      •FS     •FB     •FA      •$
17364  17364  01 15437 17374  X  365.  •      •FP     •FRACT  •FA      •$
17365  17365  11 31000 17336  X  366.  •      •TP     •0      •ANS     •$
17366  17366  45 00000 17335  X  367.  •      •HJ     •       •EXIT    •$
17367  17367  00 00000 00001  X  368.  •K1    •X      •1      •        •$
17370  17370  23 36000 00000  X  369.  •K2    •323    •36000  •00000   •$
17371  17371  00 00000 00000  X  370.  •INTGR •300    •       •        •$
17372  17372  00 00436 00000  X  371.  •TBLA  •       •TBL1   •        •$
17373  17373  00 00532 00000  X  372.  •TBLB  •       •TBL2   •        •$
17374  17374  00 00000 00000  X  373.  •FA    •00     •       •        •$

17375  17375  00 00000 00000  X  374.  •FM    •00     •       •        •$
                              X  375.  •      •ENDSUB •       •        •$
                              X  376.          SUB     ARF074        79 WORDS
                              X  377.          SUB     ARF051       334 WORDS
                              X  378.          SUB     ARF052        51 WORDS
                              X  379.          SUB     ARF054       200 WORDS
                              X  380.          SUB     ARF055        24 WORDS
```

FIG. D-3 COMPUTER PROGRAM (CONTINUED)

```
RECOIL MASS  - -CARRIAGE INERTIA, RATE, DAMPING COEFF.      - -ELEVATING SYSTEM PRELOAD, RATE, DAMPING COEFF.
CAM-BEGINNING -CAM- END- -CONST. RECOIL FRICTION- -ELEVATION- -SEAL FRICT.- -BRG. FRICT. COEFF.- -REC. PRELOAD- -TRIGGER
  3.2749000      1.1500000 02   3.5000000 07   0.              0.              1.0000000 06   1.0000000 02
  1.0900000 01   1.9400000 01   5.0000000 02   6.0000000 01    9.0000000-02    3.0000000-02   1.3750000 03   2.1900000 01

    TIME         PHI-1           PHI-2           U               PHI-1-DOT       PHI-2-DOT
  DELTA T        AXIAL CAM       TANGENT. CAM    MOMENT REACT    NORMAL REACT    SPRING FORCE        U-DOT          RECOIL FORCE
                 ROUND NUMBER    RECOIL DIST.    CRADLE ROT.     RECOIL FRICT    PROP CPL ARM    DAMP. FORCE        POWDER FORCE

  1.0000000-03   3.3608951-06   -4.2535176-06    2.9899941 01    1.1379850-02   -1.4433479-02    4.0109432-02   6.7076800-04
  1.0000000-03   0.              0.             -3.7732409 04    1.3451141 03   -9.0816433 01   -2.7424370 01   2.9505000 04
                 1.0000000      -4.1404833-05   -8.9261948-07    9.0000033 02    6.3300000-01

  1.1000000-02   9.3377762-04   -4.8116847-04    2.8428111 01    4.8505319-01   -1.7653539-01   -3.3698580 02   8.2589147 03
  1.0000000-03   0.              0.             -1.7768294 04    3.4064706 03   -9.1422310 03   -3.3541724 02   9.2756031 04
                 1.0000000       1.4714320       4.5260915-04    9.1994373 02    6.3300000-01

  2.1000000-02   5.1597353-03   -8.2101478-06    2.4462985 01    3.4903055-01    1.3187259-01   -4.1172440 02   1.5382839 04
  1.0000000-03   0.              0.              9.2367794 04    3.4520419 03   -1.7499241 04    2.8855793 02   9.1799984 03
                 1.0000000       5.4309531       4.2387210-03    1.2491918 03    6.3300000-01

  3.1000002-02   1.3381546-02   -4.2098960-06    2.0657429 01    9.1390476-01    1.0675183-01   -3.5193110 02   1.4587394 04
  1.0000000-03   0.              0.              6.3802216 04    3.1469436 02   -6.1052025 03    3.1682047 02   0.
                 1.0000000       9.2445675       1.2954977-02    1.2293096 03    6.3300000-01

  4.1000004-02   2.3337765-02    4.5135206-04    1.7419455 01    9.8972490-01    4.3349411-02   -2.9917397 02   1.3957110 04
  1.0000000-03   0.              0.             -2.6223031 04   -4.1760146 03    8.5756492 03    4.6163881 01   0.
                 1.0000000       1.2480581 01    2.3789117-02    1.1974355 03    6.3300000-01

  5.1000005-02   3.1[illegible]2-02   1.2397262-03    1.4818789 01    3.9619498-01   -1.4345415-02   -2.6031170 02   1.4489104 04
  1.0000000-03   0.              0.             -1.6552844 05   -6.2475810 03    2.3554797 04   -2.3457049 01   0.
                 1.0000000       1.5281239 01    3.2413079-02    1.2244362 03    6.3300000-01

  6.1000007-02   3.3752299-02    1.3690103-03    1.2177108 01   -7.2214451-02   -5.7805299-03   -2.2675348 02   1.5996933 04
  1.0000000-03   0.              0.             -2.0240789 05   -3.4213166 03    2.5954196 04   -1.0983007 01   0.
                 1.0000000       1.7742877 01    3.5118306-02    1.2990466 03    6.3300000-01

  7.1000008-02   3.0020944-02    8.5709606-04    1.0109600 01   -8.7462122-01   -3.3675175-02   -1.8595813 02   1.7144459 04
  1.0000000-03   0.              0.             -1.2464126 05   -2.8199455 03    1.0284425 04   -4.3982833 01   0.
                 1.0000000       1.9790382 01    3.0878084-02    1.3572229 03    6.3300000-01
```

FIG. D-4 COMPUTER OUPUT FORMAT

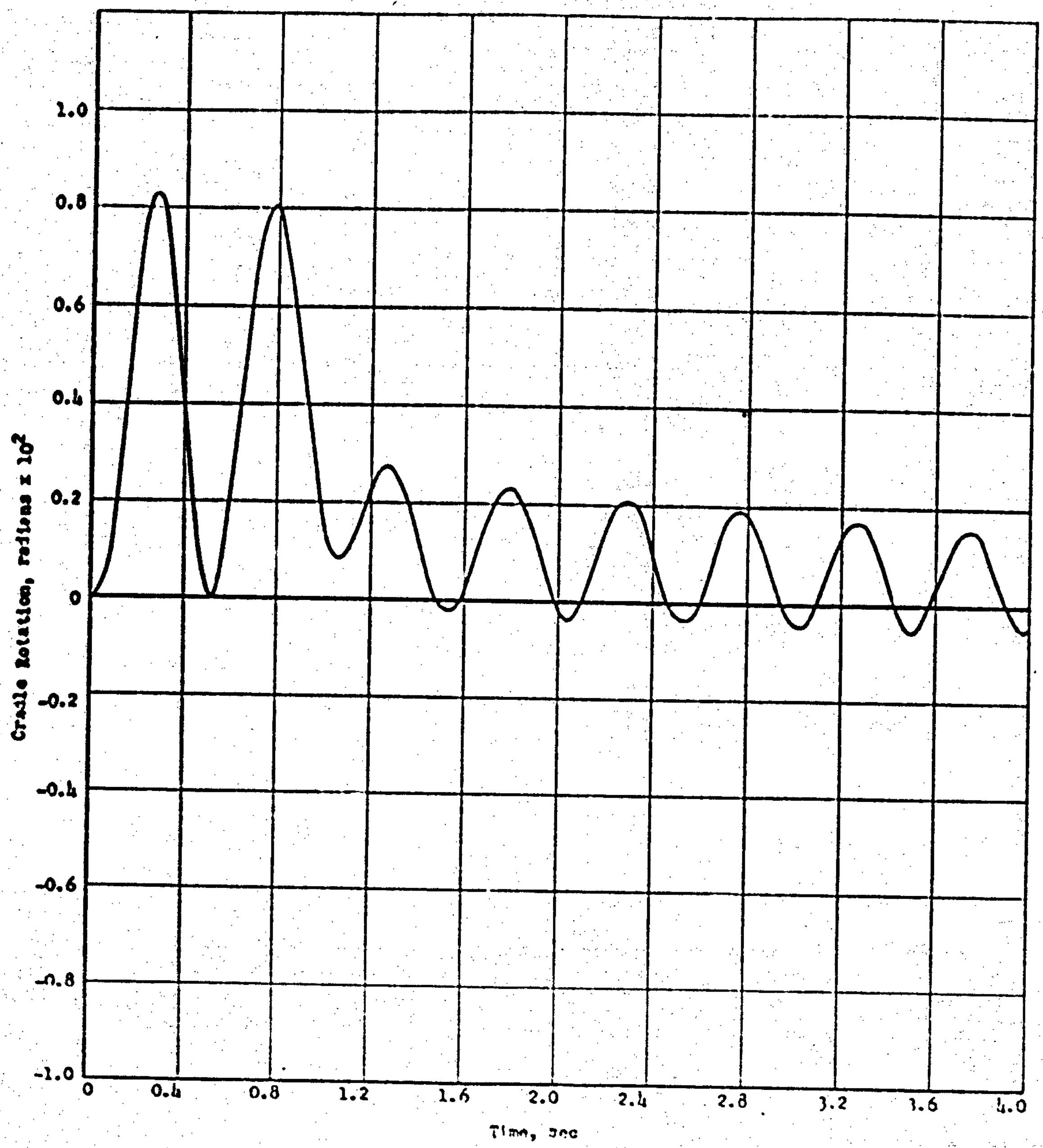

Fig. D-5 LAUNCHER RESPONSE FROM EARLY COMPUTER PROGRAM

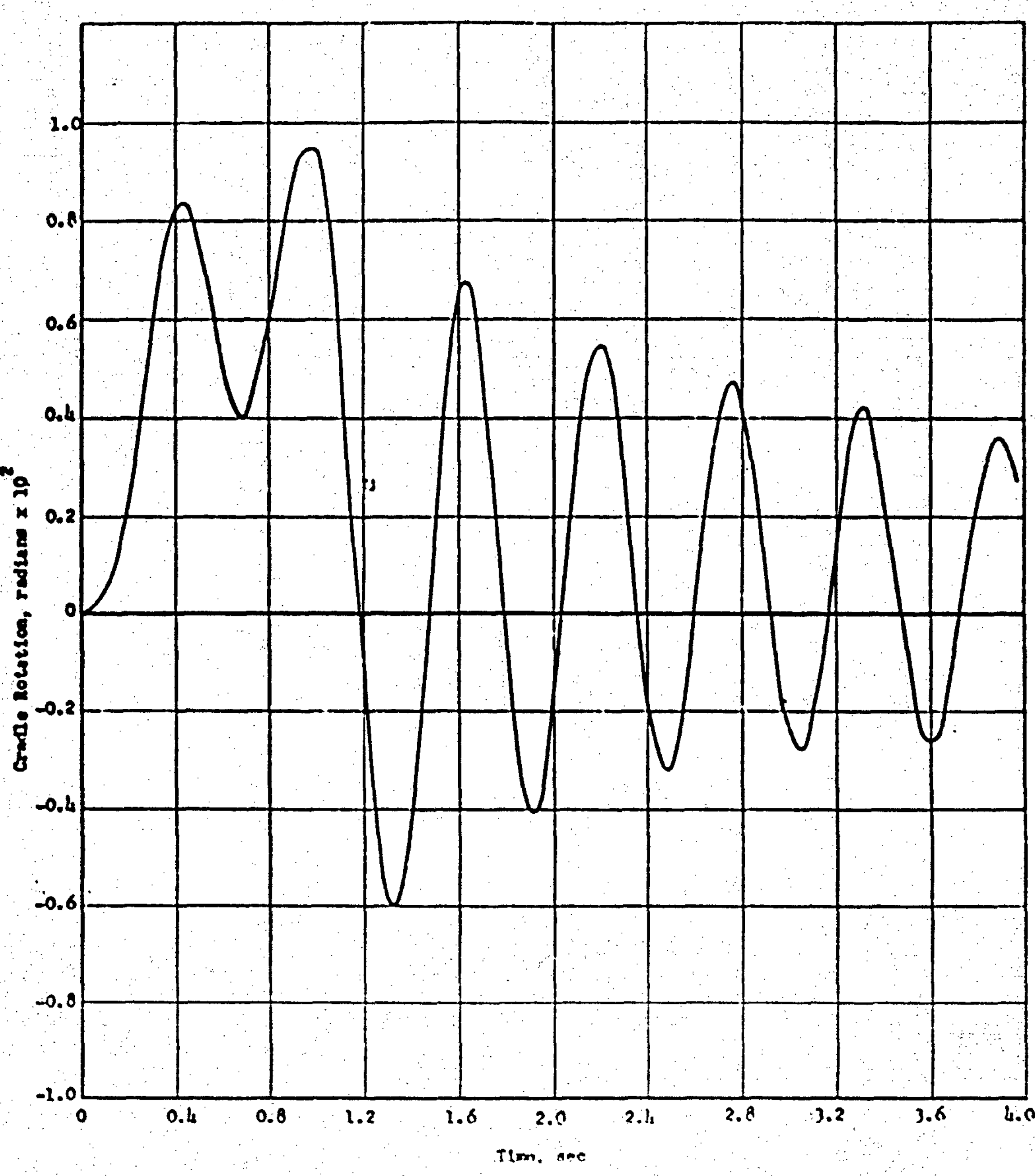

Fig. D-6 LAUNCHER RESPONSE FROM PRESENT COMPUTER PROGRAM

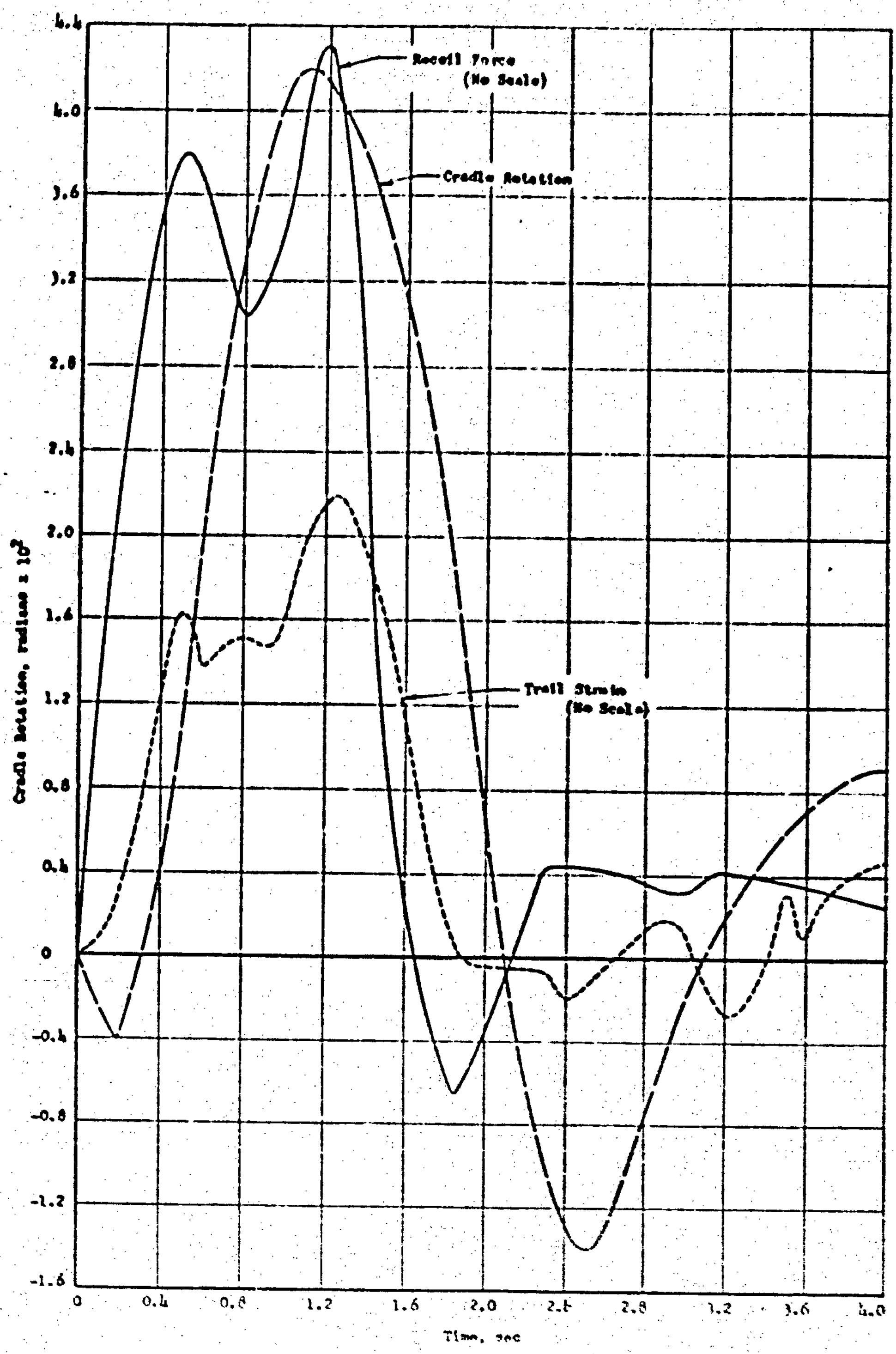

Fig. D-7 EXPERIMENTAL LAUNCHER RESPONSE

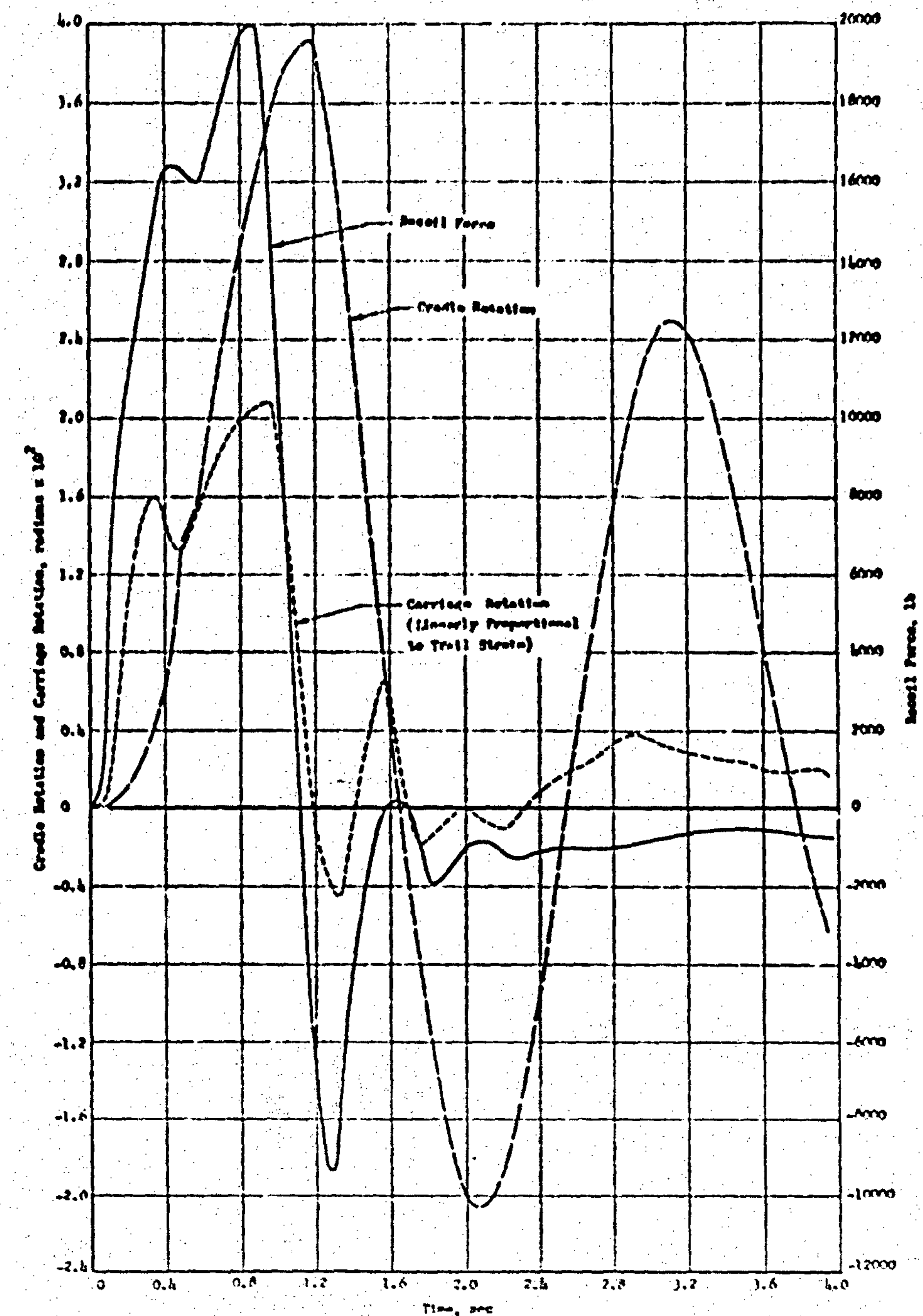

Fig. D-8 LAUNCHER RESPONSE FROM PRESENT COMPUTER PROGRAM CORRESPONDING TO EXPERIMENTAL RESPONSE

APPENDIX E

OPTIMUM ELEVATING SYSTEM PARAMETERS

Coleen Murray

I. INTRODUCTION

The purpose of this study was to determine the effects of various combinations of elevating system stiffness and damping upon gross launcher motion and to find the optimum combination of such stiffness and damping. The optimum combination was defined as that combination which yields a consistently low value of cradle displacement prior to the firing of each of the successive rounds of a burst and which concurrently yields a minimum corresponding cradle velocity. The work was based on the assumption that cradle oscillations sustained during a burst firing contribute directly to launching errors that cause dispersion of the shots of a burst. This study is concerned primarily with cradle motion, although barrel motion relative to the cradle is also a major cause of launching errors.

This study utilizes the work of Philip Meyfarth 1/ in order to define the general area of optimum damping for a given stiffness. Optimization of Meyfarth's third-order system yielded an optimum damping coefficient for any given elevating system stiffness. The damping determined by Meyfarth's work was used to indicate a value about which the damping should be varied in the Model V solutions in order to obtain the actual optimum. The ranges of optimum damping thus obtained for the several values of stiffness were then compared to each other, and a range of optimum stiffness, with corresponding optimum damping, was chosen. The third-order system was used because of the availability of the response data in the reference and the resulting simplification of the optimization procedure for the three-degree-of-freedom computer solution.

A few variations of equivalent carriage stiffness for the optimum elevating system were also investigated to determine the effect of this stiffness

---

1/ Meyfarth, P., Dynamic Response Plots and Design Charts for Third-Order Linear Systems, Research Memo No. R. M. 7401-3, Massachusetts Institute of Technology, 1958.

on cradle motion and trail hop, which is the upward deflection of the trails observed during firing of the XM70E1 launcher when the recoiling assembly is in its extreme recoil position. The values of launcher parameters maintained constant in the study are those of the XM70E1 Prototype No. 3 launcher at 0° traverse and 45° elevation.

II. DISCUSSION

A. Third-Order Analysis

The angular motion of the launcher was approximated by the motion of the following linear system with the proper conversion of units:

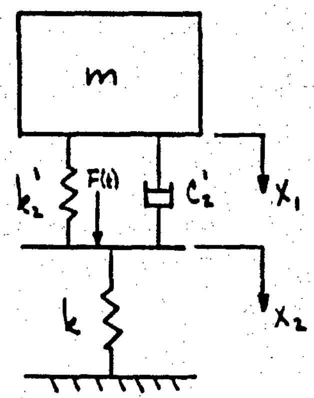

Fig. E-1 MODEL OF THIRD-ORDER SYSTEM

where

m	is an equivalent mass moment of inertia of the tipping parts about the trunnion, 7500 in. -lb-sec^2
k'_2	is the equivalent angular stiffness of the elevating system
c'_2	is the equivalent angular damping coefficient of the elevating system
k	is the combined angular stiffness of the carriages and trails, 3.5×10^7 in. -lb/radian
F(t)	is a forcing function applied to the trunnion.

The equation of motion for m is:

$$m \ddot{x}_1 = -k'_2 (x_1 - x_2) - c'_2 (x_1 - x_2) \quad \text{E-1}$$

From the statics at x_2, we have:

$$kx_2 = k'_2 (x_1 - x_2) + c'_2 (x_1 - x_2) + F(t) \quad \text{E-2}$$

By eliminating x_2 from E-1 and rewriting in terms of differential operators, one obtains:

$$D^3 x_1 (c'_2) + D^2 x_1 (k + k'_2) + D x_1 (c'_2 k/m) + x_1 (k \cdot k'_2 /m)$$

$$= (c'_2/m) \; D \; \left[F(t)\right] + (k'_2/m) \; \left[F(t)\right] \quad \text{E-3}$$

The left-hand side of Eq. E-3 may be factored into three factors, each representing a root of the system*. When two of these roots are complex conjugates, the parameters τ, ω, and ξ may be defined by the following equations:

$$\frac{c'_2 m}{k k'_2} = \frac{\tau}{\omega^2} \quad \text{E-4a}$$

$$\frac{(k + k'_2)m}{k k'_2} = \frac{(2\xi\tau\omega + 1)}{\omega^2} \quad \text{E-4b}$$

$$\frac{c'_2}{k'_2} = \frac{(\tau\omega + 2\xi)}{\omega}, \quad \text{E-4c}$$

where

τ is the constant of the factor representing the real root

ξ is the damping ratio associated with the complex-conjugate pair

ω is the undamped natural frequency associated with the complex-conjugate pair.

Let the right-hand side of Eq. E-3 be an impulse function of strength I; then, the solution of Eq. E-3 is:

---

* For a complete discussion of the following technique consult Meyfarth, Reference 1.

$$\frac{k\,k_2'}{m\,\omega^{1}}\; y(\omega t) = \frac{1}{\frac{1}{\tau\omega} - 2\xi + \tau\omega} \left\{ e^{-t/\tau} + e^{-\xi\omega t} \cdot \left[\frac{\left[\frac{1}{\tau\omega} - 2\xi\right] + \xi}{\sqrt{1-\xi^2}} \sin\sqrt{1-\xi^2}\;\omega t - \cos\sqrt{1-\xi^2}\;\omega t \right] \right\} \qquad \text{E-5}$$

The first of the two terms in the right-hand side of Eq. E-5 is an inverse exponential which decreases with increasing time; the second is the product of an inverse exponential and a sinusoidal function. The sinusoidal function will decay in the shortest time when the values of the coefficients of t in the exponents are minima. The values of τ, ω, and ξ which appeared to yield the best damping were chosen from the graphs in Reference 1 and the corresponding value of damping was then evaluated.

Figure E-2 shows the response for several values of k_2' with the corresponding optimum damping. The angular stiffness and angular damping coefficient, k_2' and c_2', were converted to values corresponding to linear restraints by multiplying by 10^{-3} (the inverse of the square of the distance from the trunnion to the elevating screw bracket).

The following comments are made on the statement preceeding Equation E-4a, concerning the pair of complex roots. Large values of stiffness always result in two of the roots being complex conjugates. However, below a certain stiffness it is possible to get three real roots for some ranges of damping. Furthermore, as the stiffness decreases, there is an increase in the range of damping which causes this. When these damping values were used as input to the computer solutions, they resulted in a continuously increasing (non-oscillatory) displacement, as shown in Figure E-3.

B. Computer Solutions

Initially, the computer solutions were investigated for the combined carriage and trail stiffness of 45×10^6 in.-lb/radian, which is about 30% higher than the measured stiffness. A range of very good response was found for stiffness of 1.0×10^4 lb/in. and damping of 360 to

540 lb-sec/in. Several graphs of cradle rotations resulting from paired values of stiffness and damping in this range are shown in Fig. E-4. The choice of an optimum combination here would be arbitrary because, at the time of each succeeding firing, the cradle displacement is uniform (Fig. E-5) and the velocity is small for all of the responses.

To illustrate that this optimum system is an improvement, its response is compared in Fig. E-6 with a response similar to that of the present weapon (with little damping). Also shown is an over-damped response, to demonstrate that an optimum damping does exist.

It was realized that there were limits on the obtainable values of stiffness and damping in the elevating system. Very high stiffness was shown to be difficult to achieve in previously built launchers, and extremely low stiffness presents a problem of stability during sighting and also is subject to excessive preload deflections. Comparison of experimental and analytical results indicates that damping corresponding to at least 90 lb-sec/in. is inherent in the launcher system; thus, no smaller damping is feasible.

Next, a much lower stiffness with increased damping was investigated to discover if cradle rotation would thus be decreased. Fig. E-3 shows that for damping between the non-oscillating range up to the maximum damping used, increased damping gives better response. Nevertheless, these responses are not as good as those with the higher spring rate (see Fig. E-7 for comparison). Also, the study of a 4-rd burst (Fig. E-8) showed that cradle rotation increased with each round.

Finally, the computer solutions were investigated for the combined carriage and trail stiffness of 35×10^6 in.-lb/radian; this is very close to the experimental value for Prototype No. 3. Although the initial maximum cradle rotation was somewhat greater than for the stiffer structure, the range of good response was similar. The optimum response still occurred for a stiffness of 1.0×10^4 to 1.4×10^4 lb/in. and damping of 360 to 540 lb-sec/in.

Trail hop was significantly affected by the carriage stiffness, k_1, as shown in Fig. E-9, which is a plot of the cradle rotation for three systems with otherwise identical parameters. The maximum negative

rotation at about 0.2 sec of the supporting structure is an indication of the relative magnitude of the hop, illustrating that trail hop greatly decreases with increasing carriage stiffness.

During tho course of the study, it was noted that the optimum damping determined from the computer solutions agreed with the optimum predicted by the third-order analysis, where linear stiffnesses from 1.0×10^4 to 1.4×10^4 lb/in. corresponded to optimum damping from 460 to 510 lb-sec/in. Such close agreement was interesting and unexpected, in that the Model V equations include the actual input force, cam path, and many nonlinear launcher effects not considered in the third-order system.

III. CONCLUSIONS

On the basis of the investigations described above, it is concluded that improved firing accuracy can be achieved for the system studied by adding damping to the elevating system. Specifically, the stiffness of the elevating system should be about 1.0×10^4 to 1.4×10^4 lb/in. and the damping of the elevating system should be about 360 to 540 lb-sec/in., for the maximum improvement.

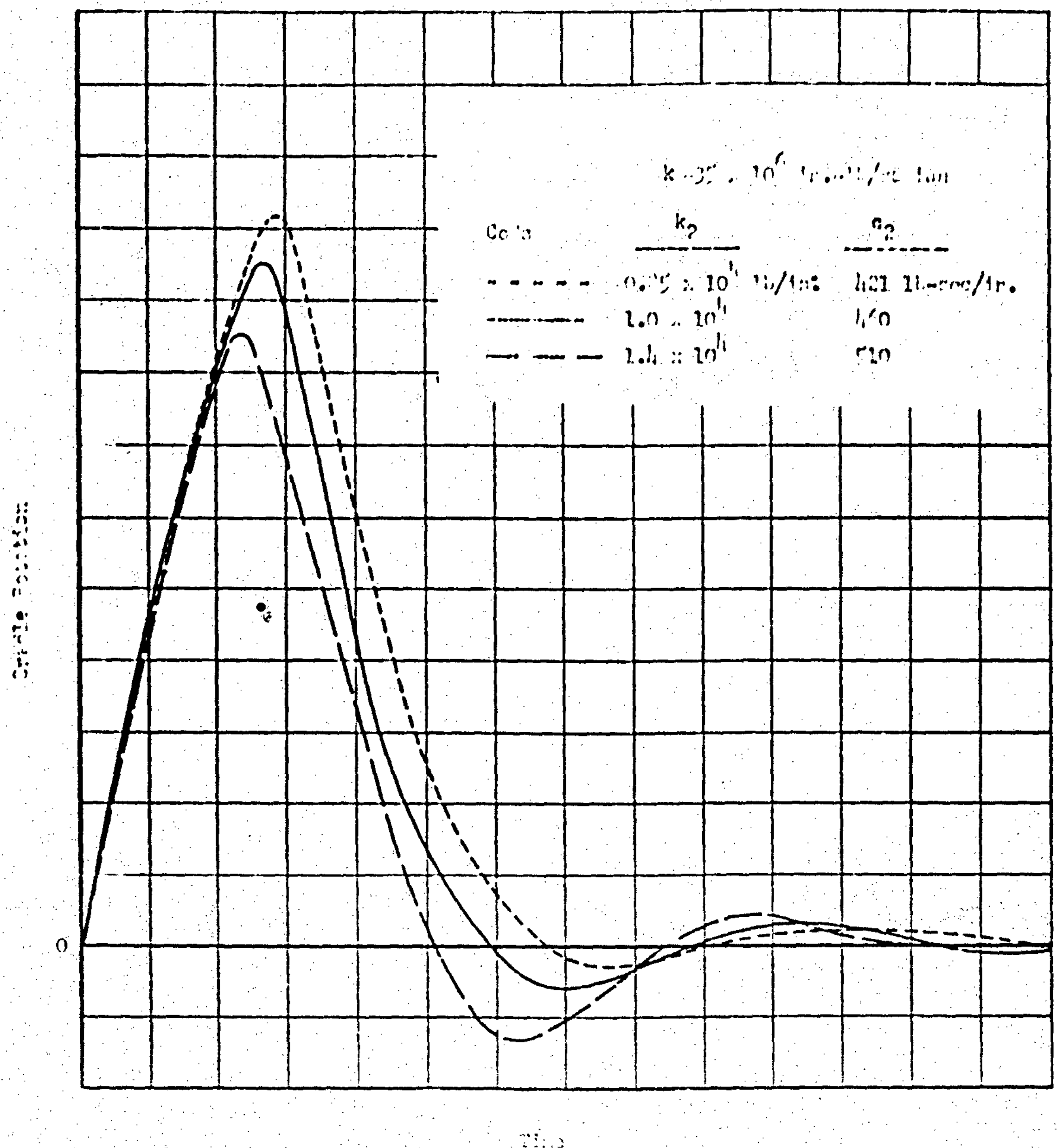

Fig. E-2 CRADLE ROTATION FROM THIRD-ORDER SYSTEM ANALYSIS

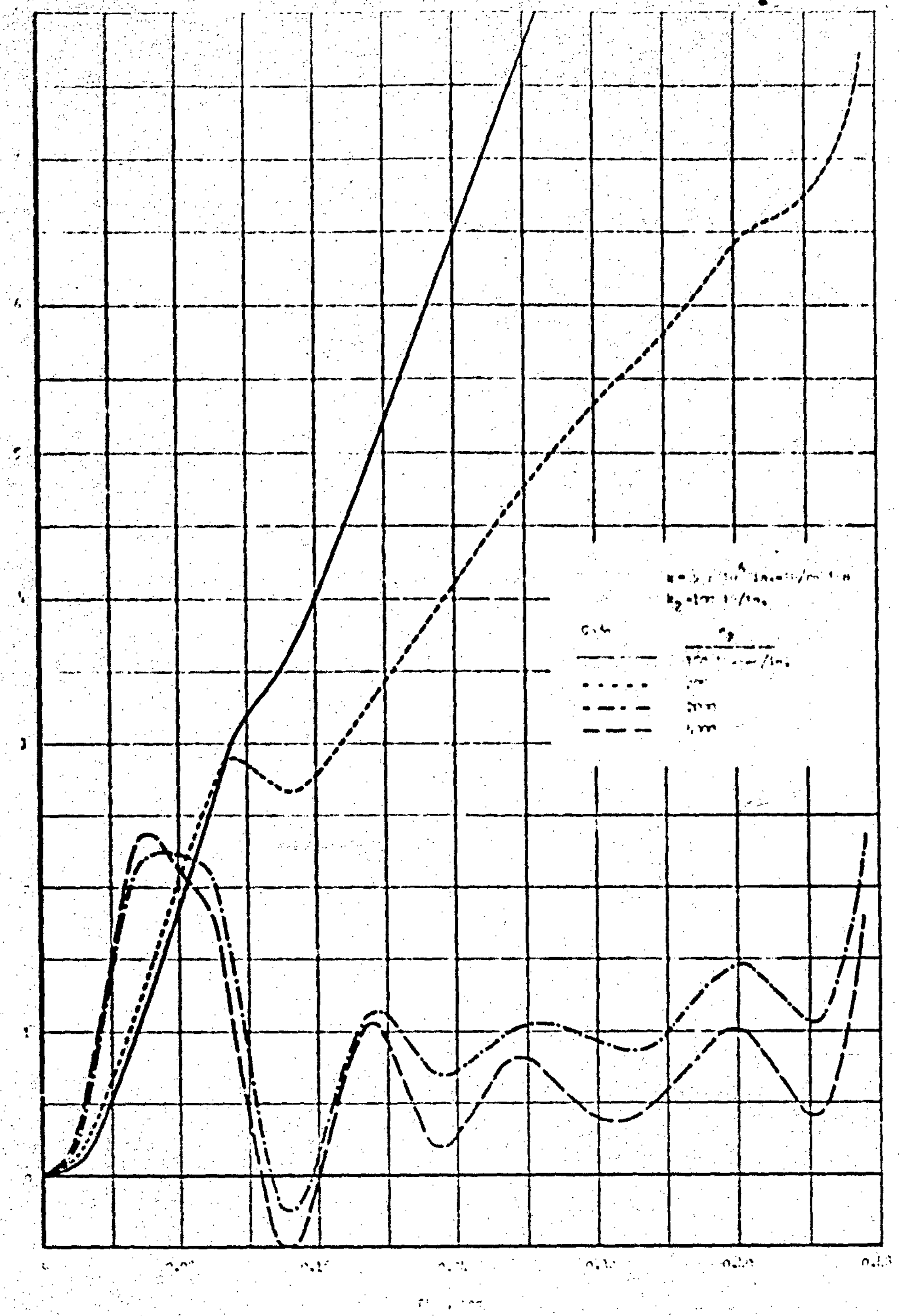

Fig. E-3 EFFECTS OF DAMPING ON CRADLE ROTATION WITH LOW ELEVATING SYSTEM STIFFNESS

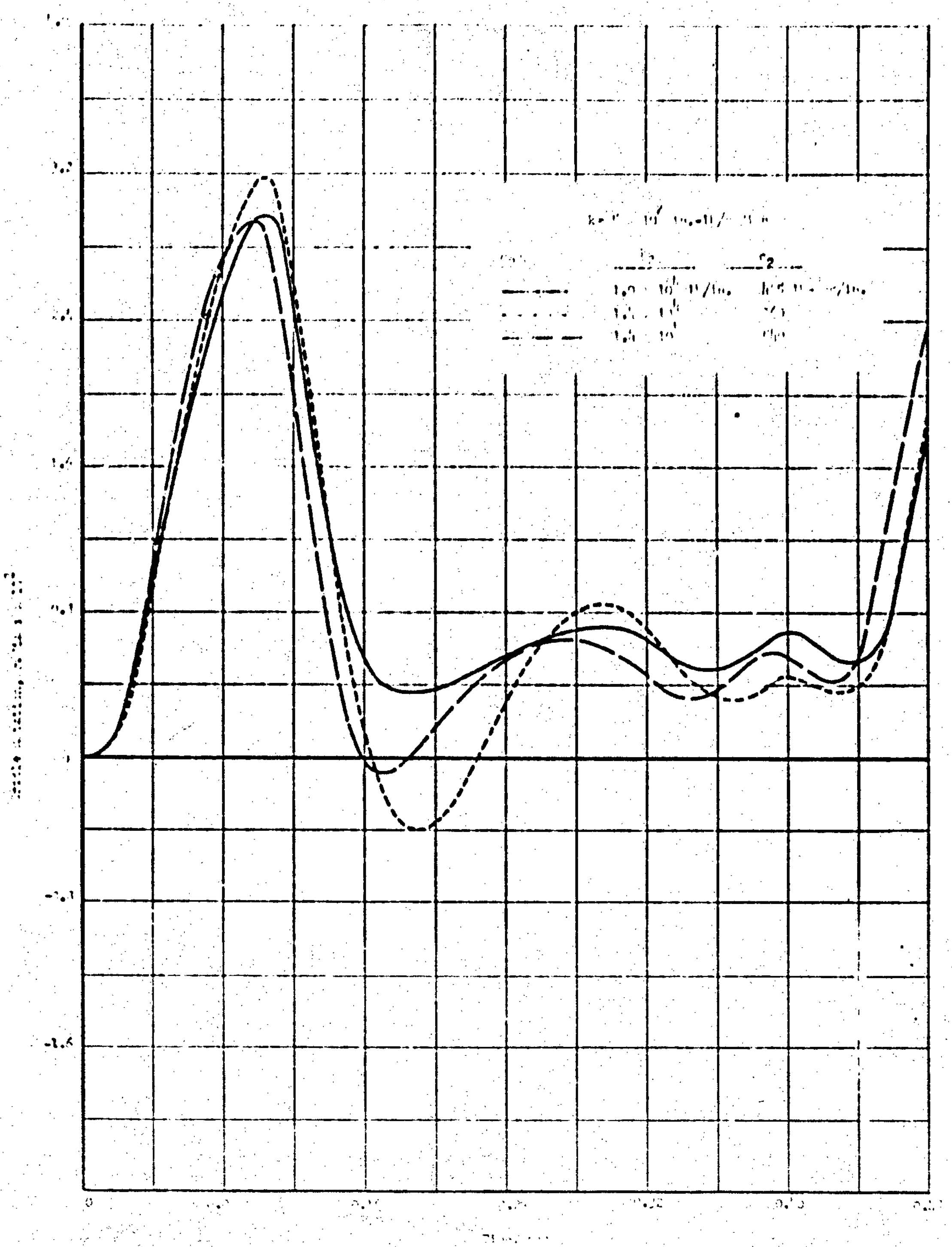

Fig. E-4 OPTIMUM RESPONSES

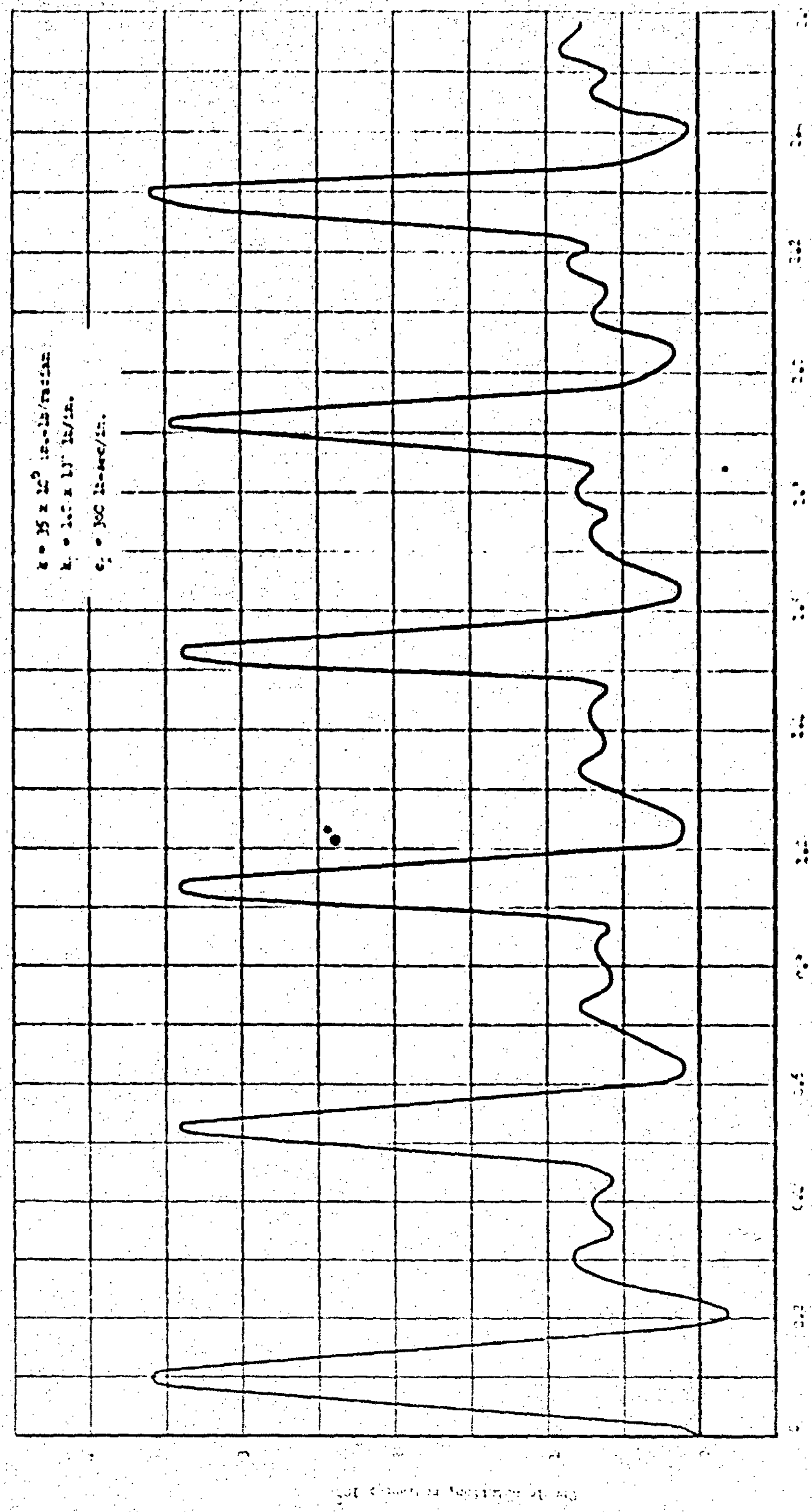

Fig. E-5 CRADLE ROTATION FOR A 6-RD BURST WITH OPTIMUM ELEVATING SYSTEM

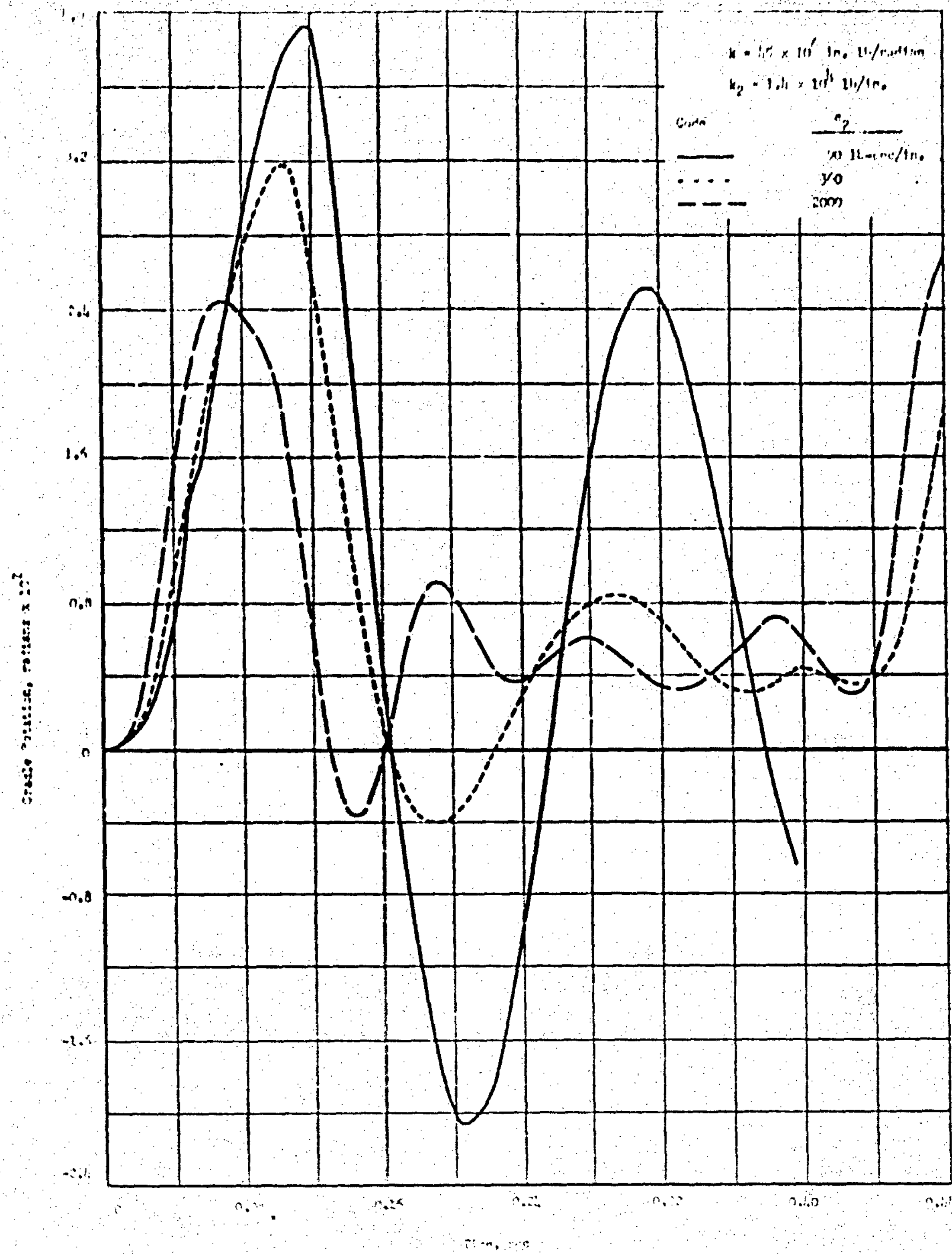

Fig. E-6 RESPONSES FOR VARIOUS ELEVATING SYSTEM DAMPING COEFFICIENTS

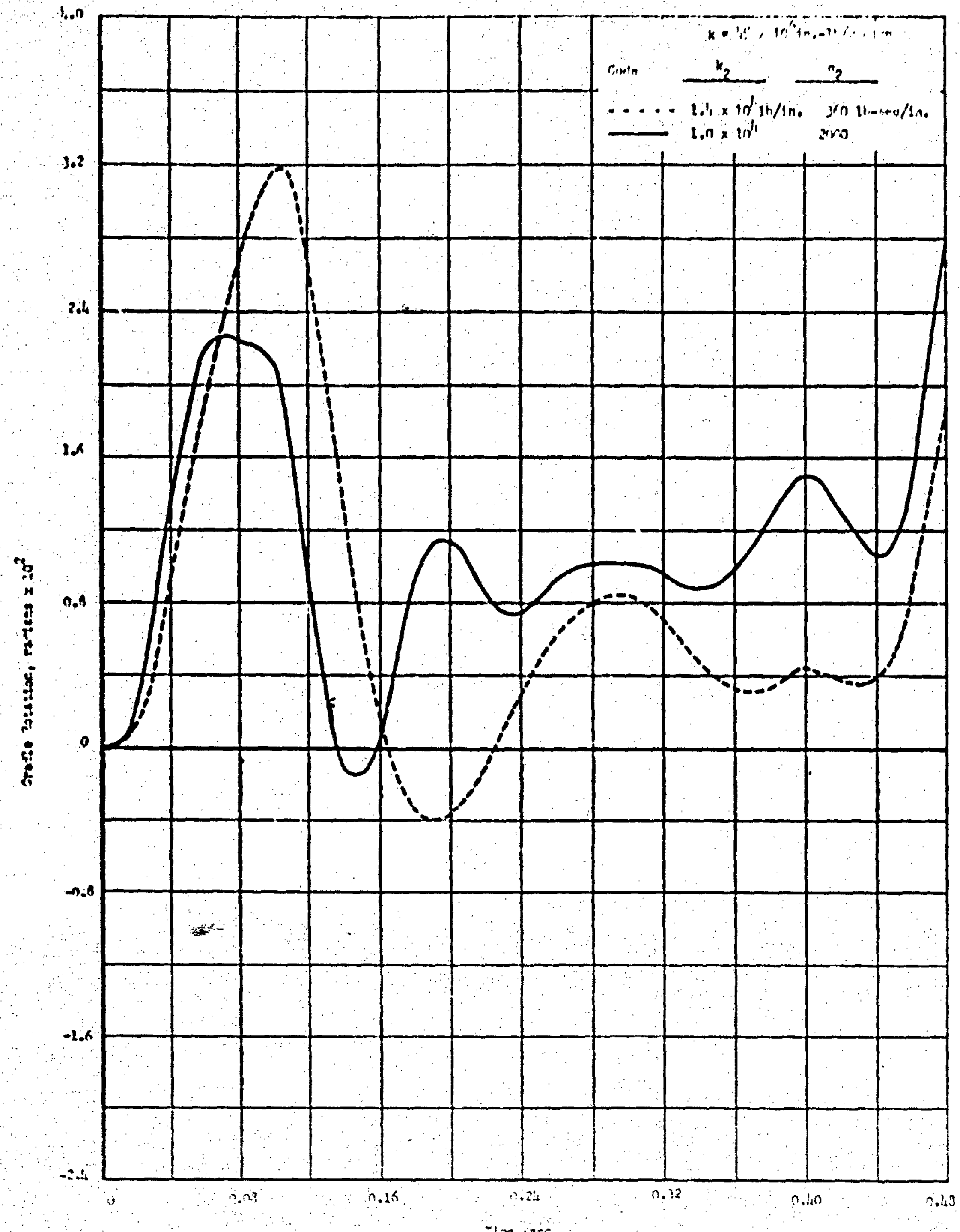

Fig. E-7 COMPARISON OF CRADLE ROTATION FOR A LOW ELEVATING STIFFNESS TO AN OPTIMUM SYSTEM

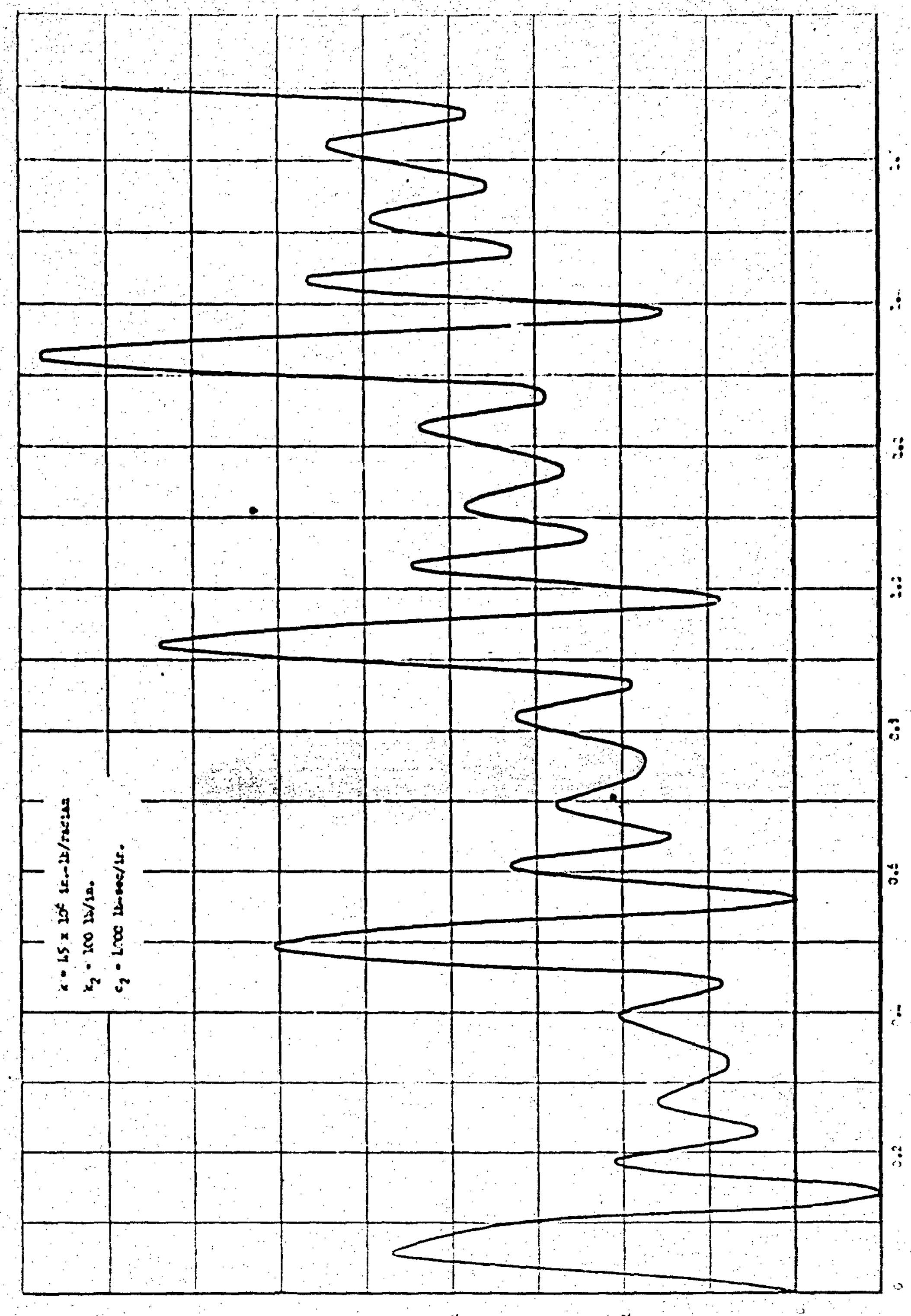

Fig. E-8 CRADLE ROTATION FOR A 4-RD BURST WITH LOW ELEVATING SYSTEM STIFFNESS

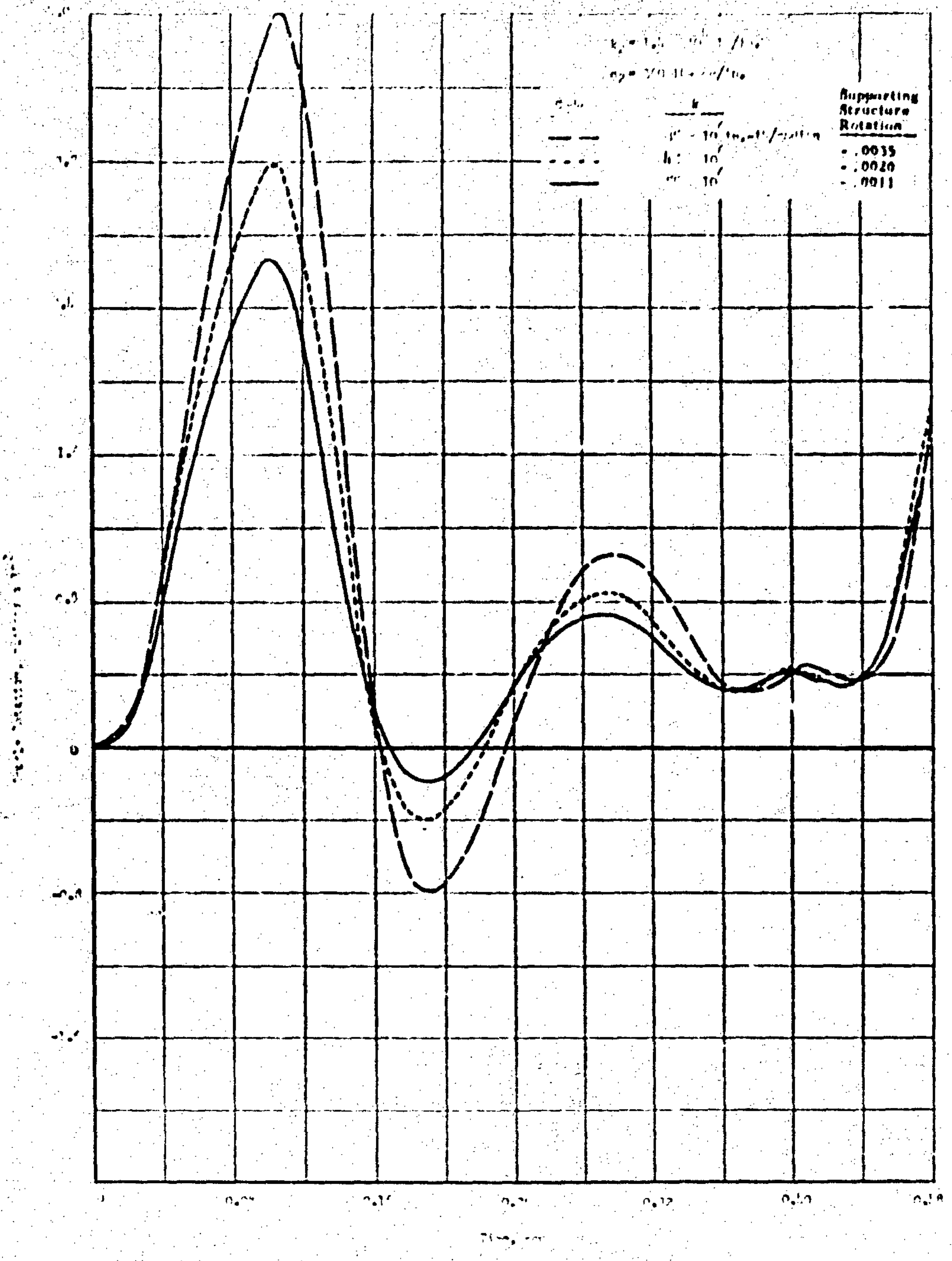

Fig. E-9 EFFECT OF CARRIAGE STIFFNESS ON CRADLE ROTATION

APPENDIX F

GENERAL EQUATIONS OF MOTION OF LAUNCHER DYNAMICS

I. INTRODUCTION

The 3-degree-of-freedom model, presented in Appendix C, was programmed for a digital computer and has been used extensively. As a 3-degree-of-freedom model, it has the advantage of relative simplicity and also reproduces much of the primary behavior of the XM70-type launcher. On the other hand, the very simplicity precludes its application to many of the presumedly secondary features of the launcher. In order to study these features, a more complete model with up to n-degrees of freedom was constructed.

The following are some of the salient features of this more complete model that are present in addition to the features of the 3-degree-of-freedom model:

1. The base of the launcher is not assumed to be fixed to a rigid foundation; instead, the trail pads and base plate are placed on visco-elastic supports which can be assigned parameter values corresponding to various terrain compositions (clay, sand, concrete, etc.). The model takes cognizance of the fact that this may be a one-way support condition so that trail hop and base hop are directly reproduced. Should the need arise, the model can be easily altered to reproduce progressive trail dig-in and base settlement.
2. It is recognized that the launcher does not recoil straight back, maintaining its position in its initial vertical plane. The tendency for three-dimensional rotation about the ball joint is allowed for. Reaction forces and moments at the ball joint, the trunnion supports, the cradle, and the recoiling parts are admitted as three-dimensional quantities.
3. The flexibility of the recoiling assembly is provided for, as are the lateral and vertical variations of center of gravity and inertial force location from shot to shot. The additional features allow the reproduction and study of the "left-right sequencing" phenomenon observed in tests of the XM70 prototype launchers.
4. The transmission of rifling torque to the launcher structure is included, as are the force parameters and geometrical freedoms necessary for interpretation of its effect.

5. The rifled firing tube is represented as a flexible piece with many degrees of freedom in both the vertical and horizontal planes. This permits the investigation of tube whip and vibrations and their effect on both the supporting structure and the projectile.

6. The projectile itself is a part of the model. The resultant effects include the variation of mass during firing and the influence of traveling forces on launcher tube motion.

7. A result of the inclusion of the increased geometrical freedom and applied forces is the introduction of Coriolis forces (in three dimensions) and gyroscopic moments not previously considered. An additional result is the inclusion of more of the coupled effects of the motion of the various launcher components.

This appendix presents a summary of the derivation of the basic equations of this model, as well as graphical and verbal definitions of the known and unknown parameters involved with the basic equations that govern the model. The motion of the launcher can be best expressed in terms of a set of interdependent right-hand three-dimensional coordinate systems, as shown in Fig. F-1. Coordinate system 1 ($[S_1]$) is fixed in the earth at the trail pads with y_1 vertical. Then, x_1 is defined by a plane through y_1 and the initial tube centerline. Systems $[S_2]$ and $[S_3]$ have origins at the ball joint and arise from a translation and a rotation through angle ($\theta_1 + \theta_2$) and the x_1, y_1 plane. Angle θ_1 is a measure of trail flexibility, while angle θ_2 os a ball-joint rotation. System $[S_4]$ arises through a rotation through angle θ_3 about y_3. Thus, y_4 coincides with y_3. System $[S_5]$ arises through a rotation through angle θ_4 about x_4; x_5 coincides with x_4. It is apparent that θ_3, θ_4, θ_5, represent freedoms at the ball joint. We arrive at $[S_6]$ by means of a translation through distance ℓ_2 and a rotation through angle $\alpha + \theta_5$; the origin of $[S_6]$ is at the trunnions. The angle α is the angle of elevation and θ_5 is the freedom in elevation permitted by the flex system. The tube base is located a distance ℓ_7 along the x_6 axis. Left-right sequencing forces the tube to swing through an angle θ_6 about an axis parallel to y_6. In addition to coordinate systems, Fig. F-1 illustrates many of the quantities which are defined on the following pages and which appear in the equations.

II. SPECIFIED QUANTITIES

ℓ_1	trail length
ℓ_2	carriage side length
ℓ_3	trunnion-to-cradle center of gravity
ℓ_4	ball joint to flex attachment
ℓ_5	y_6-position of breech center of gravity
ℓ_6	z_6-position of breech center of gravity
ℓ_7	distance from breech center of gravity to tube base
L	tube length
u_o	initial x_6-position of breech center of gravity
α	elevation angle
ξ_0	initial projectile position with reference to tube base
ℓ_8	distance from trunnion to flex attachment point
ℓ_9	horizontal (z_6) distance of cluster axle from tube centerline
β_1	carriage side orientation
β_2	flex system orientation
I	tube moment of inertia $= \frac{\pi}{4}(r_2^4 - r_1^4)$
ρ	tube mass density per unit length
m_p	projectile mass
$\left.\begin{matrix} J_x \\ J_y = J_z \end{matrix}\right\}$	mass polar inertial moments of projectile
$\left.\begin{matrix} \varphi(t), \ \varphi = \varphi^* \\ \varphi = \varphi_9 \end{matrix}\right\}$	prescribed projectile spin history
m_B	breech mass

J_{Bx}, J_{By}, J_{Bz}	mass polar inertial moments of breech
m_A	cradle mass
I_{Ax}, I_{Ay}, I_{Az}	mass polar inertial moments of cradle
m_1	concentrated mass at rear of trails (one-half trail mass)
I_{xc}, I_{yc}, I_{zc}	mass polar inertial moments of carriage about ball joint
m_B	one-half mass of trails plus mass of carriage and trunnion sides concentrated at ball joint
m_r	mass of right ($+ z_o$) cluster and projectiles
m_ℓ	mass of left ($- z_6$) cluster and projectiles
k_1, γ_1	spring and damping constants at trail rear
k_2, γ_2	spring and damping constants at trail front
k_3	angular trail and carriage stiffness (z-axis)
k_4	carriage stiffness for torque about y-axis
k_5	carriage stiffness for torque about x-axis
k_6, γ_6	spring and damping constants for flex system
E	Young's modulus (3×10^7)
μ	coefficient of friction between breech and cradle
$F(t)$	resultant "powder-gas force"
k_8	breech "stiffness" for right-left sequencing
V_n	eigen values

b_n	wave numbers $b_n^4 = \frac{\rho}{EI} V_n^2$	
	$L b_1 = 1.875$	
	$L b_2 = 4.694$	
	$L b_3 = 7.855$	
	$L b_4 = 10.996$	
	$L b_5 = 14.137$	
	$L b_6 = 17.279$	
K	recuperator preload	
k_7	recuperator spring rate	
H_1	constant recuperator friction force	
γ	oil density	
A_p	piston area	
C_o	orifice coefficient	
$\alpha_o(u)$	orifice area	
g	acceleration of gravity	
δ	proportionality constant; seal friction to recoil force	
I_B	cluster inertia moment	
R_p	cam pitch radius	
h	height of cam path development	
u_1	initial cam engagement point	$u_1 \leq u \leq u_2$
u_2	final cam engagement point	

III. LOGICAL SYMBOLS

$$H(\zeta) = \begin{cases} 0 \text{ for } \zeta \leq 0 \\ 1 \text{ for } \zeta > 0 \end{cases} \quad (\zeta \text{ generic})$$

$$\epsilon = \begin{cases} 1 \text{ for } \dot{u} < 0 \\ -1 \text{ for } \dot{u} > 0 \\ 0 \text{ for } \dot{u} = 0 \end{cases}$$

$|A|$ = absolute value of A (A generic)

IV. PHYSICAL VARIABLES (Unknowns)

y_T	trail end deflection
y_B	ball joint deflection
u	breech displacement along cradle measured from trunnion
x_ℓ	displacement of tube base: $x_\ell = u + \ell_7$
ζ	position of projectile measured from tube base; positive in x_6 direction
v	y_6-displacement of tube at point x
w	z_6-displacement of tube at point x
θ_1	angle due to "rigid" base movement $\theta_1 = \arcsin \frac{y_B - y_T}{\ell_1}$
θ_2	flexural rotation of combined carriage flexibility
θ_3	transverse angle of rotation about y_3
θ_4	angle of rotation about x_4
θ_5	elevating system flexibility
θ_6	right-left sequencing flexibility of breech
$q_n(t)$	time history for nth vibrational mode of tube in y_6-direction
$h_n(t)$	time history for nth. vibrational mode of tube in z_5-direction
$\theta_7 = \psi_y$	rotation about z_8 . . . $\psi_y = - \frac{\partial w}{\partial x}$
$\theta_8 = \psi_z$	rotation about y_8 . . . $\psi_z = \frac{\partial v}{\partial x}$
R_{6x}, R_{6y}, R_{6z}	ball joint force reactions at trunnion; positive acting on carriage; components in system 6
E_{6x}, E_{6y}	flex system force components; positive acting on carriage; components in system 5

T_{6x}, T_{6y} — trunnion moment reactions; components in system 6; positive acting on carriage

P_{cx}, P_{cy}, P_{cz} — force reaction between cradle and breech; components in system 6; positive acting on cradle

N_{cx}, N_{cy}, N_{cz} — moment reaction between cradle and breech; components in system 6; positive acting on cradle

$S_x(0, t)$, $S_y(0, t)$ — shear force between breech and tube

$M_y(0, t)$, $M_z(0, t)$ — moments between breech and tube

N_{py}, N_{pz} — force reaction between projectile and tube; components in system 6; positive when acting on projectile

M_{px}, M_{py}, M_{pz} — moment reaction between projectile and breech, when projectile is in breech; components in system 6; positive when acting on projectile

C_{px} — moment reaction between projectile and tube when projectile is in tube -- transferred rigidly to tube-breech connection; component in system 6; positive when acting on projectile

$C_5 = \cos(\alpha + \theta_5)$

$S_5 = \sin(\alpha + \theta_5)$

$C_9 = \cos \varphi$

$S_9 = \sin \varphi$

R_1 — ground reaction and gravity force at y_T

R_2 — ground reaction and gravity force at y_B

$$z_x = l_2 \cos \beta_1 - l_4 \cos \beta_2 + l_8 C_5$$

$$z_y = l_2 \sin \beta_1 - l_4 \sin \beta_2 + l_8 S_5$$

$$z = \sqrt{z_x^2 + z_y^2}$$

$$= \left[l_2^2 + l_4^2 + l_8^2 - 2 l_2 l_4 \cos (\beta_1 - \beta_2) + 2 l_2 l_8 \cos (\alpha + \theta_5 - \beta_1) - 2 l_4 l_8 \cos (\alpha + \theta_5 - \beta_2) \right]^{1/2}$$

V. DERIVATION OF EQUATIONS OF MOTION

The equations of motion were derived with the use of standard matrix techniques. These procedures are fully covered in "Elementary Matrices and Some Applications to Dynamics and Differential Equations" by R. A. Frazer, W. J. Duncan, and A. R. Collar, Cambridge University Press, 1957.

It is well known that the motion of a body can be represented by equations which characterize the motion of the center of gravity of the body together with those which characterize the rotation of the body about its center of gravity. Figure F-2 illustrates the general case. The coordinates X, Y, Z are fixed in space. while x, y, z are fixed in the body. The motion of point P is defined through the rate of change of $\bar{R}$ or, equivalently, the rates of change of $\bar{\rho}$ and $\bar{r}$. If the point P is fixed in the body, G, the rate of change of $\bar{r}$ is completely defined by the rotation of the body.

$\bar{R}$ is normally referred to X, Y, Z, as is $\bar{\rho}$. On the other hand, $\bar{r}$ is normally expressed in terms of x, y, z. If $\bar{A}$ is the matrix for transformation from X, Y, Z to x, y, z we then have

$$\bar{r} = \bar{A}\,(\bar{R} - \bar{\rho})$$

with respect to the moving coordinates the velocity of P is

$$\bar{A}\,\dot{\bar{R}} = \bar{A}\,\dot{\bar{\rho}} + \dot{\bar{r}} + \bar{\bar{w}}\,\bar{r}.$$

where $\bar{\bar{w}}$ is the rotational velocity matrix, defined through

$$\bar{\bar{w}} = -\ \dot{\bar{A}}\ \bar{A}^{-1}$$

where $\bar{A}^{-1}$ is the inverse of $\bar{A}$.

It should be noted that

$$\dot{\bar{R}} = \frac{d\bar{R}}{dt}$$

is the velocity of P with respect to the fixed coordinates and that $\bar{A}\,\dot{\bar{R}}$ merely is the result of changing the component bases.

Differentiation leads to the following expression for the acceleration referred to the moving axes

$$\bar{A}\ddot{\bar{R}} = \bar{A}\ddot{\bar{\rho}} + 2\,\bar{\bar{w}}\dot{\bar{r}} + \dot{\bar{\bar{w}}}\bar{r} + \bar{\bar{w}}^2\bar{r} + \ddot{\bar{r}}$$

The kinematic relations can be used directly to obtain the equations of motion for a point mass or the center of gravity of a rigid body. In the moving coordinate system

$$M\bar{A}\ddot{\bar{R}} = \bar{F}$$

where M is the mass and $\bar{F}$ is the force vector. For the rotational equations of motion we observe that the angular velocity can be represented as the matrix, $\bar{\bar{w}}$ or alternatively as the vector $\bar{\rho}$.

$$\bar{\bar{w}} = \begin{Vmatrix} 0 & -w_z & w_y \\ w_z & 0 & -w_x \\ -w_y & w_x & 0 \end{Vmatrix}$$

$$\bar{\rho} = (w_x, w_y, w_z)$$

Let $\bar{J}$ be the polar moment of inertia matrix of the body represented by the body axes. Then the angular momentum vector in the moving system is

$$\bar{H} = J\bar{\rho}$$

and the time rate of change of angular momentum is

$$\frac{d}{dt}\bar{H} = \bar{M} = \dot{\bar{\bar{J}}}\bar{\rho} + J\dot{\bar{\rho}} + \bar{\bar{w}}\bar{\bar{J}}\bar{\rho}$$

where $\bar{M}$ is the vector of applied moments.

<u>Coordinate Transformations</u>

The applicable coordinate systems are shown in Fig. F-1. These systems are related through the following transformations.

$$\bar{R}_2 = \bar{R}_1 - \bar{T}_{21}$$

$$\bar{T}_{21} = (\ell_1, y_B, 0)$$

$$\bar{R}_3 = \bar{A}_{32}\bar{R}_2$$

$$\bar{A}_{32} = \begin{Vmatrix} \cos(\theta_1 + \theta_2) & \sin(\theta_1 + \theta_2) & 0 \\ -\sin(\theta_1 + \theta_2) & \cos(\theta_1 + \theta_2) & 0 \\ 0 & 0 & 1 \end{Vmatrix}$$

$$\bar{R}_4 = \bar{A}_{43}\,\bar{R}_3$$

$$\bar{A}_{43} = \begin{Vmatrix} \cos\theta_3 & 0 & -\sin\theta_3 \\ 0 & 1 & 0 \\ \sin\theta_3 & 0 & \cos\theta_3 \end{Vmatrix}$$

$$\bar{R}_5 = \bar{A}_{54}\,\bar{R}_4$$

$$\bar{A}_{54} = \begin{Vmatrix} 1 & 0 & 0 \\ 0 & \cos\theta_4 & \sin\theta_4 \\ 0 & -\sin\theta_4 & \cos\theta_4 \end{Vmatrix}$$

$$\bar{R}_6 = \bar{A}_{65}\,(\bar{R}_5 - \bar{T}_{65})$$

$$\bar{T}_{65} = \left[\,\ell_2\cos\beta_1,\ \ell_2\sin\beta_1,\ 0\right]$$

$$\bar{A}_{65} = \begin{Vmatrix} \cos(\alpha+\theta_5) & \sin(\alpha+\theta_5) & 0 \\ -\sin(\alpha+\theta_5) & \cos(\alpha+\theta_5) & 0 \\ 0 & 0 & 1 \end{Vmatrix}$$

$$\bar{R}_7 = \bar{R}_6 - \bar{T}_{76}$$

$$\bar{T}_{76} = (x_f,\ 0,\ 0)$$

$$\bar{R}_8 = \bar{R}_7 - \bar{T}_{87}$$

$$\bar{T}_{87} = (x,\ 0,\ 0)$$

$$\bar{R}_9 = \bar{A}_{98}\,\bar{R}_8$$

$$\bar{A}_{98} = \begin{bmatrix} \cos\psi_Z & \sin\psi_Z & 0 \\ -\sin\psi_Z & \cos\psi_Z & 0 \\ 0 & 0 & 1 \end{bmatrix}.$$

$$
\cdot \begin{bmatrix} 1 & 0 & 0 \\ 0 & \cos \varphi^* & \sin \varphi^* \\ 0 & -\sin \varphi^* & \cos \varphi^* \end{bmatrix} \cdot
$$

$$
\cdot \begin{bmatrix} \cos \psi_y & 0 & -\sin \psi_y \\ 0 & 1 & 0 \\ \sin \psi_y & 0 & \cos \psi_y \end{bmatrix}
$$

$$
\bar{A}_{98} = \begin{bmatrix} \sin \varphi^* \sin \psi_y \sin \psi_Z + \cos \psi_y \cos \psi_Z & \cos \varphi^* \sin \psi_Z & \sin \varphi^* \cos \psi_y \sin \psi_Z - \sin \psi_y \cos \psi_Z \\ \sin \varphi^* \sin \psi_y \cos \psi_Z - \cos \psi_y \sin \psi_Z & \cos \varphi^* \cos \psi_Z & \sin \varphi^* \cos \psi_y \cos \psi_Z + \sin \psi_y \sin \psi_Z \\ \cos \varphi^* \sin \psi_y & -\sin \varphi^* & \cos \varphi^* \cos \psi_y \end{bmatrix}
$$

Utilization of these transformations leads to the following equations of motion.

VI. AUXILIARY QUANTITIES AND EXPRESSIONS

$$A_n = V_n''(0) \equiv 2\, b_n^2 / \sqrt{\rho L}$$

$$B_n = V_n'''(0) = -\frac{2 b_n^3}{\sqrt{\rho L}}\left(\frac{\text{COSH}\, b_n L + \cos b_n L}{\text{SIN}\, b_n L + \text{SINH}\, b_n L}\right)$$

$$V_n(\xi) = \frac{1}{\sqrt{\rho L}}\Big[\text{COSH}\, b_n \xi - \cos b_n \xi + \\ + \left(\frac{\text{COSH}\, b_n L + \cos b_n L}{\text{SIN}\, b_n L + \text{SINH}\, b_n L}\right)\left(\text{SIN}\, b_n \xi - \text{SINH}\, b_n \xi\right)\Big]$$

$$V_n'(\xi) = \frac{b_n}{\sqrt{\rho L}}\Big[\text{SINH}\, b_n \xi + \text{SIN}\, b_n \xi + \\ + \left(\frac{\text{COSH}\, b_n L + \cos b_n L}{\text{SIN}\, b_n L + \text{SINH}\, b_n L}\right)\left(\cos b_n \xi - \text{COSH}\, b_n \xi\right)\Big]$$

$$v_0(\xi) = -\frac{\rho g \cos\alpha}{24 EI}\left(\xi^4 - 4\xi^3 L + 6\xi^2 L^2\right)$$

$$v_0'(\xi) = -\frac{\rho g \cos\alpha}{6 EI}\left(\xi^3 - 3\xi^2 L + 3\xi L^2\right)$$

$$v(\xi,t) = v_0(\xi) + \sum_{n=1}^{\infty} V_n(\xi)\, q_n(t)$$

$$v(\xi,t) = \sum_{n=1}^{\infty} V_n(\xi)\, h_n(t)$$

$$\dot{v}(\xi,t) = \sum_{n=1}^{\infty} V_n(\xi)\, \dot{q}_n(t) + \dot{\xi} v_0' + \dot{\xi} \sum_{n=1}^{\infty} V_n'(\xi)\, q_n(t)$$

$$\dot{v}(\xi,t) = \sum_{n=1}^{\infty} V_n(\xi)\, \dot{h}_n(t) + \dot{\xi} \sum_{n=1}^{\infty} V_n'(\xi)\, h_n(t)$$

$$\theta_7(\xi,t) \equiv \psi_y(\xi,t) = -\sum_{n=1}^{\infty} V_n'(\xi) h_n(t)$$

$$\theta_8(\xi,t) \equiv \psi_z(\xi,t) = v_0'(\xi) + \sum_{n=1}^{\infty} V_n'(\xi) q_n(t)$$

$$\ddot{v}(\xi,t) = \ddot{\xi} v_0' + \dot{\xi}^2 v_0'' + \sum_{n=1}^{\infty} V_n(\xi)\ddot{q}_n + 2\dot{\xi}\sum_{n=1}^{\infty} V_n'\dot{q}_n +$$

$$+ \ddot{\xi}\sum_{n=1}^{\infty} V_n' q_n(t) + \dot{\xi}^2 \sum_{n=1}^{\infty} V_n'' q_n(t)$$

$$\ddot{w}(\xi,t) = \sum_{n=1}^{\infty} V_n(\xi)\ddot{h}_n + 2\dot{\xi}\sum_{n=1}^{\infty} V_n'\dot{h}_n + \ddot{\xi}\sum_{n=1}^{\infty} V_n' h_n +$$

$$+ \dot{\xi}^2 \sum_{n=1}^{\infty} V_n'' h_n$$

$$V_n''(\xi) = \frac{b_n^2}{\sqrt{\rho L}}\Big[\cosh b_n\xi + \cos b_n\xi +$$

$$+\left(\frac{\cosh b_nL + \cos b_nL}{\sin b_nL + \sinh b_nL}\right)(-\sin b_n\xi - \sinh b_n\xi)\Big]$$

$$V_n'''(\xi) = \frac{b_n^3}{\sqrt{\rho L}}\Big[\sinh b_n\xi - \sin b_n\xi +$$

$$+\left(\frac{\cosh b_nL + \cos b_nL}{\sin b_nL + \sinh b_nL}\right)(-\cos b_n\xi - \cosh b_n\xi)\Big]$$

$$\dot{\theta}_7 = -\sum_{n=1}^{\infty} V_n'\dot{h}_n - \dot{\xi}\sum_{n=1}^{\infty} V_n'' h_n$$

$$\dot{\theta}_8 = \dot{\xi}\, v_0''(\xi) + \sum_{n=1}^{\infty} V_n'\dot{q}_n + \dot{\xi}\sum_{n=1}^{\infty} V_n'' q_n(t)$$

$$\ddot{\theta}_1 = -\sum_1^{\infty} V_n' \ddot{h}_n - 2\dot{\xi}\sum_1^{\infty} V_n'' \dot{h}_n - \dot{\xi}^2 \sum_1^{\infty} V_n''' h_n - \ddot{\xi}\sum_1^{\infty} V_n'' h_n$$

$$\ddot{\theta}_8 - \ddot{\xi}\, v_0''(\xi) + \dot{\xi}^2 v_0'''(\xi) + \sum_1^{\infty} V_n' \ddot{q}_n + 2\dot{\xi}\sum_1^{\infty} V_n'' \dot{q}_n +$$

$$+ \dot{\xi}^2 \sum_1^{\infty} V_n''' q_n(t) + \ddot{\xi}\sum_1^{\infty} V_n'' q_n(t)$$

$$v_0''(\xi) = -\frac{\rho g \cos\alpha}{2EI}\left(\xi^2 - 2\xi L + L^2\right)$$

$$v_0'''(\xi) = -\frac{\rho g \cos\alpha}{EI}\left(\xi - L\right)$$

LET $\theta_9 = \varphi(\xi(t))$

$\varphi(\xi)$ IS THE RIFLING EQUATION

$$\varphi'(\xi) = \frac{d}{d\xi}\varphi(\xi)$$

$$\varphi''(\xi) = \frac{d^2}{d\xi^2}\varphi(\xi)$$

THEN $\dot{\theta}_9 = \dot{\xi}\,\varphi'(\xi)$

$$\ddot{\theta}_9 = \ddot{\xi}\,\varphi'(\xi) + (\dot{\xi})^2\,\varphi''(\xi)$$

$$\Delta_1 = (\dot\theta_1 + \dot\theta_2 + \dot\theta_5)^2 + (\dot\theta_3 S_5 + \dot\theta_4 C_5)^2$$

$$\Delta_2 = 2[(\dot\theta_1 + \dot\theta_2)(\theta_4 S_5 - \theta_3 C_5) + \dot\theta_3 S_5 + \dot\theta_4 C_5]$$

$$\Delta_3 = (\ddot\theta_1 + \ddot\theta_2)(\theta_4 S_5 - \theta_3 C_5) - (\dot\theta_1 + \dot\theta_2 - \dot\theta_5)(\theta_3 C_5 - \theta_4 S_5) + \\ + \ddot\theta_3 S_5 + \ddot\theta_4 C_5$$

$$\Delta_4 = (\dot\theta_3 S_5 + \dot\theta_4 C_5)(\dot\theta_3 C_5 - \dot\theta_4 S_5)$$

$$\Delta_5 = 2(\dot\theta_1 + \dot\theta_2 - \dot\theta_3 \theta_4 + \dot\theta_5)$$

$$\Delta_6 = C_5 - (\theta_1 + \theta_2) S_5$$

$$\Delta_7 = \{[\dot\theta_3^2 + (\dot\theta_1 + \dot\theta_2)^2] S_5 + (\ddot\theta_1 + \ddot\theta_2 - \theta_4 \ddot\theta_3) C_5\} l_2 \cos \beta_1 + \\ + \{(\ddot\theta_1 + \ddot\theta_2 - \theta_4 \ddot\theta_3 - 2\dot\theta_4 \dot\theta_3) S_5 - [(\dot\theta_1 + \dot\theta_2)^2 + \dot\theta_4^2] C_5\} l_2 \sin \beta_1$$

$$\Delta_8 = \dot\theta_3^2 + \dot\theta_4^2$$

$$\Delta_9 = (\dot\theta_1 + \dot\theta_2 + \dot\theta_5)(\dot\theta_3 C_5 - \dot\theta_4 S_5)$$

$$\Delta_{10} = (\ddot\theta_1 + \ddot\theta_2)(\theta_4 C_5 + \theta_3 S_5) + \ddot\theta_3 C_5 - \ddot\theta_4 S_5 + (\dot\theta_1 + \dot\theta_2 - \dot\theta_5)(\dot\theta_3 S_5 + \dot\theta_4 C_5)$$

$$\Delta_{11} = 2[(\dot\theta_1 + \dot\theta_2)(\theta_4 C_5 + \theta_3 S_5) + \dot\theta_3 C_5 - \dot\theta_4 S_5]$$

$$\Delta_{12} = [\ddot\theta_4 - (\ddot\theta_1 + \ddot\theta_2)\theta_3] l_2 \sin\beta_1 - [\ddot\theta_3 + (\ddot\theta_1 + \ddot\theta_2)\theta_4] l_2 \cos\beta_1$$

$$\Delta_{13} = (\theta_1 + \theta_2) C_5 + S_5$$

$$\Delta_{14} = (\dot\theta_1 + \dot\theta_2 + \dot\theta_5)^2 + (\dot\theta_3 C_5 - \dot\theta_4 S_5)^2$$

$$\Delta_{15} = \ddot{\theta}_1 + \ddot{\theta}_2 - \ddot{\theta}_3\theta_4 + \ddot{\theta}_5 - \dot{\theta}_3\dot{\theta}_4$$

$$\Delta_{16} = (\dot{\theta}_1 + \dot{\theta}_2 + \dot{\theta}_5)(\dot{\theta}_3 S_5 + \dot{\theta}_4 C_5)$$

$$\Delta_{17} = \left\{(\ddot{\theta}_1 + \ddot{\theta}_2 - \ddot{\theta}_3\theta_4)S_5 - \left[\dot{\theta}_3^2 + (\dot{\theta}_1 + \dot{\theta}_2)^2 C_5\right\} l_2 \cos\beta_1 + \right.$$
$$- \left\{(\ddot{\theta}_1 + \ddot{\theta}_2 - \ddot{\theta}_3\theta_4 - 2\dot{\theta}_3\dot{\theta}_4)C_5 + \left[\dot{\theta}_4^2 + (\dot{\theta}_1 + \dot{\theta}_2)^2\right]S_5\right\} l_2 \sin\beta_1$$

A. PROJECTILE EQUATIONS

$$\begin{aligned} F(t) = m_p\Big\{&\ddot{\xi} + \ddot{u} + \Delta_{13}\ddot{y}_B - (\Delta_5 + \theta_6\Delta_2)\dot{v} + (\Delta_{11} + 2\dot{\theta}_6)\dot{w} + \\ &-(\Delta_{14} + 2\theta_6\Delta_{16} + \dot{\theta}_6\Delta_{11})(\xi + u + x + L_1) + \\ &+\left[\Delta_4 - \Delta_{15} - \theta_6(\Delta_9 + \Delta_3)\right]v + \Delta_{17} - \theta_6\Delta_{12} + \\ &+\left[\Delta_{10} + \Delta_{16} + \theta_6(\Delta_8 - \Delta_{14}) + \ddot{\theta}_6\right]w\Big\} \end{aligned} \qquad \text{(F-1)}$$

$$\begin{aligned} N_{py} = m_p\Big\{&\ddot{v} + \Delta_6(\ddot{y}_B + g) + (\Delta_5 + \theta_6\Delta_2)(\dot{\xi} + \dot{u}) - (\Delta_2 - \theta_6\Delta_5)\dot{w} + \\ &-\Delta_1 v + \left[\Delta_4 + \Delta_{15} - \theta_6(\Delta_9 - \Delta_3) + \dot{\theta}_6\Delta_2\right](\xi + u + x + l_1) + \\ &+\left[\Delta_9 - \Delta_3 + \theta_6(\Delta_4 + \Delta_{15}) + \dot{\theta}_6\Delta_5\right]w + \Delta_7\Big\} \end{aligned} \qquad \text{(F-2)}$$

$$N_{pz} = m_p\Big\{\ddot{w} + (\theta_6\Delta_{13} - \theta_4)(\ddot{y}_B + q) - (\Delta_{11} + 2\dot{\theta}_6)(\dot{\xi} + \dot{u}) +$$

$$+ (\Delta_2 - \theta_6\Delta_5)\dot{v} - \left[\Delta_8 - 2\theta_6\Delta_{16} + \dot{\theta}_6\Delta_{11}\right]w +$$

$$+ \left[\Delta_{16} - \Delta_{10} + \theta_6(\Delta_8 - \Delta_{14}) - \ddot{\theta}_6\right](\xi + u + x + \ell_1) + \qquad (F\text{-}3)$$

$$+ \left[\Delta_9 + \Delta_3 + \theta_6(\Delta_4 - \Delta_{15})\right]v + \Delta_{12} + \theta_6\Delta_{17}\Big\}$$

$$C_{px} = J_x\Big\{\ddot{\theta}_9 + \Delta_3 + \theta_8 C_9\Delta_{10} + \tfrac{1}{2}\left[(\dot{\theta}_8 S_9 - \dot{\theta}_6 - \dot{\theta}_7)\Delta_5 + \dot{\theta}_8 C_9\Delta_{11} +\right.$$

$$\left. + (\theta_8 S_9 - \theta_7 - \theta_6)\Delta_{15}\right]\Big\} \qquad (F\text{-}4)$$

$$C_y = -J_y\Big\{C_9(\ddot{\theta}_6 + \ddot{\theta}_7) - \ddot{\theta}_9\theta_8 - \dot{\theta}_9\dot{\theta}_8 - \dot{\theta}_9\dot{\theta}_6 S_9 - \dot{\theta}_9\dot{\theta}_7 S_9 +$$

$$+ (\theta_6 S_9 + \theta_7 S_9 - \theta_8)\Delta_3 + C_9\Delta_{10} + S_9\Delta_{15} + \qquad (F\text{-}5)$$

$$+ \tfrac{1}{2}\left[(\dot{\theta}_6 S_9 + \dot{\theta}_7 S_9 - \dot{\theta}_8)\Delta_2 - \dot{\theta}_8 S_9\Delta_{11} + \dot{\theta}_9 C_9\Delta_5\right]\Big\} +$$

$$- (J_x - J_y)\left[\dot{\theta}_8\dot{\theta}_9 - S_9\dot{\theta}_9(\dot{\theta}_7 + \dot{\theta}_6) + C_9\Delta_{16} - S_9\Delta_4\right]$$

$$C_z = -J_y\Big\{\ddot{\theta}_8 - (\ddot{\theta}_6 + \ddot{\theta}_7)S_9 - (\dot{\theta}_6 + \dot{\theta}_7)\dot{\theta}_9 C_9 - S_9\Delta_{10} +$$

$$+ (\theta_6 + \theta_7)C_9\Delta_3 + C_9\Delta_{15} + \tfrac{1}{2}\left[(\dot{\theta}_6 + \dot{\theta}_7)C_9\Delta_2 - (S_9 + C_9)\dot{\theta}_9\Delta_5\right]\Big\} +$$

$$+ (J_x - J_y)\left[C_9\dot{\theta}_9(\dot{\theta}_7 + \dot{\theta}_6) + C_9\Delta_4 + S_9\Delta_{16}\right] \qquad (F\text{-}6)$$

B. DETERMINATION OF 6

$$\begin{aligned} k_8\theta_6 = {} & (m_\ell - m_p)(\ddot{u} + \Delta_{13}\ddot{y}_B - \Delta_{14}u + \Delta_{17}) + \\ & -(m_\ell + m_p)\,\ell_8(\Delta_{10} + \Delta_{16}) \end{aligned} \tag{F-7}$$

C. TUBE EQUATIONS

$$\begin{aligned} \ddot{q}_n + \left[V_n^2 - \Delta_1\right]q_n = {} & -\left[N_{py}V_n(\xi) + C_y V_n'(\xi)\right]H(\xi)H(L-\xi) + \\ & -\frac{B_n E I_q}{V_n^4}\cos\alpha(\Delta_1 - V_n^2) - (\Delta_2 - \theta_6\Delta_5)\dot{h}_n + \\ & +\left[\Delta_9 - \Delta_3 + \theta_6(\Delta_4 + \Delta_{16}) + \dot{\theta}_6\Delta_5\right]h_n + \\ & +\left[\Delta_{15} + \Delta_4 - \theta_6(\Delta_9 - \Delta_3) + \dot{\theta}_6\Delta_2\right]\frac{\rho A_n}{b_n^4} + \\ & -\frac{\rho B_n}{b_n^4}\Big\{\left[\Delta_{15} + \Delta_4 - \theta_6(\Delta_9 - \Delta_3) + \dot{\theta}_6\Delta_2\right](u + \ell_7) + \\ & +(\Delta_5 + \theta_6\Delta_2)\dot{u} + \Delta_6(\ddot{y}_B + g) + \Delta_7\Big\} \end{aligned} \tag{F-8}$$

$$\begin{aligned} \ddot{h}_n + \left[V_n^2 - (\Delta_8 - 2\theta_6\Delta_{16} + \dot{\theta}_6\Delta_{11})\right]h_n = {} & \\ & -\left[N_{pz}V_n(\xi) - C_y V_n'(\xi)\right]H(\xi)H(L-\xi) + \\ & +(\Delta_2 - \theta_6\Delta_5)\left[\dot{q}_n - \frac{B_n E I_q}{V_n^4}\cos\alpha\right] + \\ & +\left[\Delta_{16} - \Delta_{10} + \theta_6(\Delta_3 - \Delta_{14}) - \ddot{\theta}_6\right]\left[\frac{\rho A_n}{b_n^4} - \frac{\rho B_n}{b_n^4}(u + \ell_7)\right] + \\ & -\frac{\rho B_n}{b_n^4}\Big[\Delta_{12} + \theta_6\Delta_{17} + (\theta_6\Delta_{13} - \theta_4)(\ddot{y}_B + g) + \\ & -(\Delta_{11} + 2\theta_6)\dot{u}\Big] \end{aligned} \tag{F-9}$$

D. END SHEARS AND MOMENTS

$$
\left.
\begin{aligned}
S_y(0,t) &= -\rho g L \cos\alpha + EI \sum_1^\infty B_n g_n \\
M_z(0,t) &= -\tfrac{1}{2}\rho g L^2 \cos\alpha + EI \sum_1^\infty A_n g_n \\
S_z(0,t) &= EI \sum_1^\infty B_n h_n \\
M_y(0,t) &= -EI \sum_1^\infty A_n g_n
\end{aligned}
\right\} \qquad \text{(F-10)}
$$

E. BREECH EQUATIONS

$$
\begin{aligned}
(\rho L + m_B)\big[\ddot{u} + \Delta_{13}(\ddot{y}_B + g) - \Delta_{14} u + (\Delta_4 - \Delta_{15})\ell_5 + \\
+ (\Delta_{10} + \Delta_{16})\ell_6 + \Delta_{17}\big] = \\
= \rho L(\ell_7 + \tfrac{1}{2}L)\Delta_{14} - P_{cx} - F(t)
\end{aligned}
\qquad \text{(F-11)}
$$

$$
\begin{aligned}
m_B\big[\Delta_6(\ddot{y}_B + g) + \Delta_5 \dot{u} - \Delta_1 \ell_5 + (\Delta_4 + \Delta_{15}) u + \\
+ (\Delta_9 - \Delta_3)\ell_6 + \Delta_7\big] = \\
= -P_{cy} - S_y(0,t) - [1 - H(\xi)]N_{Py}
\end{aligned}
\qquad \text{(F-12)}
$$

$$
\begin{aligned}
m_B\big[-\Theta_4(\ddot{y}_B + g) - \Delta_{11}\dot{u} - \Delta_8 \ell_6 + \Delta_{12} + (\Delta_{16} - \Delta_{10}) u + \\
+ (\Delta_9 + \Delta_3)\ell_5\big] = \\
= -P_{cz} - S_z(0,t) - [1 - H(\xi)]N_{Pz}
\end{aligned}
\qquad \text{(F-13)}
$$

$$
\begin{aligned}
&(J_{Ex} + 2\rho L I)\Delta_3 + (J_{Ex} - J_{BY})\Delta_9 = \\
&\quad = -N_{cx} - P_{cy}\ell_6 + P_{cz}\ell_5 - C_{px} H(\xi) H(L-\xi) + \\
&\quad + [H(\xi) - 1] J_x (\ddot{\theta}_9 + \Delta_3)
\end{aligned}
\tag{F-14}
$$

$$
\begin{aligned}
&J_{BY}\Delta_{10} + (J_{Bx} - J_{Bz})\Delta_{16} = \\
&\quad = -N_{cy} + M_y(0,t) + \ell_7 S_z(0,t) + \\
&\quad + [1 - H(\xi)][(\ell_7 + \xi) N_{pz} - J_y(C_9\Delta_{10} + S_9\Delta_{15}) + \\
&\qquad - (J_x - J_y)(C_9\Delta_{16} - S_9\Delta_4)]
\end{aligned}
\tag{F-15}
$$

$$
\begin{aligned}
&J_{Bz}\Delta_{15} + (J_{BY} - J_{Ex})\Delta_4 = \\
&\quad = -N_{cz} - \ell_7 S_y(0,t) + M_z(0,t) - F(t)\ell_5 + \\
&\quad + [H(\xi) - 1][(\ell_7 + \xi) N_{py} + J_y(C_9\Delta_{15} - S_9\Delta_{10}) + \\
&\quad - (J_x - J_y)(C_9\Delta_4 + S_9\Delta_{16})] + \\
&\quad - \rho L \ell_5 [\ddot{u} + \Delta_{13}\ddot{y}_B - \Delta_{14}(u + \ell_7 + \tfrac{1}{2}L) + \Delta_{17}]
\end{aligned}
\tag{F-16}
$$

F. COUNTERRECOIL MECHANISM

$$
\begin{aligned}
F_{cx} &= -K - \epsilon H_1 - k_7(u_0 - u) - \frac{\epsilon\gamma A_p^3(1+\delta)\dot{u}^2}{2g C_0^2 \alpha_0^2} + \\
&\quad - H(u-u_1) H(u_2-u) \frac{I_B h^2}{R_p^2 (u_2-u_1)^2}\Big[2\pi \sin 2\pi \frac{u-u_1}{u_2-u_1}\Big(1 - \cos 2\pi \frac{u-u_1}{u_2-u_1}\Big)\ddot{u} + \\
&\quad + \Big(1 - \cos 2\pi \frac{u-u_1}{u_2-u_1}\Big)^2\Big] \frac{1-\epsilon}{2}
\end{aligned}
\tag{F-17}
$$

G. TRAILS AND GROUND REACTIONS

DEFINITION:

$$R_1 = \begin{cases} -k_1 y_T - \delta_1 \dot{y}_T & \text{FOR } y_T \leq 0 \\ -m_1(\ddot{y}_T + g) & \text{FOR } y_T > 0 \end{cases} \quad \text{(F-18)}$$

$$R_2 = \begin{cases} -m_3 \ddot{y}_B - k_2 y_B - \delta_2 \dot{y}_B & \text{FOR } y_B \leq 0 \\ -m_3(\ddot{y}_B + g) & \text{FOR } y_B > 0 \end{cases} \quad \text{(F-19)}$$

$$\theta_1 = \frac{y_B - y_T}{\ell_1} \quad \text{(F-20)}$$

$$\ell_1 R_1 = k_3 \theta_2 \quad \text{(F-21)}$$

H. VERTICAL EQUILIBRIUM AT BALL JOINT

$$R_1 + R_2 + \Delta_{13} R_{6x} + \Delta_6 R_{6y} - \theta_4 R_{6z} + $$
$$+ (\theta_1 + \theta_2) E_{6x} + E_{6y} = 0 \quad \text{(F-22)}$$

I. ANGULAR MOTION OF THE BALL JOINT

$$\ell_1 R_1 \theta_3 - k_5 \theta_4 + R_{6z} \ell_2 \sin \beta_1 + T_{6x} C_5 - T_{6y} S_5 +$$
$$-I_{cz}(\dot{\theta}_1 + \dot{\theta}_2)\dot{\theta}_3 - I_{xc}[\ddot{\theta}_4 - (\ddot{\theta}_1 + \ddot{\theta}_2)\theta_3 - (\dot{\theta}_1 + \dot{\theta}_2)\dot{\theta}_3] = 0 \quad \text{(F-23)}$$

$$-\ell_1 R_1 \theta_4 - k_4 \theta_3 - R_{6z} \ell_2 \cos \beta_1 + T_{6x} S_5 T_{6y} C_5 +$$
$$-(I_{xc} - I_{zc})(\dot{\theta}_1 + \dot{\theta}_2)\dot{\theta}_4 = 0 \quad \text{(F-24)}$$

$$-\ell_1 R_1 + k_4 \theta_3 \theta_4 - E_{6x} l_4 \sin\beta_2 + R_{6x} \sin(\alpha - \beta_1 + \theta_5) +$$
$$+ E_{6y} l_4 \cos\beta_2 + R_{6y} \cos(\alpha - \beta_1 + \theta_5) + I_{xc} \dot{\theta}_3 \dot{\theta}_4 + \qquad \text{(F-25)}$$
$$- I_{zc}(\ddot{\theta}_1 + \ddot{\theta}_2 - \ddot{\theta}_3 \theta_4 \cdot \dot{\theta}_3 \dot{\theta}_4) = 0$$

J. ANGULAR MOTION OF CRADLE

$$\Delta_3 I_{xA} + (I_{zA} - I_{yA}) \Delta_9 = N_{cy} - l_6 P_{cy} - T_{6x} \qquad \text{(F-26)}$$

$$\Delta_{10} I_{yA} + (I_{yA} - I_{zA}) \Delta_{16} = N_{cy} + l_6 P_{cx} - (u - l_3) P_{cz} +$$
$$- T_{6y} - l_3 R_{6z} \qquad \text{(F-27)}$$

$$\Delta_{15} I_{zA} + (I_{yA} - I_{xA}) \Delta_4 = N_{cz} + (u - l_3) P_{cy} + l_3 R_{6y} +$$
$$+ (l_5 - l_3) S_5 E_{6x} - (l_5 - l_3) C_5 E_{6y} \qquad \text{(F-28)}$$

K. LINEAR MOTION OF CRADLE CENTER OF GRAVITY

$$m_A [\Delta_{13}(\ddot{y}_B + g) - \Delta_{14} l_3 + \Delta_{17}] = \qquad \text{(F-29)}$$
$$= P_{cx} - R_{6x} - E_{6x} C_5 - E_{6y} S_5$$

$$m_A [\Delta_6(\ddot{y}_B + g) + (\Delta_4 + \Delta_{15}) l_3 + \Delta_7] =$$
$$= P_{cy} - R_{6y} + E_{6x} S_5 - E_{6y} C_5 \qquad \text{(F-30)}$$

$$m_A\left[-\theta_4(\ddot{y}_B+g)-(\Delta_{10}-\Delta_{16})\,l_3+\Delta_{12}\right]=P_{Cz}-R_{6z} \qquad \text{(F-31)}$$

L. FLEXIBLE SYSTEM FORCE

$$E_{6x}=k_6\,\frac{z_x}{z}\,l_8\,(C_5-\cos\alpha)+ \\ +b_6\,\frac{z_x}{z^2}\,l_8\,\dot{\theta}_5\left[l_4\sin(\alpha+\theta_5-\beta_2)-l_2\sin(\alpha+\theta_5-\beta_1)\right] \qquad \text{(F-32)}$$

$$E_{6y}=k_6\,\frac{z_y}{z}\,l_8\,(C_5-\cos\alpha)+ \\ +b_6\,\frac{z_y}{z^2}\,l_8\,\dot{\theta}_5\left[l_4\sin(\alpha+\theta_5-\beta_2)-l_2\sin(\alpha+\theta_5-\beta_1)\right] \qquad \text{(F-33)}$$

VII. COMPILATION OF UNKNOWNS

Unknown	Equation	Unknown	Equation	Unknown	Equation
E_{6x}	631	y_T	619	y_B	621
3	623	5	627	T_{6y}	626
R_{6x}	628	R_{6z}	630	E_{6y}	632
P_{cy}	611	N_{cx}	613	N_{cz}	615
q_n	607	6	606	C_y	604
	600	N_{pz}	602	2	620
1	624	4	622	T_{6x}	625
P_{cx}	616	R_{6y}	629	u	610
P_{cz}	612	N_{cy}	614	S_y , S_z	609
				M_z , M_y	
h_n	608	C_{px}	603	C_z	605
N_{py}	601				

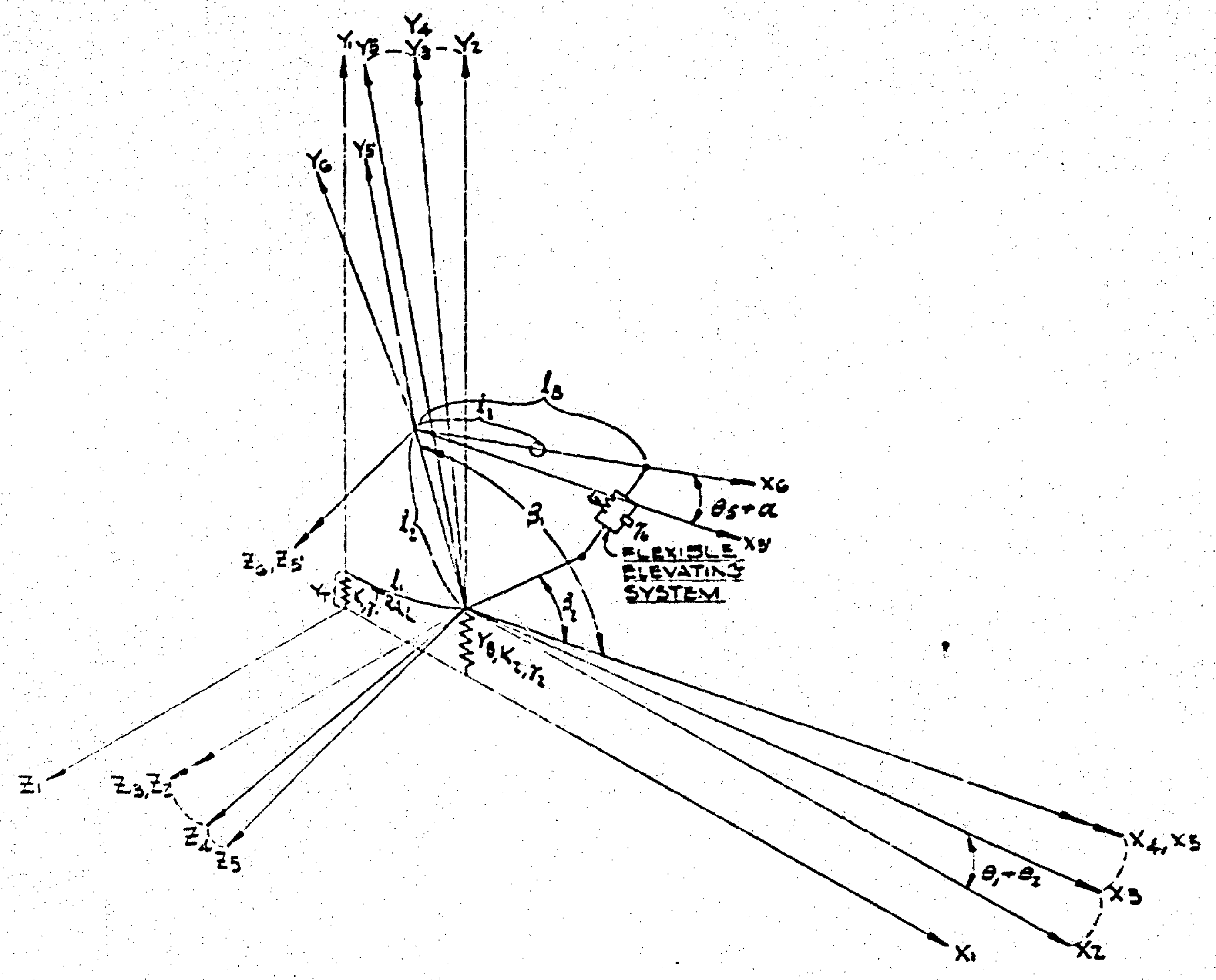

Fig. F-1 DIAGRAM OF COORDINATE SYSTEMS DESCRIBING LAUNCHER MOTION FOR MATHEMATICAL MODEL VI

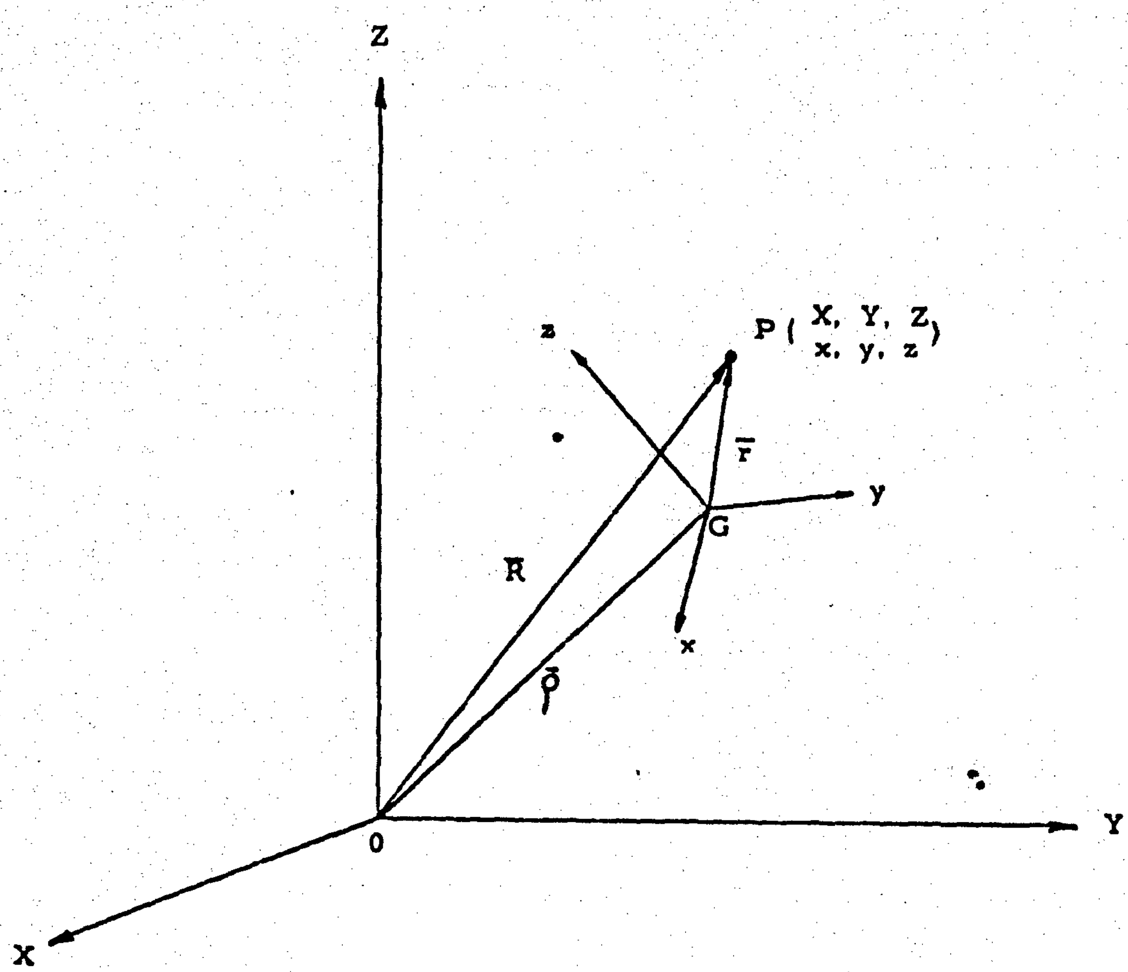

Fig. F-2 COORDINATE SYSTEM

APPENDIX G

FIXTURE DESIGNS

I. INTRODUCTION

The purpose and some of the operations of the experimental structure modifications are described in the body of the report. This appendix shows the details of the construction of the more important fixtures, the dampers, and the elevating system flexibilities. Not only the springs and dampers used on the program are shown, but also a design showing a combination spring and damper which could be used in the actual launcher. (The fixture used in the experimental program prohibited changes in elevation.)

II. FIXTURE DESCRIPTION

Figure G-1 shows the assembly of the auxiliary dampers used for the firing program. It is simply a piston submerged in a fluid inside a cylinder; the piston has orifices so that its motion gives a force approximately proportional to the square of the velocity. A detail drawing of the piston is shown in Figure G-2.

Figure G-3 shows the assembly of the flexibility added to the elevating rod; Figure G-4 gives the spring characteristics. This assembly was inserted into the present elevating system simply by moving the existing elevating screw up, and placing the spring assembly between the support in the upper carriage side and the screw. The flexibility could be removed, if desired, by replacing the spring by a rigid spacer. An alternate method was used, however, that of replacing the entire elevating screw by more rigid rods.

Figure G-5 shows a possible configuration of a spring-damper combination. The entire spring is submerged in hydraulic fluid; in this case the spring end retainers have orifice holes and act as the damper pistons. The lower, smaller spring and piston assembly is a device which acts as a fluid reserve which compensates for changes in ambient temperature. The entire assembly would be keyed so that it could transmit the torques for elevating the launcher.

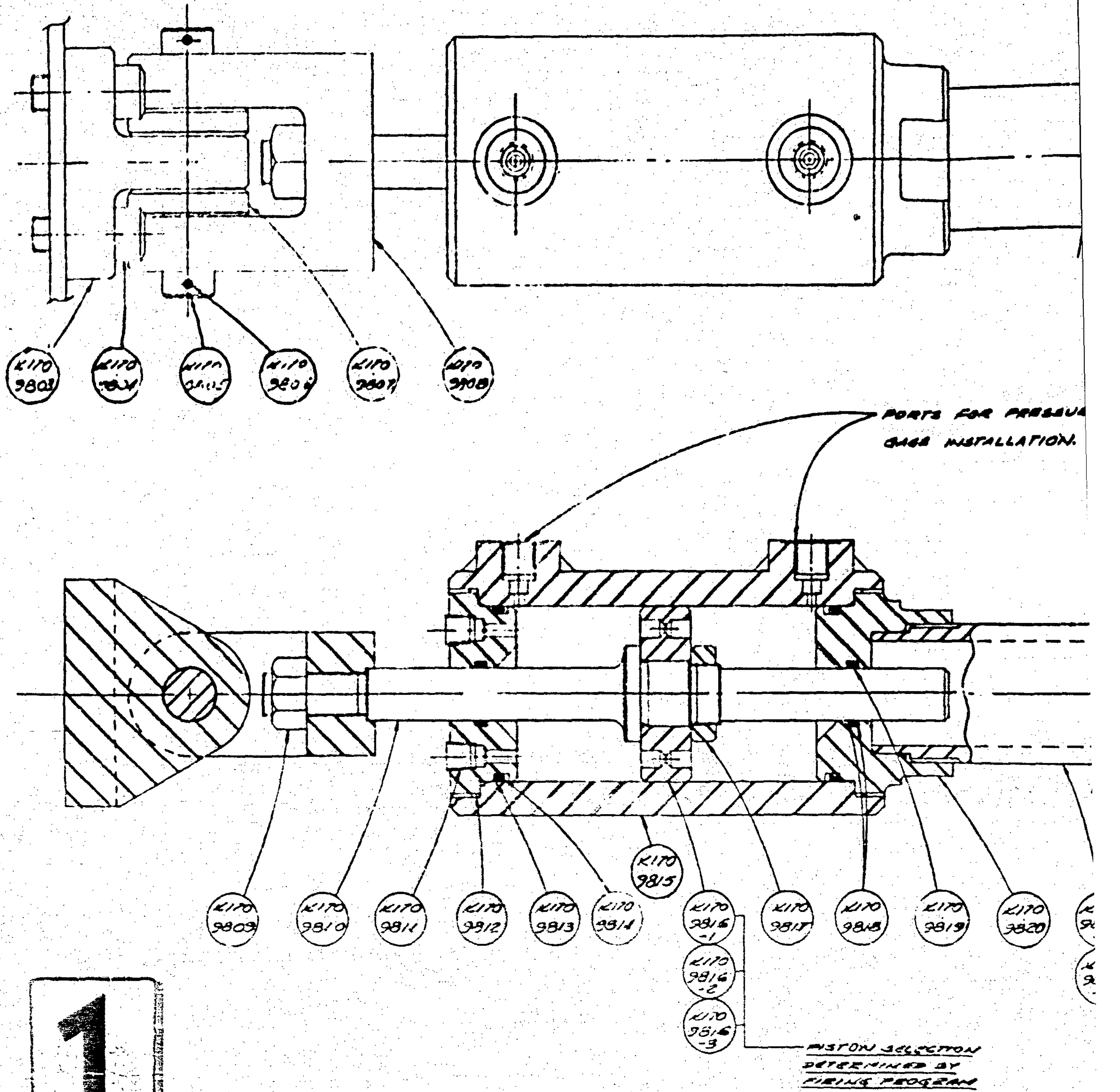

Fig. G-1 Viscous Damper As

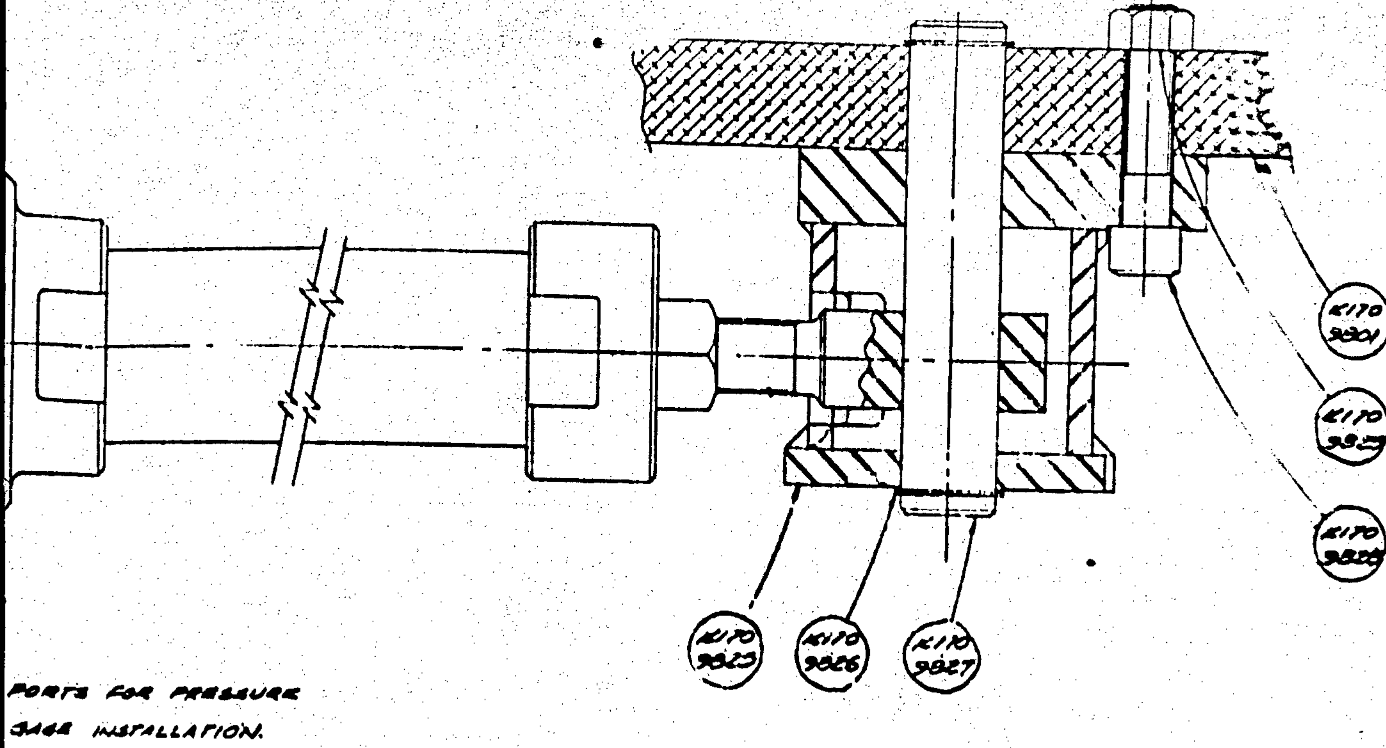

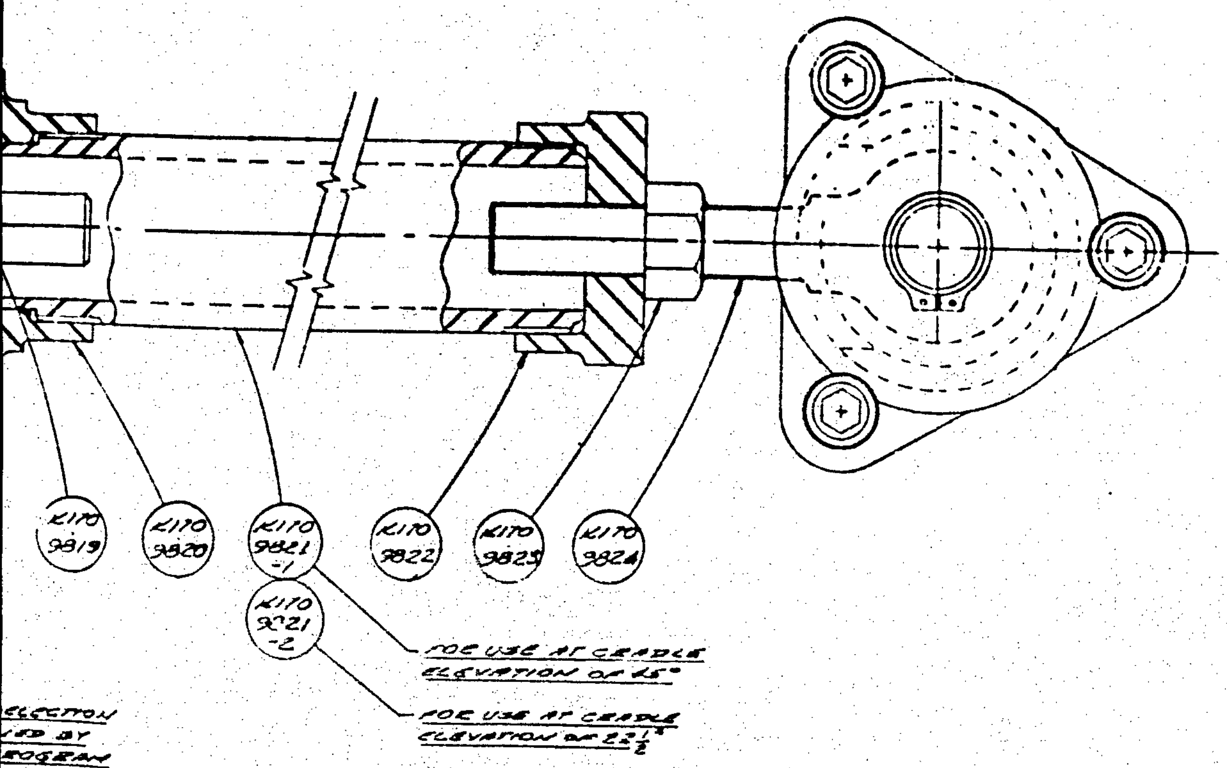

2

iscous Damper Assembly

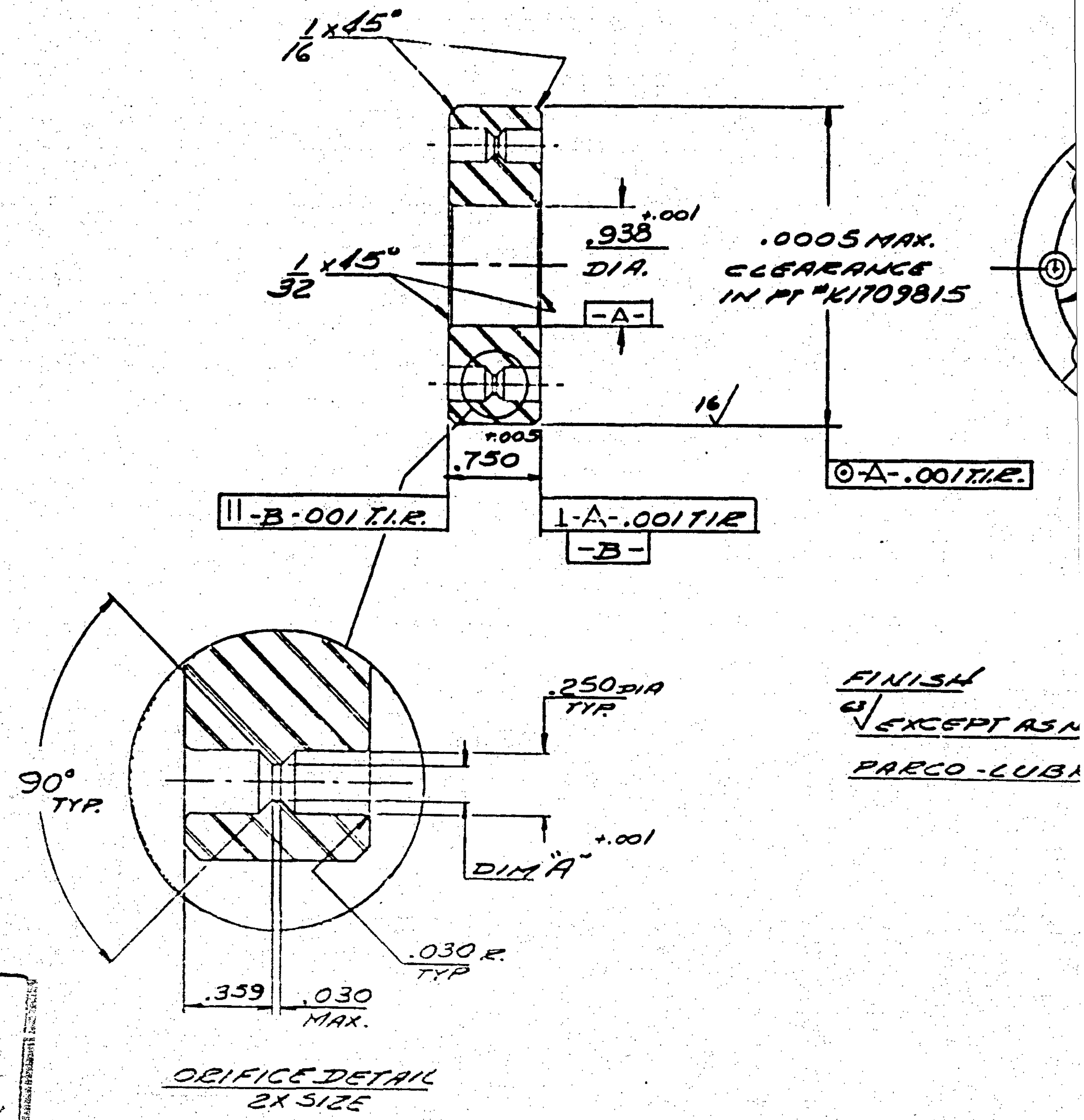

1

Fig. G-2 Damper-Pisto

PART No.	DIM "A"	No REQ.
K1709816-1	.045	2
K1709816-2	.089	2
K1709816-3		

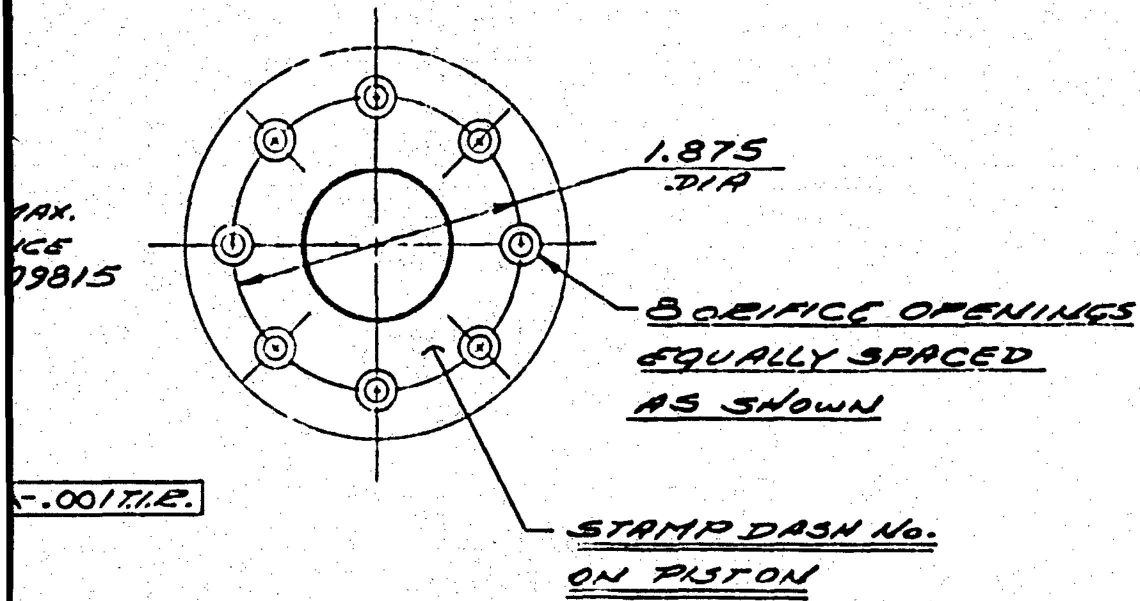

NISH
EXCEPT AS NOTED
ARCO - LUBRIZE

2

G-2 Damper-Piston

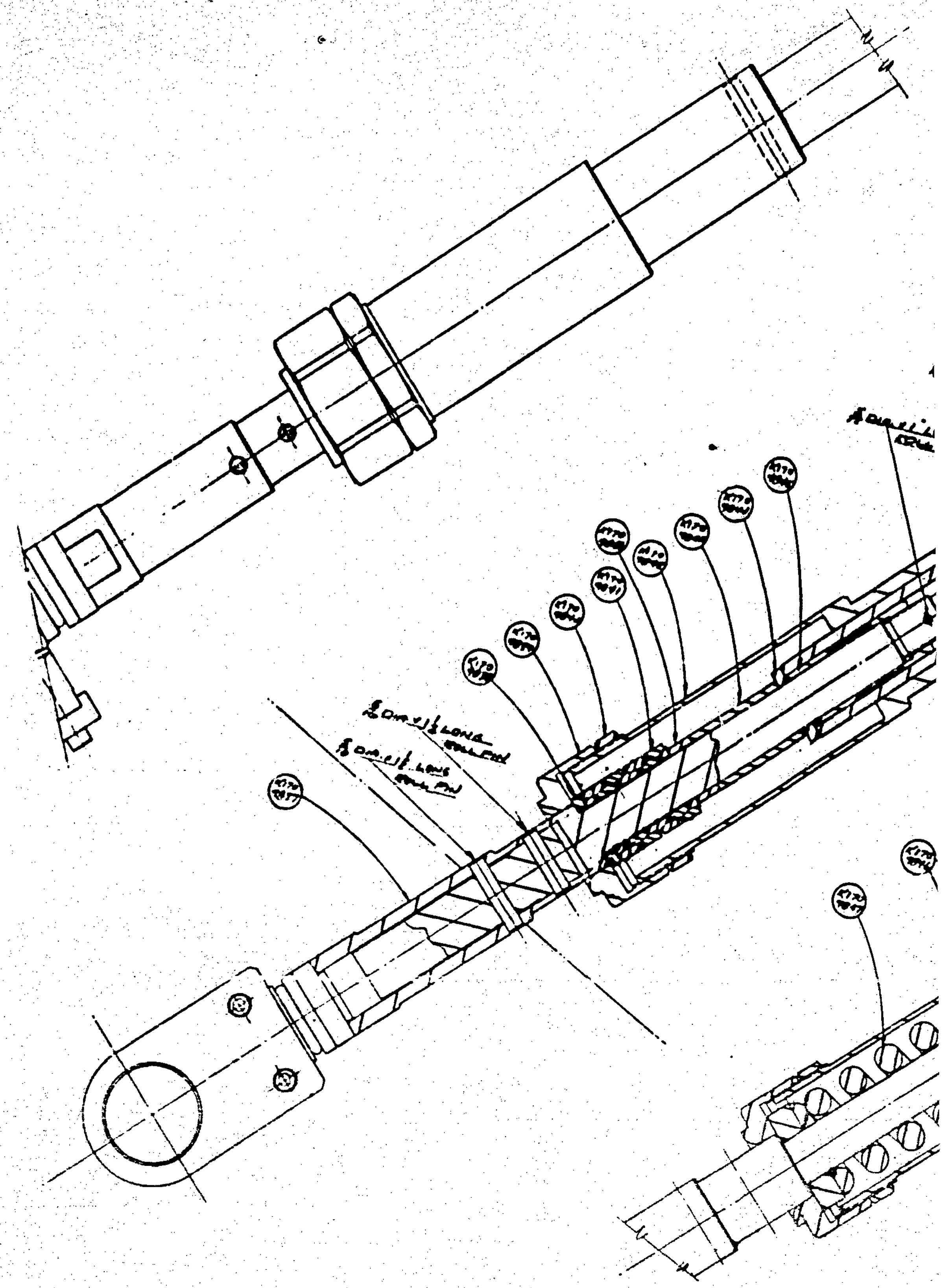

Fig. G-3 Spring Damper Combinati

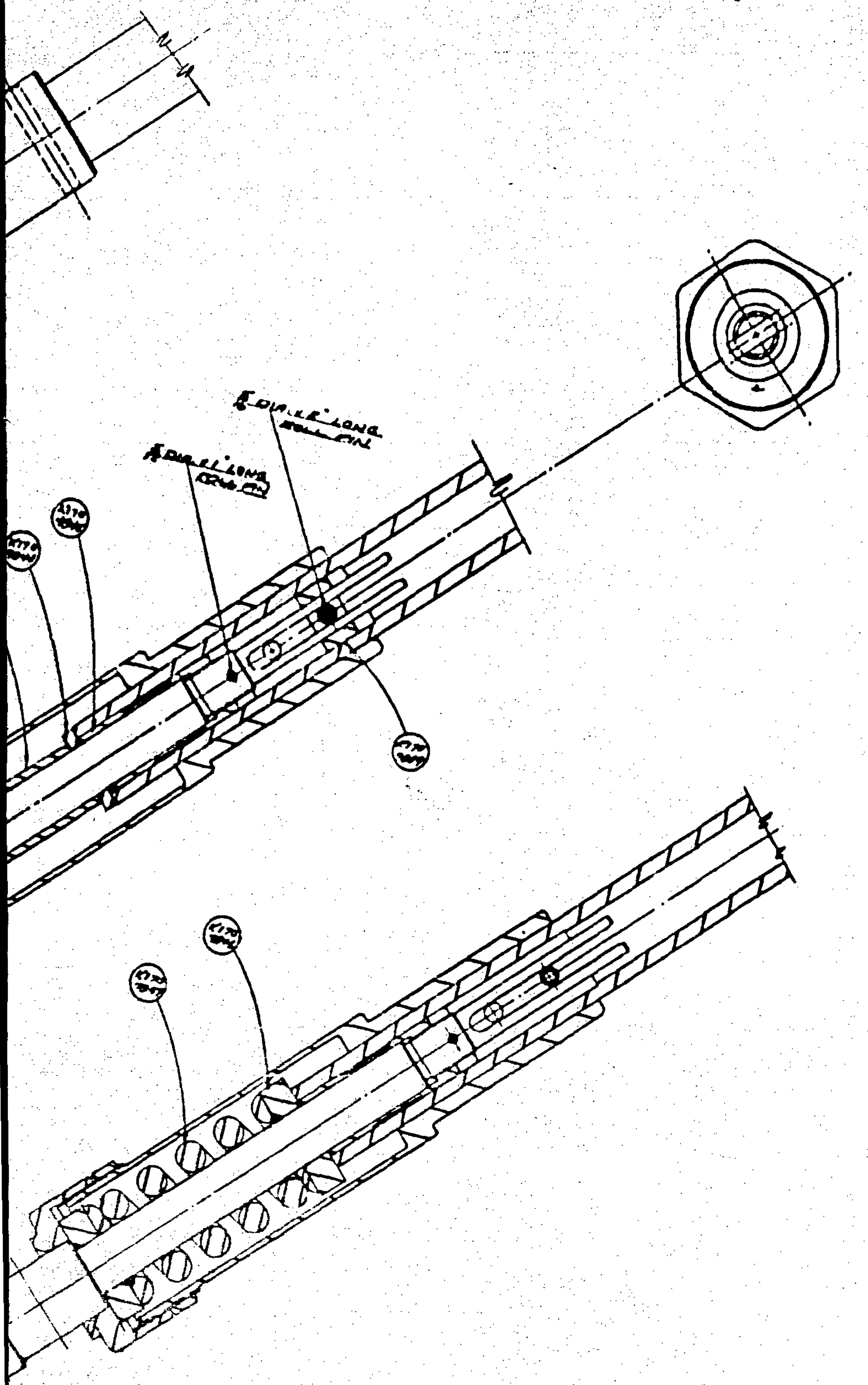

Damper Combination Assembly

2

SPRING DATA

MATL.	AISI 1095 SPRING STL.
WIRE DIA.	1/2 "
MEAN DIA.	1-7/16"
ACTIVE COILS	4-1/3
TOTAL COILS	6-1/3
RATE	7000 lb/in.
FREE HEIGHT	3-13/16
SOLID HEIGHT	3-3/16
INSTALLED HEIGHT	3-5/8
PRE-LOAD	1200 lb
DEFLECTION	.572"
MAX. LOAD	4000 lb
STRESS	115,000 p.s.i.
WOUND	R.H. - L. H.
ENDS	SQUARED & GROUND

Fig. G-4 SPRING DATA

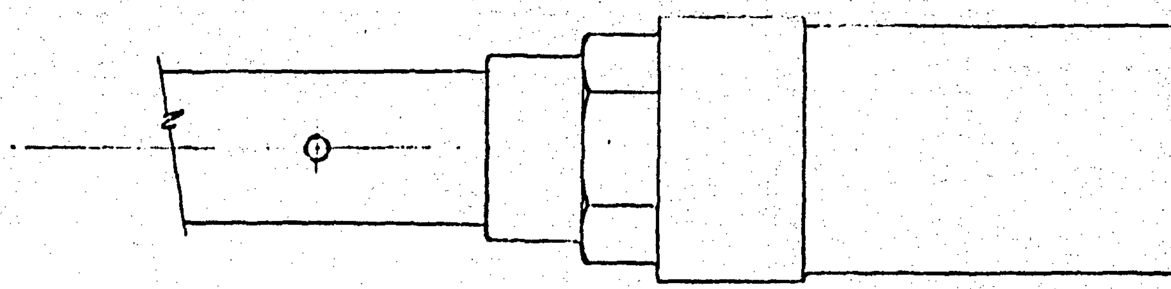

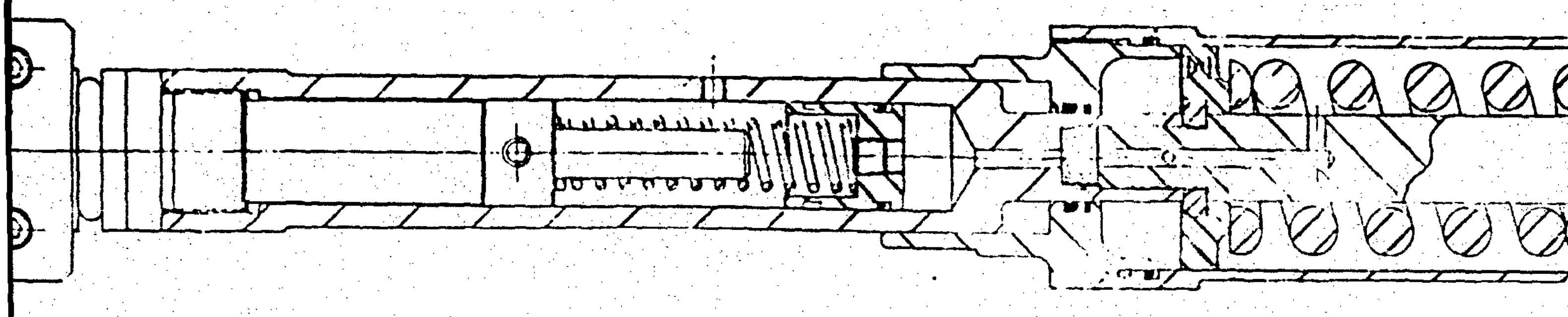

1

Fig. G-5 Spring Damper Combi

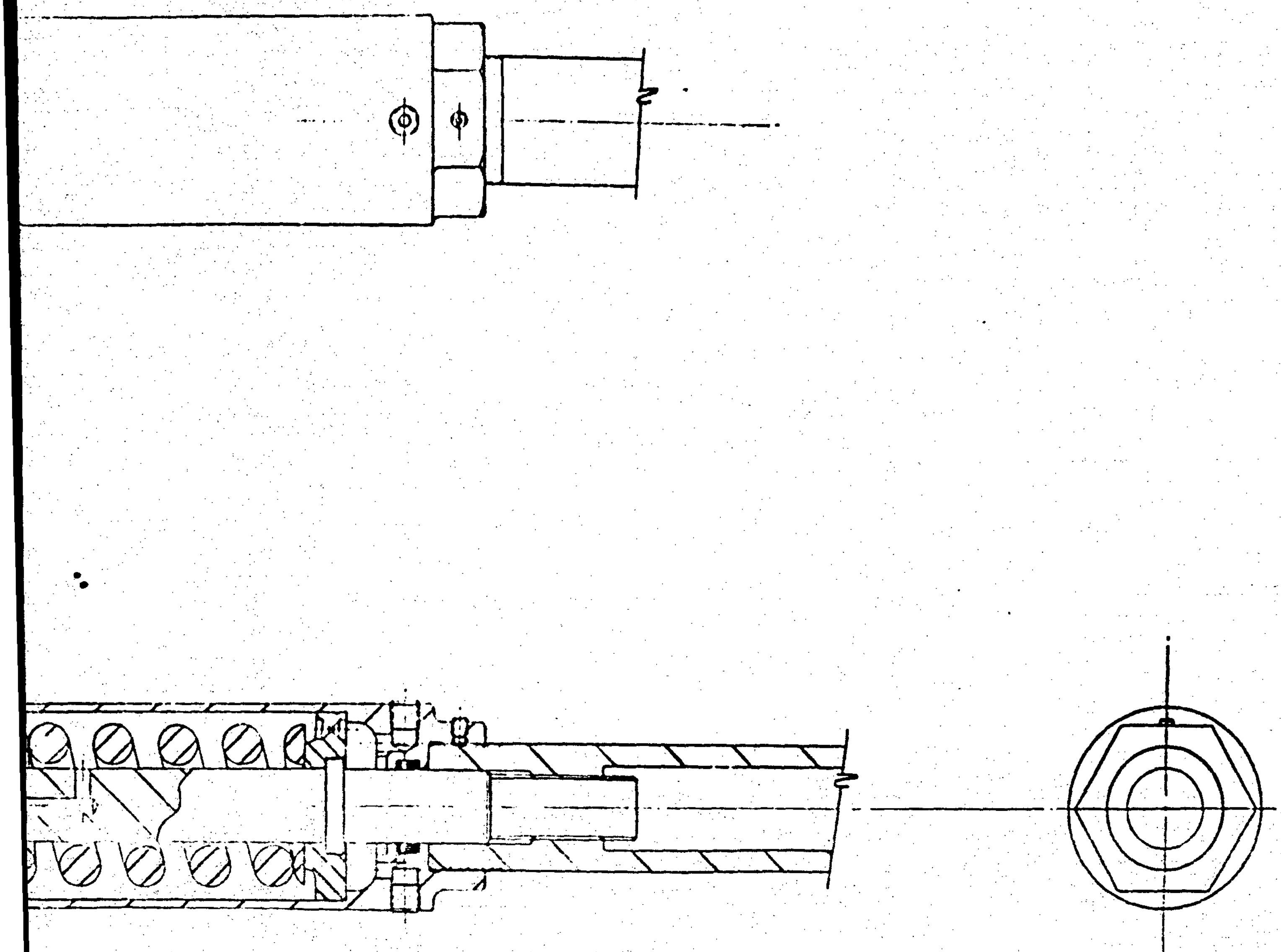

2

Spring Damper Combination

APPENDIX H

STRUCTURAL STIFFNESS MEASUREMENTS

R. M. Brach and R. H. Van Beek

I. INTRODUCTION

In order to improve launcher accuracy by choosing optimum launcher parameters, the individual effect of each significant parameter must be determined. Studies with mathematical models are being used to determine these effects, followed by firing programs to substantiate the theoretical conclusions. The success of using mathematical models for this purpose depends upon at least two major points: (1) the degree to which the models qualitatively represent the dynamics of the launcher and (2) the quantitative agreement between the mathematical model output values and actual measurements of launcher motion. In order to optimize the quantitative agreement, the numerical input values to the mathematical models should correspond closely to measured values for the actual launcher. For this reason, static stiffness measurements were made of a number of launcher structural components using Prototype No. 3 as well as the trails of Prototype No. 1. Another equally important reason for making these measurements is to enable comparison of the actual stiffness values of the manufactured parts with the intended design stiffness.

The overall, or combined, stiffness of the launcher structure below the trunnions is desired. It would also be very useful to determine which components, such as the carriage box-sections, trail hinge-pins, etc., contribute the most to the total flexibility. As it would have been time consuming and costly to disassemble the entire structure and measure the stiffness of each part, the stiffness of the entire structure was first measured, and then, wherever disassembly was simple, as for example, the removal of the trails, separate measurements were taken. An attempt was made to determine the stiffness of certain components by eliminating their contributions to flexibility by means of auxiliary stiffeners. In general, no special consideration was given to the measurement procedures to develop

extreme accuracy since stiffness values accurate within 5% to 10% were regarded as sufficient with respect to the mathematical models. Standard laboratory test machines were used wherever possible.

II. MEASUREMENTS

Static stiffness measurements were made for the following components and assemblies:

1. The entire structure below the trunnions(supporting structure).
2. The entire structure below the trunnions with the upper and lower carriage box-sections clamped together.
3. The entire structure below the trunnions with the carriage box-sections clamped together and struts inserted between the trunnions and trails. (Trails were parallel to the firing tube.)
4. The entire structure without stiffeners but traversed:
   a. 20° right
   b. 20° left
5. Elevating screw support
6. Trails:
   a. Prototype No. 3
   b. Prototype No. 1

The stiffness of the entire supporting structure was measured by applying a known load perpendicular to a bar supported through the trunnions, and measuring the deflection of the trunnions with dial gages. A side elevation of this system is shown in Fig. H-1. The load was measured with calibrated strain gages on the loading bar.

The trail stiffness was measured with the two trails clamped together by a relatively stiff fixture at their hinge-pin ends. This enabled the measurement and loading of the system to be performed as a simply supported beam (see Fig. H-2b). Again, the deflections were measured with dial gages.

The load-deflection characteristics of the jack screw supports in the upper carriage sides were measured by the procedure shown in Fig. H-2a. The compressive load applied to the screw was determined, as was the displacement of the screw relative to the upper carriage.

One parameter required by the mathematical models is a dynamic equivalent for the mass moment of inertia of the supporting structure, about a line through the ball joint perpendicular to the plane of elevation. This equivalent inertia, which permits the elastic carriage to be represented by a single flexibility and single inertia, can be measured indirectly by measuring the first mode natural frequency of the elastic carriage. In order to do this, an electro-dynamic shaker was attached to the bar through the trunnions for the purpose of applying to the launcher a harmonic force of variable frequency. The dynamic stiffness was measured as

$$k_D = \frac{Fw^2}{a},$$

where F is the applied force, w is the frequency, and a is the acceleration. Zero or very small values of the dynamic stiffness indicate resonance, and the smallest of the resonant frequencies is the first normal mode frequency.

III. DISCUSSION OF RESULTS AND CONCLUSIONS

Figure H-3 shows the load-deflection characteristics for the carriage. When converted to angular rotation about the base pivot, the average of the two sides yields a stiffness for the carriage of 32×10^6 lb-in./radian. Figure H-4 shows the stiffness of the same assembly, but with wedges between the upper and lower carriages and links of ties bolting the two together. The stiffness is 38.5×10^6 lb-in./radian. Figure H-5 shows the stiffness of the same assembly as Figure H-4, but with additional links connecting the trunnions to the trails. The stiffness is 55.5×10^6 lb-in./radian.

Figures H-6 and H-7 show the load-deflection characteristics of the carriage in full traverse, right and left, respectively. Traverse to the right stiffens the right trunnion and adds flexibility to the left trunnion, and vice versa; but there is a net decrease in the average stiffness. For both right and left traverse, the average stiffness is 25×10^6 lb-in./radian.

Figure H-8 shows the load-deflection characteristics of the lower elevating screw supports loaded in compression. This deflection occurs in the complicated structure consisting of the elevating screw gear box and its mounting.

Figure H-9 shows the load-deflection characteristics of the Prototype No. 3 trails joined at the hinge-pins and loaded as a single, simply supported beam. Converted to angular rotation, which would be produced about the base pivot, the combined stiffness of the two trails is 145×10^6 lb-in./radian. Figure H-10 gives the same data for the Prototype No. 1 trails, for which the combined stiffness is 109×10^6. The trails on the two prototypes are of different lengths, and the stiffness varies as the length squared. For purposes of comparison, the stiffness of the Prototype No. 3 trails was extrapolated to the value they would have if their length were the same as that of the Prototype No. 1 trails. This value is 223×10^6 lb-in./radian. The weight of the Prototype No. 3 trails is 385 lb; of the Prototype No. 1 trails, 351 lb. On the basis of these stiffnesses and weights, the stiffness-to-weight ratio of the Prototype No. 3 trails is computed to be 87% greater than that of the Prototype No. 1 trails.

Figure H-11 shows the results of the dynamic stiffness measurements on the carriage. The data are not conclusive, but it is probable that resonance in the first normal mode is indicated at 70 cps. The inertia of a torsional system having a stiffness of 32×10^6 lb-in./radian and a natural frequency of 70 cps agrees reasonably well with the calculated equivalent inertia of the carriage.

Each elevating screw and upper bracket assembly was loaded in compression in a universal testing machine. Fig. H-12 shows the resulting load-deflection curve for each screw-bracket assembly. The nonlinearities are due primarily to nonlinear local deflections under the balls in the ball nuts and also to clearances between the balls and the nut.

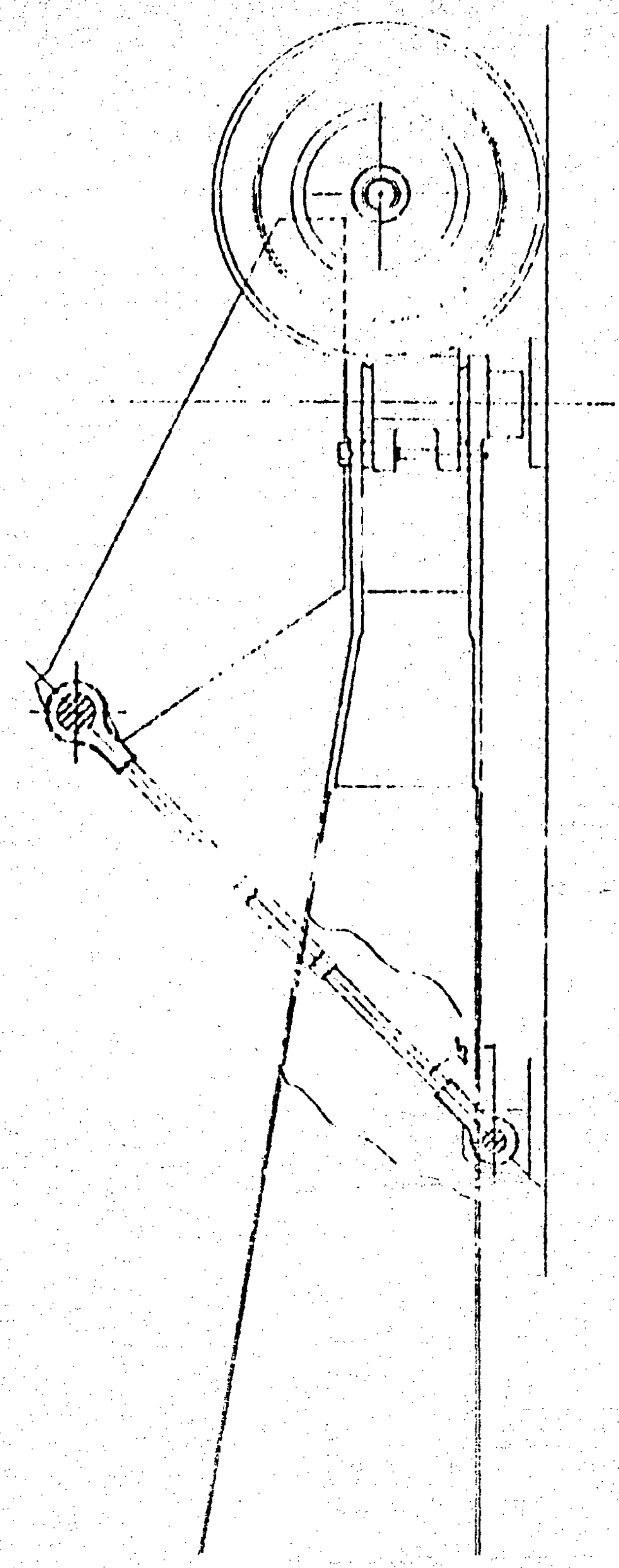

Fig. H-1 TEST SETUP FOR MEASURING CARRIAGE STIFFNESS AT TRUNNIONS

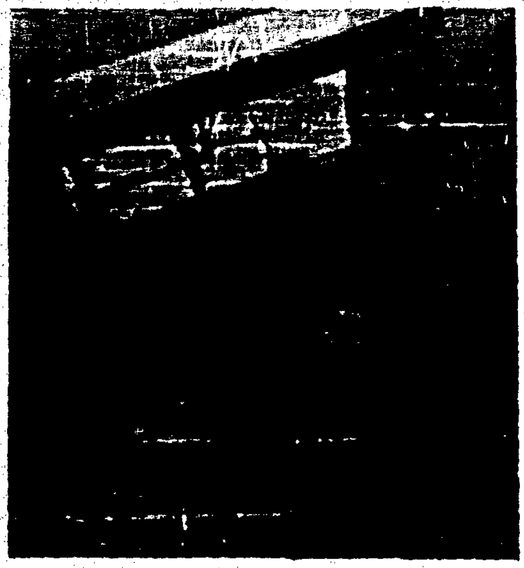

Fig. H-2a **Stiffness of Elevating Screw Support**

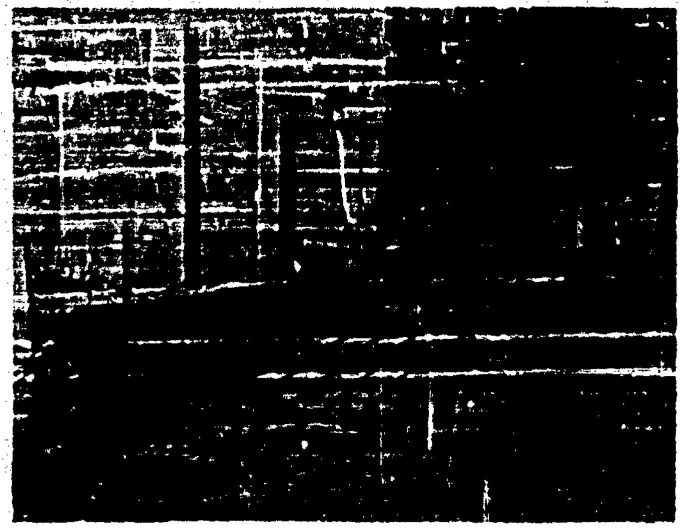

Fig. H-2b **Stiffness of Trails**

Fig. H-2c Natural Frequency of Carriage

Fig. H-2 LAUNCHER COMPONENTS UNDERGOING TESTS

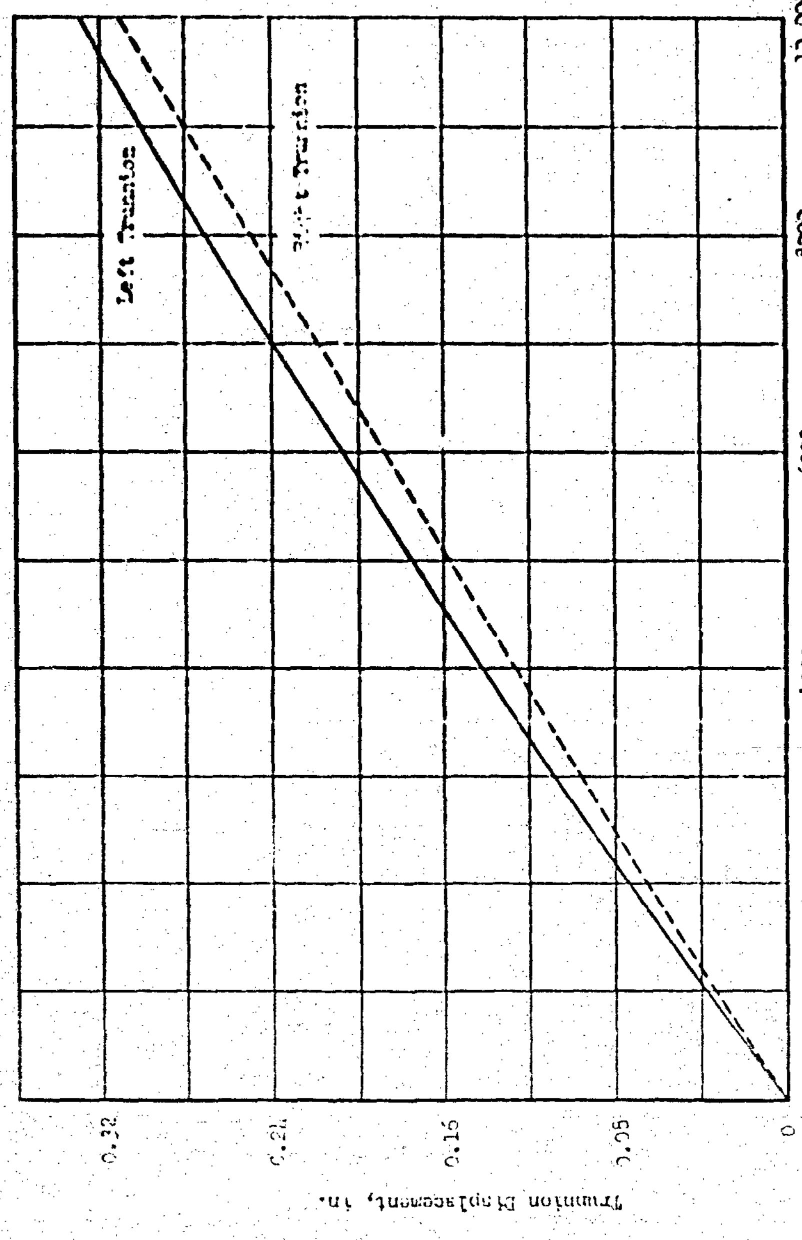

Fig. H-3 STIFFNESS OF CARRIAGE AT TRUNNIONS WITHOUT STIFFENERS

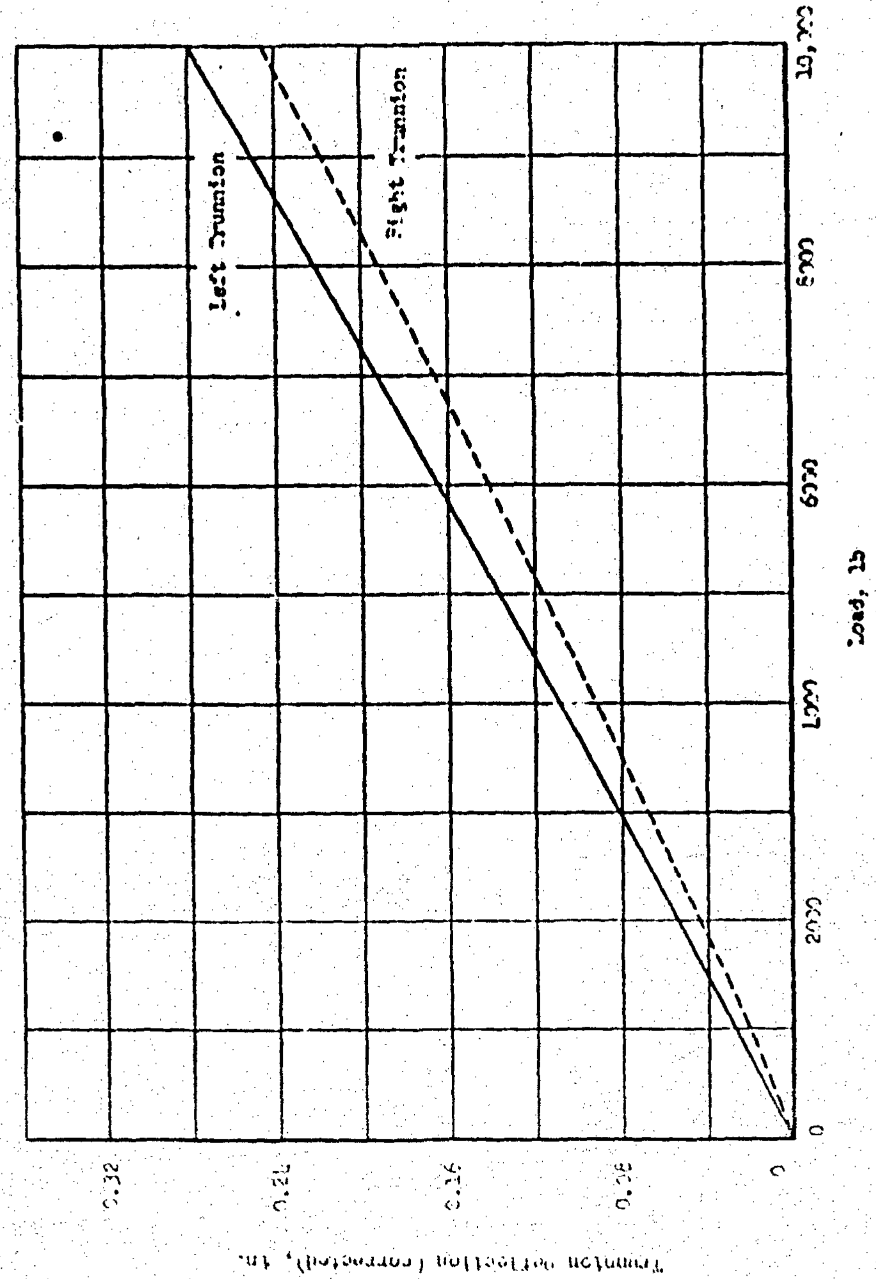

Fig. H-4 **STIFFNESS OF CARRIAGE AT TRUNNIONS WITH WEDGES AND TIES**

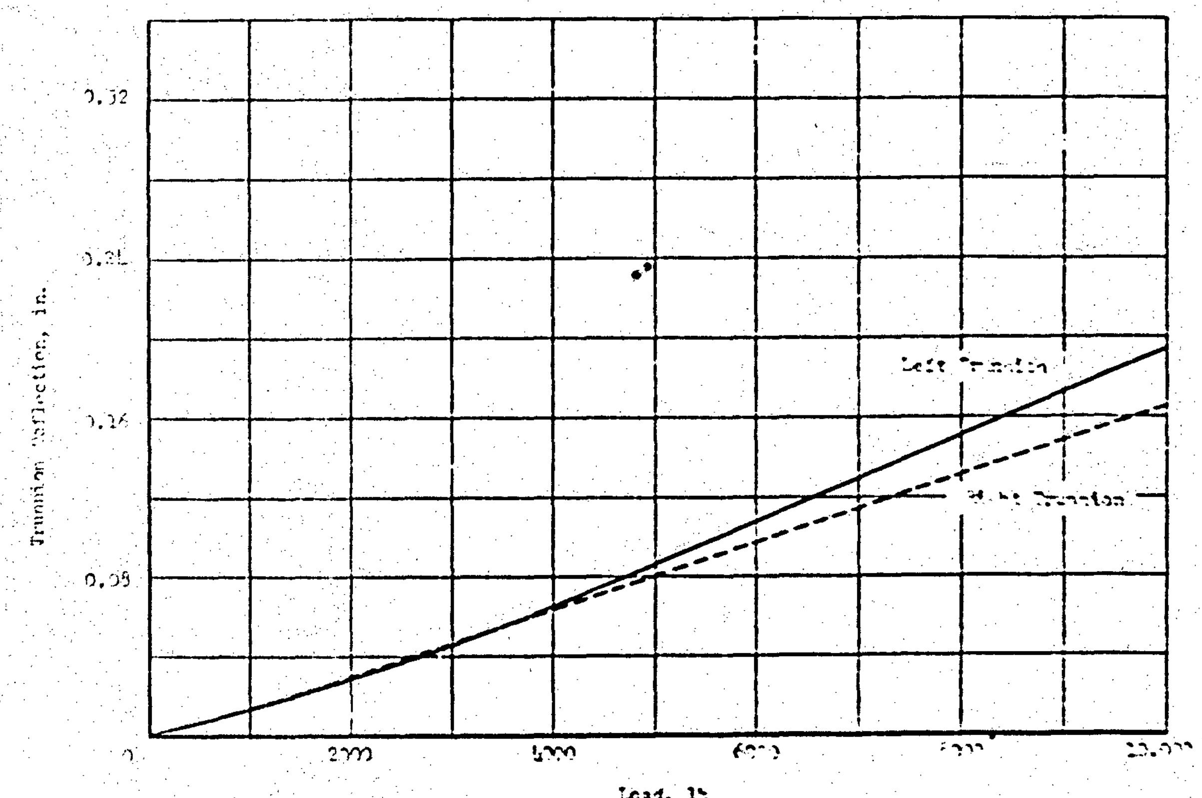

Fig. H-5 **STIFFNESS OF CARRIAGE AT TRUNNIONS WITH WEDGES, TIES, AND LINKS BETWEEN TRUNNIONS AND TRAILS**

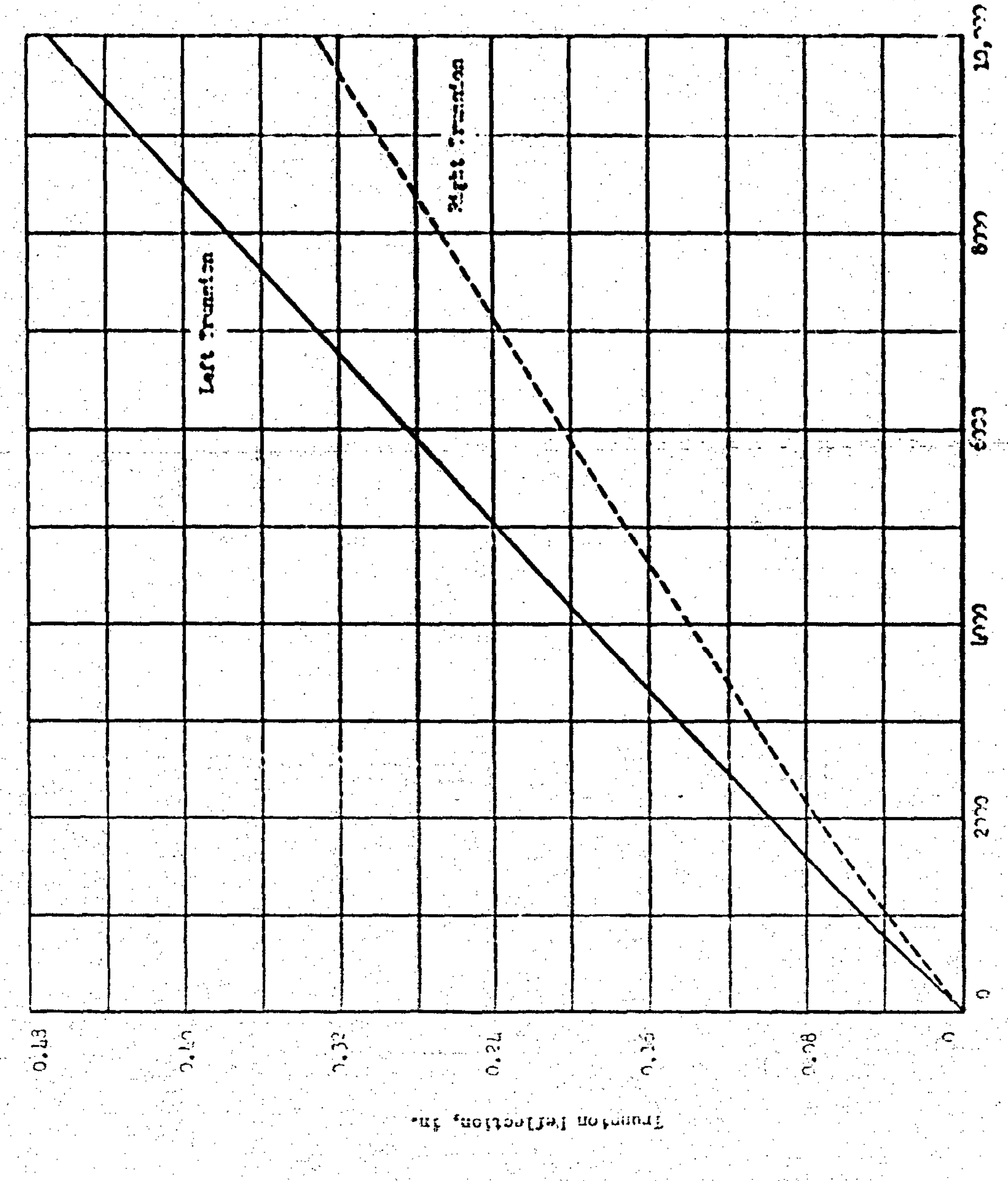

Fig. H-6 **STIFFNESS OF CARRIAGE AT FULL TRAVERSE, 20° RIGHT**

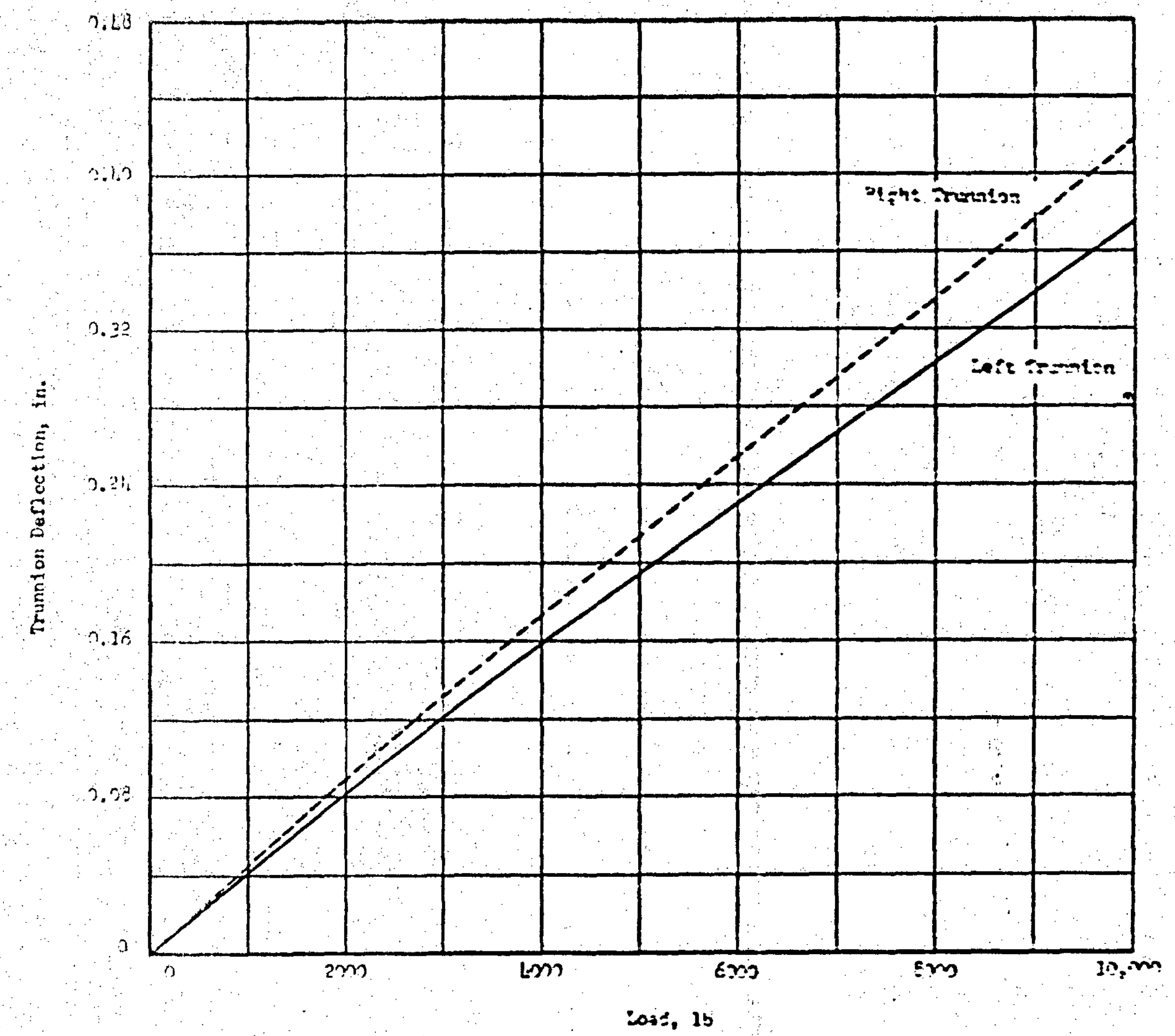

Fig. H-7 **STIFFNESS OF CARRIAGE AT FULL TRAVERSE, 20° LEFT**

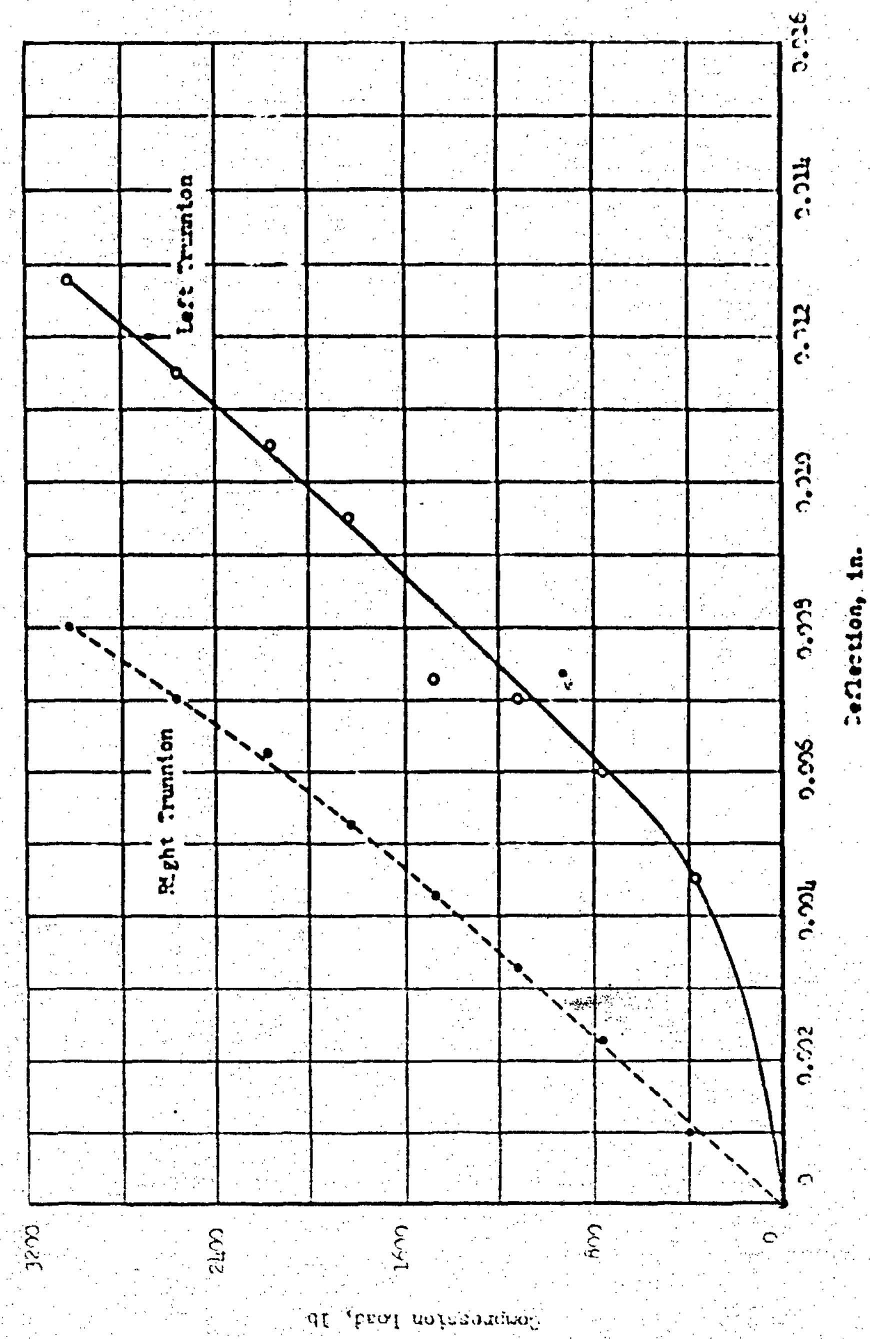

Fig. H-8 **STIFFNESS OF ELEVATING SCREW SUPPORTS**

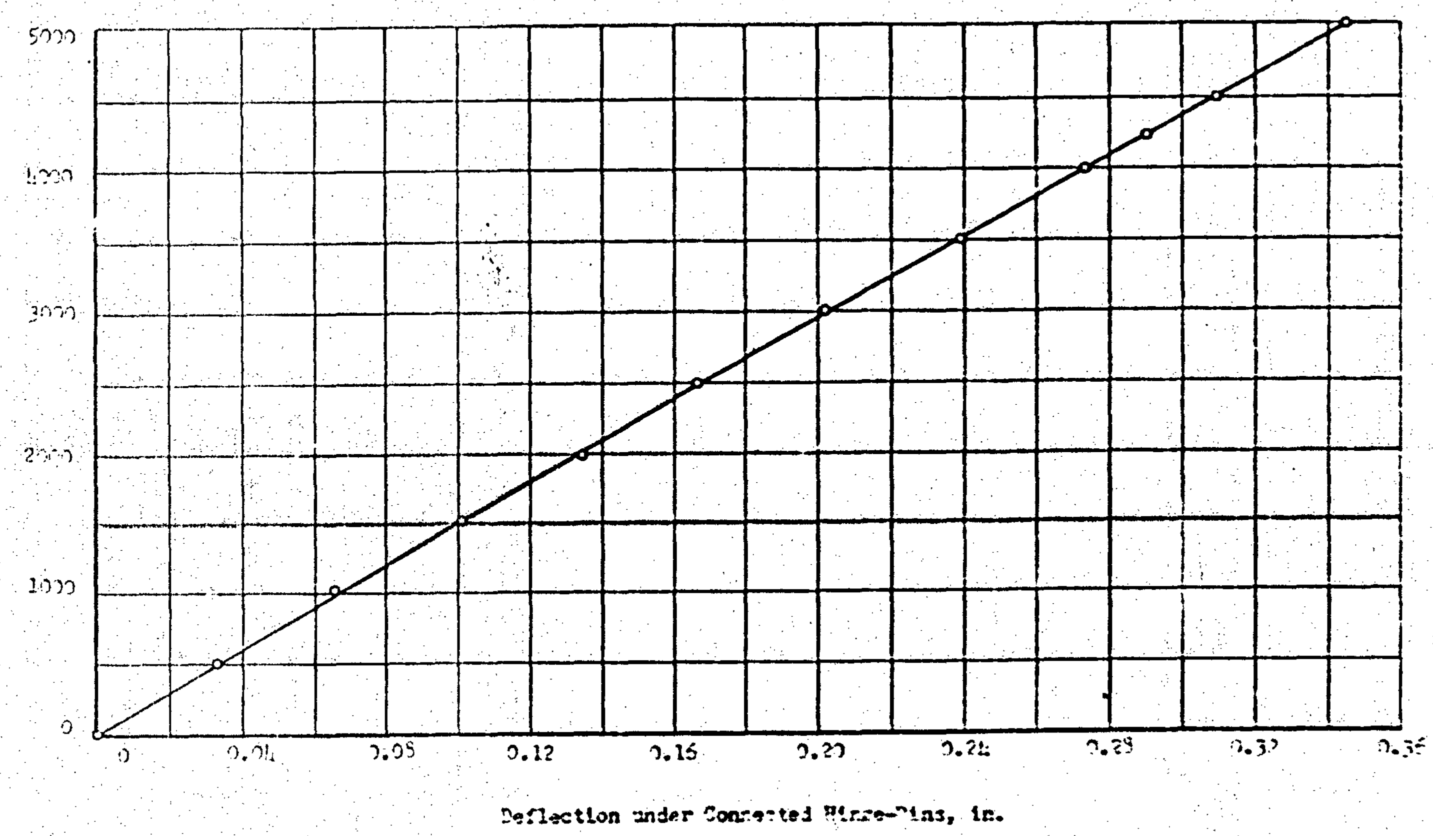

Fig. H-9 **STIFFNESS OF PROTOTYPE NO. 3 TRAILS**

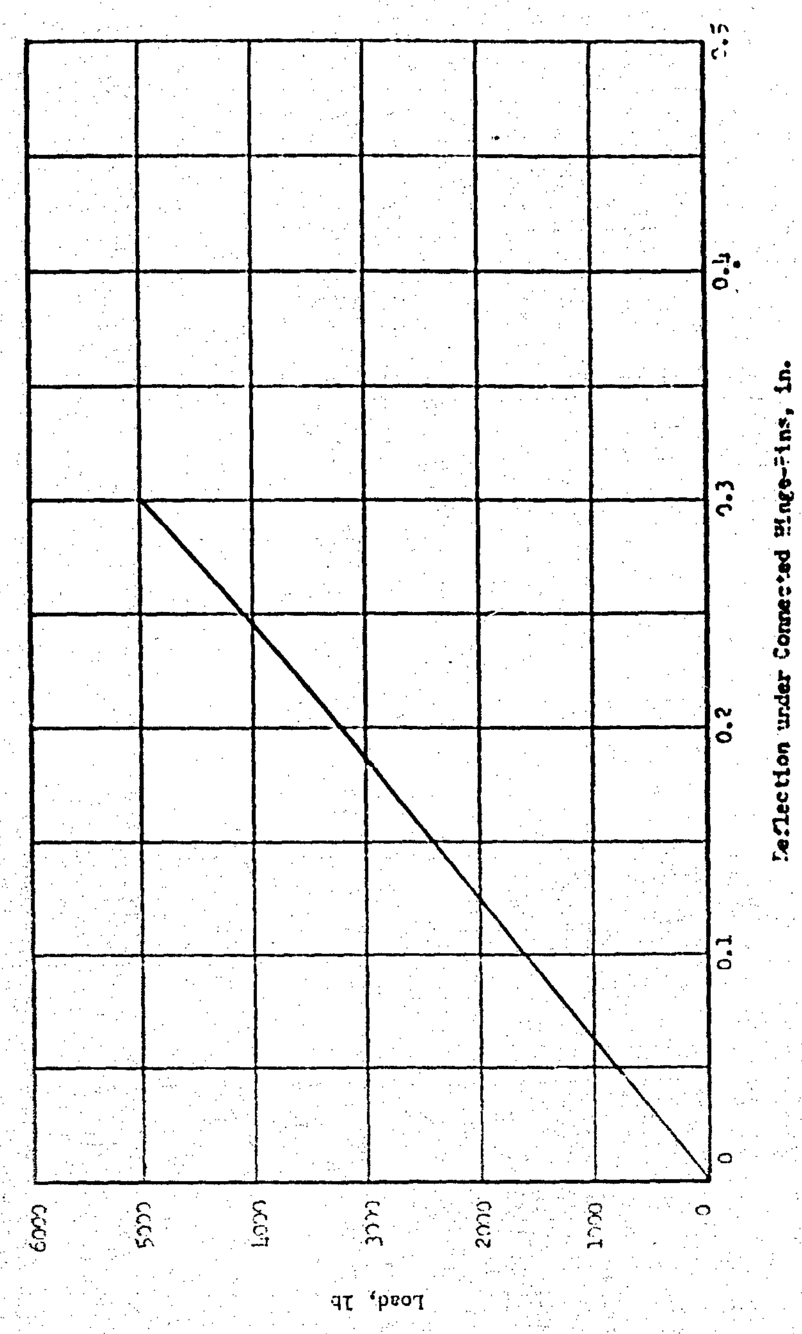

Fig. H-10 **STIFFNESS OF PROTOTYPE NO. 1 TRAILS**

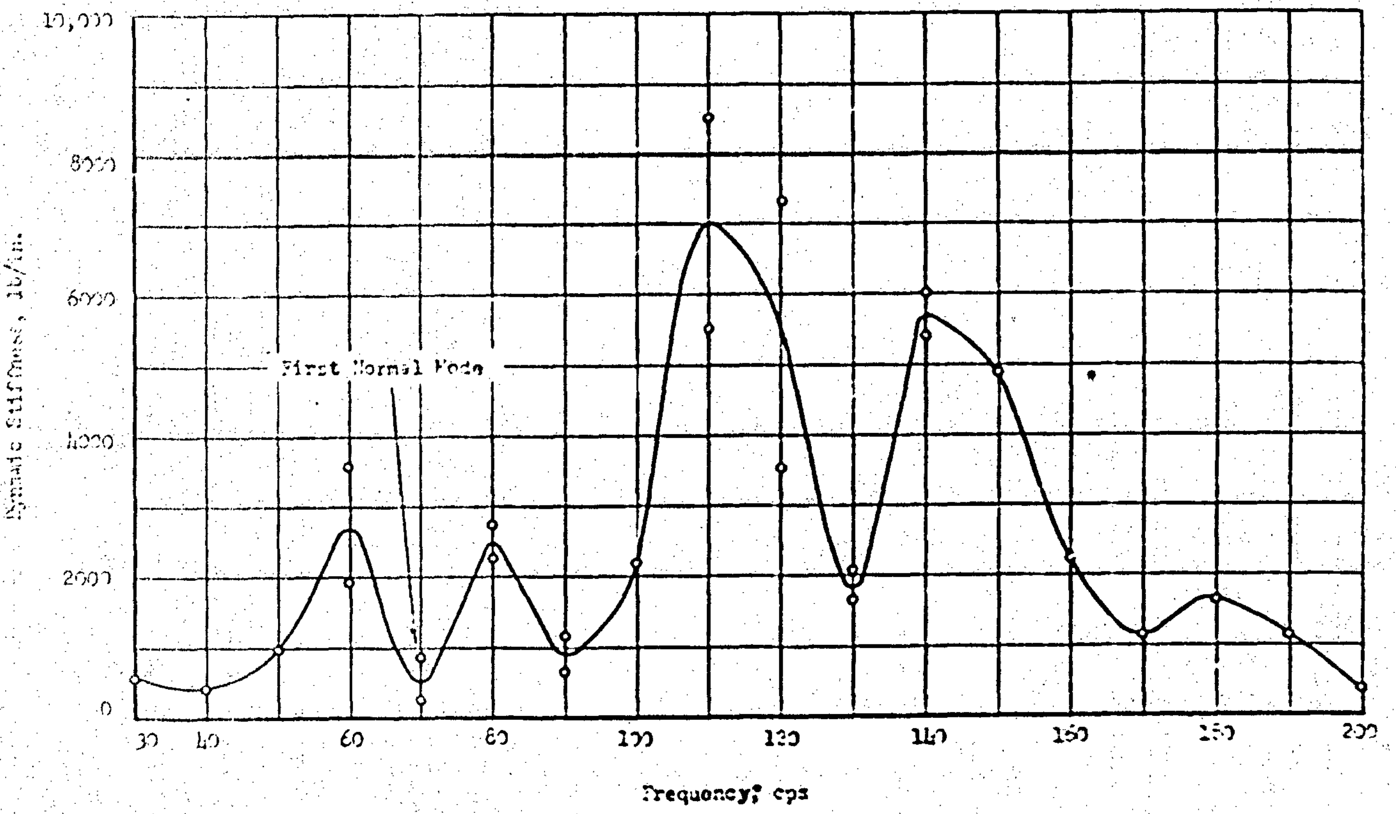

Fig. H-11 NATURAL FREQUENCY OF LAUNCHER CARRIAGE

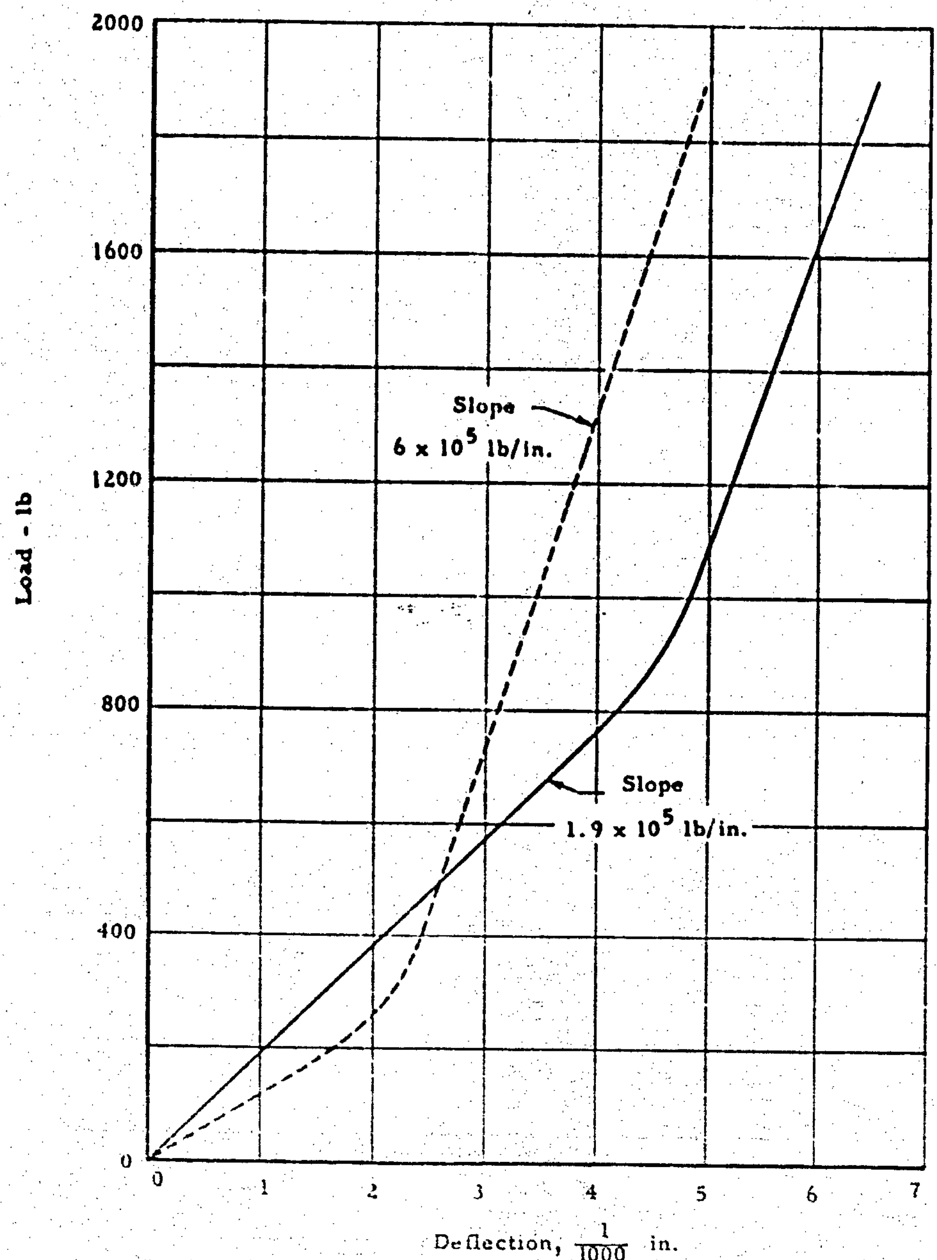

Fig. H-12 STIFFNESS OF ELEVATING SCREWS AND UPPER BRACKETS

APPENDIX I

FIRING PROGRAM

This Appendix presents a list of the firings conducted in order to obtain the launcher response in the vertical plane (see Appendix J). The instrumentation for each firing is listed as well as the structural configuration. The bursts are coded with B followed with a number; each round is individually marked by R with a corresponding number.

Because of instrumentation difficulties, some bursts were repeated. These are not listed because they were under identical conditions. Also some additional firings were made such as those to study the horizontal dispersion problem; these are described in the report body and not listed here.

TABLE I-1
FIRING SCHEDULE

Burst No.	Round No.	Zone Elevation Traverse	Target	Instrumentation	Fixtures	Movies	Comments
S. S.	R-1	$8/60^\circ/0^\circ$	No	4, 5, 6, 8, 10	None	None	To seat firing base and stakes
S. S.	R-2	$8/60^\circ/0^\circ$	No	4, 5, 6, 8, 10	None	None	and also to adjust C' recoil buf-
S. S.	R-3	$8/60^\circ/0^\circ$	No	4, 5, 6, 8, 10	None	None	fer. Checkout instrumentation.
B-1	R-4	$8/45^\circ/0^\circ$	Yes	3, 4, 5, 6, 8, 10	None	On	This will be a burst to be used
	R-5	$8/45^\circ/0^\circ$	Yes	3, 4, 5, 6, 8, 10	None	Target	for comparison purposes but
	R-6	$8/45^\circ/0^\circ$	Yes	3, 4, 5, 6, 8, 10	None	(See	also to check out the left-right
	R-7	$8/45^\circ/0^\circ$	Yes	3, 4, 5, 6, 8, 10	None	Comments)	sequencing. Have a movie cam-
	R-8	$8/45^\circ/0^\circ$	Yes	3, 4, 5, 6, 8, 10	None	Black &	era on the target to record se-
	R-9	$8/45^\circ/0^\circ$	Yes	3, 4, 5, 6, 8, 10	None	White	quence. Regular 16MM camera
							at high speed.
B-2	R-10	$9/45^\circ/0^\circ$	Yes	3, 4, 5, 6, 8, 10	None	On target	Same as previous burst
	R-11	$9/45^\circ/0^\circ$	Yes	3, 4, 5, 6, 8, 10	None	On target	
	R-12	$9/45^\circ/0^\circ$	Yes	3, 4, 5, 6, 8, 10	None	On target	
	R-13	$9/45^\circ/0^\circ$	Yes	3, 4, 5, 6, 8, 10	None	On target	
	R-14	$9/45^\circ/0^\circ$	Yes	3, 4, 5, 6, 8, 10	None	On target	
	R-15	$9/45^\circ/0^\circ$	Yes	3, 4, 5, 6, 8, 10	None	On target	
B-3	R-16	$9/45^\circ/0^\circ$	Yes	3, 4, 5, 6, 8, 10	None	On target	Repeat of previous burst to
	R-17	$9/45^\circ/0^\circ$	Yes	3, 4, 5, 6, 8, 10	None	On target	check similarity of results.
	R-18	$9/45^\circ/0^\circ$	Yes	3, 4, 5, 6, 8, 10	None	On target	(Mainly to check the similarity
	R-19	$9/45^\circ/0^\circ$	Yes	3, 4, 5, 6, 8, 10	None	On target	of target patterns.)
	R-20	$9/45^\circ/0^\circ$	Yes	3, 4, 5, 6, 8, 10	None	On target	
	R-21	$9/45^\circ/0^\circ$	Yes	3, 4, 5, 6, 8, 10	None	On target	

Burst No.	Round No.	Zone Elevation Traverse	Target	Instrumentation	Fixtures	Movies	Comments
B-4	R-22	9/45°/0°	Yes	3, 4, 5, 6, 8, 10	None	None	To complete a set of three records
	R-23	9/45°/0°	Yes	3, 4, 5, 6, 8, 10	None	None	at this condition for comparison.
							Record round sequence through
							target.
B-5	R-24	9/45°/0°	Yes	3, 4, 5, 6, 8, 10	la, 3	None	Large damper holes. Record
	R-25	9/45°/0°	Yes	3, 4, 5, 6, 8, 10	la, 3	None	round sequence through target.
S. S.	R-26	9/45°/0°	No	3, 4, 5, 6, 8, 10	la, 3	None	Single shot repeat of preceding
							burst.
S. S.	R-27	9/45°/0°	No	3, 4, 5, 6, 8, 10	la, 3	None	Repeat of preceding test.
B-6	R-28	9/45°/0°	Yes	3, 4, 5, 6, 8, 10	la, 3	None	Change to small diameter holes
	R-29	9/45°/0°	Yes	3, 4, 5, 6, 8, 10	la, 3	None	in hydraulic damper. Record
							round sequence through target.
S. S.	R-30	9/45°/0°	No	3, 4, 5, 6, 8, 10	la, 3	None	Single shot repeat of preceding
							test.
S. S.	R-31	9/45°/0°	No	3, 4, 5, 6, 8, 10	la, 3	None	Repeat of preceding test.
B-7	R-32	9/45°/0°	Yes	3, 4, 5, 6, 7	la,3,4,5,6	None	Small dia. holes in damper coil
	R-33	9/45°/0°	Yes	3, 4, 5, 6, 7	la,3,4,5,6	None	spring in elevating system.
S. S.	R-34	9/45°/0°	No	3, 4, 5, 6, 7	la,3,4,5,6	None	Single shot repeat of preceding
							test.
S. S.	R-35	9/45°/0°	No	3, 4, 5, 6, 7	la,3,4,5,6	None	Repeat of preceding test.

Burst No.	Round No.	Zone Elevation Traverse	Target	Instrumentation	Fixtures	Movies	Comments
B-8	R-36	9/45°/0°	Yes	3,4,5,6,7,8	2,3,4,5,6	None	Small dia. damper holes,
	R-37	9/45°/0°	Yes	3,4,5,6,7,8	2,3,4,5,6	None	record target sequence.
S. S.	R-38	9/45°/0°	No	3,4,5,6,7,8	2,3,4,5,6	None	Single shot repeat of preceding test.
S. S.	R-39	9/45°/0°	No	3,4,5,6,7,8	2,3,4,5,6	None	Repeat of preceding test.
B-9	R-40	9/45°/0°	No	3,4,5,6	1b	None	Install ring springs into
	R-41	9/45°/0°	No	3,4,5,6	1b	None	elevating system.
S. S.	R-42	9/45°/0°	No	3,4,5,6	1b	None	Single-shot repeat of preceding test.
B-10	R-43	9/45°/0°	No	3,4,5,6,7	1b, 3	None	Repeat of previous test with
	R-44	9/45°/0°	No	3,4,5,6,7	1b, 3	None	damper added. Small dia. holes.
B-11	R-45	7/45°/0°	No	3	1a	None	No recoil pressure
	R-46	7/45°/0°	No	3	1a	None	

The following fixtures were required for the experimental firings of Pilot No. 3 at Ft. Sheridan. The corresponding numbers in the following list will be used in the firing schedule.

1. Variable flexibility elevating rods with: a.) coil springs and b.) friction damped ring springs,
2. Rigid elevating rods,
3. Hydraulic dampers between carriage sides and cradle with interchangeable pistons,
4. Shorter pad placement on the trails,
5. Trunnion-to-trail stiffening struts,
6. Brackets and wedges for stiffening the carriage box-sections.

The following instrumentation was required for the experimental firings of Pilot No. 3 at Ft. Sheridan. The combination of instruments to use for each particular firing will be found on the firing schedule. Each of the following list will be referred to by number.

1. One strain gage on the rear plate of the recoiling parts for a firing signal.
2. One strain gage on each trail.
3. Two linear pots between cradle and ground, one on each side of the cradle, perpendicular to it at 45° elevation, a few inches behind the cradle front. Maximum expected motion, $\pm$ 3 in.
4. One strain gage on each elevating rod including the fixtures. Maximum expected strain, 300×10^{-6} in./in.
5. Two linear pots, one on each side of the launcher, trunnion to ground, parallel to the cradle at 45° elevation. Expected maximum motion, $\pm$ 3/4 in.
6. Two linear pots, one on each side, trunnion to ground, perpendicular to the cradle at 45° elevation. Maximum expected motion, $\pm$ 1/2 in.
7. Two strain gages, one on each damper rod, to measure tension and compression. Maximum expected strain, 200×10^{-6} in./in.
8. One linear pot on each trail end, perpendicular to the ground. Maximum expected vertical displacement (+6, -1/4) in.

   (The firing base will be staked to prevent rearward displacements.)
9. Strain gages on the indexing system shafts.
10. Recoil system pressure (one gage, right or left side)

INSTRUMENTATION NOTE: Gages 1, 2 and II (rear plate, trail, & recoil pressure) will be used for all firings unless otherwise noted.

APPENDIX J

EXPERIMENTAL LAUNCHER RESPONSE CURVES

I. INTRODUCTION

The list of the firings and the instrumentation for each burst in Appendix I shows that a very large amount of data was recorded. The most significant portion of this data is that which actually illustrates the response of the launcher. In order to limit the amount of data to a reasonable level, only the cradle response and trail strain are shown. (Exceptions to this are Fig. 22 and 23 in the body of the report.) These curves are presented for each of the structural configurations.

II. DISCUSSION

The cradle response is shown in inches of displacement. This is the motion of the cradle front perpendicular to the plane containing the trunnions and firing tube. If the trunnions remain motionless, this cradle motion, by dividing by the proper distance, gives cradle rotation. For this purpose, the trunnion motion in the vertical plane was found experimentally to be negligible; dividing the cradle displacement by 60 in. is a good approximation of cradle rotation.

If the trails respond primarily in their first mode shape, the trail strain is approximately proportional to the angular deflection of the trail at its connection with the lower box member. Again, experiments show that the use of the trail strain to indicate rotation is a good assumption. This strain and the cradle displacement serve to show the launcher response.

The following figures show the cradle response and trail strains for the birst conditions described in Appendix I.

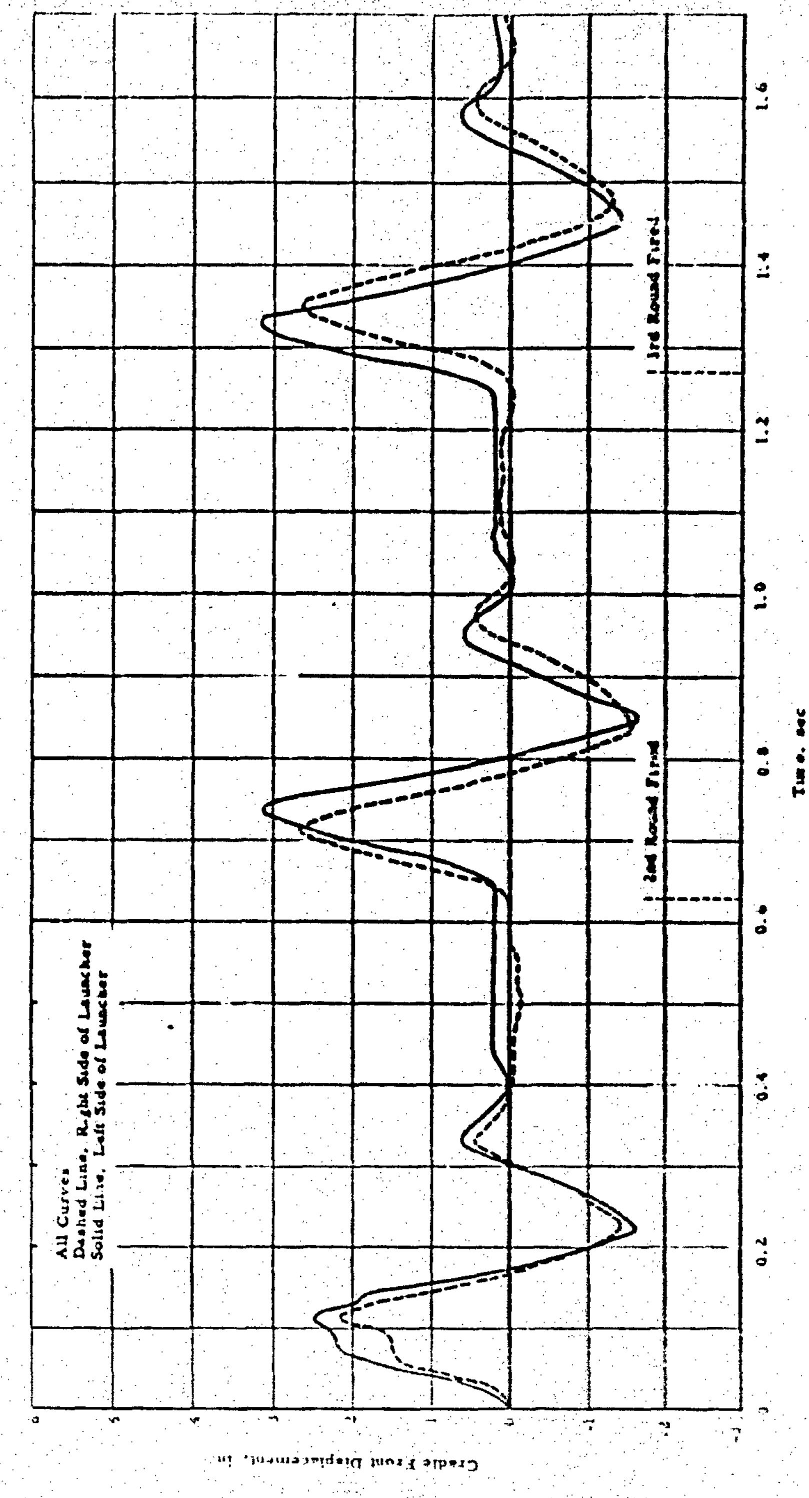

Fig. J-1 CRADLE MOTION, BURST B-2

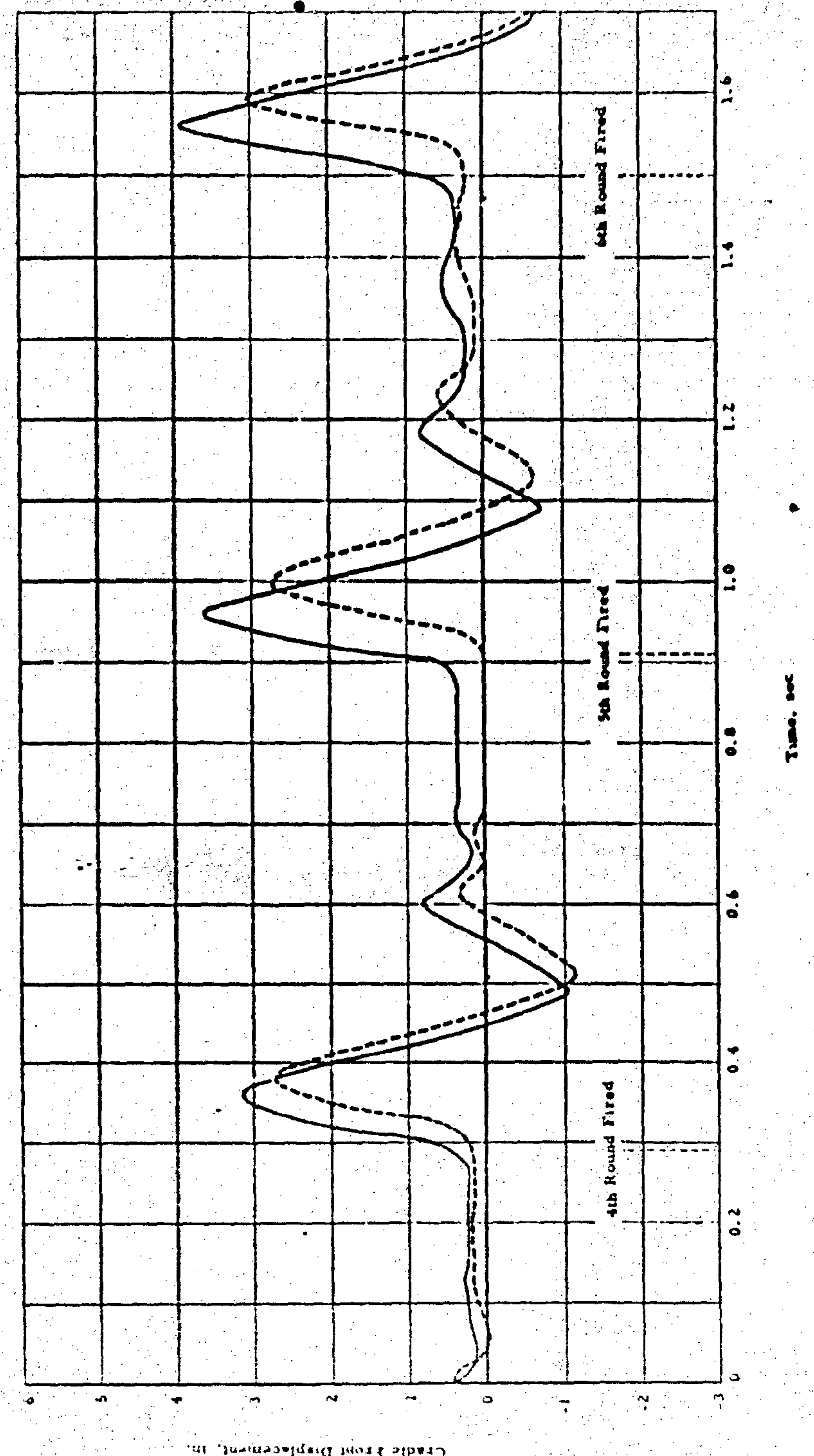

Fig. J-2 CRADLE MOTION, BURST B-2

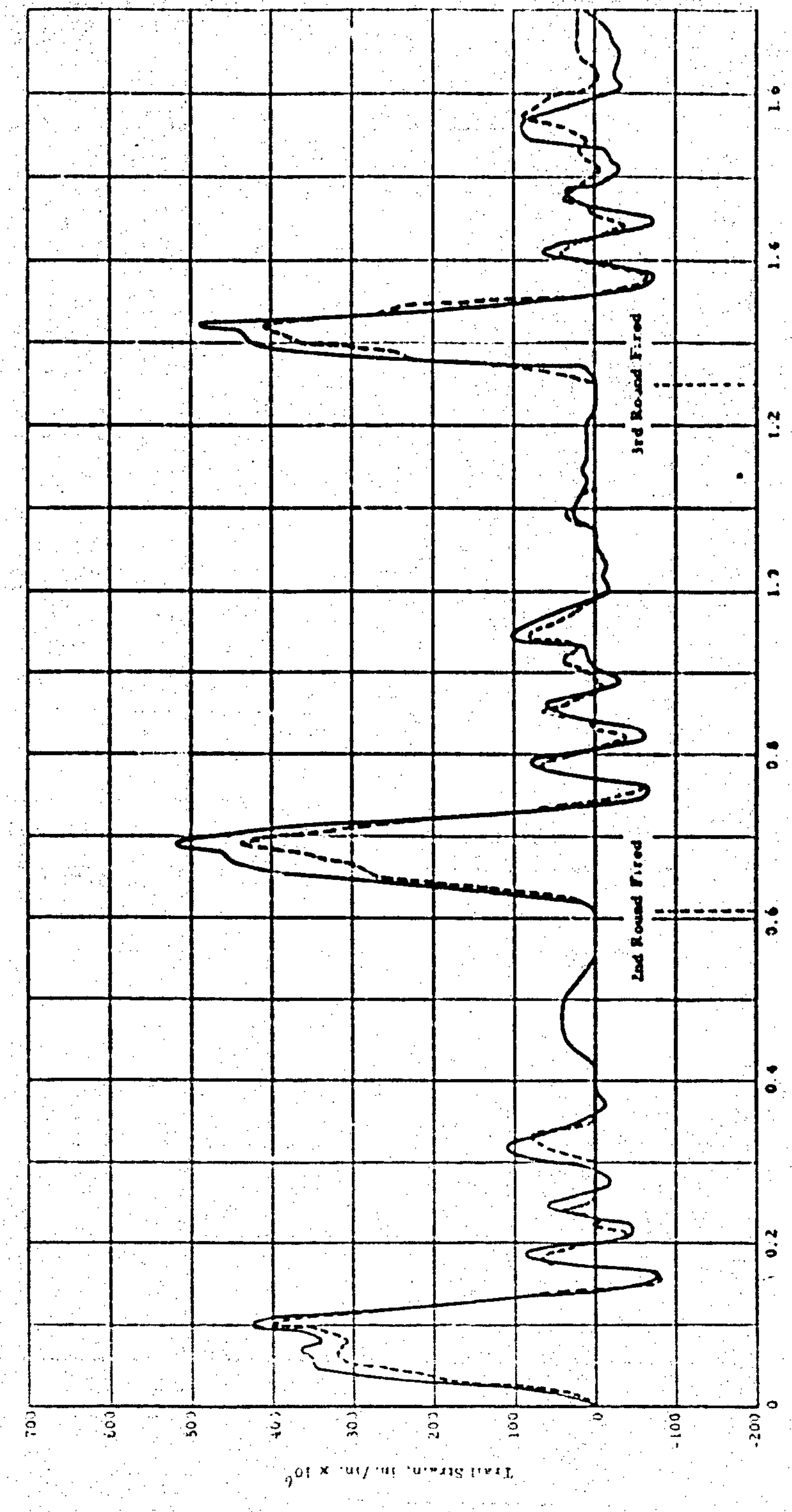

Fig. J-3 TRAIL STRAIN, BURST B-2

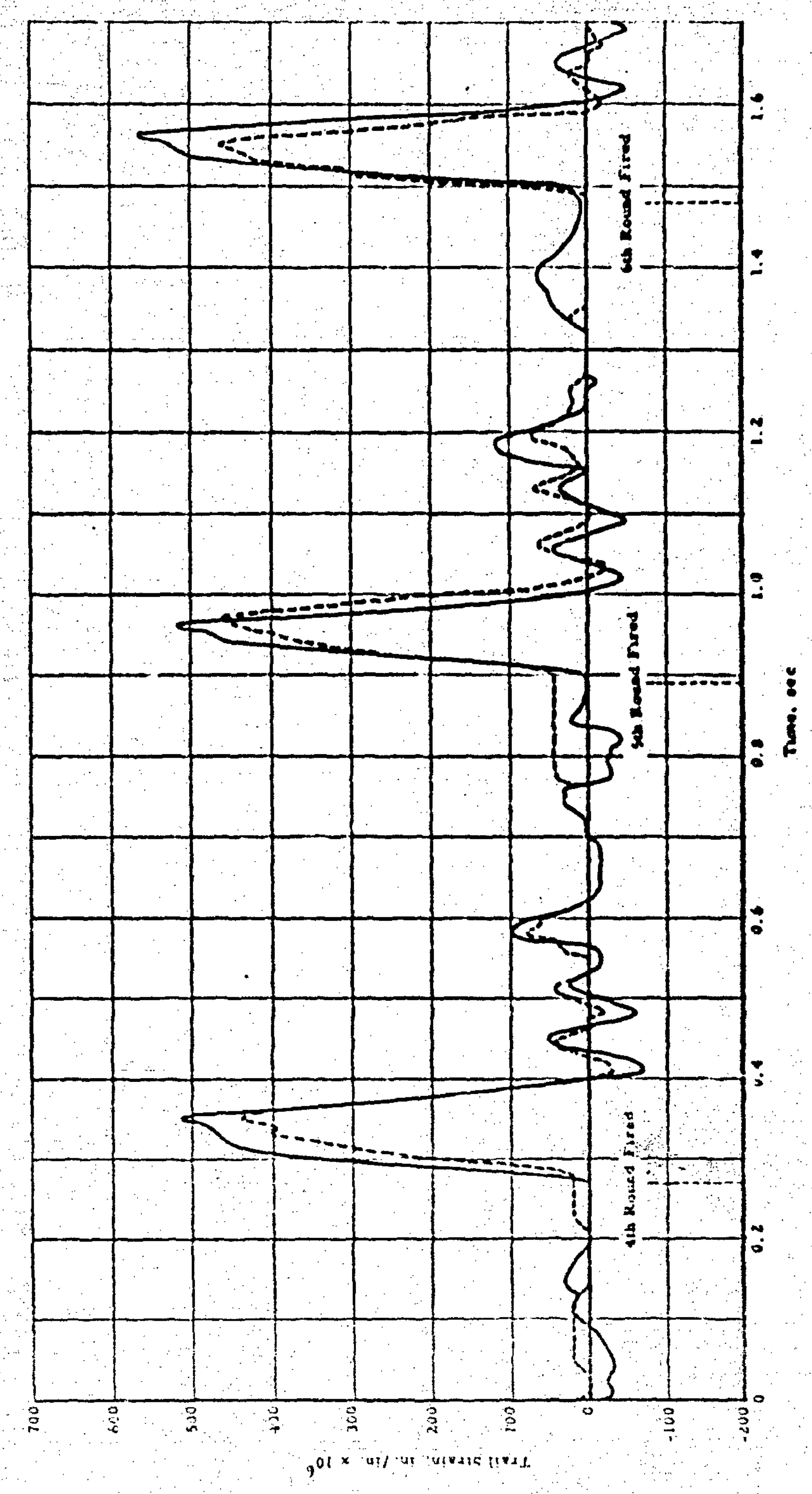

Fig. J-4 TRAIL STRAIN, BURST B-2

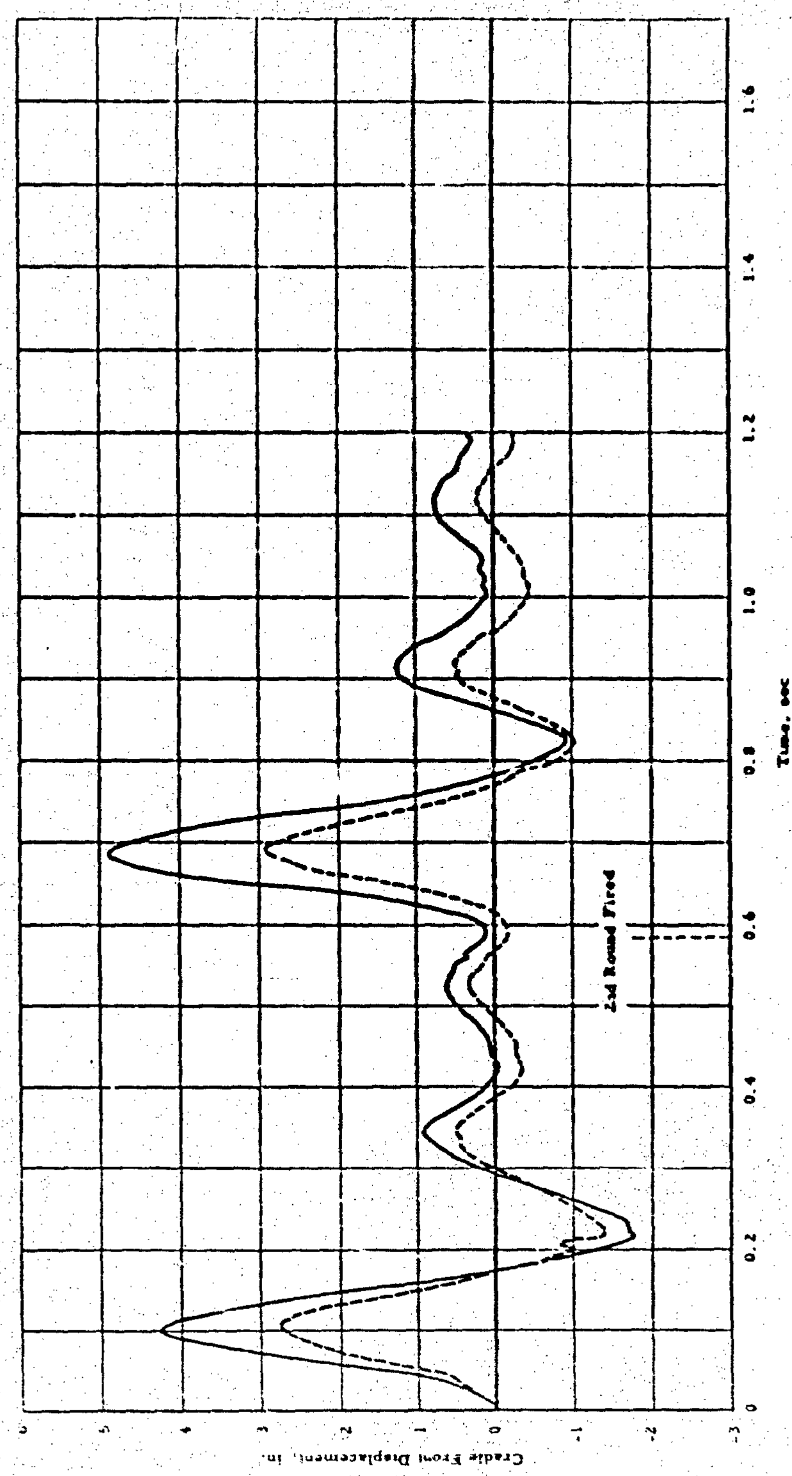

Fig. J-5 CRADLE MOTION, BURST B-5

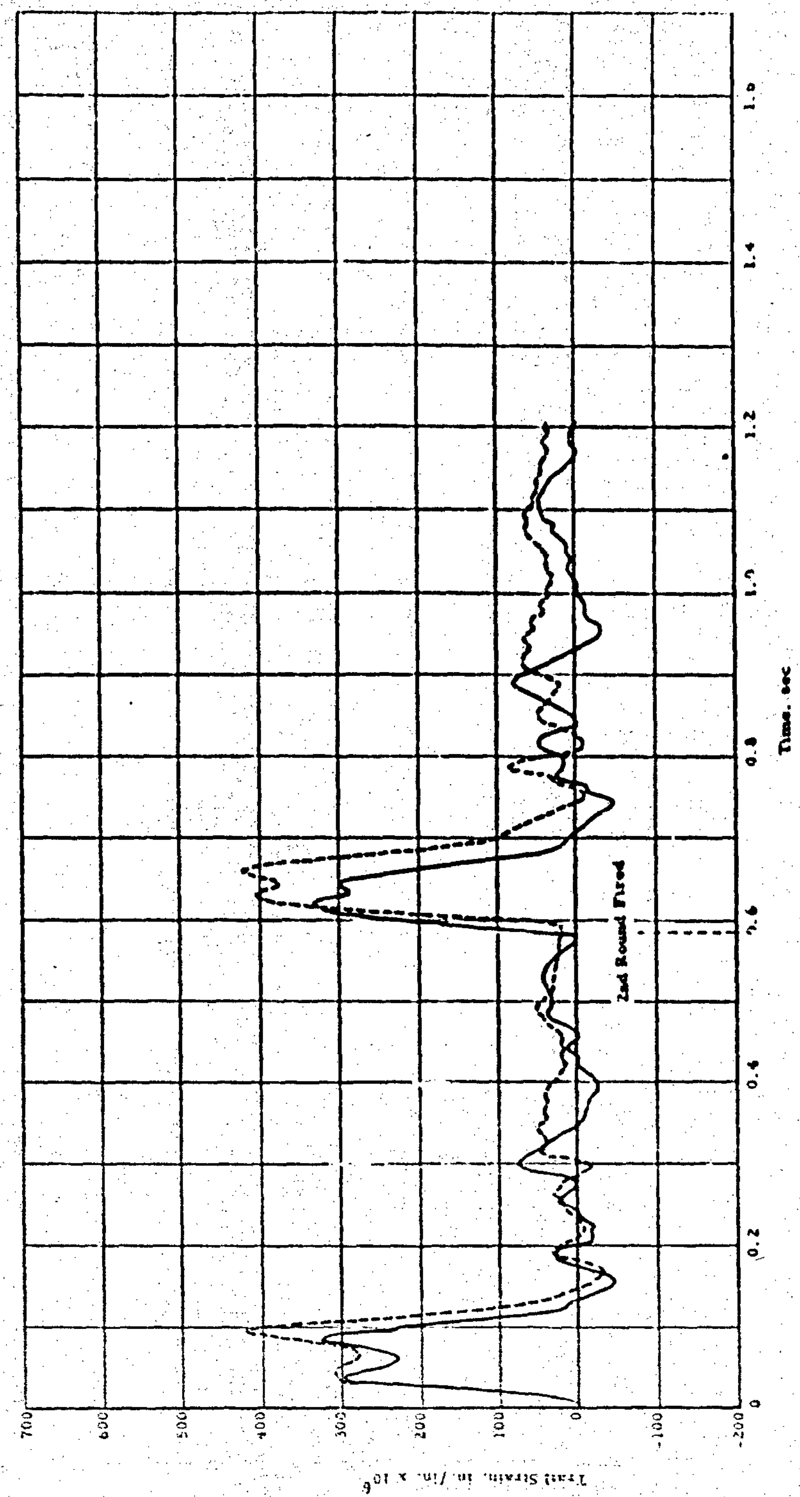

Fig. J-6 TRAIL STRAIN, BURST B-5

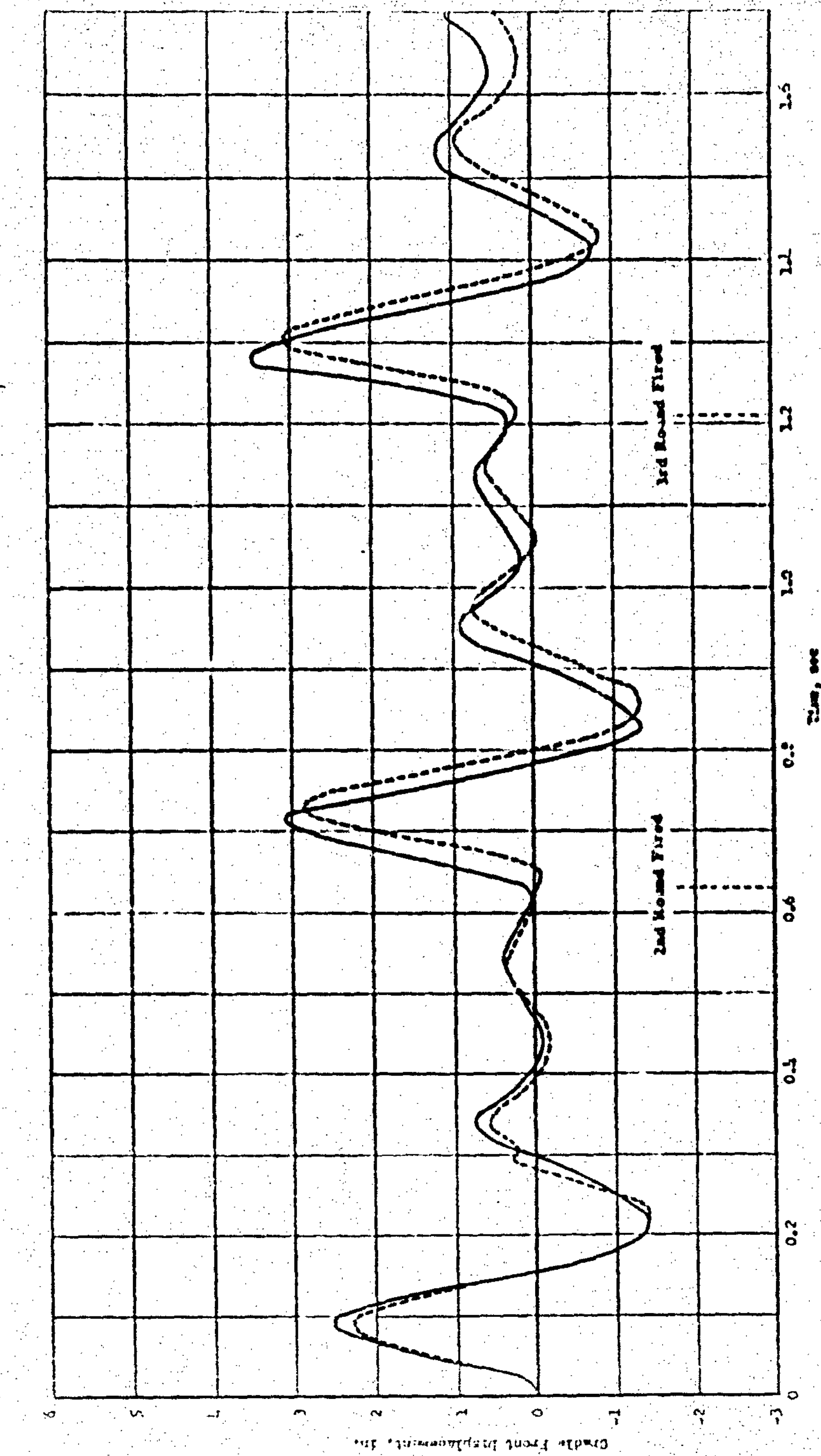

Fig J-7 CRADLE MOTION, BURST B-6

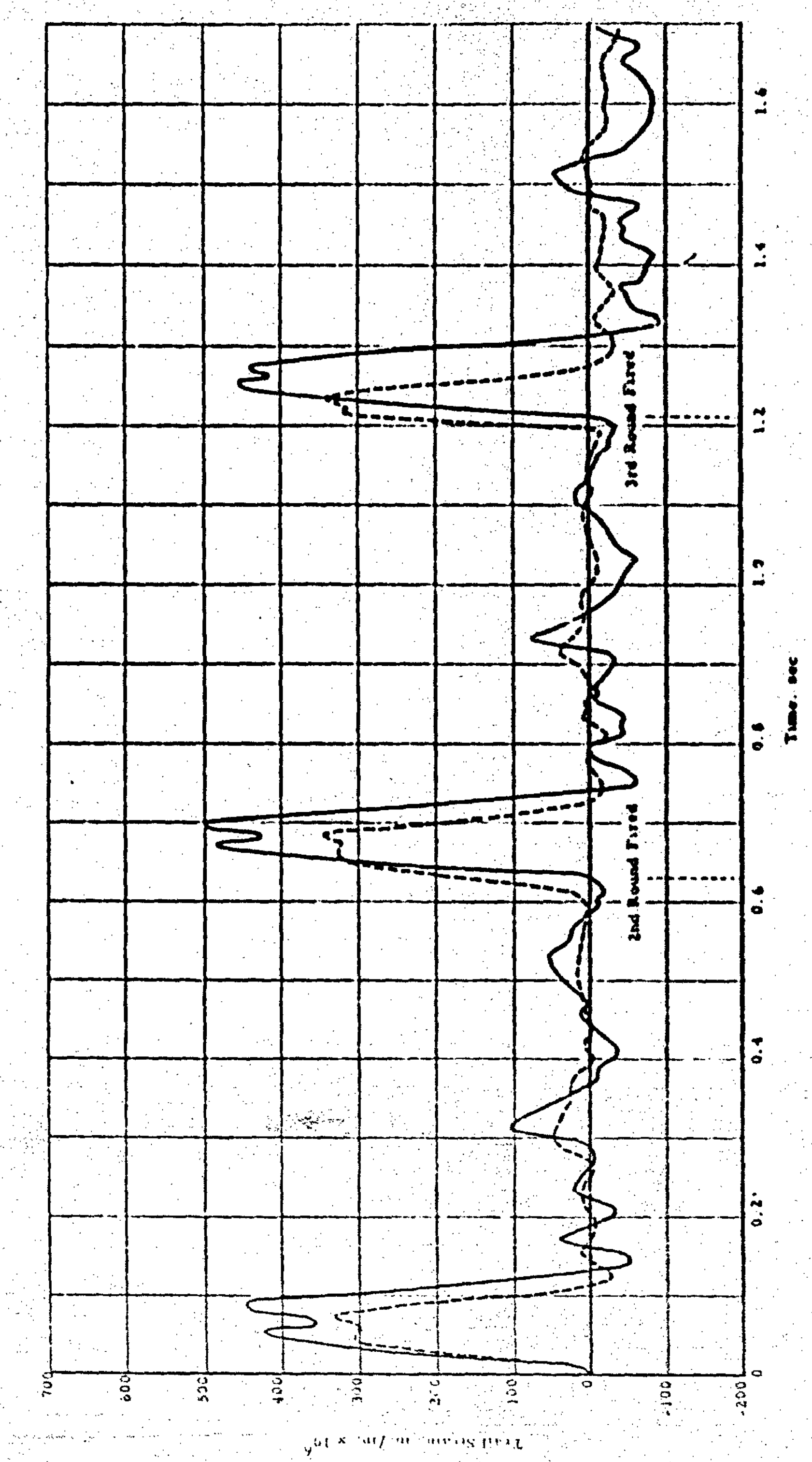

Fig. J-8 TRAIL STRAIN, BURST B-6

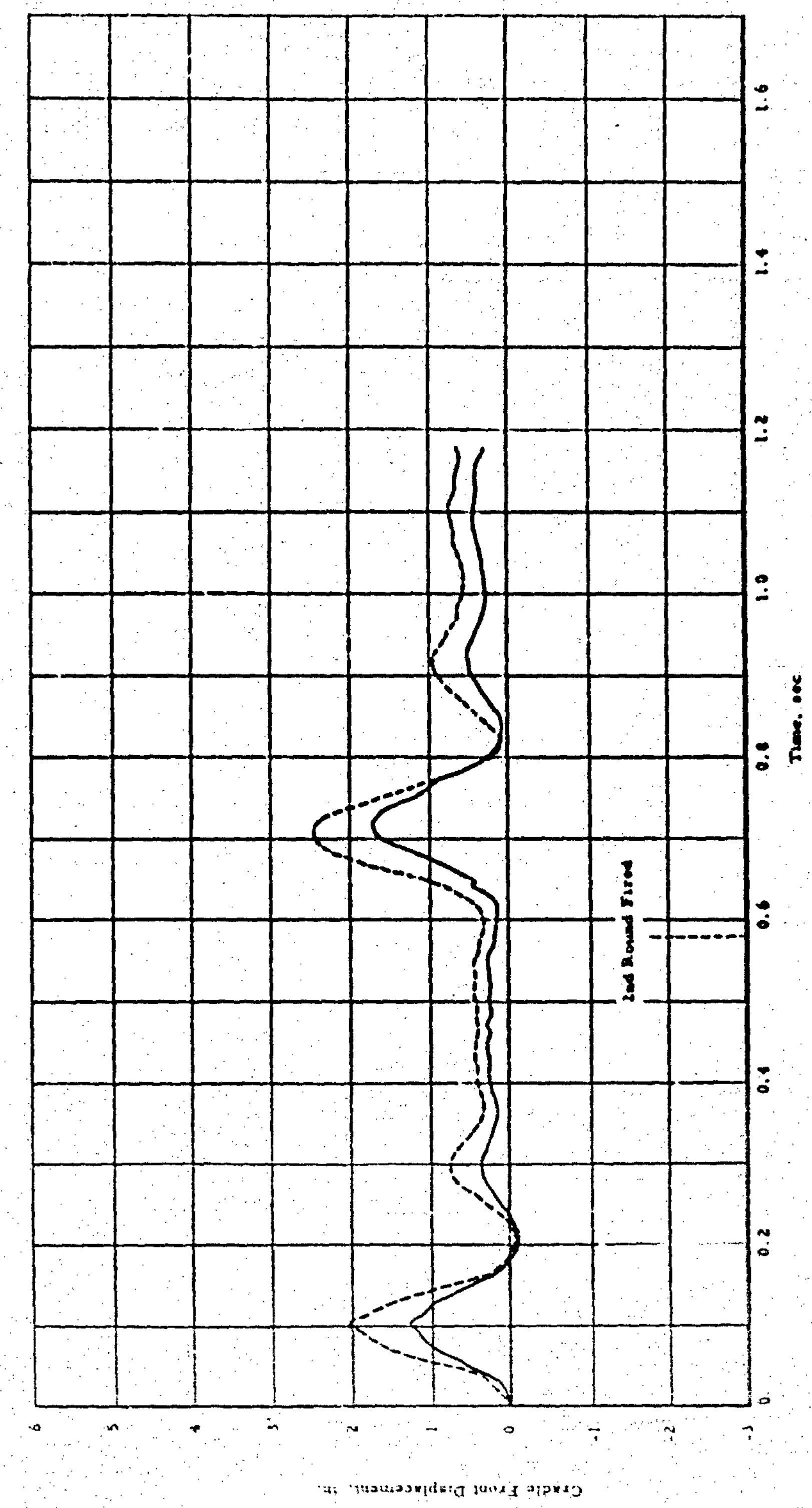

Fig. J-9 CRADLE MOTION, BURST B-7

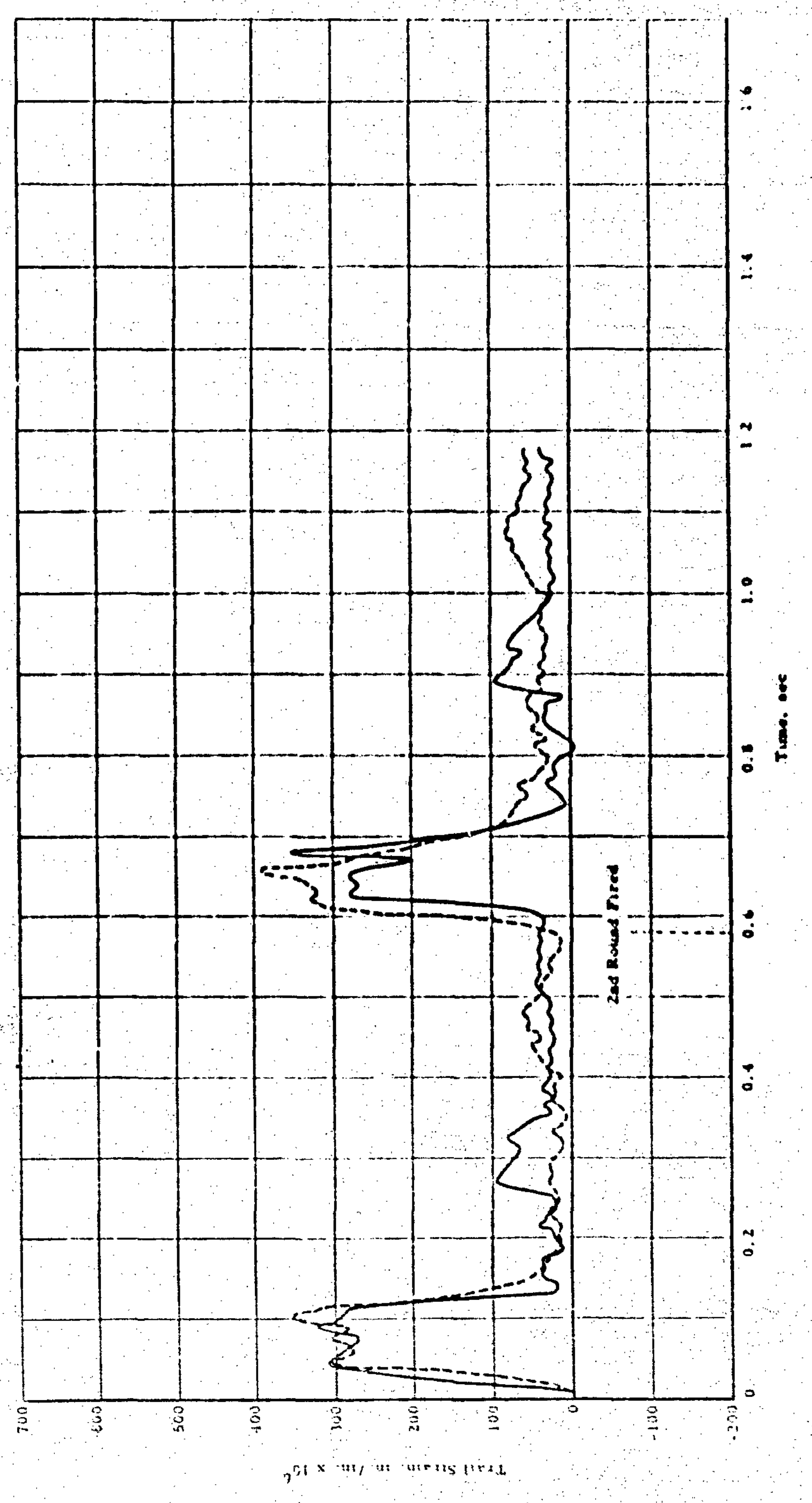

Fig. J-10 **TRAIL STRAIN, BURST B-7**

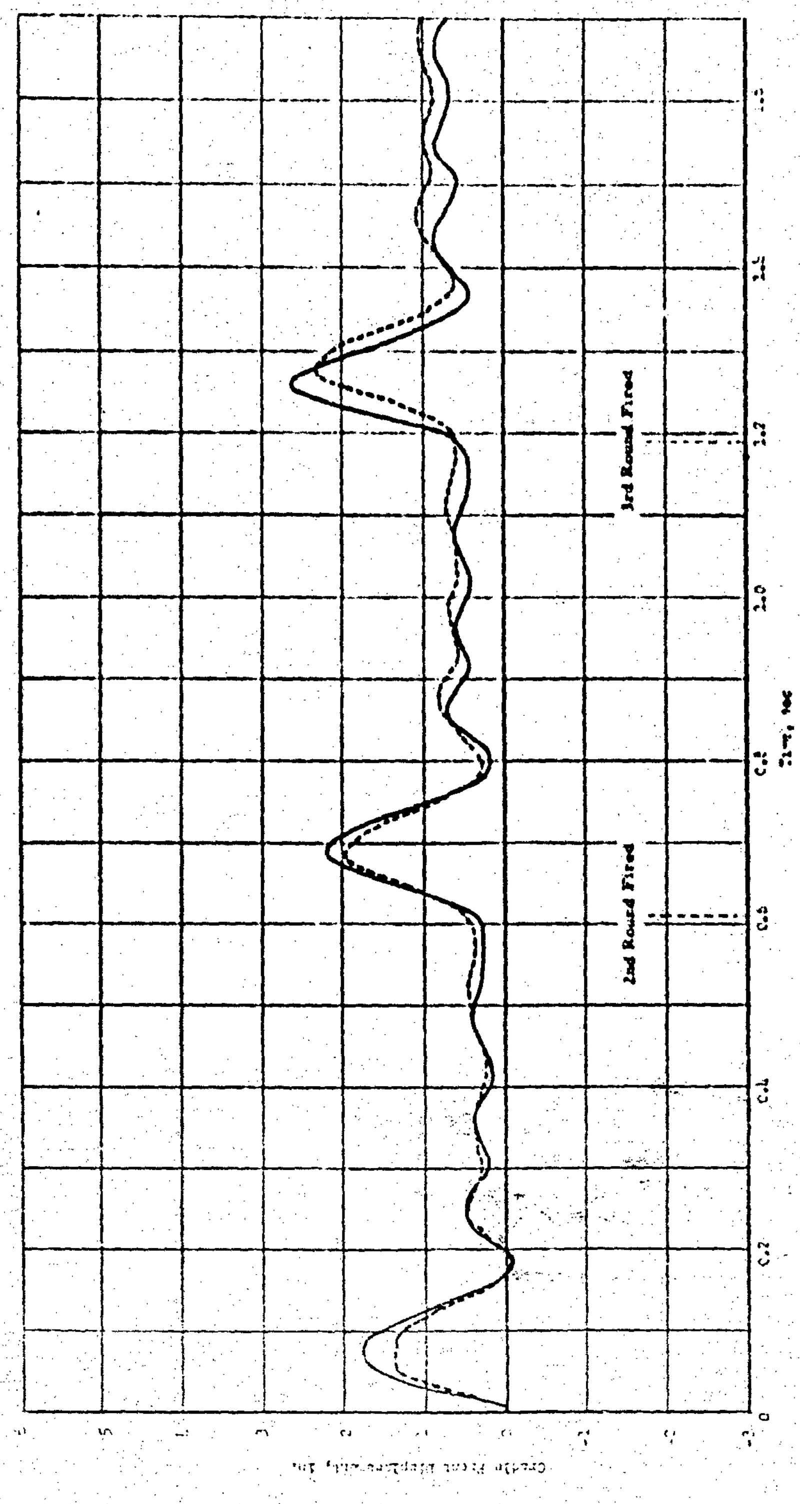

Fig. J-11 **CRADLE MOTION, BURST B-8**

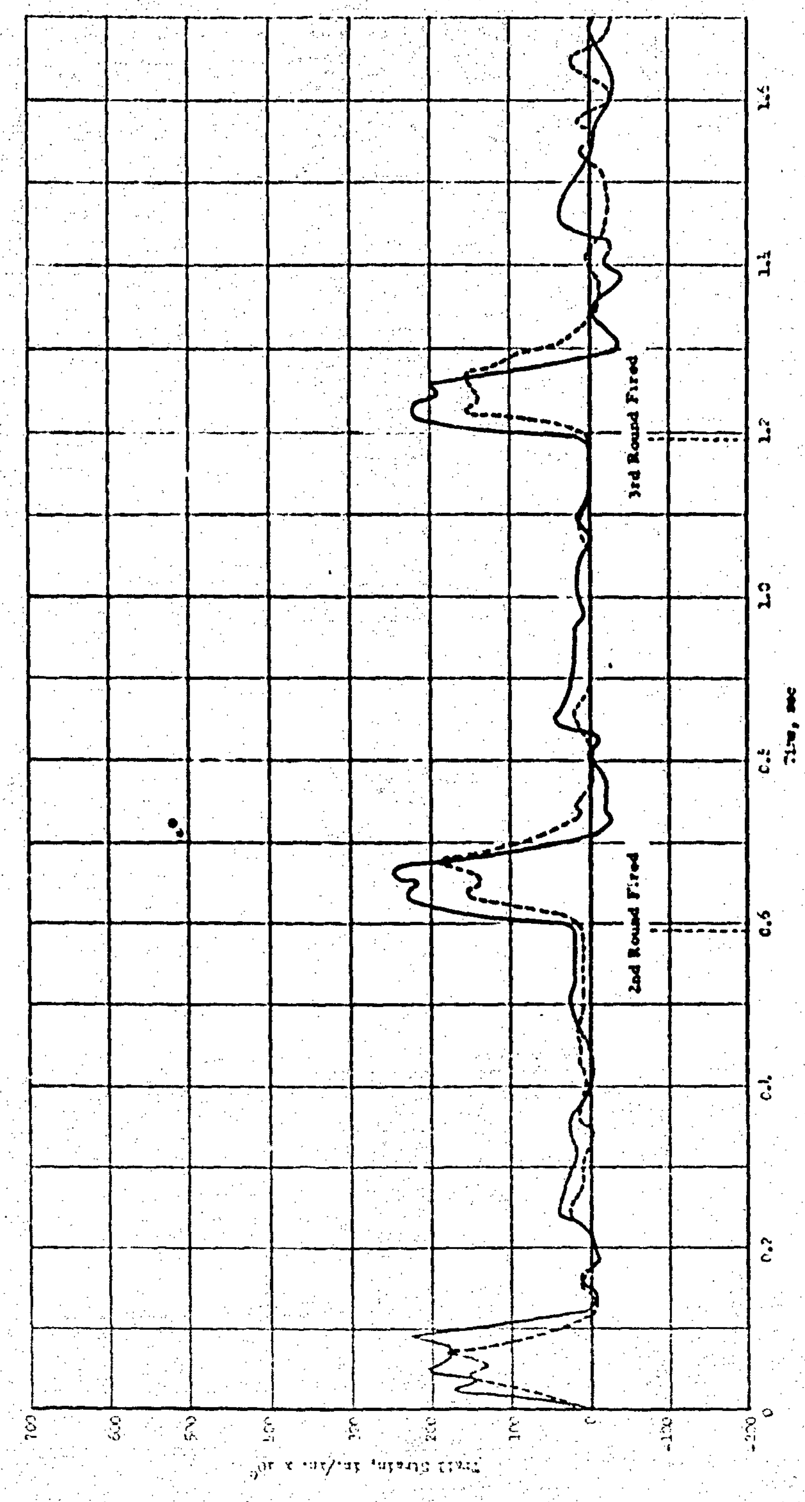

Fig. J-12 TRAIL STRAIN, BURST B-8

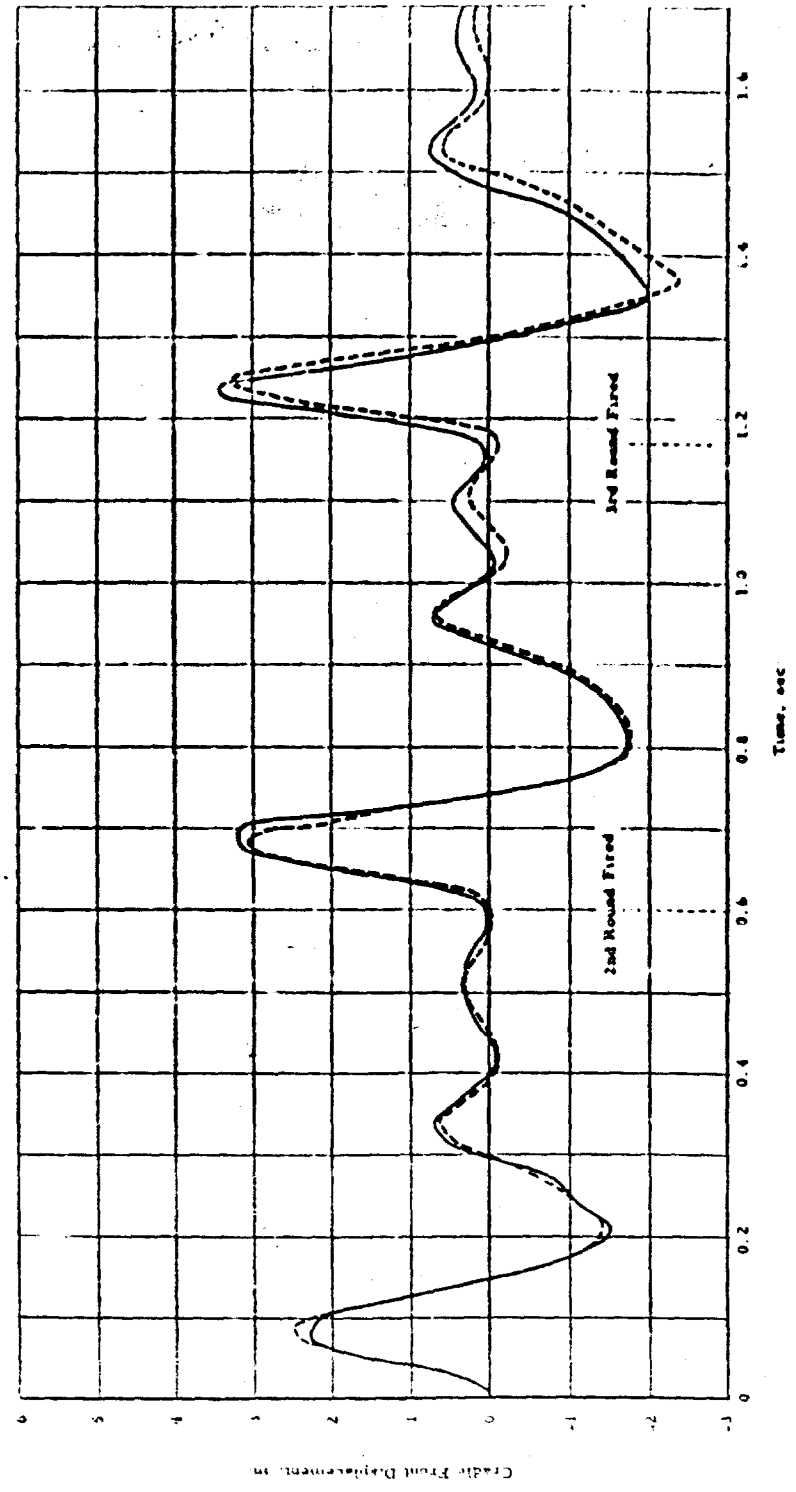

Fig. J-13 CRADLE ROTATION, BURST B-9

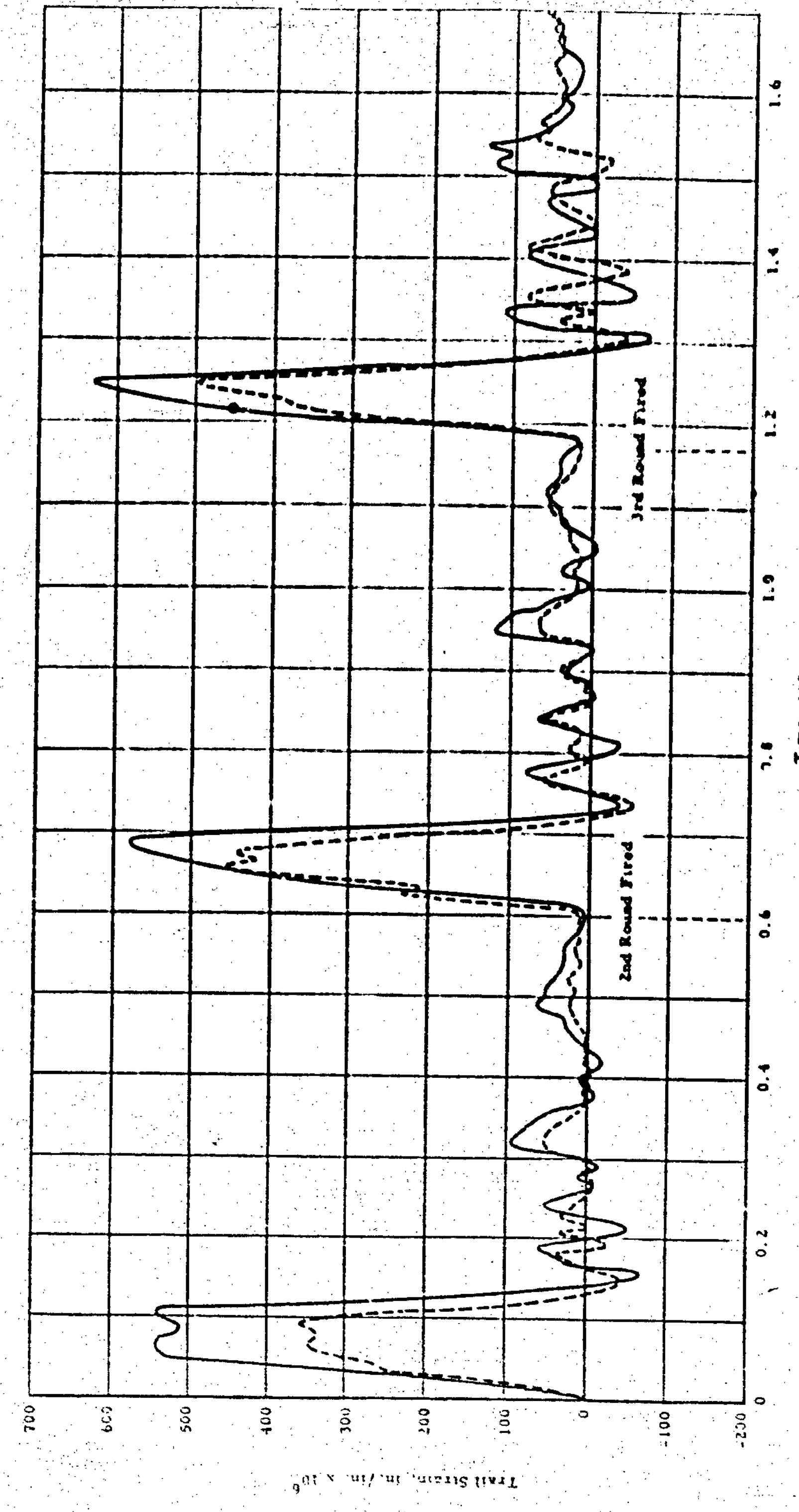

Fig. J-14 **TRAIL STRAIN, BURST B-9**

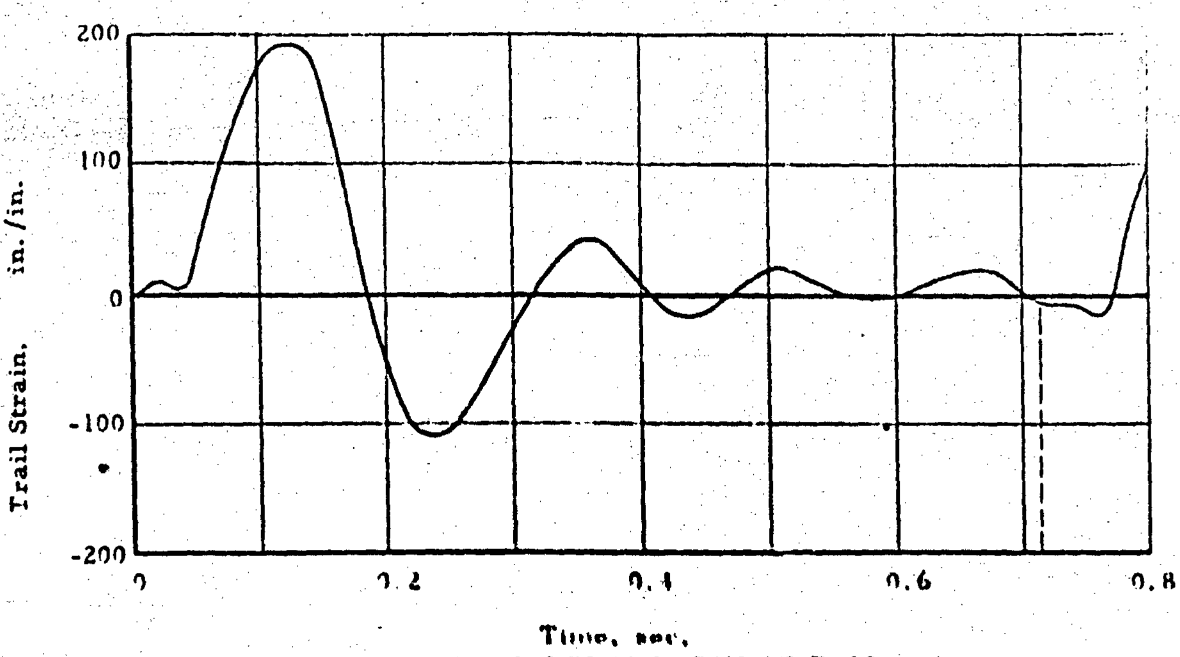

Fig. J-15 TRAIL STRAIN, BURST B-10

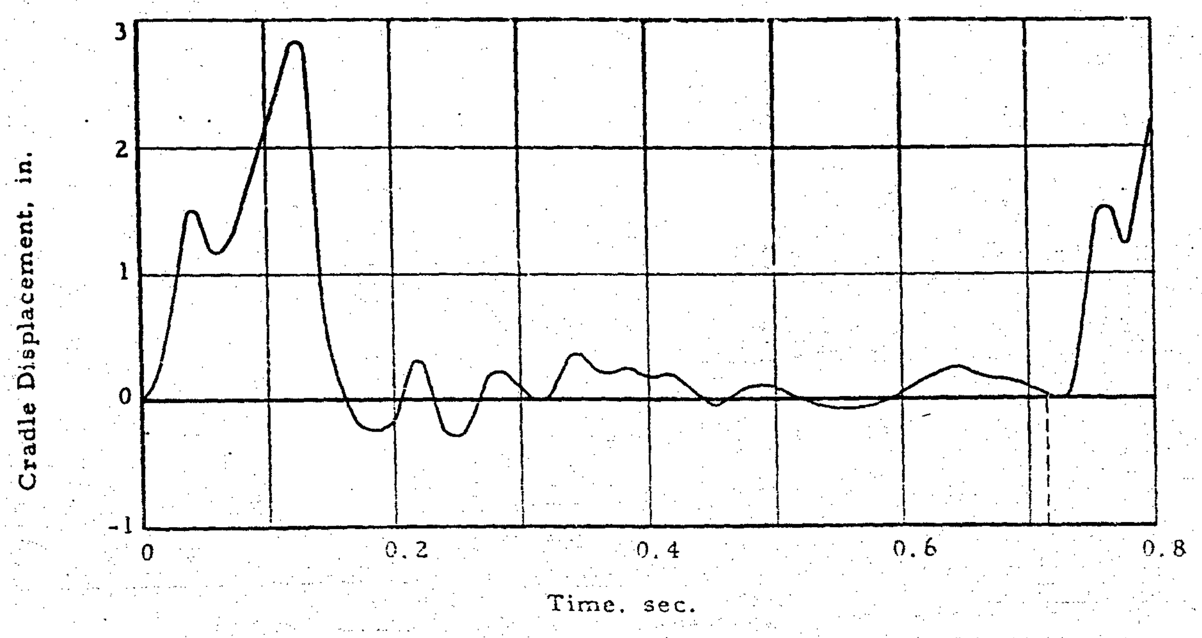

Fig. J-16 CRADLE MOTION, BURST B-10